University of Strathclyde

Strathclyde Institute of Pharmacy and Biomedical Sciences,
University of Strathclyde,
Glasgow, G4 0RE

The Expression and Function of IL-33 within the CNS and during the Pathogenesis of Multiple Sclerosis

A thesis submitted in fulfilment of the requirements for the degree of Doctor of Philosophy

Debbie Allan

Glasgow, Scotland, February 2015

In Loving Memory of
Elisabeth Milne

Acknowledgements

Firstly I would like to thank my supervisor Dr Hui-Rong Jiang for making this PhD possible. I would also like to thank Prof. William Harnett for his constant support and guidance; you have been a calming presence in stressful times.

I would like to thank Mark who has helped with many EAE experiments when I have freaked out or managed to injure myself! I would also like to give a big thank you to Karen. Unfortunately, you came at the end of my PhD but you have helped me with writing up, stats (which we both know I hate!) and viva prep and I am very grateful. You really kept me calm, motivated and were always there when I needed you-Thanks!

I have been very fortunate to make such great friends at Strathclyde who I will miss immensely. I would like to thank Sarah, Alison, Jenny, Kara, Nicola, Rhona and Felicity for the great chats (although we may have distracted the rest of Level 5!) and relaxing dinners. You guys have kept me sane and helped me persevere through all the microscopy and image analysis, of which there was a lot! I would like to thank all my new friends at BioOutsource (there are too many to name) who have given great advice over this past year writing up and have kept me motivated to finish! I couldn't ask for a better team to work with!

As anyone who has finished a PhD knows it can stressful and tiring and can often spill into your personal life. So, on that note I would like to thank all the people behind the scenes who have had to put up with research papers everywhere and bad moods! Thanks to my mum who has always been supportive of my research, thanks for always being there for me- I bet you are glad it is over! Your love and encouragement has helped a lot over the past few years. Thanks to my aunt and uncle who have always encouraged me and thanks for all the delicious dinners you have made me! Unfortunately, my gran cannot be here today to witness me completing my PhD but she was there at the beginning and I hope she would have been proud – I dedicate this thesis to you, you are missed every day!

I would also like to thank my extended family- the Norris' (and granny Gray). Thanks for all your support over the last few years and for including me in all your family events, it has made the time fly in! Sorry if I have bored you to tears with all the thesis chat!

Last but not least I would like to thank my amazing boyfriend Greg. I don't know where to begin. You have helped me in every way, more than you know. Not only have you helped practically with my thesis but you have been my rock. I appreciated everything you have done. Thank you.

‘This thesis is the result of the author’s original research. It has been composed by the author and has not been previously submitted for examination which has led to the award of a degree.’

'The copyright of this thesis belongs to the author under the terms of the United Kingdom Copyright Acts as qualified by University of Strathclyde Regulation 3.50. Due acknowledgement must always be made of the use of any material contained in, or derived from, this thesis.’

Signed:

Date:

Abstract

Multiple Sclerosis (MS) is a chronic autoimmune disease of the central nervous system (CNS) effecting millions of people worldwide. The pathology of MS is characterised by the demyelination of neurons. Though the root cause of MS remains elusive a combination of genetic, environmental and infectious factors are thought to contribute. IL-33 has previously been shown to be protective (e.g. atherosclerosis), or detrimental (e.g. asthma), in certain disease states. IL-33 and ST2 (IL-33R) are highly expressed within the CNS and have been shown to exacerbate Experimental Autoimmune Encephalomyelitis (mouse model of Multiple Sclerosis). In-situ staining was used to indicate expression of IL-33 and ST2 in the CNS at different stages of EAE disease. IL-33 remained unchanged throughout the time course of disease. However, ST2 expression was upregulated during cellular infiltration. Within naïve and EAE mice IL-33 and ST2 were both expressed on astrocytes and neurons. In acute and chronic MS tissues IL-33 was highly expressed by neurons and axons. Within the lesions IL-33 was present on damaged axons as well as microglia and ODCs. ST2 displayed a diffuse staining in control and MS tissues, however within the lesion site of acute and chronic MS samples ST2 surrounded damaged axons and was present on several ODCs. The potential for IL-33 to affect myelination was investigated using an in-vitro culture system. IL-33 significantly reduced myelination within rat cultures, however no significant effect was observed within the mouse culture system. The main findings from EAE tissues were corroborated in human MS tissue and the implications this may have on understanding the disease course of MS are discussed.

Table of Contents

Table of Figures

Abbreviations

AD	Alzheimer's Disease
ALS	Amyotrophic lateral sclerosis
APC	antigen presenting cell
ATP	adenosine triphosphate
BBB	blood brain barrier
BSA	bovine serum albumin
cDNA	complimentary deoxyribonucleic acid
CFA	complete freuds adjuvant
CIA	collagen induced arthritis
CNS	central nervous system
CO_2	carbon dioxide
CSF	cerebrospinal fluid
CVO	Circumventricular Organs
DAB	diaminobenzidine
DAPI	4'-6-diamidino-2-phenylindole
DC	dendritic cell
dH_2O	distilled water
DIV	days in vitro
DM^+	differentiation media plus insulin
DM^-	differentiation media without insulin
DMEM	Dulbecco's Modified Eagle Medium
E	embryonic day
EAE	experimental autoimmune encephalomyelitis
EBV	epstein barr virus
EC	endothelial cells
EGF	epidermal growth factor
ELISA	enzyme-linked immunosorbent assay
E2	estrogen
FBS	Foetal bovine serum
FGF	fibroblast growth factor
GalC	galactocerebroside
GFAP	glial fibrillary acidic protein
H & E	Haematoxylin and eosin
HBSS	Hank's balanced saline solution
HMGB1	high-mobility group box 1
HRP	horse radish peroxidase
IBD	Irritable Bowel Disease
IFN	interferon
ICAM	intracellular adhesion molecule-1
Ig	immunoglobulin
IL-	Interleukin
KO	knock-out
LINGO-1	leucine rich repeat and Ig domain-containing 1
mAb	monoclonal antibody

MAG	myelin Associated Glycoprotein
MAPK	mitogen-activated protein kinase
MBP	myelin basic protein
MCP	monocyte chemoattractant protein-1
MHC	major histocompatibility complex
MRI	magnetic resonance imaging
MOG	myelin oligodendrocyte protein
mRNA	messenger ribonucleic acid
MS	multiple sclerosis
NeuN	neuronal nuclei
NRG	neuregulin-1
NVU	neurovascular unit
OPCs	oligodendrocyte progenitor cells
ODCs	oligodendrocyte progenitor cells
pAb	polyclonal antibody
PBS	phosphate buffered saline
PCA	passive cutaneous anaphylaxis
PCR	polymerase chain reaction
PDGFα	platelet derived growth factor alpha
PFA	paraformaldehyde
PI	post immunisation
PLL	poly-L-lysine
PLP	proteolipid protein
PM	plating media
PNS	peripheral nervous system
PPMS	primary progressive MS
PSA-NCAM	polysialylated neural cell adhesion molecule
PTX	pertussis toxin X
RN	reactive nitrogen species
RO	reactive oxygen species
Rpm	revolutions per minute
RRMS	relapsing remitting MS
RT	room temperature
SC	spinal cord
SD	standard deviation
SD	Sprague Dawley
S.E.M	standard error of the mean
SIGIRR	single immunoglobulin IL-1R- related molecule
SPMS	Spontaneous Progressive MS
TCR	T cell receptor
TGF	tumour growth factor
TLR	toll Like Receptor
TMEV	Theiler’s murine encephalomyelitis virus
TNF	tumour Necrosis Factor
UC	ulcerative colitis
VCAM	vascular cell adhesion molecule 1
WM	white Matter

WT	wild-Type

1. Introduction

1.1 The Central Nervous System

The mammalian central nervous system (CNS) contains an astounding 100 billion neurons (Faingold 2004). Each individual neurons converses with thousands of other neurons within the CNS, forming the most complex communication and information transfer system in existence. The CNS consists of the spinal cord and brain (cerebral hemispheres, midbrain, cerebellum, diencephalon, pons and medulla oblongata). The brain is perceived as the 'control center' and directs functions such as information processing, perception, motor control, arousal, homeostasis, motivation, memory and learning. The main cell types localized to the CNS are neurons, oligodendrocytes, astrocytes and microglia (see table 1.1 for cells and functions) which are separated from the periphery nervous system (PNS) by the blood brain barrier (BBB) made from endothelial cells, astrocytes and pericytes.

The Neuron

The main component of the CNS is an electrically excitable cell known as the neuron. This term was first coined by Vilhelm von Waldeyer in 1891, stemming from the Greek word for "sinew". Each neuron is comprised of a cell body which projects branched processes termed dendrites, and a long slender projection called an axon. The cell body contains the nucleus of the neuron and is therefore involved in protein synthesis and metabolic processes. Dendrites contain organelles such as Nissle bodies and mitochondria. They also receive neuronal signals from neighboring neurons

via synapses (Li et al. 2004; Uno & Else 1989) and represent the only structural unit within the CNS that conducts nerve impulses (Fodstad 2002).

There are two types of neuronal cells: myelinated and non-myelinated. The myelin sheath that surrounds the axons of myelinated neurons enables the rapid propagation of nerve impulses crucial to neuronal function. During myelination, regular intervals (or gaps), are created between the myelin sheaths, which are called the 'Nodes of Ranvier' (Caldwell et al. 2000). These gaps contain sodium/potassium (Na^+/K^+) ATPases, sodium/calcium (Na^+/Ca^{2+}) exchanges and voltage gated Na^+ channels that generate action potentials along the axons (Caldwell et al. 2000; Craner et al. 2004; Greene et al. 1988). The myelin sheath increases the membrane resistance and enhances axonal depolarisation between action potentials. Interestingly, the Nodes 'regenerate' the action potential as it moves along the axons via Na^+ voltage channels. As previously mentioned, the main function of myelin is to insulate the axons and allow for the clustering of Na^+ channels at the Nodes of Ranvier (Caldwell et al. 2000). This is achieved through the high lipid content of the myelin components, which contribute to the construction of myelin. Myelin consists of glycolipid (mainly galactocerebroside, GalC) and its sulphated analogue sulfatide, cholesterol and phospholipid (Coetzee et al. 1996; Swapna et al. 2006). The Nodes of Ranvier allow the action potential to 'jump' from one node to the next creating a rapid propagation of an impulse. Therefore, both myelin sheaths and the Nodes of Ranvier are required to create fast and efficient nerve impulse propagation (Huxley & Stampfli 1948) (Figure1.1).

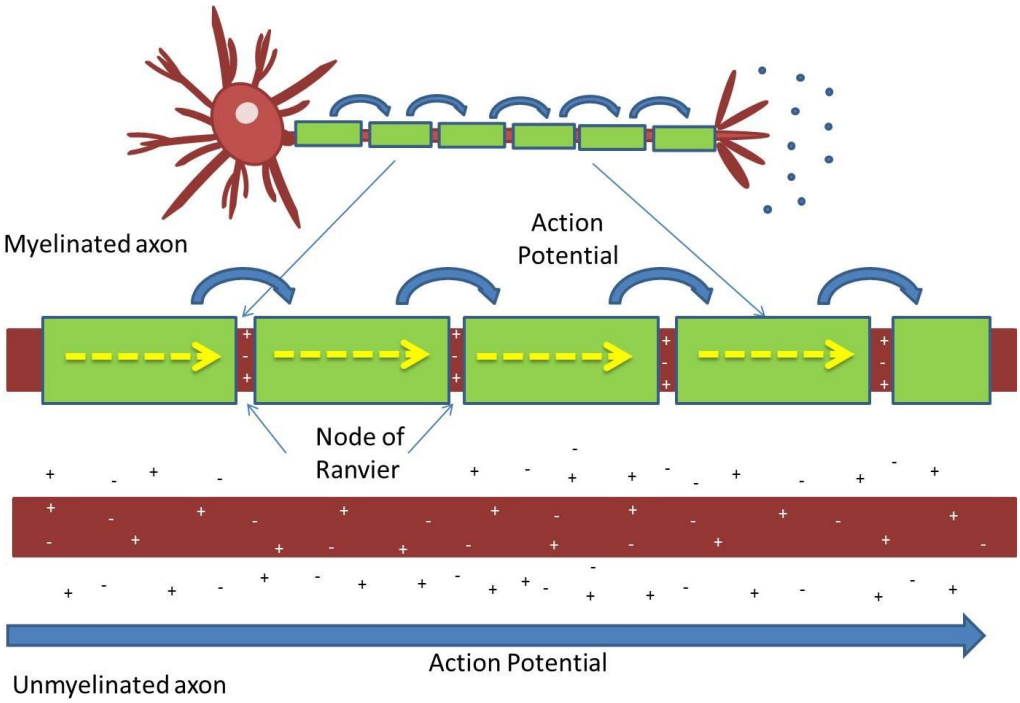

Figure 1.1 Myelination aids action potentials. In a myelinated axon, the current is forced down the nerve until it reaches ion channels at the Nodes of Ranvier (sections of unmyelinated axon) which propagate the action potential to the next node (salutatory conduction). Myelin prevents the action potential from dissipating across the membrane (unmyelinated axon).

Glia cells

Neuroglia (or glia), are cells that surround neurons in the CNS. Depending on the region of the brain, glial cells can outnumber neurons by up to 10-15 times. These cells support the various neuronal components, allowing them to fulfill their functions effectively. Glial cells are involved in: guiding neuronal precursors to their destination during development; supporting myelination; and ensuring a stable CNS by surveying the surrounding environment and maintaining homeostasis. Glial cells were originally thought to solely have a supportive role within the CNS; however, recent evidence suggests that these cells have been underestimated in terms of function, as they perform intricate and essential roles within the CNS (Hilgetag & Barbas 2009).

Glia cells can be divided into microglia and macroglia cells. Astrocytes are the most abundant type of macroglia cell in the nervous systems. Other cell types include oligodendrocytes and Schwann cells, both of which generate myelin; provide support and insulation to the axons in CNS and peripheral nervous system (PNS) respectively.

Oligodendrocytes

In early life oligodendrocyte progenitor cells (OPCs) eventually become myelin producing oligodendrocytes (ODCs) which are distributed throughout the CNS within the white and grey matter (Miller 1996). OPC migration is directed by regulatory signals including growth factors such as platelet derived growth factor (PDGF) (Spassky et al. 2001), fibroblast growth factor (FGF), hepatocyte growth factor (Ohya et al. 2007; Yan & Rivkees 2002) and chemotropic molecules (Jarjour et al. 2003). Major myelin component formation begins when the OPC enters the terminal differentiation stages and switches to a pre-myelinating ODCs. Other studies have also shown that the electrical activity produced from axons can control the proliferation of ODCs (Barres et al. 1993).

Myelination by ODCs is enhanced by the down-regulation of polysialylated neural cell adhesion molecule (PSA-NCAM) (Charles et al. 2000) and leucine rich repeat and Ig domain-containing 1 (LINGO-1) (Mi et al., 2005). LINGO-1 is a transmembrane protein expressed by neurons and ODCs during their early development. LINGO-1 knock-out (KO) mice showed higher numbers of mature ODCs and myelinated axons than wild type (WT) littermates (Mi et al. 2005). Other reports suggest that the lack of inhibitory signals such as γ-secretase (Watkins et al. 2009) and CXCR2 (Kerstetter et al. 2009) promotes myelination, whereas Notch 1 signaling inhibits ODC differentiation. In culture, inhibition of γ-secretase (a Notch 1 protease) by DAPT (*N*-[(3,5-Difluorophenyl)acetyl]-L-alanyl-2-phenyl]glycine-1,1-dimethylethylester) increased the number of MBP^{+}ODCs and myelinated axons (Watkins et al. 2009). CXCR2 was thought to help promote the proliferation of OPCs (with the help of PDGF) as it is the potential receptor for CXCL1 involved in ODC proliferation (Nguyen & Stangel 2001). However, blocking CXCR2 enhances remyelination and potentiates recovery in a lysophosphatidylcholine-induced demyelination model as well as the classical MOG_{35-55} induced Experimental Autoimmune Encephalomyelitis (EAE) (Kerstetter et al. 2009). Although various inhibitors of myelination have been reported, there has been less success in identifying a molecule which enhances myelination within the CNS. In contrast, Schwann cells in the PNS were shown to respond to neuregulin-1 (NRG, an EGF-like growth factor) and promote myelination (Brinkmann et al. 2008). However, *in vitro* studies have shown that this cannot be applied to the CNS, implying that ODCs in the CNS utilise a different signaling pathway to regulate myelination than that adopted by Schwann cells within the periphery (Brinkmann et al. 2008).

ODCs support myelin up to 100 times their weight (McTigue & Tripathi 2008) but their energy consumption means they are very susceptible to pathology. The complex differentiation process and the unique metabolism of ODCs are often vulnerable under pathological conditions. ODCs consume large quantities of oxygen and adenosine triphosphate (ATP) which results in toxic

by-product production (hydrogen peroxide, H_2O_2). Such a by-product needs to be metabolised effectively; otherwise it can cause CNS degradation and ODC apoptosis (Mouzannar et al. 2001). Myelin synthetic enzymes (HMG-CoA reductase, succinic dehydrogenase, NADH dehydrogenase, dioxygenase and glucose-6-phosphate dehydrogenase (Todorich et al. 2009)require iron as a co-factor (JR & SL 1996). This in turn causes the production of free radicals and lipid peroxidases (Braughlers et al. 1986) which can directly damage intracellular compartments of ODCs. In addition, ODCs have low concentrations of glutathione (anti-oxidant enzyme) making them even more susceptible to damage due to build-up of oxidants (SK & BH 1996). Other factors such as proinflammatory cytokines are also able to induce ODC loss directly. For example, the cytokine TNF-α binds to its receptor, expressed by the ODCs, resulting in ODC apoptosis via p55-TNF binding (Jurewicz et al. 2005). Damage induced by IFN-γ is more complex, as it only affects the proliferating ODCs yet has very little effect on the immature ODCs and no effect on mature ODCs (Horiuchi et al. 2006). Indirectly, ODCs can be damaged due to the effect of inflammatory mediators on microglia and astrocytes, which produce reactive oxygen (RO) and nitrogen (RN) species, thereby impairing mitochondria function of ODCs (Stewart et al. 2000).

Astrocytes

Astrocytes (‘star shaped’ cells) (Schnitzer & Karschin 1986) generally fall into two main subtypes, fibrous and protoplasmic. Fibrous astrocytes have long fibre-like projections and are found in the white matter. In contrast, protoplasmic astrocytes are found in the grey matter and have stems from which smaller branches arise in a globoid fashion. Both types of astrocyte have widespread contact with blood vessels. Although both subsets form junctions between distal processes of nearby astrocytes, the projections arising from protoplasmic astrocytes encase synapses, whereas fibrous

astrocytes are associated with the Nodes of Ranvier (Ffrench-Constant & Miller 1986). Other astrocyte-like glial cells include Muller's cells within the retina, pinealocytes in the pineal gland and pituicytes in the pituitary gland. These cell types contain various astrocyte-related molecules such as glial fibrillary acidic protein (GFAP) and exert similar functions (Jessen & Mirsky 1983).

Astrocytes organise themselves within specific domains in CNS, these domains rarely overlap (Bushong et al. 2002) and can encompass approximately four neurons, hundreds of dendrites and interact with hundreds of thousands of synapses (Halassa et al. 2007). Astrocytes have a role in the migration of developing axons during development (Powell & Geller 1999), and in the formation of synapses (Krzisch et al. 2014). Astrocytes are also involved in synaptic pruning via the release of complement, molecule Clq, marking the synapse for destruction by microglia (Stevens et al. 2007).

Astrocytes also regulate ions (Li et al. 1998) and fluids in CNS (Papadopoulos et al. 2004) which are essential for maintaining the tissue homeostasis. They display regular increases in intracellular calcium, which is important in their interaction with other astrocytes and neurons. A further function of astrocytes is their involvement in CNS metabolism as they take up glucose from the blood vessels and distribute the energy metabolites (Pellerin & Magistretti 1994). Furthermore, astrocytes store massive quantities of glycogen which can sustain neuronal activity during high demand and hypoglycaemia (Suh et al. 2007). In addition to their role in the CNS, astrocytes also control local blood flow within the CNS via the regulation of blood vessel diameter (Mulligan & Macvicar 2004). Astrocytes achieve this through the release of mediators such as prostaglandins (Dabertrand et al. 2013) nitric oxide (NO) and arachidonic acid (Chen & Chen 1998).

Astrocytes respond to CNS injury such as inflammation or demyelination by a process called astrogliosis which can often lead to scar formation. Mild or moderate astrogliosis is associated with non-penetrating trauma and mild infection (Bushong et al. 2002). However, severe astrogliosis is associated with CNS focal lesions and severe infections. This arises in response to neuroinflammation in diseases such as multiple sclerosis (MS). During astrogliosis astrocytes change their morphology and molecular expression of proteins. During mild or moderate astrogliosis, there is very little tissue remodeling and astrocytes often return to an appearance similar to that in healthy tissue once the damage has been resolved (Bushong et al. 2002). In contrast, during severe diffuse astrogliosis, there is a significant increase in GFAP expression, cellular hypertrophy, extension of processes, and extensive proliferation of astrocytes (Sofroniew 2010). The non-overlapping, even distribution of astrocytes in the healthy CNS (Bushong et al. 2002) is also replaced by reactive proliferating astrocytes which then overlap with other astrocyte projections in close proximity (Wilhelmsson et al. 2006). This overlapping is usually widespread over areas which are in close proximity to focal lesions. However, astrogliosis is also beneficial to CNS as it localises the severe tissue damage to a contained area and prevents the spread of inflammation beyond the dense barrier, which surrounds the glial scar.

It is predicted that mediators of astrogliosis could be produced by a variety of CNS cells such as neurons, microglia, ODCs or pericytes. Such regulators include cytokines (IL-6, LIF , CNTF, TNF-α, INF-γ, IL-1 and IL-10); lipopolysaccharide (LPS) and other TLR ligands; glutamate and noradrenalin (neurotransmitters); ATP; ROS; hypoxia; glucose deficiency; β-amyloid; NH_4^+ and cell proliferation regulators such as endothelin-1 (Acosta et al. 2006; Akaoka et al. 2001; Andreiuolo et al. 2009; Araque et al. 1999).

Microglia

Microglia make up between 5-20% of the total glial population, depending on the CNS localisation. Microglia can either be resting in healthy CNS tissues or become activated or reactive microglia producing cytotoxic molecules under disease conditions (Colton & Gilbert 1987). Microglia can also become phagocytic (macrophages) in certain circumstances (Marin-Padilla 2011), for example they can engulf invading micro-organisms and debris.

Microglia are often activated before any other glial cells in CNS injury, as they are extremely sensitive to even slight changes in their microenvironment, such as differences in ion homeostasis (Nimmerjahn et al. 2005). Activated microglia cells can either be classically activated M1 or alternatively activated M2 microglia cells. M1 microglial cells are usually associated with a reaction against viral and bacteria that are activated by the TLR ligand, LPS and IFN-γ, TNFα and cell surface markers CD86 and CD68. In comparison, M2 microglia are usually activated by IL-13 and IL-4 and express arginase 1, Ym1, CD206 and IL-10associated with parasite infection, tissue repair and may have neuroprotective effects (Kobayashi et al. 2013).

Table 1.1 CNS Resident cells and functions.

Cells	Function
Neuron	1. Sends and receives nerve impulses. 2. Myelinated axons contain Nodes of Ranvier. 3. Nodes of Ranvier contain ion channels which aid the propagation of nerve impulses.
ODC	1. Produces myelin which insulates the axon. 2. Myelin enables the rapid propagation of nerve impulses.
Astrocyte	1. Involved in the early migration of axons. 2. Helps the formation of synapses and is involved in synaptic pruning. 3. Takes up glucose and distributes energy metabolites. 4. Regulates pH and blood flow. 5. Form scars during astrogliosis.
Microglia	1. Early defence against pathogens. 2. Monitors the environment for any changes in e.g. pH or ions. 3. Phagocytose antigens and scavenge cell debris. 4. M1 microglial cells are involved in viral and bacterial pathogens. 5. M2 microglial cells are usually associated with parasite infections and tissue repair.

The Blood Brain Barrier (BBB)

The BBB exists as a barrier between the blood and the brain parenchyma to provide the first line of defense against infiltration by micro-organisms and auto-reactive immune cells (Abbott et al. 2006; Abbott et al. 2010). There is a network of cells and molecules involved in maintaining the integrity of the BBB including endothelial cells (EC), pericytes, astrocytes, neurons and extracellular matrix proteins which collectively form the neurovascular unit (NVU) (Abbott et al. 2006). ECs form exceptionally tight junctions and have a very low incidence of pinocytosis. Tight junctions are an essential requirement for BBB function. They not only form a barrier (by transmembrane and cytoplasmic proteins linked to an action-based cytoskeleton) to prevent cells and substances from entering the CNS but also may help to maintain the cell polarity of endothelial cells, via Polarity protein 3 (PAR-3), which is essential for the function of epithelial cells within the BBB (Izumi et al. 1998). Adhesion proteins, such as Claudin 3 and 5, are transmembrane proteins and also play a role in controlling BBB permeability via tight junctions (Pfeiffer et al. 2011). However various transport mechanisms are in place on the ECs within the BBB to facilitate the passage of polar nutrients. For examples the GLUT-1 and Na^+K^+ ATPase transporters in ECs allow the passage of molecules such as glucose and ions, as well as the release of toxic by-products and macromolecules from the CNS (Devraj et al. 2013). ECs rely on the cross-talk between resident cells and the extracellular matrix in order to maintain diffusion properly (Bernanke et al. 2008). Pericytes are cells which embed themselves within the basement membrane of the ECs. A lack of pericytes can result in an increase in pinocytosis and permeability, thus resulting in a ‘leaky’ BBB (Amulet et al. 2010).

Astrocyte end-feet are also involved in the structure of the BBB; they wrap themselves around ECs and the microvessel walls. The astrocyte end-feet highly express orthogonal array particles containing the water channel

aquaporin 4, as well as the K^+ channel Kir4.1, thus allowing for volume and ion regulation (Abbott et al. 2006; Abbott 2002). Wnts are a family of extracellular matrix glycoproteins, which regulate intracellular signaling via cell surface receptors (Frizzled and low-density-lipoprotein like receptors). In essence, Wnt signaling prevents the phosphorylation of β-catenin, allowing the translocation of β-catenin to the nucleus and regulation of cell transcription (MacDonald et al. 2009). Wnts signaling has been shown to be increasingly important in the development and maintenance of the BBB (Liebner et al. 2008) and potentially in the communication between cells of the NVU.

During CNS inflammation, the breakdown of the BBB has been correlated with clinical disease and lesion formation in both rodent and human tissues (Bennett et al. 2010). It has been shown that there is a relationship between tight junction pathology (shown by ZO-1 disorganisation) with focal lesions in the white matter in EAE induced mice. While tight junctions in regions of the CNS not associated with inflammation remained intact. The tight junction pathology has been shown to precede clinical signs of EAE and is correlated with clinical signs of EAE (Bennett et al. 2010).

1.2 Multiple Sclerosis (MS)

Immune cells are important components of a healthy immune system. The development and maturation of T and B lymphocytes in the central lymphoid organs, thymus and bone marrow, are strictly regulated to ensure cells respond to exogenous pathogens, but not self-antigens, via positive and negative selection processes. When, self-antigen-recognising, lymphocytes do escape to the periphery, peripheral tolerance (occurring in secondary lymphoid organs) comes into play and renders these autoreactive immune

cells inactive or anergic (Janeway & Walport 2001).

Paul Enrich first suggested that the immune system could endanger itself by producing self-reactive autoantibodies. Noel Rose further demonstrated that by injecting rabbits with thyroglobulin resulted in lesions similar to that seen in Hashimoto's Thyroiditis. Later, Enrich described this as 'horror autotoxicus', which was subsequently known as autoimmune disease (Steinman & Nussenzweig 2002). Autoimmune disease develops through the breakdown of central and peripheral tolerance. The failure of these mechanisms results in T cells, which are able to bind to self-peptides with high affinity, being present in the circulation. These cells mount an immune attack against specific tissue proteins. These immune responses then result in tissue damages and develop diseases such as rheumatoid arthritis, Crohn's disease and MS (Steinman & Nussenzweig 2002).

MS is an organ-specific autoimmune disease as the immune system mounts an attack on the CNS i.e. the spinal cord and brain myelin tissues, resulting in the damage of myelin sheaths (demyelination), axons and neurons (neurodegeneration). MS affects 2.5 million people worldwide, and is most prevalent in young adults, between 20-40 years of age. However, MS is a disease of all ages, as there are many cases of pediatric MS (McLaughlin et al. 2009).

MS symptoms and subtypes

MS is a chronic demyelinating disease of the CNS and is the leading cause of neuronal disability in the developed countries (Hemmer et al. 2006). There are four clinical forms of MS; relapsing-remitting (RRMS), secondary progressive (SPMS), primary progressive (PPMS) and progressive-relapsing (PRMS) (Comabella & Khoury 2012). Most MS patients suffer from RRMS, which as the name implies, involves remission (approximately 6-8 weeks)

after a relapse. SPMS can be found in patients who, previously were diagnosed with RRMS and involves a progressive decline with fewer remissions. PPMS occurs in approximately 10-15% of patients and involves a continual deterioration and reduced life expectancy (Cottrell et al. 1999). Finally PRMS is where MS patients get continually worse with occasional relapses. The most common symptoms of MS include paralysis, fatigue, weakness, bladder and bowel incontinence, spasticity pain, sensory disturbances, loss of balance and coordination and visual disturbances (Kenealy et al. 2003; Palmer 2013). As the name implies (sclerae, meaning scars/lesion) lesions in the brain and spinal cord is typical of MS. MS is characterised by the presence of demyelination, multifocal inflammation, reactive gliosis and ODC/ axonal loss (Comabella & Khoury 2012). Repeated demyelination results in scar tissue around the demyelinated and damaged axon. MS lesions in CNS are visualised using gadolinium and MRI imaging and are directly correlated with disease severity (Wolinsky 1999).

Lucchinetti and colleagues (Lucchinetti et al. 2000) described the four patterns of MS lesions. Patterns I and II are very similar, the active lesions are associated with T cell and macrophage inflammation. However pattern II also has immunoglobulins (Igs) and complement C9neo deposition. Both lesion types are normally found around veins and venules with a defined border and perivenous extensions. Furthermore, a high number of ODCs are present in the inactive plaques. Within pattern III lesions there is no Ig deposition but they do contain T cells, macrophages and activated microglia. These lesions are mainly associated with inflamed vessels within the demyelinated plaque. Pattern III lesions, unlike I and II, show diffuse spreading into the surrounding white matter, due to the lack of a defined border. Furthermore, these lesions only involve the loss of myelin-associated glycoprotein (MAG) but not the other myelin markers (such as MBP/MOG) and within the inactive plaque few ODCs are present. Finally, pattern IV reveals T cells and macrophages but not Ig or complement deposition. The

lesion has defined edges and complete loss of ODCs in active and inactive areas, with no sign of remyelination (Lucchinetti et al. 2000b).

MS etiology

The exact cause of MS disease is currently unclear, however scientific evidence has suggested that MS occurs as a result of a combination of genetic, environmental and infectious factors. The increase of disease prevalence (2-5 %) in first degree relatives of MS patients, which rises to 20-35% increase in monozygotic twins, suggests that genetics have an important role to play in the development of MS. Studies of a well characterised MS data set suggest MS susceptibility is associated with the histocompatibility complex (HLA in humans), specifically HLA-DR and –DQ genes e.g. HLA-DR15. HLA-DR15 encompasses genes such as, cytotoxic T lymphocyte-associated antigen (CTLA-4) (Alizadeh et al. 2003), Interleukin 1 (IL-1) (Sospedra & Martin 2005) and the estrogen receptor (Hensiek et al. 2002). Studies have implied that polymorphism in genes for CCR2 (Miyagishi et al. 2003) may result in protection, whereas polymorphisms in genes such as IL-4 (Karakus et al. 2013), IL-2 (Cavanillas et al. 2010) and vitamin D (Niino et al. 2000) increase the risk of developing MS.

An additional trend in MS occurrence is that it is more prevalent in females than males. Some studies have depicted oestrogens as pathogenic, whereas androgens, such as testosterone, are thought of as protective(Kurth et al. 2014). Symptoms are found to be worse during menstruation and during pregnancy less relapses are observed. This is then linked with a post-natal disease rebound (Runmarker & Andersen 1995) suggesting a regulatory effect of pregnancy hormones on MS progression. Further studies using the Foxp3-DTR mouse strain have indicated that oestrogen (E_2) can protect EAE mice from the clinical and histological signs of EAE in a Treg- independent manner. E_2 treatment of Foxp3-DTR mice showed a decreased expression of

CCL2 but enhanced IL-10 and IL-13 secretion associated with protection possibly due to regulatory B cells (Subramanian et al. 2011). Treatment of MS patients with estriol, with levels approximate to those seen in women 6 months pregnant, showed reduced lesions in RRMS patients(Sicotte et al. 2002). Despite this, no clear link between the sex chromosomes and MS occurrence has been confirmed (Sospedra & Martin 2005a; Runmarker & Andersen 1995; Sicotte et al. 2002).

Apart from the genetic factors, environmental factors have also been implemented in the susceptibility/ exacerbations of MS. These factors include altitude, exposure to sunlight and viral infections.

Altitude may have its role to play in MS incidence. A study conducted in 1967 investigated MS incidence rate on genetically similar populations living at different altitudes, in Switzerland. The results showed, that in areas of low altitude there was high MS incidence, compared to areas of high altitude with low incidence of MS disease. One possible explanation for this difference is the increase of short wavelength ultraviolet radiation at high altitudes compared to low (Hayes 2000). This may also support the role of vitamin D in MS development. Sunlight is required for the synthesis of pre-cholecalciferol within the skin. Pre-cholecalciferol is the precursor for the hormone 1, 25-dihydroxycholecalciferol (1,25-$(OH)_2D_3$). It has been hypothesised that sunlight may utilise 1,25-$(OH)_2D_3$ to protect individuals from developing MS, as the areas with low vitamin D, due to low intensity solar radiation and a low vitamin D diet, demonstrate an increase in MS prevalence (Hayes 2000). Furthermore, experimental evidence from animal studies has confirmed that 1,25-$(OH)_2D_3$ inhibits disease progression (Nashold et al. 2000) and polymorphisms in vitamin D receptor (VDR) have been associated with MS susceptibility (Hayes 2000).

The prevalence of MS is also increased in areas further north or south of the equator. Scotland has one of the highest incidences of MS in the world.

Consistent with this geographical distribution, Asia and Africa, which predominantly lie on the equator, have low prevalence (http://www.mstrust.org.uk). Interestingly several studies have shown that people who move to a different area of the world before the age of 15 have a similar risk of MS disease as the local people in the new area. However, they retain the risk associated with the birthplace, if moving after age 15. This suggests that environmental factors also have a role in MS development (Sospedra & Martin 2005a).

Other environmental conditions, such as viral infection, are also contributing factors in the development of MS disease. Persistent viruses, such as herpes or retroviruses are most likely to be involved in the pathogenesis of MS. The majority of MS patients have been seen to have a high antibody titer to Epstein Barr virus (EBV) compared to age matched controls with low antibody titers for EBV (Levin et al. 2011). The presence of HHV-6 DNA and anti-HHV6 IgG and IgM antibodies in the serum and cerebrospinal fluid (CSF) of MS patients (Ramroodi et al. 2013) further suggests that infection may be involved in the pathology of MS leading to demyelination. Infectious agents may induce MS by molecular mimicry or bystander activation. Molecular mimicry can occur due to the cross-linking of potentially self-reactive T cells with a viral antigen initiating immune cells to cross the BBB and recognise CNS antigens e.g. MBP (Olson et al. 2001). Bystander activation of autoimmune T cells can also occur independently of the TCR via superantigens, cytokines or pattern recognition e.g. TLR 4, the receptor for LPS. The inflammatory damage resulting from infection causes injury to self-tissue and initiates the release of autoantigens (Nogai et al. 2005).

Research into the correlation between infection and MS incidence has further suggested that MS relapses often follow systemic infections such as virus infection, implying that viruses can trigger an MS relapse. This is supported by experimental evidence in MS disease models which showed that spontaneous CNS inflammation developed in mice housed in a non-sterile

environment, but not in mice housed in a sterile pathogen-free environment (Goverman et al. 1993).

1.3 EAE, an animal model for MS disease

As discussed previously, MS is a complex disease and its development is influenced by a variety of factors such as genetic background, environmental factors and viral infections (Sospedra & Martin 2005a). Furthermore, clinically there are four subtypes of the disease, which affect patients with different clinical symptoms and prognosis. However, research into understanding the complex immunomechanisms of MS disease has been restricted by the difficulties of obtaining CNS tissues from MS patients. An effective *in vivo* model is thus essential for the investigation of the immunopathogenesis of MS disease to better understand the disease and to develop drugs for patients. EAE is the most common animal model used to understand the immune mechanisms surrounding MS, such as the involvement of cytokines and chemokines in CNS inflammation, how encephalogenic cells enter the (once thought to be completely immune privileged) CNS, as well as the demyelination/ remyelination processes.

Toxic agents can be used to induce a CNS demyelination animal model (cuprizone model) to investigate the mechanisms of demyelination and remyelination; however there is no immune cell infiltration in this model as it mainly affects ODCs and thus is not an accurate model of MS (Wergeland et al. 2011). The Theiler's murine encephalomyelitis virus (TMEV) model is induced by Theiler's virus. The model is used to investigate the role of viral infections in CNS damage and mimics chronic progressive MS (Tsunoda & Fujinami 2010) as viruses can cause relapse in MS patients. The most widely used *in vivo* model of MS is the EAE model. EAE mimics inflammatory cells infiltrating the CNS and inflicts myelin-specific damage resulting in the

demyelination and degeneration of axons. These events result in clinical symptoms in animals such as limp tail, hind limb gait, hind limb paralysis and then forelimb paralysis after which the experiment is usually terminated. EAE was first stumbled upon in the 19th century during the development of a rabies vaccine (Kuerten & Angelov 2008). In 1949 Olitisky *et al* managed to induce EAE in mice as a model for researching demyelinating disease (Olitsky & Yager 1949). Since then, EAE has been induced in many species of animals such as rats (Weissert et al. 1998), guinea pigs (Tselios et al. 2000) and marmoset monkeys (Jagessar, Heijmans, Blezer, et al. 2012).

Several different myelin proteins have been identified to initiate EAE in rodents such as MBP, which encompasses 30-40% of the myelin sheath. Although some strains of mouse are highly susceptible to these proteins (B10.Pl and PL/J) revealing a monophasic EAE. Other common mouse stains including C57BL/6 are resistant to MBP immunisation. PLP is another common antigen used to induce EAE, it induces a chronic-relapsing EAE in SJL mice but again C57BL/6 mice are resistant to PLP. C57BL/6 mice are however, susceptible to MOG protein and its peptide MOG $_{35\text{-}55}$ initiating a monophasic disease. To induce EAE, myelin antigens such as MBP, PLP or MOG are injected subcutaneously after being emulsified with Complete Freud's adjuvant (CFA). CFA is a potent inflammatory agent which contains inactivated dried mycobacteria in mineral oil. CFA enhances the maturation of antigen presenting dendritic cells (DCs) and stimulates a Th1/Th17-like response (Kai et al. 2006; Billiau & Matthys 2001). The exotoxin produced from *Bordtella pertussis,* pertussis toxin (PTX), is injected intraperitoneally along with MOG and CFA and contributes to BBB permeability, cell infiltration and further promotes an inflammatory response (Falnes & Sandvig 2000). Furthermore, if EAE is initiated in C57BL/6 mice with MOG and CFA, in the absence of PTX, a peripheral pathogenic T cell response is initiated but no histological or clinical EAE is observed (Hofstetter et al. 2003) further confirming the importance of PTX in the pathogenesis of EAE.

Different animal models and different types of EAE models have been useful in research to understand the different clinical courses of MS (Kuerten & Angelov 2008). Spontaneous EAE models in genetically modified mice are also available (Pöllinger et al. 2009) for example, MOG-specific TCR transgenic SJL/J mice can spontaneously develop relapsing-remitting EAE. These mice develop classical signs of EAE such as tail and hind limb paralysis with worsening disease (Pöllinger et al. 2009). EAE can also be induced passively by adoptive transfer of myelin specific T cells, collected from immunised mice, to naïve animals. The passively transferred T cells can be labelled to distinguish between the transferred myelin specific T cells and the host T cells. While the classical MOG-induced EAE has been shown to result in inflammation mainly restricted to the spinal cord, passive induction of EAE is useful as it also produces brain inflammation, which is also often observed in MS patients (Stromnes & Goverman 2006). It is important to take into account that experimental conditions such as the animal species, strain, sex, age, whether passive or active induction was used, timing, frequency and dosage of the molecules or agents being studied will affect the disease susceptibility and thus the results of the study.

EAE does however have its limitations, the most obvious one being the species differences between rodents and humans (Handel et al. 2011). Also MS is often seen as a spontaneous relapsing-remitting disease however most EAE models require the active immunisation of myelin antigens in CFA. Furthermore, these mouse models of MS usually use inbred mice, limiting the usefulness of this breed-specific data (Handel et al. 2011a). EAE is not influenced by complex factors such as genetics or environmental impacts, which is important in the spontaneity of MS, and thus should also be taken into consideration when utilising a mouse model, and this can lead to a limited understanding (Handel et al. 2011a). Despite this, EAE is invaluable to MS research and can provide useful information for us to understand the

underlying mechanisms of MS disease and develop new therapeutic strategies for patients (Farooqi et al. 2010). Indeed, some MS disease-modifying drugs have been developed for clinical use due to successful experiments using EAE models (Massacesi et al. 2005; Hartung et al. 2002).

1.4 Immunopathogenesis of MS and EAE

MS is a chronic immune-mediated demyelinating disease which inflicts varying degrees of disability depending on the subtype in question and damage inflicted (sensorimotor, cerebellar, visual, cognitive and neuropsychiatric) (Lim & Constantinescu 2010). Over the years, extensive research has been carried out both *in vitro* and *in vivo* in order to understand the complex events entailed in MS pathogenesis.

The inflammation associated with MS and EAE is usually a result of CNS antigens getting released into the periphery via the cervical lymph nodes where they are activated. These antigens are then presented to T cells within the periphery and initiate the activation and expansion of inflammatory cells (Wucherpfennig & Strominger 1995; Furtado et al. 2008). Recent research evidence suggests that Th1 and Th17 cells are the main contributors to the development of MS and EAE. However the importance of $CD8^+$ T cells, B cells and innate immune cells, such as macrophages and neutrophils, should not be overlooked (Piccio et al. 2002; Nowak et al. 2009; Sayed et al. 2010). The activated immune cells migrate towards the BBB where they bind to adhesion molecules before crossing BBB and enter into CNS (Furtado et al. 2008; Piccio et al. 2002). After entering CNS, the T cells are restimulated by local and infiltrating APCs (microglia/astrocytes/B cells/DCs) (Steinman 1999). These activated inflammatory T cells then initiate damage of myelin and ODC lysis by secreting immune molecules such as IFN-γ and IL-17 and by the activation of resident CNS cells to release cytotoxic molecules (ROS and RNS) (Lorenz et al. 2003). All of these processes lead to demyelination and damage of the axons, the hallmark of EAE and MS. Interestingly partial

or full remyelination, mainly mediated by ODCs entering the demyelinated area, occurs simultaneously as demyelination is ongoing and involves many of the same cells and molecules (Rodriguez 2007). Thus understanding the exact functions of immune cells and molecules in the inflammation leading to MS/EAE and the subsequent demyelination and remyelination processes are essential to develop new therapeutic strategies for patients.

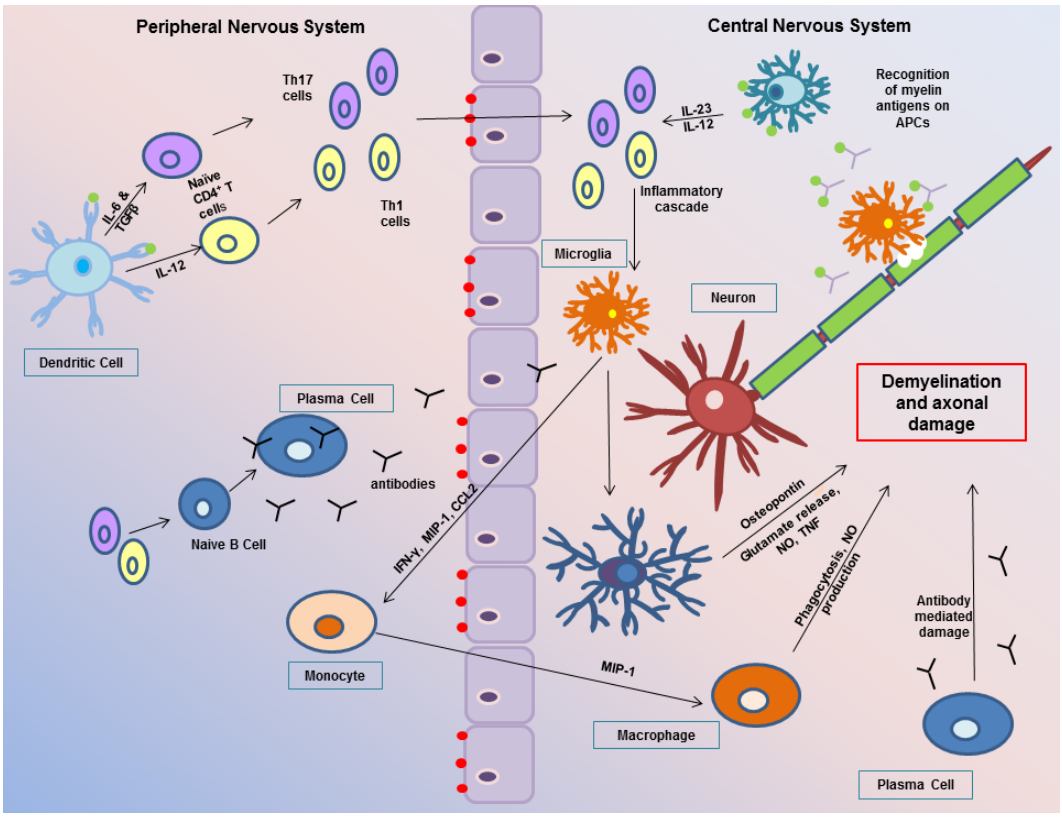

Figure 1.2 Immunopathogenesis of MS and EAE. Naïve T cells are primed within the periphery by APCs, such as DCs and differentiate to IL-6 and TGF-β secreting or IL-12 producing Th17 and Th1 cells respectively. These T cells cross the BBB via adhesion molecules and enter CNS where they are re-stimulated with myelin antigens presented by the local APCs such as microglia. This then initiates an inflammatory cascade involving the secretion of cytokines and molecules involved in myelin and axonal damage. Activated microglia are also able to produce inflammatory factors to attract more inflammatory cells and enhance the pathogenesis. Plasma cells produce antibodies, which cross the BBB and aid in the demyelination (Adapted from Constantinescu *et al*. 2011).

CNS inflammation

Peripheral activation of CNS antigen specific T cells are often activated by unknown mechanisms in the periphery, which results in the activation of CNS glial cells and the upregulation of MHC and adhesion molecules (Frank et al. 2006; Wucherpfennig & Strominger 1995; McMahon et al. 2005). In order for the encephalogenic T cells to inflict the necessary neuroinflammation seen in EAE they must first cross the BBB. T cells not specific for myelin antigens can enter the CNS but only T cells specific for CNS antigens are able to persist within the CNS and initiate the recruitment of other inflammatory cells such as macrophages, neutrophils, mast cells and $CD8^+$ T cells through secretion of IL-9, TNF and GMCSF (Nowak et al. 2009; Sayed et al. 2010; Ousman & David 2001).

T cell extravasation from the blood onto the BBB involves strong adhesive forces between cells and the microvessels allowing for the T cells to pass into the parenchyma via T cell tethering, rolling and capture (Nandi et al. 2004). The rolling and capture of T cells on an intact BBB involves α-integrins and vascular CAM (VCAM). In non-inflammatory conditions, adhesion molecules such as intracellular CAM (ICAM) and VCAM are expressed constituently on the endothelium and are subsequently up-regulated during the course of EAE. The migration of T cells into the CNS involves an activated endothelium and the attachment of T cells to the endothelium via these cell adhesion molecules (Elices et al. 1990). Previously, it has been shown that antibodies produced against the $\alpha_1\beta_1$-integrins prevent the development of EAE and this was the main mechanisms of MS drug natalizumab. In recent studies, it was elucidated that $\alpha_1\beta_1$-integrins are important in the passage of $\alpha_1\beta_1$ T cells, but not $\alpha_1\beta_1$ antigen presenting cells (APCs), granulocytes or macrophages, into the CNS, via deletion of the β_1 and initiating disease. In these experiments $\alpha_1\beta_1$ T cells failed to accumulate in the CNS due to poor adhesion to brain endothelial cells (Bauer et al.

2009). In order to withstand the force of blood flow along the microvessel, T cells need to enhance the strength of the interactions they have with integrins and VCAMs by endothelial-T cell signaling through G protein independent interactions (Grabovsky et al. 2000; Vajkoczy et al. 2001). Once within the CNS, resident APCs (microglia and astrocytes) and infiltrating APCs (e.g. DCs), which present myelin proteins, will reactivate these T cells locally and initiate a cascade of events including chemokine secretion and recruitment of macrophages and additional T cells into the CNS (Stromnes & Goverman 2006a).

There are different subsets of CD4 T cells including Th1, Th2, Th17, Th9 and T regulatory cells (Figure 1.2). Th1 cells produce proinflammatory cytokines such as IL-2, IFN-γ and TNF-α which are often involved in inflammation, cell mediated immunity and autoimmunity. The transcription factors involved in Th1 cell differentiation and function include T-bet, STAT1, STAT4 and C-Rel (Bettelli et al. 2004). Th2 cells are associated with antibody-mediated responses, extracellular parasites and conditions associated with allergies such as asthma (Mosmann & Sad 1996). GATA3, JunB, STAT6 and c-maf are all required for Th2 differentiation and are associated with IL-4, IL-5 and IL-13 cytokine production (Bettelli et al. 2004). Interestingly, Th1 and Th2 cells are mutually inhibitory as IFN-γ inhibits Th2 cell differentiation and function and vice versa with IL-4 on Th1 cells (Mosmann & Sad 1996; Damsker et al. 2010). Th17 cells are a separate $CD4^+$ subset of T cells which produce IL-17A, IL-17F, IL-21 and IL-9, and are involved in autoimmunity, similarly to Th1 cells (Langrish et al. 2005). Furthermore, T bet is not only associated with Th1 cell differentiation but it also regulates the IL-23R transcription, thus affecting Th17 cells as they rely on IL-23 for their development and survival (Gocke et al. 2007). Th9 cells are another distinct subpopulation of $CD4^+$ T cells. They are ascribed the name due to the production of IL-9. Th9 cells are induced by TGF-β and IL-4 and are mainly associated with allergic disease involving mast cell responses (Staudt et al. 2010). There are several subpopulations of T regulatory cells (Tr1, Treg, Th3

etc.), T reg cells utilise FOXP3 and produce TGF-β and IL-10 which have been implicated in the regulatory role of Tregs (Joetham et al. 2007). Patients lacking FOXP3 develop excessive autoimmune disease (Yagi et al. 2004). $CD4^{+}CD25^{+}$Treg cells selected within the thymus are called natural Treg (nTreg) cells while peripherally generated cells are called induced Treg (iTreg) cells (Chen et al. 2003).

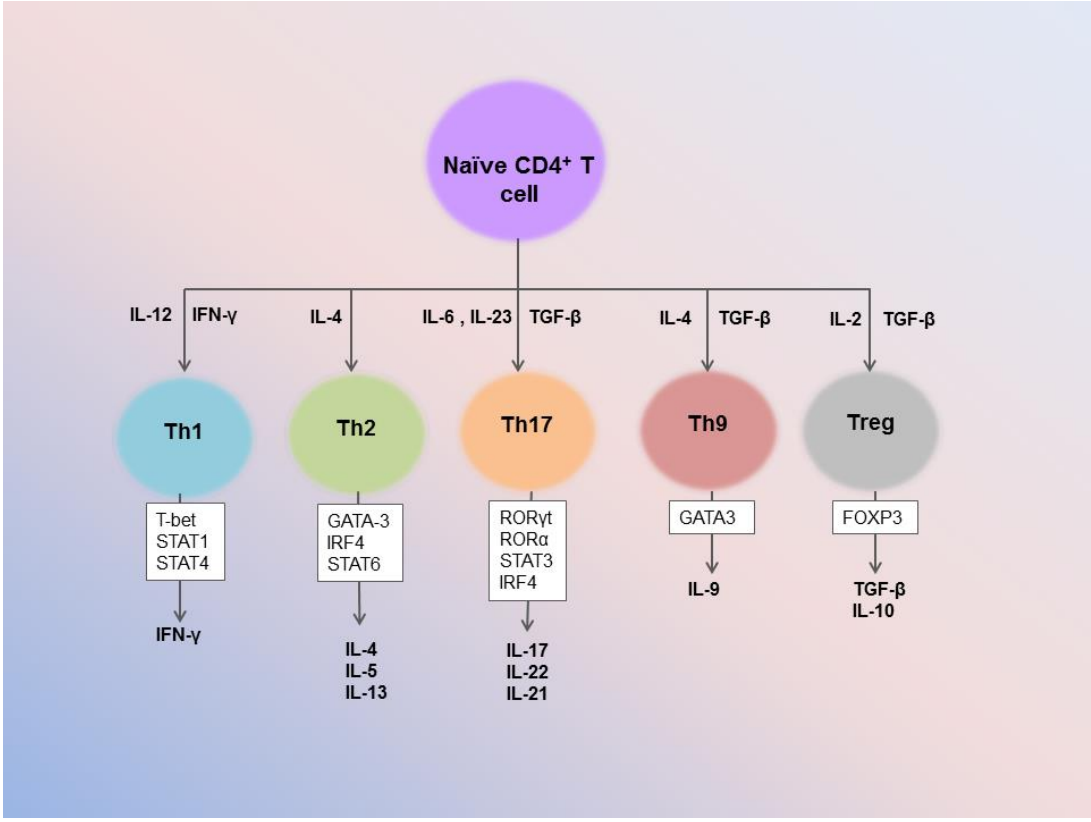

Figure 1.3 CD4+ T cell subtype differentiation. The main subtypes of $CD4^{+}$T cells are Th1, Th2, Th17, Th9 and Treg cells. The cytokine environment and the transcription factors utilized affect T cell subset differentiation. Naïve T cells (Th0) can become Th1 cells under the influence of IL-12 and IFN-γ, utilizing T-bet, STAT1 and STAT4 transcription factors. Th1 cells are usually associated with a pro-inflammatory environment. Th2 cells, known for their involvement in allergy, are produced in an IL-4-rich environment. Th2 cells use GATA3, IRF4 and STAT6 and produce cytokines such as IL-4, IL-5 and IL-13. Th17 cell functions are similar to Th1 cells and are usually associated with the same pro-inflammatory environment. They need IL-6, IL-23 and TGF-β for differentiation, as well as RORγt, RORα,

STAT3 and IRF4. Th17 cells are associated with the production of IL-17, IL-22 and IL-21. Th9 cells rely on GATA3 signalling and produce IL-9. T regulatory cells, known for their immune-modulating role in disease, need IL-2 and TGF-β for differentiation. They express FOXP3 and produce IL-10 and TGF-β to dampen down an immune response.

Previous studies suggested that MS is predominantly a Th1-mediated disease. This conclusion was based upon the findings that IL-12 is required for the differentiation of Th1 cells, and IL-12p40$^{-/-}$ mice are resistant to EAE (Cua et al. 2003). Also, MS patients given IFN-γ (Th1 cytokine) treatment have been found to display a more severe disease (Panitch et al. 1987). Surprisingly, IFN-γ KO mice developed more severe EAE with a higher rate of mortality when compared with the control WT littermates (IFN-γ$^{+/+}$ and IFN-γ$^{+/-}$ mice) (Ferber et al. 1996). This suggested that Th1 cells are not solely responsible for the inflammation and demyelination observed in MS/EAE development and that other mechanisms are involved.

As mentioned above, both T-bet and STAT1 are transcription factors that are needed for the differentiation of precursor Th cells into Th1 T cells (Bettelli et al. 2004). Previous studies have also demonstrated that T-bet$^{-/-}$ mice are resistant to EAE. STAT1$^{-/-}$ mice however, are still susceptible to EAE and these mice have IFN-γ^{+}Th1 cells. Furthermore, T-bet$^{-/-}$ STAT1$^{-/-}$ double KO mice are also resistant to EAE (Bettelli et al. 2004). These results further confirmed that Th1 cells may not be the only effector cells in the development of MS and EAE and indicates another cell which utilized T-bet but not STAT1 and can still initiate disease in STAT1$^{-/-}$ KO mice. It was later discovered that the cytokine IL-23 is comprised of the subunit p40 of IL-12 but also a p19 subunit, which is unique to IL-23 (Oppmann et al. 2000). Cua *et al* further discovered that only mice deficient of both IL-23p19$^{-/-}$ and IL-12p40$^{-/-}$ were resistant to EAE development, whilst IL-12p35$^{-/-}$ were still susceptible to EAE (Cua et al. 2003). These results indicated that IL-23, but not IL-12, was essential for the development of EAE; similar data were also observed in other autoimmune disease models. These included the

rheumatoid arthritis disease model: collagen induced arthritis (CIA) and IBD using IL-12p35 x IL-10 KO mice, which developed spontaneous IBD whereas IL-23p19 x IL-10 KO mice did not (Langrish et al. 2005; Yen et al. 2006). Following research then focused on identifying the immune cells, which required IL-23 in their cell differentiation and function. Langrish and colleagues discovered that IL-23 is essential for the development of Th17, but not Th1 cells, as IL-23p19$^{-/-}$ and WT mice had similar numbers of MOG specific IFN-γ-producing cells in EAE. In contrast, IL-17 producing cells were absent from the IL-23p19$^{-/-}$ mice. Furthermore, treatment of draining lymph node (DLN) cells with rIL-23 expanded Th17, but not Th1 cells (Langrish et al. 2005).

Other studies have also shown the importance of Th17 cells in EAE development via IL-9 production (Nowak et al. 2009). Naïve mice, which received IL-23 expanding PLP-specific CD4^{+}T cells developed severe EAE compared to naïve mice which received IL-12-expanding PLP specific CD4^{+}T cells. These results suggest that IL-23 and Th17 cells are more effective at initiating EAE than IL-12 and Th1 cells *in vivo* (Langrish et al. 2005). Other reports have also confirmed the importance of Th17 in EAE development through investigating the migration of Th17 cells into the CNS. Th17 cells produce CCL20 (chemokine) and express CCR6 (chemokine receptor). In inflamed joints synovial cells secrete CCL20, attracting Th17 cells to the inflammation site (Hirota et al. 2007). The up regulation of CCL20 and CCR6 is evident in CIA as well as EAE. Indeed, in CCR6-deficient mouse strains, Th17 cells were unable to migrate to the CNS and no EAE was induced (Yamazaki et al. 2008) indicating the importance of Th17 cells in EAE pathogenesis. However, O'Conner *et al*. reported that Th17 cells alone were not able to induce EAE, and that both Th1 and Th17 cells were required for the disease development. Furthermore, Th1 cells were capable of homing to the CNS better than Th17 cells. It was thus suggested that Th1 cells might migrate to the CNS and induce the inflammation and recruitment of cells, which facilitates the entry of Th17 cells into the CNS (Connor et al. 2009).

Some recent advances in the understanding of immune T cell phenotype switching *in vivo* have added a new level of complexity to the immune mechanisms of MS/EAE. For example, a study investigating phenotype switching during ocular inflammation, using HEL-specific TCR transgenic mice, led to the discovery of the instability of Th17 cells *in vivo* (Shi et al. 2009). The results show that Th1 cells adoptively transferred into recipient mice still expressed IFN-γ after 10 days, but Th17 cells in the recipient mice lost the expression of IL-17 and instead expressed IFN-γ or both IL-17 and IFN-γ. Further studies showed IFN-γ expressing Th17 cells also expressed T-bet with no detectable levels of ROR-γt. In contrast, Th1 cells retained their phenotype independently of the environmental milieu (Shi et al. 2009). The unstable phenotype of Th17 cells *in vivo* may help to explain the discrepancies in the data in the literature. For example, whilst Langrish *et al.* suggested that Th17 cells are essential for the induction of EAE, O'Conner *et al.* reported the need for Th1 cells in Th17-mediated inflammatory reactions. Additionally, detection of IL-17$^+$IFN-γ$^+$ cells in MS brain lesions further supports phenotype switching of Th17 cells in MS disease (Kebir et al. 2009).

A recent report from Kroenke and colleagues suggested that the types of inflammatory cell recruited into CNS are dependent on the mediating CD4$^+$ effector cells (Kroenke et al. 2008). IL-12p70 and IL-23 polarised T cells were taken from the lymph nodes (LNs) of SJL mice primed with PLP and produced IL-1 and IL-17 cells, respectively. These cells were then adoptively transferred into naïve mice. Th17 driven EAE has been shown to be enriched with neutrophils and extends into the deep parenchymal white matter, whereas Th1 driven EAE is enriched with macrophages and the lesions are confined to the subpial white matter (Kroenke et al. 2008). These findings are consistent with observations from MS tissues that some forms of MS lesions are dominated by neutrophils in the CNS with elevated IL-8 (Th17) whereas other forms are enriched with macrophages (Th1) (Griffin et al. 2012; Wojkowska et al. 2014). Additionally, Th17-mediated EAE involved atypical

brain inflammation by gaining entry into the CNS via the choroid plexus (Reboldi et al. 2009) whereas Th1-mediated EAE induced only spinal cord inflammation (Stromnes et al. 2008).

A further subset of $CD4^+$ T cells are the Tregs, the discovery of which brought a new aspect to MS/EAE research. Impaired Treg cell populations have been linked to MS pathology. Treg cells depend on the CD46 co-stimulatory pathway for their induction, MS patients have between a 4- and 6-fold decrease in CD46-stimulated IL-10 secretion compared to healthy controls (Astier et al. 2006). Furthermore, $FOXP3^+CD25^+CD4^+$ Treg cells were reduced in RRMS patients compared to healthy controls or patients with other neurological diseases (Venken et al. 2008). There was also a reduction in FOXP3 expression on $CD25^{high}$ $CD4^+$ T cells. Interestingly, it was additionally shown that Treg cells appeared to accumulate within the CSF of RRMS patients but not in SPMS or optic nerve disease (OND) (Venken et al. 2008). Overall numerous studies have shown that Treg cells play an important regulatory role in the development of EAE as the transfer of $CD25^+CD4^+$ T cells was protective in EAE by reducing cell infiltration into the CNS (Kohm et al. 2002).

Although MS and EAE are regarded as Th1 and Th17 driven immune condition, other cells such as CD8 T cells, macrophages, neutrophils, B cells and the resident CNS glial cells also play their part in the development of MS and EAE. An early study surprisingly observed that $CD8^+$ cells are more prevalent in MS brain tissue than $CD4^+$ T cells (Cabarrocas et al. 2003) and are found within the region of demyelinated axons (Deb et al. 2010) as well as the CSF and brain of MS patients (Skulina et al. 2004; Battistini et al. 2003). Unlike $CD4^+$ T cells, $CD8^+$ T cells are able to induce death directly by the release of cytotoxic molecules such as granzymes and perforin, as well as by displaying ligands for death signals such as Fas-L and TNF-α (Alderson & Tough 1995; Brehm et al. 2005) CD8 T cells can be activated by MHC I molecules found on almost all nucleated cells (Lehner & Cresswell

2004). Furthermore, in paraffin MS brain tissues it was shown that MHC-I was up-regulated in neurons and ODC cells during MS disease, immediately prior to demyelination occurring (Höftberger et al. 2004). CNS microglia cells were also reported to cross-present antigens to $CD8^+$ T cells (Beauvillain et al. 2008). The data suggests that $CD8^+$ T cells play an important role in the pathogenesis of MS disease. Indeed a study investigating acute axonal injury in active demyelination within MS lesions has shown that the numbers of $CD8^+$ T cell and macrophage in CNS lesions correlated with axonal damage in MS (Bitsch et al. 2000). Furthermore, EAE is also reported as being induced by $CD8^+$ T cells in C57BL/6 mice (Sun et al. 2001). Also, regulatory $CD8^+$ T cells, characterised by the lack of CD28 expression, were reported to induce tolerised DCs (Najafian et al. 2003). This is supported by a report identifying $CD122^+$ regulatory $CD8^+$ T cells, which produce IL-10 and suppress IFN-y production (Endharti et al. 2005; Cho et al. 2008) and deletion of this population exacerbates EAE (Lee et al. 2008).

Studies indicate a role for B cells, in MS and EAE, by acting as APCs for self-reactive T cells, by co-stimulating and recruiting T cells and by the production of myelin-specific antibodies that result in myelin destruction (Jagessar, Heijmans, Oh, et al. 2012). Normally, B cells cannot pass through the BBB however, during an inflammatory response they can enter the CNS, along with complement, to promote inflammation (Knopf et al. 1998). B cells can be stimulated to produce antibodies due to viral or self-antigens, super-antigens or via bystander stimulation (Qin et al. 1998). Antibodies opsonise myelin for phagocytosis or activate complement resulting in MAC (membrane activation complex) formation causing cytotoxic effects and demyelination (Mead et al. 2002). Furthermore, B cells can produce cytokines (such as IL-6), which in combination with TGF-β can facilitate the generation of pathogenic Th17 cells and the production of pro-inflammatory cytokines (Bettelli et al. 2008). Moreover, B cells can promote a Th1 response by enhancing IFN-γ production (Menard et al. 2007). In studying EAE induced in marmoset

monkeys, Jagessar et al. demonstrated that B cells contribute to MS and EAE pathology. Depletion of $CD20^+$ B cells, using anti-BLys and anti-APRIL antibodies, impairs the activation of Th17 and cytotoxic T cells, which are important in EAE induction (Jagessar, Heijmans, Oh, et al. 2012). Further studies suggest that B cells from MS patients have demonstrated impaired IL-10 production compared to healthy patients. This implies that B cells aid in the pathogenesis of MS and although only pattern II lesions are indicative of antibodies and complement deposition this is the most common lesion type seen and further demonstrates the importance of B cells in many patients with MS (McLaughlin et al. 2009). This research has led to the clinical testing of therapies, which deplete B lymphocytes in MS patients. An incidence of where this was demonstrated was when a patient with RRMS received Rituximab treatment (anti CD20 antibodies, CD20 is present on mature B cells but not plasma cells) had depleted B cells for 6 months, which was associated with no relapses or new lesion formation for 9 months (Stüve et al. 2005). Early studies showed the presence of immunoglobulins in the CSF of MS patients (Morris-Downes et al. 2002). Furthermore, B cells are elevated in most MS patients; a study has identified short-lived plasmablasts to be the main B cell contributor to the pathogenesis seen during MS (Cepok et al. 2005). Interestingly, in SPMS, follicles containing B cells and DCs have been identified. B cell follicles allow B cells to clonally expand and become memory cells or the antibody secreting plasma cells (Serafini et al. 2004). These observations further suggest a role for B cells in MS pathology. Meningeal B cell follicles have also been found close to grey matter lesions and meningeal inflammation (Magliozzi et al. 2007).

Demyelination

It is often the case that chronic MS lesions are defined by infiltration of lymphocytes and other inflammatory cells, extensive demyelination, axonal loss and gliosis (Kuhlmann et al. 2008). Interestingly, a lot of the same molecules involved in demyelination are also important mediators of the remyelination process, both of which occur simultaneously *in vivo*. It is the balance between the demyelination and remyelination, which determines the clinical consequence of a relapse or remission (Foote & Blakemore 2005).

B cells are thought to contribute to the demyelination seen in MS by the opsonisation of myelin (Jagessar, Heijmans, Bauer, et al. 2012; Weissert et al. 1998) as demonstrated by the presence of oligoclonal IgG bands (bands of IgG in more than 95% of MS patients), as well as an IgG increase in the CSF of MS patients) (Link & Huang 2006). Autoantibodies produced by B cells have a clear role to play in CNS demyelination, as seen in pattern II lesions (present in 50% of patients) having extensive antibody and complement deposition (Lucchinetti et al. 2000). Autoantibodies to MOG and other myelin proteins (e.g. PLP and MBP) result in demyelination by the fixation and activation of the complement cascade (Piddlesden et al. 1991). As previously mentioned, $CD8^+$ T cells can induce demyelination via MHC I molecules present on neurons and ODCs via Fas-FasL signaling and perforin (present in $CD8^+$ T cell granules) (Kivisäkk et al. 1999). Cytotoxic T cells secrete perforin, which causes the generation of holes in the membranes of cells, resulting in cellular lysis, and is often the cause of ODC death (Kivisäkk et al. 1999), cytoplasmic vacuolation, and the breakdown of the nuclear envelope. Moreover perforin mRNA is expressed in the CSF cells and blood mononuclear cells of MS patients (Kivisäkk et al. 1999; Matusevicius et al. 1998). Clinically, the use of plasma exchange in these patients has been shown to reduce the neurological symptoms of MS (Weinshenker et al. 1999).

Microglia have often been found to be activated before the onset of symptoms and cellular infiltration into the brain. They are deemed effective APCs and can potentiate the demyelination process by presenting myelin antigens to lymphocytes. Furthermore, a demyelinating model using cuprizone treatment microglia accumulated within the demyelinated regions (Remington et al. 2007) . However, microglia also have a protective role to play during neuropathology as they engulf dead cells and destroyed myelin which, if left to build up would result in extensive damage and demyelination to the axons.

Remyelination

ODCs are the myelin-producing cells of the CNS and thus the key players in the remyelination process, and the main target cells during inflammation induced demyelination. However previous evidence suggests that OPCs are mainly responsible for the remyelination process, rather than the surviving ODCs within the lesion.

Numerous studies suggest that many immune cells and molecules involved in inflammation and demyelination are also important for remyelination to occur (Rodriguez 2007). A study using the *taiep* rat, which is devoid of an inflammatory response, has shown stunted remyelination. Remyelination was however, evident in the presence of inflammation suggesting that the molecules needed for inflammation are also needed to initiate remyelination,(Foote & Blakemore 2005). T cells and B cells are also important in promoting remyelination (Bieber et al. 2003), was shown using recombinant activation gene-1 (Rag-1)-deficient mice, which cannot produce mature B or T cells. These were assessed for remyelination after lysolecithin-induced demyelination and Rag-1 deficient mice did not have the same extent of remyelination as that of the WT control mice (C57BL/6 mice). The authors suggested that T cells and B cells produce factors that are needed

for OPC migration and viability (Bieber et al. 2003).

Another controversial point in the remyelination process is the requirement of antibodies. Antibodies are the main players in the demyelination process, which mainly involve the IgG class. However, the presence of IgM antibodies is imperative in remyelination. It has been found that IgG binds to complement with high affinity, however IgM antibodies bind to complement with high avidity (Miller et al. 1994). Two monoclonal antibodies have been identified to be important in remyelination (sHIgM22 and sHIgM46) which binds to antigens on ODCs promoting remyelination (Warrington et al. 2000). Treatment of MS patients with the above antibodies, over a one month period, was found to reduce the lesions observed in MRI scans (Pirko et al. 2004). This suggests that antibodies may function to prevent ODC death or have some involvement in the activation of OPCs to produce myelin.

Many immune cells and molecules that are associated with demyelination are also an important component of remyelination and thus it has been shown that remyelination occurs in areas of ongoing demyelination. The clinical outcome of the disease is influenced by the CNS inflammation, and the subsequent demyelination and remyelination processes. Thus understanding the mechanisms of CNS inflammation, demyelination and remyelination will help to develop therapeutic strategies for MS patients through promoting remyelination and inhibiting demyelination in the CNS.

A role for systemic Inflammation in MS disease

Systemic infections in the periphery can also have an effect on the development of CNS inflammation. Autoimmune diseases such as Crohn's disease (Yang & Lichtenstein 2002) and rheumatoid arthritis were reported to be exacerbated by systemic infections (Perry et al. 2003; Edwards et al. 1998). In the case of MS, systemic infections can cause relapses of disease

(Moreno et al. 2011). MS patients are considered to be at risk of a relapse four or five weeks after an infection (e.g. respiratory) (Sibley & Bamford 1985). It has been postulated that IFN-γ and TNF-α are involved in exacerbating MS pathogenesis during systemic infection by facilitating T-cell infiltration into the CNS thus enhancing localised inflammation (Panitch 1994). Cytokines released during systemic cell damage such as IL-1β, IL-6 and TNF-α can also directly cause an inflammatory response by binding to the receptors on circumventricular organs (CVO) that lack an intact blood brain barrier (Perry et al. 2003; Takahashi et al. 2013). Cytokines can interact with the vagal nerve which stimulates neurons within the brain stem (Perry 2004; Mascarucci et al. 1998) or via the endothelial cells/ perivascular macrophages within the BBB, which indirectly induce the transcription of factors needed for CNS inflammation (Matsumura & Yamagata 1996). If a macrophage is already 'primed' during on-going inflammation within the brain it will generate a larger response than an unprimed macrophage (Gifford & Lohmann-Matthes 1987). In the EAE model systemic challenge with bacteria-derived toxins was able to enhance the clinical symptoms of the disease thus also providing additional evidence for the involvement of systemic infection in the exacerbation of CNS inflammation.

1.5 Interleukin (IL-) 33 cytokine

IL-33 is a member of the IL-1 cytokine superfamily which is generally pro-inflammatory and all the members share a similar beta trefoil structure. The other family members include IL-1α, IL-1β and IL-18 (Schmitz et al. 2005).

Table 1.2 IL-1 cytokine superfamily

Name	Receptor	Co-Receptor	Function
IL-1α	IL-1R1	IL-1RacP	Proinflammatory
IL-β	IL-1R1	IL-1RacP	Proinflammatory
IL-1Ra	IL-1R1	IL-1RacP	Antagonist for IL-1α and IL-β
IL-18	IL-18Rα	IL-18Rβ	Proinflammatory
IL-36Ra	IL-1Rrp2	N/A	Antagonist for IL-36α, IL-36β and IL-36γ
IL-36α	IL-1Rrp2	IL-1RacP	Proinflammatory
IL-37	Unknown	Unknown	Anti-Inflammatory
IL-36β	IL-1Rrp2	IL-1RacP	Proinflammatory
IL-36γ	IL-1Rrp2	IL-1RacP	Proinflammatory
IL-38	Unknown	Unknown	Unknown
IL-33	ST2	IL-1RacP	Th2 responses/ proinflammatory

(Dinarello 2011)

IL-1 and IL-18

The IL-1 family proteins have been largely associated with inflammation (Werman et al. 2004). As mentioned above, IL-1 has two forms, IL-1α and IL-1β, which are structurally related (Schmitz et al. 2005). IL-1α has been established as mainly an intracellular mediator of inflammation which is released upon cell damage, IL-1α usually exerts its effects in an autocrine fashion (Woodworth et al. 1995). IL-1β needs to be cleaved by caspase 1 (IL-1β converting enzyme ICE) in order to become active (Martinon et al. 2002). There are two IL-1 receptors, IL-1RI containing the intracellular (TIR)

signaling domain, and IL-1RII (Hirotani et al. 2005). The binding of IL-1α or IL-1β to the IL-1RI results in the activation of cellular responses. However IL-1RII is a decoy receptor (Lang et al. 1998) and binds to excess IL-1 without inducing signaling pathways. IL-1β enhances the differentiation of Th17 cells, which are pivotal in inflammation and autoimmune diseases (Sutton et al. 2009). Studies showed that IL-1R1$^{-/-}$ mice are resistant to EAE as IL-1 (in conjunction with IL-23) signaling is necessary for the production of Th17 cells (Sutton et al. 2006). IL-1 is expressed on monocytes and macrophages in the PNS; within the CNS, IL-1 is expressed on neurons, astrocytes, ODCs and endothelial cells (Zhang et al. 1998; Davies et al. 1999; Sairanen et al. 1997). Furthermore, EAE induced in rats, along with recombinant human IL-1Rα, resulted in reduced clinical disease course, paralysis and weight loss. Excess IL-1β has been linked to an increase in susceptibility to MS and is present in MS lesions (Martin & Near 1995; Badovinac et al. 1998; de Jong et al. 2002).

The IL-18 sub-family consists of IL-18 and the IL-18 binding protein (IL-18BP), which acts in a similar manner to a decoy receptor. IL-18 is present on monocytes, macrophages and DCs (Schmitz et al. 2005; Smith 2011). Similarly to IL-1β, IL-18 is synthesised as a 23kDa peptide (Pro-IL-18) which is inactive until it is cleaved by caspase-1. Pro-IL-18 can also be activated by extracellular enzymes such as, protease 3, cathepsin G and serine proteases (Raupach et al. 2006; Sugawara et al. 2014). IL-18Rβ is recruited to form a heterotrimeric complex with IL-18Rα and IL-18, which then recruits adaptor proteins such as MyD88 and activates pathways involving NF-κB (Thomassen et al. 1998). IL-18, IL-18α and β have been identified in Purkinje cells, astrocytes (within the cerebellum), and the medial habenula neurons, amongst others. In addition, studies have indicated that IL-18 can be produced by microglia and astrocytes (*in vitro*) upon stimulation with LPS (Conti et al. 1999; Sugama et al. 2007), and may be involved in the activation of microglia (Mori et al. 2001). Research into the role of IL-18 in MS/EAE suggests that prolonged or repetitive activation of microglia can lead to

pathological forms associated with MS (Kuno et al. 2005). Moreover microglia are thought to act as antigen presenting cells (APCs) by presenting antigens to naïve T cells in the mouse model of MS (EAE), as well as secreting cytokines (IL-6, IL-23, IL-1β and TGF-β) associated with the differentiation and activation of Th17 cells (thus driving pathology). The role of IL-18 in microglia cell activation is confirmed by another study using IL-18 KO mice which had reduced levels of microglia activation and subsequent clearance of bacteria and viruses (Sugama et al. 2004). Interestingly, IL-18 mRNA levels are elevated in the brain and spinal cord of mice with EAE which correlated with an increase in caspase-1 within these regions, and increased severity of disease. Over-expression of the IL-18 decoy receptor (IL-18BP) can prevent the induction of EAE (Schif-Zuck et al. 2005). MS patients also express increase IL-18 in their peripheral blood monocytes (Huang et al. 2004). Furthermore, there is an increase in IL-18 in the serum and CSF of MS patients in comparison to control groups (Losy & Niezgoda 2001).

The newest member of the IL-1 family is IL-33, which was first identified by Schmitz *et al*. in 2005 (Schmitz et al. 2005). The human IL-33 gene is located on chromosome 9p24.1 while the murine equivalent is present on chromosome 19qC1 (Schmitz et al. 2005). Sequence analysis databases have since shown that mouse and human IL-33 are 55% identical at the amino acid level (Schmitz et al. 2005). As an IL-1 family member, IL-33 most closely resembles IL-18. Both IL-18 and IL-33 are the only IL-1 members not linked to the IL-1 gene cluster on human chromosome 2 (Moussion et al. 2008; Carriere & Roussel 2007).

IL-33 biology

IL-33 was originally described as a nuclear factor from high endothelial venules (NF-HEV) as it associates with chromatin in the nucleus of HEV endothelial cells *in vivo*. However, it also has transcriptional regulatory

properties suggesting a dual function of IL-33 as both a nuclear factor and a cytokine (Moussion et al. 2008; Carriere & Roussel 2007). Similarly, IL-1α and HMGB1 regulate transcription within the nucleus, but also act as pro-inflammatory cytokines (Werman et al. 2004; Rovere-Querini et al. 2004). Initial studies suggested that IL-33 was cleaved by caspase 1 from a pro-peptide (30kDa) into a mature active (18kDa) peptide (Cayrol & Girard 2009). However, more recent studies (Lüthi et al. 2009) have shown that, unlike IL-1 and IL-18, the un-cleaved 30kDa IL-33 is the bioactive form, which is inactivated by caspases -3 and -7 (apoptosome caspases) (Cayrol & Girard 2009) and it is released upon apoptosis or necrosis of cells similar to that of an alarmin which alerts the immune system to damage.

After identifying IL-33, Schmitz et al. further studied the expression of IL-33 and reported that IL-33 mRNA was highly expressed in the stomach, lung, spinal cord, brain and skin tissues. Low levels of IL-33 mRNA were expressed in the lymph nodes, spleen, pancreas, kidney and heart. Furthermore, murine resting dendritic cells and activated macrophages were also seen to express IL-33 mRNA, whilst in human samples IL-33 only observed in activated dendritic cells and macrophages whilst human NK cells, Th1, Th2, Th0 and PBMC cells showed no IL-33 mRNA expression (Schmitz et al. 2005). Other studies indicated that IL-33 is constitutively expressed at the protein level on endothelial cells, epithelial cells (Pichery & Mirey 2012) and pancreatic stellate cells (Masamune et al. 2010). In vitro, IL-33 has been shown to be expressed in super-confluent but not sub-confluent endothelial cells and endothelial cells do not express IL-33 if they have advanced through the G_1 phase of the cell cycle (Küchler et al. 2008). Alternative splicing of IL-33 creates several mature mRNA from a single gene resulting in functionally and structurally different proteins. Hong *et al* were the first group to discover a splice variant of IL-33, which lacks the exon 3 (Hong et al. 2011). Some recent studies further confirmed other splice variants of IL-33, which lacks exons 4 and 5 (Tsuda et al. 2012a). Full-length

IL-33, and variants lacking exon 4 and 4-5 where all located in nuclear fractions whereas the IL-33 variant lacking exon 3 was detected in the cytoplasmic fraction, indicating that IL-33 also exists within the cytoplasm of cells (Tsuda et al. 2012). These findings were confirmed by the discovery that IL-33 was located in cytoplasmic vesicles, as well as within in the nucleus. IL-33 is thought to utilise the nuclear pore complex to be transported between the nucleus and the cytoplasm where it can reside in cytoplasmic vesicles and be secreted by living cells during biomechanical overload (Kakkar et al. 2012).

IL-33 is the ligand for the orphan receptor ST2 (Schmitz et al. 2005). ST2 also encompasses the IL-1 receptor accessory protein (IL-1RAcP) (Table 1.2) to form a functional receptor for IL-33 (Liew et al. 2010; Lingel et al. 2009). IL-1RAcP is also utilised by other IL-1 family members such as IL-1α and IL-1β (Chackerian et al. 2007). ST2 has four variants: soluble ST2 receptor (sST2, also known as a decoy receptor), a transmembrane ST2 receptor (ST2L) and two novel variants (ST2V and ST2LV) (Tominaga et al. 1999). Similarly to other IL-1 cytokines, IL-33 signals through the TIR domain of IL-1RAcP, utilising pathways such as MYD88, IRAK 1 and IRAK 4 to activate proteins such as NF-κB p65, ERK, p38 and JNK mitogen-activated protein kinases (MAPKs) (Liew et al. 2010; Brint et al. 2002; Choi et al. 2012; Ali et al. 2011). This leads to the production of immune cytokines such as IL-5 and IL-13. TNF receptor associated factor 6 (TRAF 6) has been implicated in IL-33 signaling through pathways such as p38, NF-κB and JNK and is an essential adapter molecule for the formation of the ST2 ligand complex (Funakoshi-Tago et al. 2008; Choi et al. 2009).

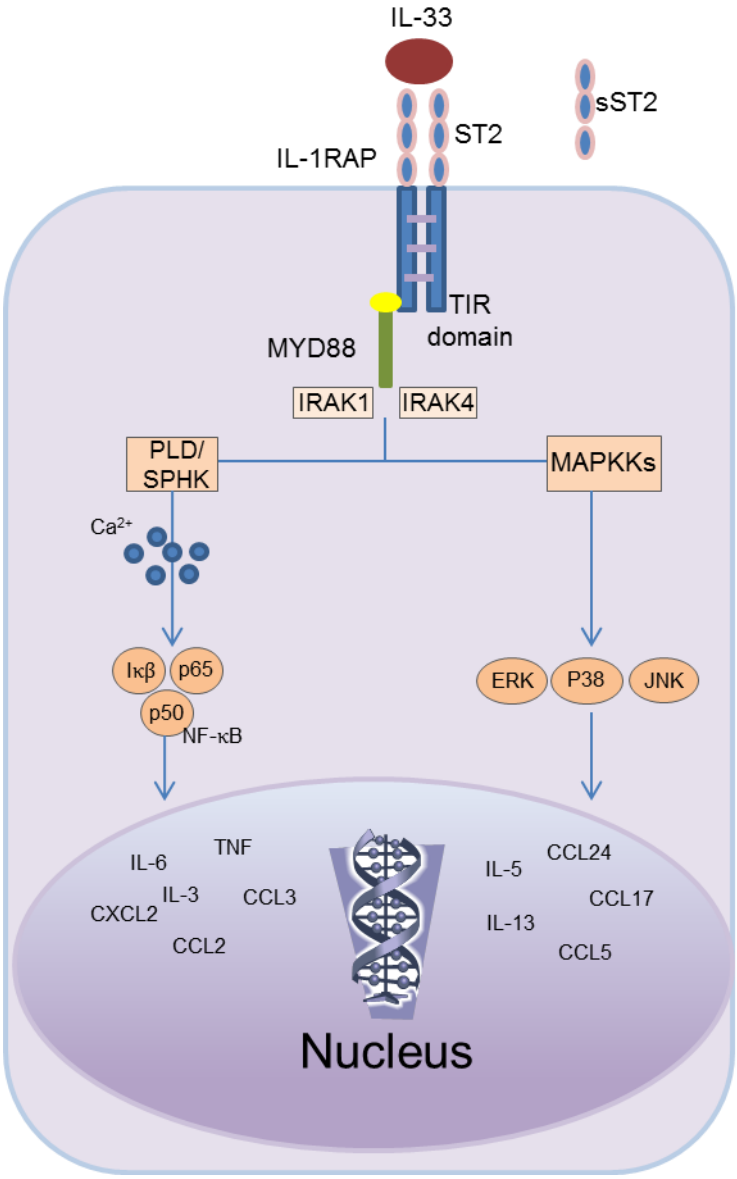

Figure 1.4 IL-33 Signalling Pathway. IL-33 binds to ST2 and associated adaptor receptor IL-1RAP. Once bound, IL-33 signals through the TIR domain and activates MyD88, IRAK1 and IRAK4. This in turn recruits NF-κB p65, ERK, p38 and JNK. These proteins influence the production of cytokines such as IL-6, IL-5, IL-13 and chemokines such as CCL2, CCL5 and CCL24 within the nucleus of the cell.

ST2 has been found to be present on Th2 $CD4^+$ T cells but not Th1 cells (Löhning et al. 1998), mast cells (Moritz et al. 1998a), macrophages (Kurowska-Stolarska et al. 2009), basophils (Kondo et al. 2008), NK cells, NKT cells (Smithgall et al. 2008) and DCs (Yanagawa et al. 2011) have also been shown to possess the ST2 receptor and therefore can be activated by IL-33. Although IL-4 can induce ST2 it is not necessary for ST2 expression on Th2 cells (Löhning et al. 1998). IL-33 can drive Th2 cells by the production of IL-5 and IL-13 but not IL-4, these Th2 cells differ from the classical Th2 cells. Instead of activation via IL-4 they are stimulated by IL-33 via ST2 on the surface of the Th2 cells secreting IL-5 and IL-13. Furthermore, IL-33 stimulated the differentiation of these Th2 cells via Toll/IL-1R through MyD88, MAPKs and NF-κB, unlike classical pathways such as STAT6 and GATA3 (Kurowska-Stolarska et al. 2008; Hayakawa et al. 2007).

SIGIRR (single immunoglobulin IL-1R- related molecule) is another negative regulator of IL-33-mediated signaling though the ST2L similar to that of the decoy receptor (sST2). SIGIRR is also expressed on Th2 but not Th1 cells. IL-33 can bind the SIGIRR receptor and specifically inhibit IL-33/ST2 signaling. Furthermore SIGIRR-deficient Th2 cells produce more IL-5, IL-4 and IL-13 than WT cells (Bulek et al. 2009).

IL-33 and diseases

Allergies such as anaphylactic shock, asthma and dermatitis are usually associated with the production of IgE antibodies, which bind to Fc receptors on mast cells, the cross-linking of the bound IgE leading to degranulation and the release of inflammatory mediators (Pushparaj et al. 2009). ST2 has been found to be highly expressed on mast cells (Moritz et al. 1998b) and IL-33 induced the degranulation of IgE-sensitised mast cells *in vitro* (Pushparaj et al. 2009). IL-33 increases the production of IL-5 and IL-13 and augments a Th2 response leading to increased goblet cell hyperplasia via ST2 and

MYD88 pathways and thus airway hyper responsiveness. Mast cells and basophils are mediators of asthma and can induce IL-13 upon stimulation by IL-33 (Kondo et al. 2008). During anaphylaxis and dermatitis (serum and skin inflammation respectively), there was an increase in IgE and IL-33 expression observed in patient samples compared to healthy controls. In the murine model of IgE-mediated passive cutaneous anaphylaxis (PCA), IL-33 increased vascular permeability to a similar level to that of the allergen employed (DNP-HSA). Furthermore, when IL-33 was administered in conjunction with this allergen an additive effect was observed in IgE sensitive mice, in particular, enhanced mast cell degranulation in an ST2-dependent manner (Pushparaj et al. 2009). As previously mentioned IL-33 can drive IL-5-producing T cells in an allergen-induced asthma model via ST2 on their surface. ST2 KO BALB/c mice demonstrated an attenuated disease course, the administration of IL-33 enhanced IL-5 production by T cells and enhancing the airway inflammation in WT and IL-4 KO mice. Soluble ST2 sequestered circulating IL-33 and inhibited the T cell-induced airway inflammation suggesting a role for IL-33 in allergen-induced asthma (Kurowska-Stolarska et al. 2008; Hayakawa et al. 2007).

IL-33 and sST2 are increased in the inflamed mucosa of patients with ulcerative colitis (UC) compared to that observed in control biopsies (Pastorelli et al. 2010). The presence of IL-33 was also determined by western blotting in the cytoplasm and nucleus of intestinal epithelial cells and in the lamina propria mononuclear cells (Pastorelli et al. 2010). However, ST2 mRNA was decreased in the intestinal epithelial cells of UC patients. Furthermore IL-33 and sST2 were up regulated in patients with UC, compared to control healthy patients, suggesting a possible disease biomarker. Infliximab (anti-TNF-α) treatment reduced IL-33 due to an increase in sST2 in UC via TNF modulation of IL-33 and sST2 in IEC (Pastorelli et al. 2010).

IL-33 can also have a role to play in the controlling *Trichuris muris (T.muris*; a gastrointestinal nematode) infections, which relies heavily on a Th2 response. Results have shown that during *T. muris* infection, IL-33 mRNA is enhanced and the subsequent protein expression drives the expulsion of the parasite, reducing worm burden. IL-33 treatment administered at the beginning of the parasite infection is able to induce a Th cell switch from a Th1- to a Th2-mediated response. However, when given during a chronic *T. muris* infection IL-33 fails to reduce worm burden and expulsion by failing to induce the Th cell switch (Humphreys et al. 2008). In 1998, it was discovered that when anti-ST2 antibody was injected into BALB/c mice infected with the intracellular protozoan parasite *Leishmania major* reduced parasite load. This was due to a switch from a pathogenic Th2 to a protective Th1 response, suggesting a role for IL-33 in the resolution of Leishmania infections (Xu et al. 1998).

IL-33 and ST2 are also implicated in diseases such as atherosclerosis, cardiovascular damage, obesity and septicaemia. IL-33 and ST2 mRNA were both identified on vascular cells and tissues in C57BL/6 mice and primary human ECs and expression was increased in $Apo^{-/-}$ mice, which develop atherosclerotic plaques, compared to controls. Furthermore, IL-33 treatment of $Apo^{-/-}$ mice reduced artherosclerosis development. IL-33 exerted this effect by increasing the production of Th2 cells and the production of cytokines such as IL-5 and IL-13, shifting the Th phenotype from a Th1 type response to a Th2 type and initiating antibody production (IgA, IgE and IgG_1) whilst decreasing IFN-γ expression (associated with a Th1 response). Furthermore, sST2 sequesters circulating IL-33, thus lowering IL-5 and IL-13 whilst increasing levels of IFN-γ, resulting in an exacerbated disease course (Miller et al. 2008). Other studies on cardiovascular disease also identified ST2 on cardiomyocytes. The presence of the decoy receptor (sST2), thought to mop up excess IL-33, has been seen to aggregate cardiomyocyte damage. Both cardiomyocytes and cardiac fibroblasts express IL-33 mRNA, and when exposed to mechanical strain the expression of ST2 and IL-33 are up-

regulated. Studies have shown that IL-33 blocks cardiomyocyte hypertrophy upon administration of angiotensin II and phenylephrine which correlates with a decrease in ROS generation, thereby suggesting a cardioprotective role for IL-33 (Sanada et al. 2007). McLaren *et al* (McLaren et al. 2010) reported that IL-33 reduced the number of residing macrophages within an atherosclerotic plaque and also reduced the conversion of macrophages into foam cells, which are the main players in atherosclerosis. Overall the results have shown that IL-33 can induce a shift from a Th1 response to a Th2 response, thus has a protective role in atherosclerosis disease.

In a spontaneous obese model (*ob/ob*), mice were treated with PBS or IL-33, which decreased epididymal white adipose tissue (eWAT) by 9.9%. Additionally, treating mice with IL-33 resulted in the accumulation of Th2 cytokines (IL-5, IL-6, IL-10 and IL-13) in serum and the local accumulation of Th2 cells in WAT, which contained more IL-5 producing T cells and macrophages than PBS tissues. Moreover the $CD45^{+}F4/80^{+}$ cells present in IL-33 *ob/ob* treated mice had more M2 macrophages present within the WAT compared to PBS controls, which had more M1 macrophages present. These findings suggest a role for IL-33 in reducing the chronic inflammation associated with obesity, through increasing the recruitment of Th2 cells and production of Th2 cytokines, as well as M2 polarisation (Miller et al. 2010).

IL-33 also has a role to play in septicemia, the presence of IL-33 enhances neutrophil actions, essential for bacterial clearance during sepsis. This occurs by preventing the down regulation of CXCR2 and interfering with TLR signaling (Alves-Filho et al. 2010).

In autoimmune diseases, IL-33 and ST2 have been reported as being expressed within the synovia of RA patients and to exacerbate CIA. Furthermore, in resting synovial fibroblasts little IL-33 was seen, and the expression of IL-33 was enhanced when cells were treated with TNF-α and IL-1β. Immunised ST2 KO DBA/1 mice showed a reduced disease severity

compared to WT mice. This coincided with a decrease in IL-17, IFN-γ and TNF-α production and reduced mono- and poly-morphonuclear cells. Furthermore, IL-33 exacerbated CIA via inflammatory cytokines secreted by mast cells (Xu et al. 2010).

In summary, a large volume of research studies have shown that IL-33 has an important role in a wide range of immune-mediated diseases. As an alarmin molecule, IL-33 plays an essential part in alerting the immune system to inflammation and damage. In the case of Th1 or Th2-mediated diseases, IL-33 can attenuate or potentiate the inflammation, and therefore may be potential therapeutic reagents or targets for patients.

IL-33 in CNS and CNS diseases

IL-33 is an important immunemodulatory cytokine, and the highest levels of IL-33 mRNA are expressed by the brain and spinal cord tissues in mice (Schmitz et al. 2005), suggesting that IL-33 may have CNS-specific functions. Many recent studies have focused on understanding the role of IL-33 within the CNS. Using western blot analysis, IL-33 was reported expressed on both endothelial cells and astrocytes (epithelial- like cells of the CNS) at an mRNA and protein level in *in vitro* glial cultures (Yasuoka et al. 2011). The authors determined ST2 to be located on astrocytes and microglia, highlighting potential autocrine and paracrine regulation of IL-33 within the CNS (Yasuoka et al. 2011; Schmitz et al. 2005; Hudson et al. 2008).

Since this discovery, studies have been conducted in an attempt to understand the role of IL-33 within the CNS. Genetic studies of Alzheimer Disease (AD) patients suggested that IL-33 might play a role in Alzheimer's protection (Yu et al. 2012). IL-33 was shown to be localised to chromosome 9p24 and this may be a genetic determent of Alzheimer's disease.

Polymorphisms of the IL-33 gene have been associated with increased risk of AD (Chapuis et al. 2009) and genetic variants can induce susceptibility of late AD in a Han Chinese population (Yu et al. 2012). Other studies have investigated the expression of ST2 during subarachnoid haemorrhage in the CSF from 21 patients. ST2 is upregulated in cells within the CSF of patients suffering from a subarachnoid haemorrhage, suggesting ST2 involvement in the inflammation (Kanda et al. 2006). Additionally, the active gene in subarachnoid haemorrhage (Dvs27) also encodes IL-33, implying a role for IL-33 in the CNS pathogenesis surrounding this condition (Inoue & Takeda 1999). Amyotrophic lateral sclerosis (ALS) is a neurodegenerative disease resulting in the death of motor neurons. IL-33 secretion was decreased in ALS patients potentially due to neuron apoptosis, not necrosis, thus IL-33 would be cleaved and thereby undetectable. However, sST2 was also upregulated and this has the role of mopping up the excess IL-33, preventing IL-33 signaling through ST2L (Lin et al. 2012).

Another study investigating the role of IL-33 in the protozoan parasite infection *Toxoplasma gondii* (*T. gondii*) using animal models indicated that ST2L, sST2 and IL-33 mRNA expression was significantly up regulated in *T.gondii*-infected BALB/c mouse brains compared to controls. T.gondii requires a balanced Th1/ Th2 responses for the effective control of parasites. T1/ST2$^{-/-}$ mice bred on a BALB/c background showed greater brain pathology than control mice due to and the production of IFN-γ, iNOS and TNF-α suggesting a role of IL-33 in the effective control of parasites (Jones et al. 2010).

As an important immune cytokine highly expressed in the CNS tissues, the role of IL-33 in the development of autoimmune MS disease is of particular interest. A recent report by Yasuoka and colleagues using an EAE model has shown that IL-33 is upregulated on astrocytes in lesions (Yasuoka et al. 2011). ST2 mRNA was increased in mice with EAE compared to control

C57BL/6 mice and ST2 KO BALB/c mice presented exacerbated EAE in comparison to WT mice (Jiang et al. 2012). The importance of IL-33 in the development of MS disease is confirmed by a report from the group of Christophi which showed that IL-33 was increased in MS patient plasma compared to controls. Using fresh frozen brain sections from MS patient brains, Christophi also employed RT-PCR and ELISA to determine that IL-33 was upregulated in tissues of MS patients compared to controls. Additionally, using immunohistochemical staining, IL-33 was shown to be expressed on astrocytes in plaques, periplaques and NAWM of MS patients, however only trace amounts of IL-33 were seen in normal control patients (Christophi et al. 2011). The exact role of IL-33 however is less clear. Our report suggests that the administration of exogenous IL-33 into EAE mice (at disease onset) resulted in an attenuated EAE course due to a switch from a Th1 to a Th2 response associated with the production of IL-5 and IL-13 (Jiang et al. 2012). Moreover AAMØ have been established as protective during EAE and in this study high expression of $MR^{+}PD\text{-}L2^{+}$ (AAMØ surface markers) macrophages was observed in the IL-33 treated EAE mice (Jiang et al. 2012). In contrast, another study has shown that the administration of IL-33-neutralising antibody during early onset of EAE attenuated the disease. Both IL-17 and IFN-γ production was reduced and the production of IL-10 and TGF-β was increased, suggesting that IL-33 has a pathogenic and not protective role to play in EAE (Li et al. 2012a). It is not clear what has caused these different results, thus further investigation is required to clarify the role of IL-33 in EAE.

1.5 Research Aims

The current findings through research employing CNS cell culture, animal models and patient's samples have suggested that IL-33 is likely to play an important role in the development of MS and EAE. It is also likely that IL-33, an important immunomodulatory cytokine, modulates MS/EAE development through mediating peripheral and CNS inflammation, CNS demyelination and

remyelination. Despite research providing an understanding of the role of IL-33 in mediating immune responses, little is known about the exact role and underlying mechanisms of IL-33 function in CNS compartment. The aims of this thesis are therefore:

1. To further characterise the expression of IL-33 and its receptor ST2 in normal and EAE CNS tissues and investigate whether the expression levels correlates with disease severity;
2. Investigate the co-localisation of IL-33 and ST2 with CNS resident cells;
3. Investigate the expression of IL-33 and ST2 in normal and MS patient CNS tissues;
4. Determine the function of the IL-33/ST2 signaling pathway in CNS myelination utilising an i*n vitro* myelinating system.

Data obtained from this study will provide novel insights into the expression and function of IL-33 and ST2 in the development of MS disease. In particular, the study will provide important information on the functional role of IL-33 within the CNS, and may lead to new therapeutic strategies for patients.

2. Materials and Methods

2.1 Mice

Female C57BL/6 mice were purchased from Harlan Laboratories, UK or bred in house at Strathclyde and Glasgow University animal facilities under U.K Home Office guidelines. Mice aged 7-12 weeks old were used in all EAE experiments and embryonic day 13.5 (E13.5) mice were used for the mouse myelinating culture system.

2.2 Rats

For the rat myelinating culture system, Sprague Dawley (SD) rats were used and maintained in the Biological Services Facilities, University of Glasgow and under U.K Home Office guidelines.

2.3 Experimental Autoimmune Encephalomyelitis (EAE)

Mice were given a subcutaneous (s.c) injection on the lower back with 100µg of MOG_{35-55} peptide (New England Peptide, USA) in 50µL of PBS (pH 7) emulsified with CFA (5.5mg/mL of Mycobacterium tuberculosis strain H37RA, Difco). Control mice received PBS emulsified with CFA. Each mouse also received intraperitoneal (i.p.) injection of 100ng/100µl of pertussis toxin (PTX) (Tolcris bioscience 70323-44-3) in PBS on days 0 and 2 post-immunisation.

2.4 Clinical Evaluation

During the course of EAE each mouse was ear marked with a number, the disease progression was monitored for the duration of the disease by clinically evaluating the stage of disease using a 5 point monitoring system. At time of immunisation mice showed no changes in motor function, when handled the tail became tense and hind limbs spread apart. When walking no gait or head tilting was observed, this was referred to as Score 0. At Score 1, the mice begin to develop a limp tail with little/ no tension when handled. As the disease progressed, the limp tail was accompanied by hind limb weakness (i.e., the hind limbs did not spread when lifted) and showed a 'wobbly walk' (Score 2). As severity of EAE increased, at approximately day 18 post immunisation, mice develop complete paralysis of the hind limbs and spinning when picked up by the tail (Score 3). This quickly leads to partial front limb paralysis and minimal movement (Score 4) and Score 5, where the mice can no longer move/ spontaneous rolling in the cage. Within these studies mice were not allowed to develop disease beyond Score 3 after which they were culled.

2.5 Evaluation of lymph node and spleen cell culture

The spleens were collected from naïve, PBS and EAE C57BL/6 mice and put in 5ml of RPMI(PAA 1640). The spleens were mashed in a sterile petri dish with RPMI using a syringe and sterile Nitrex mesh. The cells left in the RPMI media was filtered into a falcon tube. The cell suspension was then centrifuged at 1300 rpm for 5 minutes. Lysis buffer was added to the spleen cells for 5 minutes at room temperature. After 5 minutes the spleen cells were topped up with 20ml of RPMI medium and centrifuged for 5 minutes at 1300rpm. Spleen cells were re suspended in 10ml RPMI. Cells were counted

using Trypan blue (Sigma T8154) and cells were suspended at a concentration of $4x10^6$ cells/mL. Cells were plated into 24 well plates and treated with either media, or MOG for 48 hours. The supernatant for each was taken for ELISA analysis.

2.6 ELISA (Enzyme Linked Immunosorbent Assay)

ELISA was performed using a 96 well high binding ELISA plates (Greiner bio-one cat. UK, Number655061). Plates were coated overnight at 4°C with coating antibody for the cytokine of interest diluted in 1x coating buffer (ebioscience kit). The plates were then washed using PBS Tween (0.5%) five times leaving to soak for 1 minute between washes. Wells were then blocked using assay diluent (ebioscience ELISA kit) for 1 hour. Plates were washed again and the standards and samples were added to each plate and incubated overnight at 4°C. The following day plates were washed and then incubated with the detection antibody, secondary antibody conjugated to horse-radish peroxidase (HRP), for 1 hour at room temperature. Excess HRP was removed by washing and the substrate was then added (ebioscience ELISA kit) for 15-30 minutes, the reaction was stopped using 1M sulphuric acid (H_2SO_4). The absorbance was then read using an Epock Biotek plate reader at 492nm.

Table 2.1. ELISA antibodies

Antibody	Dilution	Supplier
IFN-γ		
Coating antibody	1:1000	ebioscience
Recombinant antibody	1:500	ebioscience
Detection antibody	1:1000	ebioscience
IL-17		
Coating antibody	1:250	ebioscience
Recombinant antibody	1:125	ebioscience
Detection antibody	1:150	ebioscience
HRP	1:250	ebioscience

2.7 CNS Tissue Dissection

Adult mouse brain dissection

Mice were sacrificed by CO_2 asphyxiation. Allergen exposure was reduced by spraying the fur with 70% ethanol (Sigma). This also prevented hair contaminating the tissue. The head was removed using scissors making sure not to damage the cortical region of the spinal cord below. An incision was made in the skin near the brain stem and the skin was pulled back exposing the skull. The occipital region of the skull was cut and using curved tweezers the skull was removed in sections by positioning the tweezers underneath the skull, not touching the brain and lifting upwards. Once the skull had been carefully removed, the brain was then detached from the optic nerve and surrounding nerve fibres by carefully positioning scissors underneath the brain. The brain was removed from the skull cavity by inserting curved tweezers underneath the brain and gently lifting it out. The brain was placed in Optimal Cutting Temperature compound (OCT) or 4% paraformaldehyde (4%PFA) (Fisher Scientific) for immunohistochemical staining.

Adult mouse spinal cord dissection

The fur was lifted up using tweezers and an incision running from the neck to the tail was made. The skin was then pulled back to reveal the spinal column. Incisions were made at the cervical, and coccyx regions and along the sides of the spinal column to detach it from the body. Using a 5ml syringe filled with 1X PBS and a 19G needle, the spinal cord was flushed out of the spinal column. The needle was inserted into the sacrum end and PBS inserted into the spinal column and the spinal cord was flushed out from the cervical opening. Once removed the spinal cord was either placed in 10% formalin for

fixation and paraffin embedding or cut and embedded in OCT for frozen sectioning.

2.8 Paraffin processing of murine tissues

The freshly dissected tissue was fixed in a 10% formalin solution for 48-72 hours at room temperature. Coronal sections of the brain and spinal cord were then processed using an automated paraffin processor. The tissues were rinsed in tap water for 1 hour then dehydrated gradually though 70%, 80%, 95% ethanol for 45 minutes each followed by three changes of 100% alcohol for 1 hour each. The tissues were then cleaned in histoclear (derivative of xylene) twice for 1 hour each time. Next the tissues were immersed in paraffin for 3 hours to perfuse the tissue. The sections were then removed from the processer and embedded in a block of paraffin and left to harden on a cool block. Each paraffin block was cut into 3µm sections using a microtome after which they were placed to float in a 40°C water bath containing distilled water and transferred onto Superfrost Plus glass slides to dry.

2.9 Processing of frozen murine tissues

Spinal cord tissues were embedded in OCT and frozen on dry ice. Tissues were cut using a cryostat (Shandon, Thermo Scientific) into 7µm sections and stored at -20°C before staining.

2.10 Haematoxylin and eosin staining (H and E)

Paraffin slides were heated in an oven at 60°C for 35 minutes to soften the wax. The slides were then deparaffinised and hydrated through histoclear and a graded alcohol series (histoclear, 100% ethanol, 90% ethanol and 70% ethanol for 3 x 5 minutes each). Sections were then outlined using a wax pen and rehydrated in wash buffer for 3 x 5 minutes. The slides were placed in Haematoxylin Z (Thermoscientific) for 7 minutes and then washed under running water. Next, the slides were dipped 12 times in 1% acid/alcohol solution and washed in running tap water. The slides were then left in Scott's Tap Water Substitute (STEWS) for 2 minutes, the tissues morphology was checked at this stage under a brightfield microscope. Following incubation in STEWS the tissues were washed in running water then incubated in EOSIN (thermoscientific) for 1 minute and further washed for 2 minutes. The tissue is then dehydrated by 10 dips in 70% ethanol and absolute ethanol (x2) then incubated in histoclear (National Diagnostics) for 1 minute (x3). The sections were then mounted using DPX (National Diagnostics) onto Superfrost Plus glass slides.

2.11 Luxol fast blue staining

Paraffin sections were deparaffinised and hydrated to 95% alcohol and incubated with Luxol fast blue solution in an oven overnight at 56°C. The slides were washed in 96% ethanol and then washed with tap water. The slides were then incubated in 0.1% lithium carbonate for 30 seconds to differentiate the myelin staining. The differentiation was then continued in 70% ethanol for 30 seconds and then washed in tap water. The staining was checked visually using the microscope to ensure differentiation was complete. The slides were then counterstained with Cresyl violet for 30-40 seconds and washed in distilled water. Slides were next placed into 100% alcohol then histoclear for 2 x 5 minutes and mounted onto Superfrost Plus glass slides.

2.12 Immunoenzyme staining

Frozen murine tissues

Spinal cord sections were immersed in ice cold fixative (75 % acetone and 25% ethanol) for 10 minutes and left to dry at room temperature. Sections were then outlined using a wax pen and rehydrated in wash buffer for 3 x 5 minutes. The slides were incubated for 30 minutes in blocking buffer (0.1% BSA (Sigma A7906), PBS and horse serum (10%) within a moisture chamber. Tissues were added to wash buffer (TBS (Sigma T6066) Tween 0.5% (Sigma P5927) and primary antibodies were added and incubated overnight at 4°C. The following day sections were washed in wash buffer before adding the biotinylated secondary antibody for 2 hours at room temperature. Tissues were washed in TBS Tween as previously described. Horse-radish peroxidase (HRP, ebioscience) was added (1:500) for 30 minutes at room temperature. Following washing with TBS Tween DAB (3, 3'-Diaminobenzidine, (Vector)) solution was added for 10-30 minutes at room temperature. The sections were washed in TBS and then dH_2O and

counterstained with hematotoxylin for 1 minute before rinsing under tap water. Sections were mounted using an aqueous tissue mounting medium.

Paraffin murine tissues

Paraffin slides were heated in an oven at 60°C for 35 minutes to soften the wax. The slides were then deparaffinised and hydrated through histoclear and a graded alcohol series (histoclear, 100% ethanol, 90% ethanol and 70% ethanol for 3 x 5 minutes each). The sections were then rinsed in distilled water for 5 minutes. To quench the endogenous peroxidase activity the tissues were incubated in 0.5% hydrogen peroxidase in methanol. The slides were then washed (TBST buffer) for 5 minutes. The slides were next incubated with sodium citrate in a pressure cooker for antigen retrieval and then left to cool then washed for 5 minutes in tap water. The tissues were “blocked” using 1% BSA 10% horse serum in PBS for 1 hour. The primary antibodies (anti-IL-33 1:40 and anti-ST2 (1:500)) were incubated overnight with the tissues at 4°C. The tissues were next left for 1 hour at room temperature. The slides were then washed and incubated with the appropriate biotinylated antibody for 1 hour at RT. Next the slides were washed and incubated with HRP for 1 hour at RT. After the HRP was washed off, antibody binding was visualised using Impact DAB (Vector) or AmecRed (Vector) solution and the reaction then stopped with tap water. Finally, the slides were counter stained using haematoxylin, dehydrated through a graded alcohol series (70%-95%-100%-histoclear) and then mounted using hydromount.

Double immunohistochemical staining was performed by repeating the above procedure, however using alkaline phosphatase in place of HRP and visualising with Vector® blue.

2.13 Immunofluorescent staining

OCT spinal cord sections were fixed with ice cold fixative (75 % acetone and 25% ethanol) for 10 minutes and left to dry at room temperature. Paraffin sections were deparaffinised and rehydrated as previously described. Sections were then outlined using a wax pen and rehydrated in wash buffer for 3 x 5 minutes. The slides were next incubated for 30 minutes in blocking buffer within a moisture chamber. Tissues were washed in wash buffer and then primary antibodies were added and the tissues incubated overnight at 4°C. Sections were immersed in wash buffer before adding the secondary labelled antibodies and incubated for 1 hour. Tissues were then washed as before and mounted in DAPI hardest (Vector Laboratories) and sealed with clear nail varnish. Using an epi-florescent microscope, images were captured of the spinal cord sections at magnifications of 10, 20 and 40 times.

Table 2.2. Primary antibodies used during the Immunohistochemical staining of murine tissues.

Antibody	Species	Isotype	Dilution	Supplier
IL-33	Goat	IgG	1:40	R and D Systems
IL-33	Rat	IgG	1:60	R and D Systems
ST2	Rabbit	IgG	1:200	Sigma
ST2	Rat	IgG	1:100	MD Bioscience
NeuN (clone A60 MAB377)	Mouse	IgG1	1:100	Millipore
GFAP	Rabbit	IgG	1:500	DAKO
Iba1	Goat	IgG	1:100	WAKO

Table 2.3. Isotype control antibodies used during the Immunohistochemical staining of murine tissues.

Species	Isotype	Dilution	Supplier
	IgG		Vector
Rat		1:1000	
Mouse		1:200	
Rabbit		1:100	

Table 2.4. Secondary (biotinylated) antibodies used during the Immunohistochemical staining of murine tissues.

Species	Dilution	Supplier
Rat	1:100	BD pharmagen
Mouse	1:100	eBioscience
Rabbit	1:100	Vector

Table 2.5. Fluorescent Antibodies used during the Immunohistochemical and immunocytochemical staining

Antibody	Species	Dilution	Supplier
Streptavidin FITC	N/A	1:200	Vector
Streptavidin Texas Red	N/A	1:143	Vector
TRITC	Mouse	1:100	Invitrogen
TRITC	Rabbit	1:100	Invitrogen
TRITC	Goat	1:100	Invitrogen

2.14 In Vitro Myelinating Cultures

This protocol of generating myelinating spinal cord cultures (Sorensen et al. 2008) has been modified from Thomson et al., (Thomson et al. 2006) for use in rats.

Isolation of the corpus striatum

Neurospheres were derived from the corpus striatum of P1 Sprague Dawley rats. Pups were killed by i.p injection of euthathal in accordance to UK Home Office guidelines.

Using a dissection microscope, the brain was removed from the skull and separated into the two cerebral hemispheres using a scalpel (no.22 blade). Both hemispheres were orientated into a sagittal position. The tissue directly surrounding the striatum was isolated by making an incision at the front of the corpus callosum and then a second incision at the lateral ventricle; once isolated it was placed rostrally. The caudate nucleus of the striatum was then removed using curved forceps (Dumont no. 5) and placed into a bijou containing 1 ml of L-15 medium.

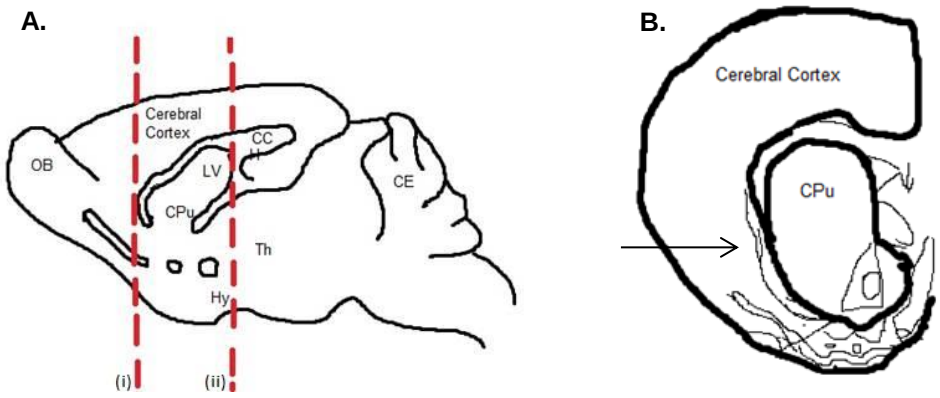

Figure 2.1 Extraction of rat striatum from P1 rat brain. A. Sagittal section of rat brain from P1 SD rats. To remove the striatum from each hemisphere

two incisions were made. The first incision was made at the frontal tip of the corpus callosum (i) and the second at the lateral ventricle (ii). B. When the section surrounding the striatum has been removed from the rest of the cerebral hemisphere it is placed in a rostral orientation where the striatum is easily visible and can be removed with curved forceps. Figures adapted from Budantsev et al., 2007 and Gammie et al ., 2004. *Abbreviations: cc, corpus callosum; CE, cerebellum; CPu, caudate-putamen complex (striatum);H, hippocampus; Hy, hypothalamus; LV, lateral ventricle, OB, olfactory bulb; S, septum; Th, thalamus.*

Creation of neurospheres

The striata were gently titrated using a glass Pasteur pipette and centrifuged for 5 minutes at 800rpm (~136RCF). The supernatant was removed and the pellet re-suspended in 2ml of neurosphere medium (NSM) and added to an uncoated T75cm^3 flask (Fisher Scientific). The volume within each flask was made up to 20ml and supplemented with 20 ng/mL of mouse sub maxillary gland epidermal growth factor (EGF, R and D systems) to promote sphere formation.

Neurospheres were grown at 37ºC/5% CO_2 changing two thirds of the media every 2-3 days. Growth of neurospheres usually took approximately 7 days before they were large enough to be plated down to form astrocytes.

Generation of Astrocyte Monolayer

Coverslips (13mm, VWR) were coated in 13.3µg/ml poly-L-lysine (PLL) (Sigma-Aldrich, Dorset, UK) for 3 hours at 37°C. The PLL was then removed and the coverslips washed 3 times in sterile dH_2O. The coverslips were then placed into a 24 well plate and left to air dry before use.

Neurospheres were transferred into a 50ml falcon tube and centrifuge for 5 min at 800rpm (~136RCF). The supernatant was removed and the pellet was re-suspended in 2ml DMEM + 10% FBS and triturated using a glass Pasteur

pipette. The volume of medium was made up to 12ml of DMEM + 10% FBS and 500µl of cells were added to each well (~50,000 cells/ coverslip). The volume of each well was then made up to 1ml (using DMEM + 10% FBS) and samples incubated at 37ºC/5% CO_2. The cells were maintained by removing half the medium and replacing it with fresh medium. Growth took 7 days before the astrocytes formed a confluent monolayer on the coverslip.

Dissociated spinal cord cultures

Myelinating spinal cord cultures were generated as described previously (Sorensen et al. 2008).

Isolation of embryonic rat and mouse spinal cord

Time-mated Sprague Dawley female rats or C57BL/6 female mice were killed at embryonic day E15.5 and E13.5 respectively by overdose of CO_2 (day of plugging denoted as E0.5). The abdominal skin and fur were sterilised with 70% ethanol. A lower incision was made and the uterus removed and placed in ice cold HBSS (Hank's balanced salt solution (GIBCO, Invitrogen, cat. number 14170)).

Embryos were dissected from the gravid uterus and decapitated approximately 3mm rostral to cervical flexure. The cranial 5- to 6- mm sections of spinal cord from E15.5/E13.5 embryos were dissected, stripped of meninges and placed in a bijoux containing 1mL of HBSS.

Generation of myelination spinal cord cultures

The tissue was gently triturated using a glass Pasteur pipette and then enzymatically dissociated by adding 100µl of 10X trypsin (Sigma, T3924) and 100µl of 1% collagenase (Sigma, C9722) for 15 minutes at room temperature. Enzymatic activity was stopped by adding 2mL of SD solution

containing 0.52mg/mL soybean trypsin inhibitor (Sigma, T9003), 3.0 mg/mL BSA (Sigma), and 0.04mg/mL DNase (sigma) to prevent cell clumping.

The cells were triturated and spun at 800rpm for 5 minutes and the pellet was re-suspended in plating medium. A live cell count was performed using a haemocytometer and trypan blue stain.

For the rat culture, three coverslips supporting the astrocytes were placed in a 35mm petri dish and the dissociated rat spinal cord cells were plated onto the coverslip with a density of 150, 000 cells/50µl.

For the mouse cell cultures the mouse dissociated spinal cord cells were plated onto a coverslip with a density of 150, 000 cells/50µl, and 50 µl per coverslip.

The cells were left to attach for 2 hours in 37ºC/5% CO_2 after which 400µl of plating medium and 600µl of differentiation medium containing 0.5mg/mL insulin (Sigma) was added. The cultures were fed three times a week with differentiation medium (DM (+)) by removing half the media and replacing it with fresh media. After day 12, insulin was removed from the differentiation medium (DM (-)) to promote myelination. The cultures were maintained for 26-28 days at 37ºC/5% CO_2 (Sorensen et al. 2008).

Treatment

Cells were incubated with 100ng IL-33 (R and D systems) from day 12-28. Cells were fed three times a week by removing 500µl of medium and replacing it with 500µl of fresh medium containing the required treatment.

2.15 Immunocytochemistry

Cells were fixed with 4% paraformaldehyde (PFA) (Fisher Scientific F/1451PB17) for 20 min, washed in PBS and then permeabilised with 0.5% Triton X-100 (Sigma, T9284) for 15 min (RT) and finally added to blocking buffer for 30 min (RT). Fixed and permeablised cells were incubated overnight at 4°C with primary antibody diluted in blocking buffer. After washing with PBS, an appropriate fluorochrome conjugated secondary antibody (Table 4.) was added for 15 min (RT). Coverslips were then washed in PBS followed by dH_2O and mounted in Vectashield (Vector labs).

Table 2.6. Primary antibodies used for Immunocytochemistry

Antibody	Species	Isotype	Dilution	Supplier
IL-33	Goat	IgG	1:40	R and D Systems
IL-33	Rat	IgG	1:60	R and D Systems
ST2	Rabbit	IgG	1:200	Sigma
ST2	Rat	IgG	1:100	MD Bioscience
NeuN (clone A60 MAB377)	Mouse	IgG1	1:100	Millipore
GFAP	Rabbit	IgG	1:500	DAKO
SMI-31 (Ab24570)	Mouse	IgG1	1:1000	Abcam
MBP (clone 26)	Mouse	IgG2a	1:100	Chemicon
O4	Mouse	IgM	1:200	Millipore
Olig2	Rabbit	IgG	1:500	Millipore

Live immunocytochemistry

Cells were incubated with primary antibodies in 50µl of primary antibodies diluted in DMEM at 4°C for 30 minutes. The cells were then immediately fixed with 4% PFA for 20 minutes. The coverslips were next blocked in blocking buffer for 30 minutes at RT. After washing with PBS an appropriate fluorochrome-conjugated secondary antibody was added for 15 minutes. Coverslips were then washed in PBS followed by dH_2O and mounted in Vectashield (Vector labs).

2.16 Image capture and analysis

Image capture

All images taken for analysis of cell number, morphology and axonal/myelin quantification were obtained using an Olympus BX51fluroscent microscope. For myelin analysis, a minimum of thirty images were taken per experiment. Images were taken in a random fashion, ten images per coverslip. For myelin analysis images were taken at X10 magnification and for cell counting images were taken at X20 magnification.

Quantification of axonal density

Cells were stained for the neurofilament marker SMI-31 to visualise the axons and images were taken at X10 magnification. The images were analysed using the software Image J. Using this software each image was separated into three channels i.e. blue, red and green channels. The channel which corresponded with the SMI-31 stained cells was converted into a black and white image. The axonal density is calculated by finding the percentage

of SMI-31 pixels compared to the total number of pixels within the image (Figure 2A).

Quantification of myelinated axons

Oligodendrocytes and myelin were stained with the myelin marker MBP and a minimum of ten images per cover slip were taken at x 10 magnification. Using Image J software the red, green and blue channels of each image was separated, the channel which matched the myelin/ODC channel was converted to a black/white image. ODC/myelin density was calculated as the number of positive pixels expressed as a percentage of the total number of pixels per field of view (Figure 2B)

As MBP (or any other myelin marker) does not differentiate completely between the myelin produced and the ODC itself the myelin sheaths need to be manually highlighted using Adobe Photoshop elements ® (blue) and measure using a macro in Image J. To determine the percentage of myelinated axons the myelin pixels are divided by the SMI-31 (axon) pixels in the same field.

Cell counting

To quantify cell populations images were taken at x20 magnification from three coverslips per experiment. The immune-positive cells associated with DAPI (nuclear stain) were counted using the Image J cell counter. Cell counts were expressed as a percentage of the total number of $DAPI^+$ nuclei in the field of view.

IL-33 and ST2 quantification

The expression of IL-33 and ST2 in EAE and MS tissues was quantitated using Image J utilising the threshold plugin and adjusting the brightness and contrast the percentage of IL-33 and ST2 pixels were calculated per field of view.

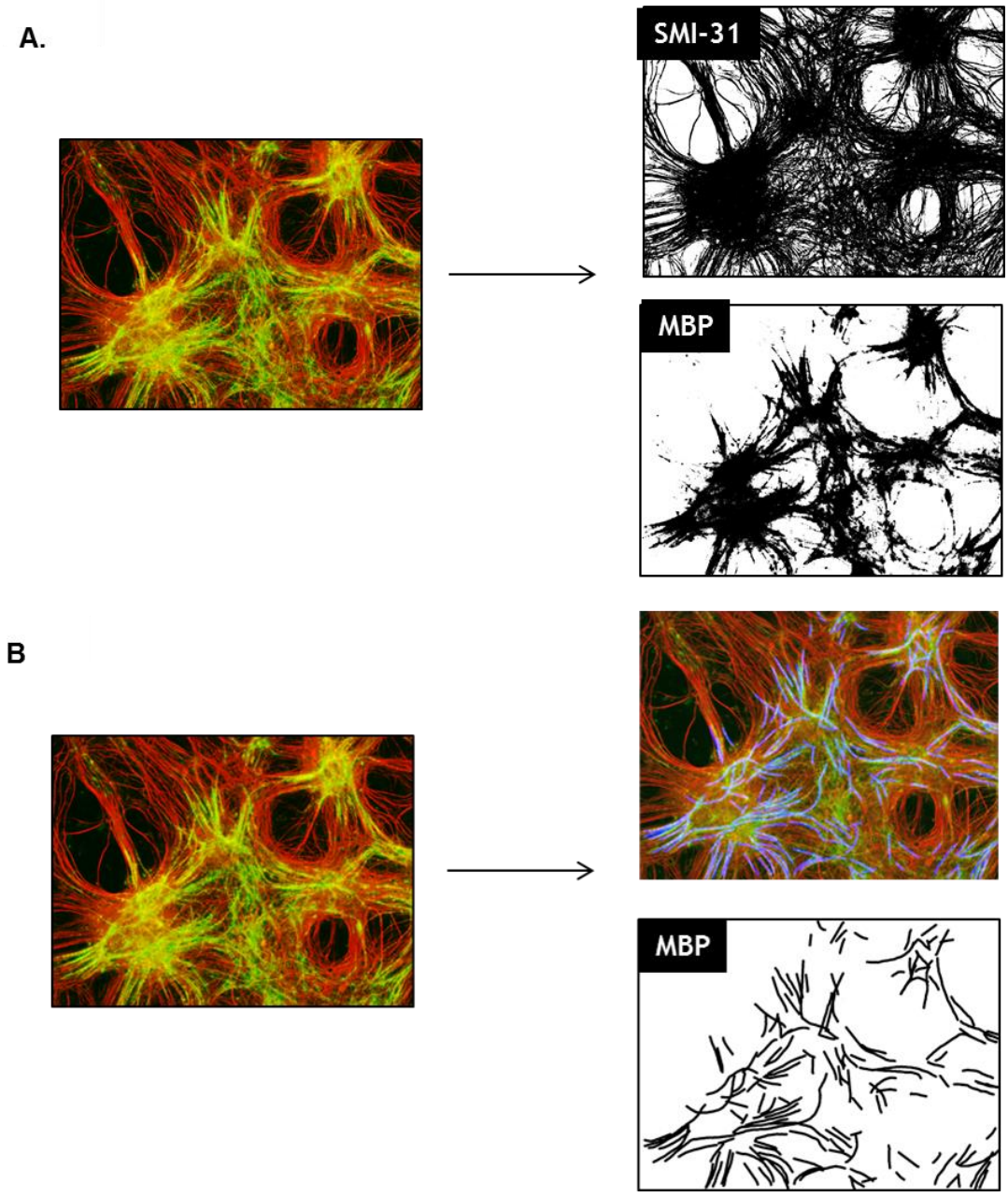

Figure 2.2 Quantification of axons and myelin. Axonal density was calculated my splitting each image into the individual channels in image J. The channel corresponding to SMI-31(axons) in red was changed to a black and white image. The axonal density was calculated by dividing the percentage of black pixels (SMI-31 $^{+}$) by the total number of pixels in that field (A). The percentage of myelinated axons was quantified by placing a transparent layer on top of the image in Adobe Photoshop® and drawing over the myelin (blue). The myelin was then quantified by using a macro within Image J. Myelination was expressed as the total number of myelin pixels / total number of SMI-31 pixels (B).

Statistical analysis

The data reported here were compiled from 3 experiments and analysed in the statistical package JMP 8.0 (S.A.S) using linear models. Percentage axonal density and percentage myelinated axons were analysed to determine the difference between days *in vitro* (DIV) (days 12, 18 and 28) and between control and IL-33 treated cultures at day 28DIV. Microglia, astrocytes and oligodendrocyte counts were compared between treated (IL-33) and untreated (media alone) cultures at day 12, 18 and 28 DIV. Including "Days In Vitro" as a factor enabled the differences between timepoints to be assessed. Significant differences between groups ($p<0.05$) were determined by Student's t-test for the most complex term in the minimal model. Significant pairwise differences ($p<0.05$) among groups were determined using Tukey's All Pairs adjusted p-values for the most complex term in the model.

2.17 Myelin Quantification Macro (written by John Annan)

```
//set the thresholds here
thresh_red = 33;
thresh_green = 79;
thresh_blue = 128;

//get the name of the open image, and the folder it came from
iTitle=getTitle;
imageDirectory = getDirectory("image");
print (imageDirectory);
print ("Image name,Red Black,Red White,Green Black,Green White,Blue Black,Blue White")

//build a list of all images in the folder
fList=getFileList(imageDirectory);
selectWindow(iTitle);
run("Close");

//start the loop to open files
for (i=0; i<fList.length; i++){
        //check that file is a valid image
        if (endsWith(fList[i],"tif")) {
        //if it is valid, open it
        open(imageDirectory + fList[i]);

        //build names of color component images
        iTitle=getTitle;
        iTitleRed=iTitle + " (red)";
```

```
iTitleGreen=iTitle + " (green)";
iTitleBlue=iTitle + " (blue)";


//split image into colour components
run("RGB Split");

//get red and blue areas and threshold

string="image1=["+iTitleGreen + "] operation=AND image2=[" + iTitleBlue+"] create";
run("Image Calculator...", string);
iTitleAND = getTitle;
setThreshold(thresh_blue, 255);
run("Threshold", "thresholded remaining black");
run("Invert");

//measure areas
getStatistics(area, mean, min, max, std, histogram);
n_blue_black=histogram[0];
n_blue_white=histogram[255];

//close windows
selectWindow(iTitleAND);
run("Close");
selectWindow(iTitleBlue);
run("Close");


//get red threshold
selectWindow(iTitleRed);
setThreshold(thresh_red, 255);
```

```
run("Threshold", "thresholded remaining black");
run("Invert");

//measure areas
getStatistics(area, mean, min, max, std, histogram);
n_red_black=histogram[0];
n_red_white=histogram[255];

selectWindow(iTitleRed);
run("Close");

//get green threshold
selectWindow(iTitleGreen);
setThreshold(thresh_green, 255);
run("Threshold", "thresholded remaining black");
run("Invert");

//measure areas
getStatistics(area, mean, min, max, std, histogram);
n_green_black=histogram[0];
n_green_white=histogram[255];

selectWindow(iTitleGreen);
run("Close");

//display results
print
(iTitle+","+n_red_black+","+n_red_white+","+n_green_black+","+n_green_wh
ite+","+n_blue_black+","+n_blue_white);

}
```

2.18 Human Brain samples

The samples used within this chapter were from Professor Hans Lassmann's laboratory in Vienna, Austria. These samples have been extensively characterised and housed within the care of one of the most esteemed MS pathologists. The samples identified in this chapter range from acute to chronic, 36-83 years old and both female and male MS and control samples. This array of tissues samples has given a good overview of the expression of IL-33 and ST2 within certain variables. Although, perhaps hundreds of patient samples would be needed for a more coherent understanding of the expression of these molecules this however, is beyond the scope of this study. Chronic MS differs from acute MS in that the demyelination is usually more extensive due to persistent inflammation over a long period of time.

Table 2.7. Healthy control samples used in the identification of IL-33/ ST2 expression. Table details the identification number of the tissue sample, tissue type and the age and sex of the patient from whom it originated**.**

Tissue	Type	Age	Gender
132-92-5	Healthy Control	65	Male
421-92-5		80	Female
8-01-1		36	Female
579-91-3		46	Female
28-03-2		42	Female
68-93-4		83	Male

Table 2.8. Acute MS tissue samples used in the identification of IL-33/ ST2 expression. Table details the identification number of the tissue sample, tissue type and the age and sex of the patient from whom it originated.

Tissue	Type	Age	Gender
581-96-10D	Acute MS	35	Male
90-09-6		69	Female
A01-144		34	Female
S403-97		45	Male
270-99-2		45	Male
Spanien C2		40	Male
70-93-6		78	Male

Table 2.9 Chronic MS tissue samples used in the identification of IL-33/ ST2 expression. Table details the identification number of the tissue sample, tissue type and the age and sex of the patient from whom it originated.

Tissue	Type	Age	Gender
146-01-8	Chronic MS	41	Male
67-05-9		34	Male
39-03-15		67	Male
144-90-3		77	Female
244-94-7		81	Female
285-81-6		78	Female
72-83-6		64	Female

2.19 Immunohistochemistry of Human samples

Paraffin embedded tissues were dewaxed in xylene for 2 x 15 minutes then rinsed in 96% ethanol twice. Endogenous peroxidases were blocked with a 0.02% solution of hydrogen peroxidase in methanol for 30 minutes. The sections were then further rinsed in 96% ethanol and rehydrated gradually through 96%-70%-50% ethanol and then distilled water. The slides then underwent antigen retrieval using 0.01M citrate buffer at pH6.0 (IL-33) or EDTA (ST2 and all other antibodies) at pH 8.0 in a pressure cooker for 1

hour. Slides were left to cool then washed in TBS for 2 x 5 minutes. To block the non-specific staining slides were incubated with 10%FCS/DAKO (DAKO S3006) buffer for 20 minutes. The primary antibodies were incubated in 10%FCS/DAKO buffer overnight at 4°C (200 µl/ tissue). Slides were then washed with TBS 3 x 5 minutes and incubated with the appropriate biotinylated antibody in 10% FCS/DAKO for 1 hour at room temperature on a shaker. The biotinylated antibody was then washed off as previously described and Avidin–Peroxidase was added in 10%FCS/DAKO for 1 hour at room temperature on the shaker. Slides were next washed in TBS and developed in DAB and then tap water was used to stop the reaction after visual inspection under a microscope. IL-33 staining was enhanced using copper sulphate solution for 5 minutes. The slides were then counterstained in haematoxylin for 7 seconds and rinsed in tap water. Slides were dehydrated through graded alcohol 50%-70% then 3 x 96% and Butle acetate. Slides were mounted with eukitt and left to dry.

Double immunohistochemical staining was performed by repeating the above procedure however using alkaline phosphatase in place of HRP and visualising with Fast Blue.

Table 2.10. Primary antibodies used during the Immunohistochemical staining of human tissues.

Antibody	Species	Isotype	Dilution	Supplier
IL-33	Mouse	IgG1a	1:100	Enzo Lifescience
ST2	Rabbit	IgG	1:100	Sigma
GFAP	Rabbit	IgG	1:100	DAKO
SMI-31 (Ab24570)	Mouse	IgG1	1:100	Abcam
SMI-32	Mouse	IgG1	1:100	Stenberger Monoclonals Inc
CD68	Mouse	IgG	1:100	Abcam
Iba1	Goat	IgG	1:100	Wako
CA II	Sheep	IgG	1:500	Abcam

Table 2.11. Secondary antibodies used during the Immunohistochemical staining of human tissues.

Antibody	Species	Dilution	Supplier
Biotin	Sheep α mouse	1:500	Jackson Immunoresearch
Biotin	Donkey α mouse	1:250	
Biotin	Donkey α rabbit	1:2000	

Table 2.12. Detection antibodies used during the Immunohistochemical staining of human tissues.

Antibody	Species	Dilution	Supplier
Avidin Peroxidase	N/A	1:100	Jackson Immunoresearch
Alkaline Phosphatase	N/A	1:100	
DAB	N/A	N/A	Vector
Avidin Cy2	N/A	1:100	Jackson Immunoresearch
Cy3	Donkey α rabbit	1:200	
Cy5	Donkey α rabbit	1:200	
Cy3	Donkey α sheep	1:100	
Dylight	Donkey α mouse	1:100	
Dylight	Horse α mouse	1:100	

2.20 Reagents

Phosphate Buffer Saline (PBS) 10X (1L H_2O) pH 7.0

NaCL	80g		Sigma
KCL	2 g		Sigma
$Na_2HPO47H_2O$	11.5g	Sigma	
$Na_2HPO47H_2O$	2g	Sigma	

Phosphate Buffer Saline (PBS) 1 X (1L H_2O) pH 7.0

PBS 10X	100 ml	
dH_20	900ml	

Tris-buffered Saline (TBS) 10X (1L H_2O) pH8.4

Trizma Base	61g	Sigma
NaCl	90g	Sigma

Tris-buffered Saline (TBS) 1 X Tween (0.05%) (1L H_2O) pH8.4

TBS 10X	100ml	
dH_20	900ml	
Tween 20	500 µl	Sigma

Sodium Citrate (0.05% Tween) (1 L, pH6.0)

Sodium Citrate	2.94g	Sigma
dH_20	1000 ml	
Tween 20	500 µl	Sigma

Blocking Buffer (1% BSA, 10% Horse serum)

1x PBS	45 ml	
BSA	0.5g	Sigma
Horse Serum	5ml	

Ethylenediaminetetraacetic acid (1mM EDTA, 0.05% Tween 20, pH8.0)

EDTA	0.37g	Sigma
dH_2O	1000ml	

1M Sulphuric Acid

18M Sulphuric Acid	27.8ml
dH_2O	474.4 ml

-

1 M Tris-HCl

Tris base	60.5g	Sigma
dH_2O	500 ml	

Adjust to pH 9.0 using 1 N HCl

Hydrogen Peroxidase Block (0.5%)

Methanol	50ml	VWR
H_2O_2	250µl	Sigma

70% Ethanol

Absolute ethanol	700 ml	Sigma
dH_2O	300ml	

Poly-L-Lysine (PLL)

PLL hydrobromide	25 mg	Sigma
dH_2O	6.25 ml	

* Dissolve in 6.25ml sterile H2O. Sterilise by filtering through a 0.22µ filter and store at -20°C in 66ul aliquots

Collagenase

Collagenase	20mg	Sigma
Leibovitz L-15 media	20 ml	Invitrogen

Sterilise using 0.22µ filter and store at -20°C.

<u>Neurosphere media</u>

Glucose (30%)

D-glucose	30g	Sigma
dH_2O	100ml	

Sodium hydrogen carbonate (7.5%)

NaHCO3	7.5g
dH_2O	100ml

DMEM/ F12 (10X)

DMEM (high glucose) 1 sachet	Invitrogen

Ham's F-12 Nutrient Mix		Invitrogen
Sterile dH_2O	5500ml	

Hepes (1M)

HEPES	23.8g	Sigma
dH_2O	100ml	

Putrescine

Putrescine	96.6 mg	Sigma
dH_2O	100ml	

Selenium (3mM)

Sodium Selenate	1mg	Sigma
dH_2O	1.93 ml	

Progesterone

Progesterone	1mg	Sigma
95% Ethanol	1.59ml	Sigma

Hormone mix (10X)

10X DMEM/F12	25ml	Invitrogen
30% Glucose	5ml	
0.5% $NaHCO_3$	3.75 ml	
1M Hepes	1.25 ml	
dH_2O	187.5 ml	
Apo-human transferrin	250mg	Sigma
Human insulin	6.25ml	Sigma
Putrescine (600NM)	25ml	Sigma
Sodium selenite (3mM)	25ml	Sigma
Progesterone	25ml	Sigma

Epidermal growth factor (EGF)

Recombinant murine EGF	1mg	Peprotech
Sterile dH_2O	1 ml	

Use at a final concentration of 4ng/ml (4nl EGF/ 20mlneurosphere media)

Neurosphere medium

DMEM/F12(x10)	25ml
Hormone mix (x10)	25ml

30% glucose 5ml
7.5% NaHCO3 3.75ml
1M Hepes 1.25ml
L-Glutamine (200nM) 2.5ml

Astrocyte growth medium

DMEM(1g/L) 179ml		Invitrogen
Foetal bovine serum	20ml	Biosera
L-Glutamine(200nM)	1ml	

Plating medium

DMEM (4.5g/L glucose)	50ml
Horse serum	25ml
HBSS	25ml

Differentiation medium (DM)

Biotin (1mg/ml)

Biotin	100mg
1M NaOH	100ml

Dilute 1 in 100 with dH2O filter using a 0.22n filter and store at -20°C. Use at a final concentration of 10ng/ml

Hydrocortisone

hydrocortisone	100mg
dH2O	27.6ml

* Dilute 1 in a 1000 by adding 20Nl to 19.88ml of sterile H2O to create a 10NM stock. Filter through a 0.22N filter and store in 250Nl aliquots at -20°C.

Insulin (500ng/ml)

Insulin(bovine pancreas)	100mg
10mM HCl/H2O	200ml

Differentiation medium + insulin (DM+)(50ml)

DMEM (4.5g/L glucose)	47.25ml
Biotin (1mg/ml)	50 µl
N1 supplement (100X)	500 µl
Hydrocortisone (10nM)	250 µl
Insulin(0.5mg/ml)	1 ml

Differentiation medium –insulin (DM -)

DMEM (4.5g/L glucose)	48.2 ml
Biotin (1mg/ml)	50ul
N1 supplement (100X)	500µl
Hydrocortisone (10nM)	250µl

SD inhibitor

Trypsin inhibitor (soybean)	13 mg
DNase 1 (bovine pancreas)	1mg
BSA fraction V	75mg
Leibovitz	25 ml

4% Paraformaldehyde (PFA)

Paraformaldehyde	40g
Phosphate buffer (0.1M)	1000ml

0.5% Triton X -100

Triton X-100	0.5ml
dH_2O	100ml

Ice cold fixative

Acetone	700ml
Ethanol	300 ml

Scott's tap water substitute (STEWS)

Sodium hydrogen carbonate	10g
Magnesium sulphate	100g
dH_2O	5L

Acid/Alcohol (0.3%)

Ethanol	2800ml
dH_2O	1200ml
Conc HCl	12ml

3. IL-33 and ST2 expression in the CNS tissues of naïve and EAE mice

3.1 Introduction

As introduced previously, IL-33 is a member of the IL-1 superfamily of which there are currently 11 members (see Table 1.2) (Schmitz et al., 2005). Schimitz et al. reported that the mRNA of IL-33 is expressed by many tissues such as the stomach, lung and skin. Low level expression was also observed in the lymph nodes, spleen, pancreas, kidney and heart, as well as endothelial cells, DCs and macrophages in mice. Furthermore, a high level of murine IL-33 mRNA was expressed by the brain and spinal cord tissues. In humans, IL-33 is present on mast cells, DCs, lung fibroblasts, dermal fibroblasts and endothelial cells in the mammary, prostate and lungs (Schmitz et al., 2005). This resulted in an intensive search to understand the function of IL-33 in the CNS. Indeed several studies have suggested that IL-33 plays an important role in CNS neurodegenerative diseases such as AD, ALS and Toxoplasma gondii (Chapuis et al. 2009; Jones et al. 2010; Lin et al. 2012).

MS and EAE are primarily mediated by Th1/Th17 driven responses, with enhanced Th2 and Treg responses during the recovery phase (Venken et al. 2008; Weaver et al. 2005). As IL-33 recruits Th2 cells and produces IL-5 and IL-13, this suggests that IL-33/ST2 has an important role to play in EAE/MS through modulating the peripheral immune responses (Komai-Koma et al. 2007). The exact function of IL-33 in the CNS is not clear. IL-33 has been identified on astrocytes and brain endothelial cells in culture (Yasuoka et al. 2011) and within tissues (Christophi et al., 2011). ST2 has been identified on astrocytes but also microglial cells, implying a possible autocrine or paracrine IL-33 function (Yasuoka et al. 2011; Schmitz et al. 2005; Hudson et al. 2008).

To understand the function of the IL-33/ST2 signaling pathway in the CNS and its contribution towards the development of MS/EAE, I first studied the expression of IL-33 and ST2 in the spinal cord and brain tissues of naïve, PBS-treated (PBS) and MOG-immunised (EAE) mice. I investigated whether the expression levels in the CNS tissues correlated with the clinical disease severity observed. The aims of this chapter were therefore:

1. To characterise EAE clinical profile and immune responses in EAE mice compared to control mice.

2. To study the CNS pathology associated with EAE using immunohistochemical staining and Luxol blue staining.

3. To determine the expression of IL-33 and ST2 within the spinal cord and brain of control and EAE mice, and whether there is a correlation between the expression levels and clinical severity.

3.2 Results

Clinical score of MOG and PBS immunised C57BL/6 mice

EAE was induced in C57BL/6 mice as described in the Materials and Methods chapter. Two groups of female C57BL/6 mice were immunised with MOG+CFA or PBS+CFA s.c. at day 0, together with an i.p. injection of 100ng of PTX at day 0 and 2. MOG-induced EAE in C57BL/6 background mice is a self-remitting monophasic disease model. EAE mice started to develop clinical symptoms at days 9-12, demonstrating a limp tail and a gait in their walk. By day 18, the peak of the disease, mice developed complete hind limb paralysis and partial forelimb paralysis. After day 18 the mice began to enter a recovery phase where partial but not full recovery was observed at day 28 (Figure 3.1). Control mice, immunised with PBS+CFA, and naïve mice developed no clinical signs of disease.

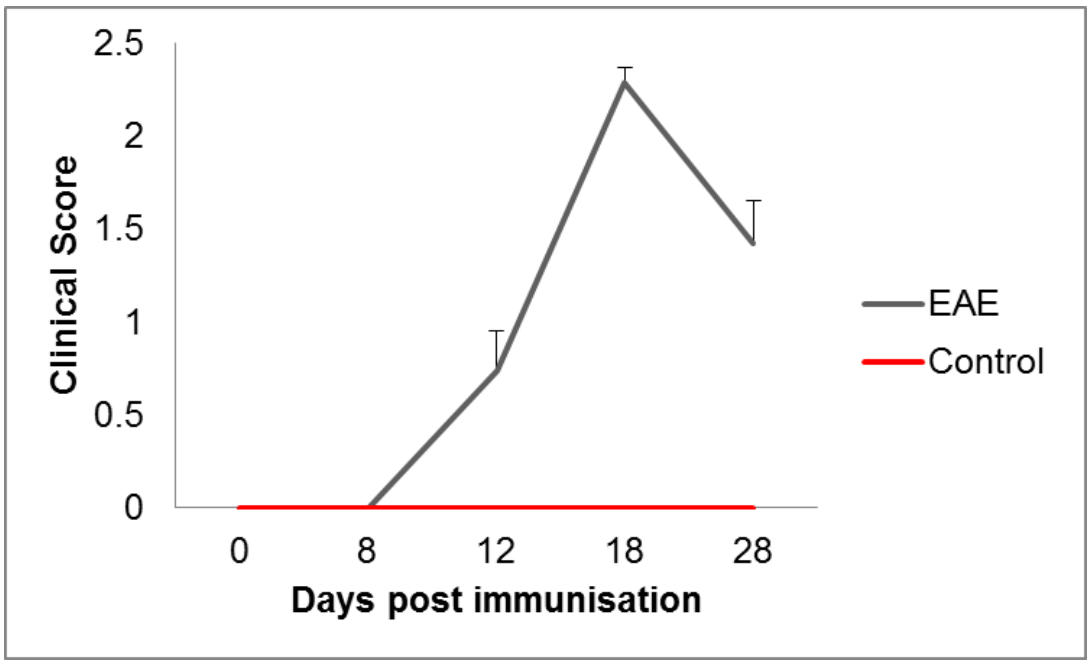

Figure 3.1 EAE clinical score of PBS and MOG immunised mice. EAE was induced in C57BL/6 mice by immunisation with MOG_{35-55}+ CFA+PTX

while controls received PBS+CFA+PTX. Clinical symptoms were then monitored/ EAE mice are shown in black n=3, control PBS+CFA immunised mice are shown in red n=3. Graph shows mean and standard errors of daily clinical scores. The data are representative of 3 experiments.

Cytokine production by the spleen cells of MOG- and PBS immunised mice

I then went on to study the systemic immune responses of EAE and control mice. The spleen is useful in determining the cytokine profile during EAE. When MOG and CFA were injected through the skin, the antigen was drained into the LNs, and presented to naïve T cells. The spleen has a similar action but drains mainly from the blood. Once activated, lymphocytes migrate from the lymph nodes to the spleen to proliferate and secrete cytokines (Yang et al. 2002). To evaluate the immune responses in MOG-immunised EAE and PBS-immunised control mice, mice were sacrificed at day 18 post immunization (PI) and spleens were harvested and cultured *in vitro* with MOG or medium alone as a control. The supernatants were collected for ELISA measurement of IL-17 and IFN-γ (Figure 3.2). Our data showed that only the splenocytes, collected from MOG-immunised EAE mice and subsequently re-stimulated with MOG *in vitro*, significantly increased levels of IL-17A and IFN-γ (Figure 2). Cells harvested from untreated or PBS-immunised mice did not show any IL-17A and IFN-γ production, suggesting an antigen-specific production of cytokines. This data was in agreement with Murphy et al., who demonstrated that IL-17 and IFN-γ producing $CD4^+$ T cells (Th1/Th17) are likely the most important effector T cell subsets in the development of MS and EAE (Murphy et al. 2010).

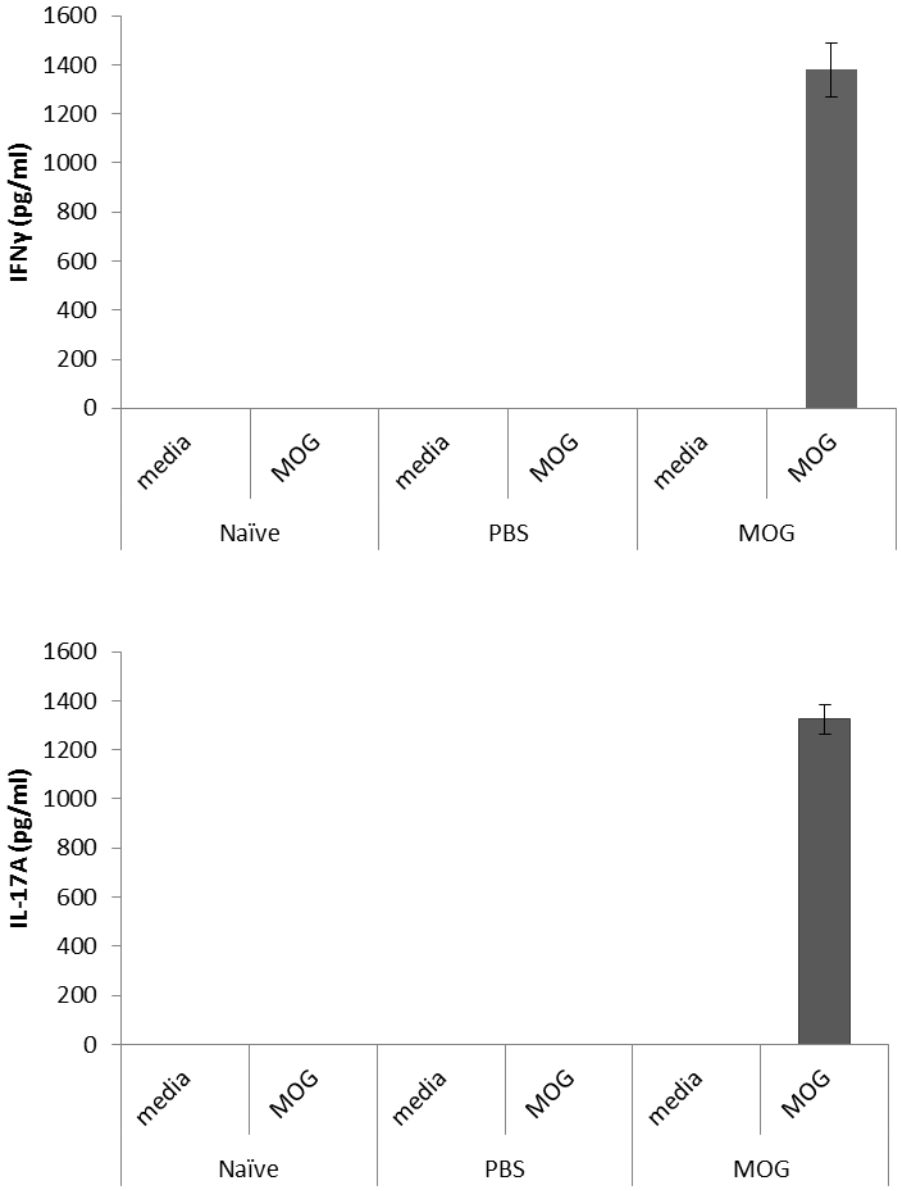

Figure 3.2 Cytokine production by spleen cells at peak of EAE disease. Spleen cells from D18 PI were cultured and treated with medium or medium containing MOG_{35-55} for 48 hours. The supernatants were collected and ELISA was performed for IFN-γ **(A)** and IL-17A **(B)** representative of pulled data, mean ± S.E.M, n=1

Histology of spinal cord tissues from naïve, and PBS or MOG immunised mice

To understand the clinical symptoms of EAE development in the mice, I proceeded to use H&E staining to examine the spinal cord morphology in

control and then the EAE mice. Spinal cords were harvested from naïve and PBS-immunised mice at day 18 PI, fixed in PFA and embedded in paraffin. The results show that naïve (Figure 3.3A) and day 18 PBS-immunised mice (Figure 3.3B) spinal cord tissues have similar tissue morphology. There was no sign of cellular infiltration or inflammation in the white or grey matter of the spinal cord tissues. The normal morphology of the spinal cord in PBS-immunised mice, confirmed that PBS immunised mice had no clinical signs of EAE disease (Figure 3.1). Furthermore, their splenocytes produced non-detectable MOG-specific IL-17 and IFN-γ (Figure 3.2).

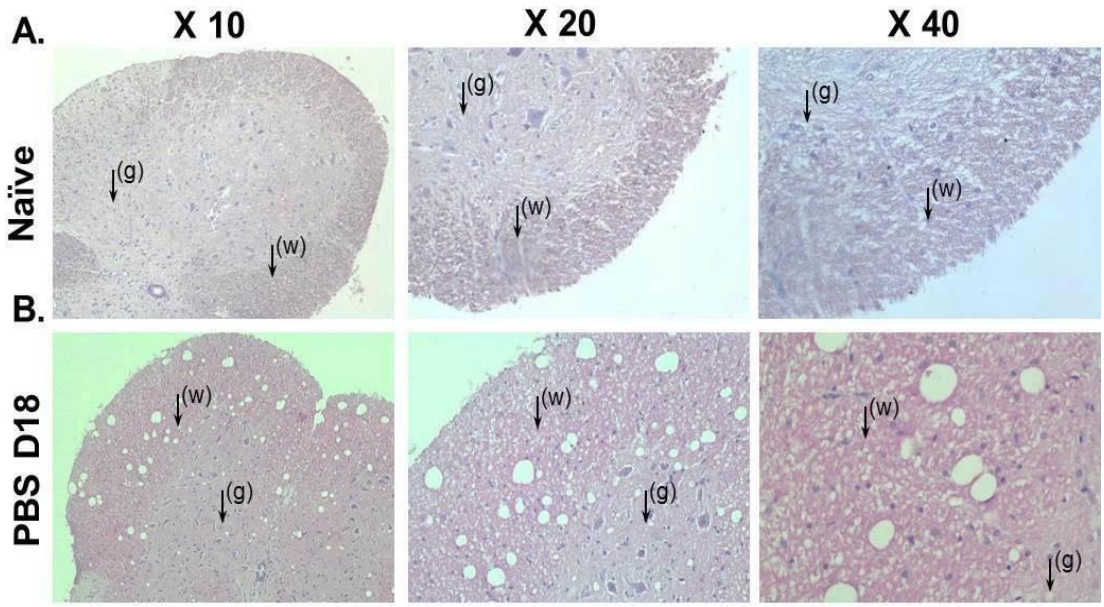

Figure 3.3 Histological analysis of spinal cord tissues from naïve and PBS-immunised mice. Spinal cords were harvested from naïve **(A.)** and PBS+CFA-immunised mice (Day 18) **(B.)** and subjected to H&E staining. White matter **(w)** and grey matter **(g)** are indicated with arrows.

Next I examined the spinal cord sections harvested from the EAE mice at day 8, 18 and 28 PI. The data showed that spinal cord harvested on day 8 post immunisation (Figure 3.4A) had low occurrence of leukocyte infiltration within the tissues. In contrast, there was significant leukocyte infiltration within the spinal cord white matter at day 18 PI (the peak of EAE when mice had severe paralysis (Figure 3.4B). At the recovery stage of EAE, day 28 PI,

there was a reduced level of leukocyte infiltration observed in the spinal cord tissues (Figure 3.4C).

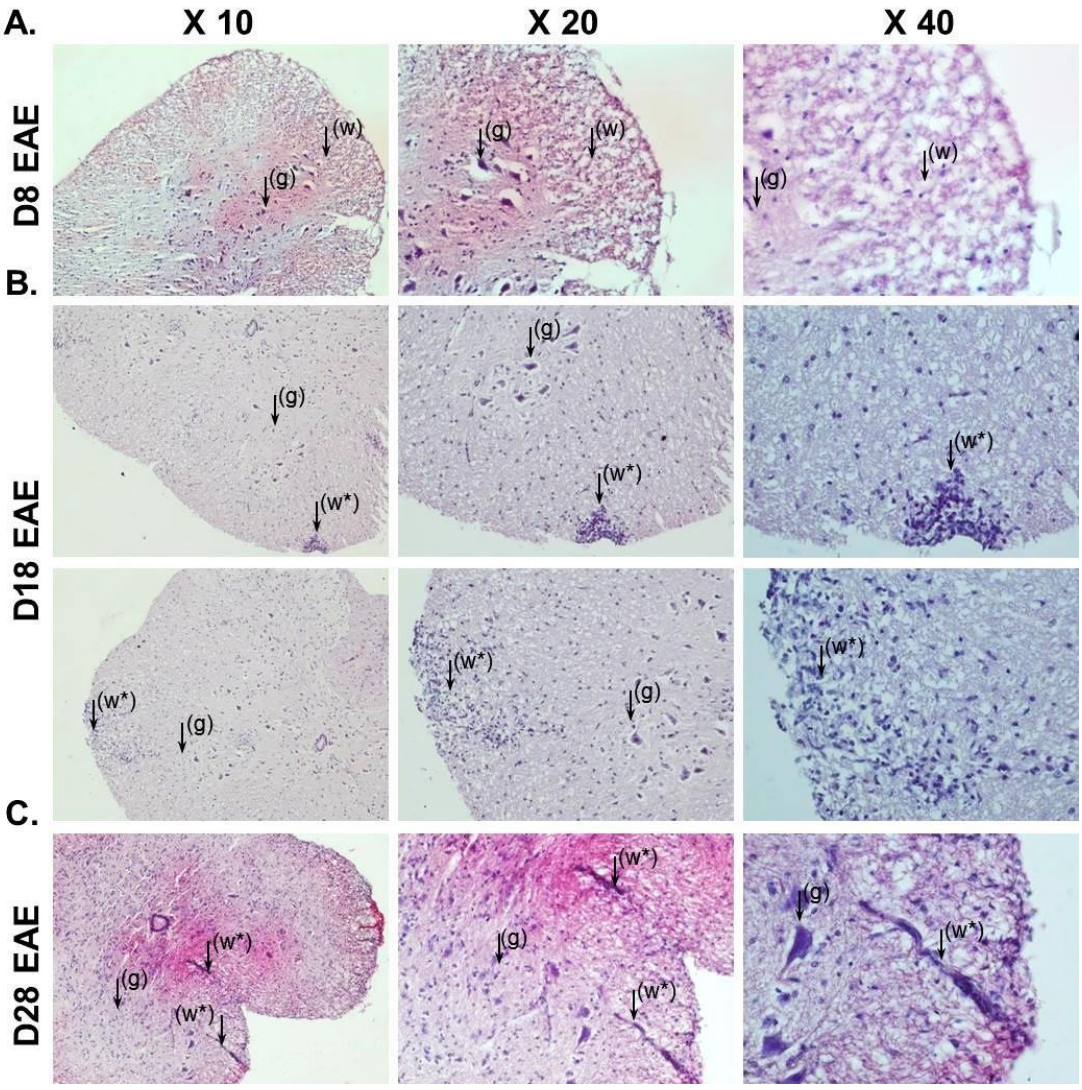

Figure 3.4 Histological analysis of EAE spinal cord sections. Spinal cords were harvested from EAE mice and were stained with H & E. Tissue morphology at day 8 **(A),** day 18 **(B)** and day 28 **(C)** post immunisation are shown. Normal white matter **(w)**, white matter with areas of cell infiltration/ inflammation **(w*)** and grey matter **(g)** are indicated by arrows.

As MS is an inflammatory demyelinating autoimmune disease, I then examined the myelin loss in the spinal cord tissues collected from naïve, PBS- and EAE-immunised mice, with a myelin-specific stain (Luxol fast blue). Neuronal cell bodies were counterstained with cresyl violet. As expected, in

control animals (Figure 3.5) intact myelin was seen within the white matter (w) and neuron cell bodies within the grey matter (g). Intact myelin was also observed in the spinal cord tissues of PBS-immunised mice, which confirmed that inflammation in EAE was a specific response to the MOG antigen injection. General peripheral activation of the immune system did not induce antigen-specific activation of T cells; therefore it resulted in no observable inflammation or demyelination in the CNS tissues (Figure 3.5). In EAE mice, at early stage day 8 PI, there was no myelin loss within spinal cord tissues (Figure 3.6A). At the peak of disease (Figure 3.6B) there were areas of demyelination - determined by the lack of Luxol fast blue staining (w*). This correlated with cellular infiltration observed in the H&E staining (Figure 3.4B). These results (Figure 3.4B and 3.6B) show the extent of damage to the spinal cord during EAE. After the peak of the disease (Figure 3.6C), the mice began to recover from the paralysis, and the clinical score was reduced. However, the areas of demyelination were still apparent suggesting the loss of myelin was not repaired at the resolution stage.

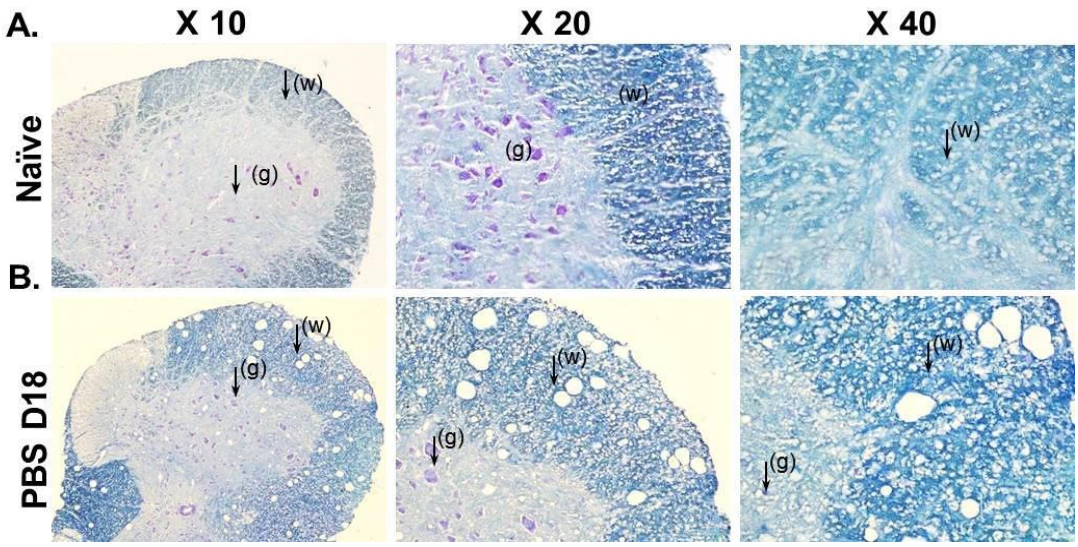

Figure 3.5 Luxol fast blue staining of control tissue. Spinal cords were harvested from naïve **(A.)** and PBS + CFA **(B.)** immunised mice (Day 18), stained with Luxol fast blue and counterstained with cresyl violet. White matter **(w)** and grey matter **(g)** are indicated with arrows.

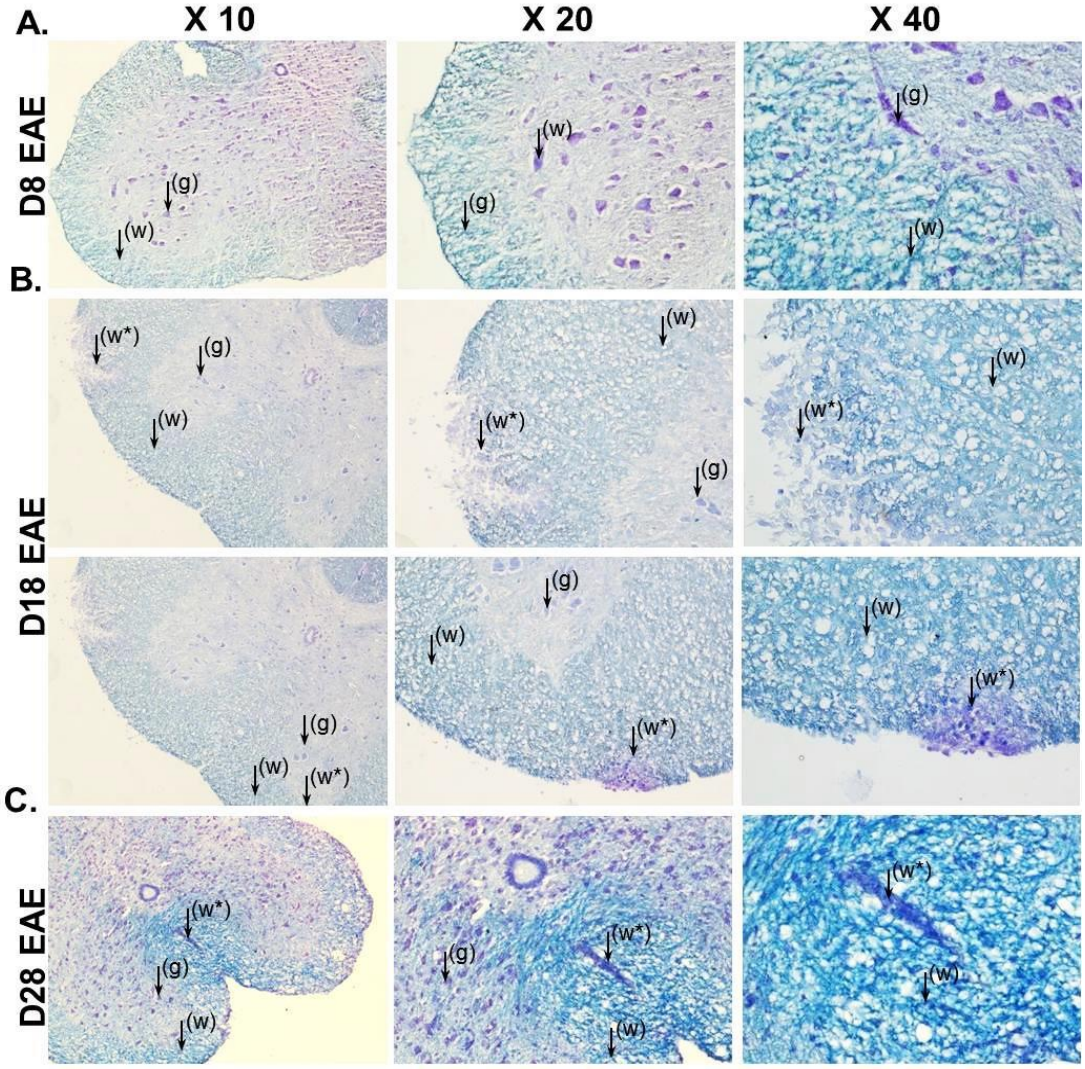

Figure 3.6 Luxol fast blue staining of EAE tissue. Spinal cords were harvested from EAE mice and were stained with Luxol fast blue. Tissue morphology at day 8 **(A)** day 18 **(B)** and day 28 **(C)** post immunisation are shown. Normal white matter **(w)**, white matter with areas of cell infiltration/ inflammation **(w*)** and grey matter **(g)** are indicated by arrows.

IL-33 expression in spinal cord tissues

IL-33 mRNA is highly expressed by the spinal cord and brain (Schmitz et al., 2005). Here, immunohistochemical staining was used to determine the distribution of IL-33 within the CNS of naïve, PBS- and MOG-immunised mice at day 18 PI. Firstly, I confirmed the specificity of IL-33 staining by using

an isotype antibody, which produced a negative result (Figure 3.7A), as anticipated. In naïve spinal cord, a nuclear distribution of IL-33 was observed within the white (w) and grey matter (g) of the spinal cord. However, IL-33 also showed a cytoplasmic distribution within the grey matter. Similar IL-33 staining was observed in tissues from naïve (Figure 3.7B) and PBS-immunised (Figure 3.7C) mice. This indicates that non-specific peripheral activation of the immune system did not alter the expression pattern or levels of IL-33 within the spinal cord. Furthermore, quantitative analysis of the IL-33 immunohistochemical staining (Figure 3.8) in the spinal cord tissue has shown that there was no difference in the expression of IL-33 in naïve and EAE tissues (Figure 3.9).

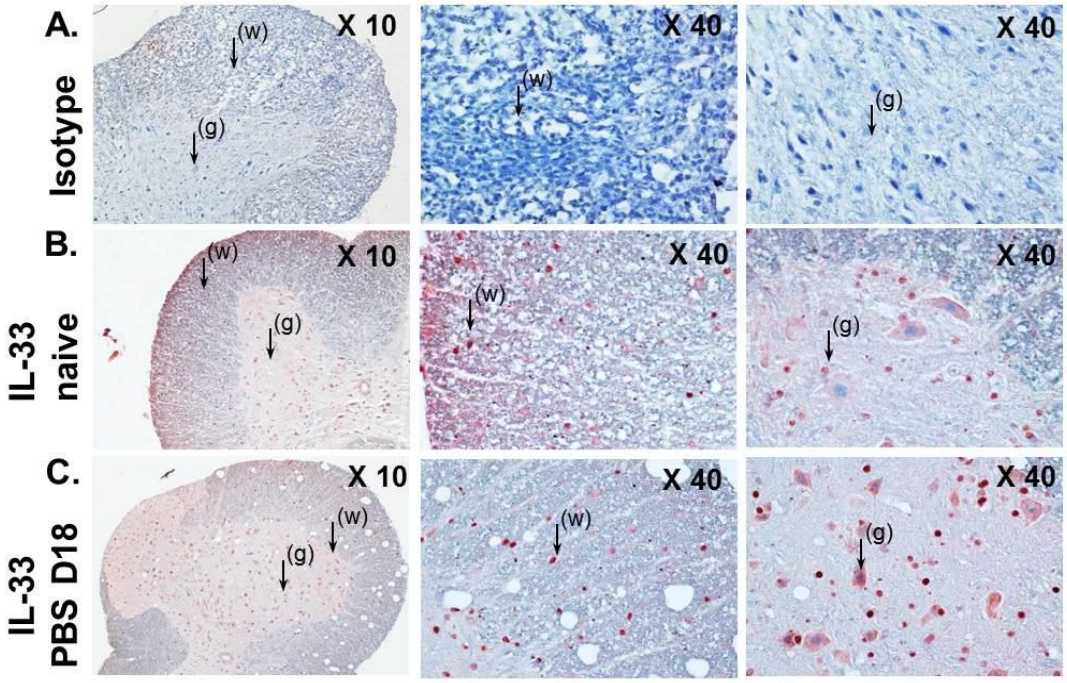

Figure 3.7 IL-33 expression on spinal cord sections of naïve and PBS immunised mice. Spinal cords were harvested from naïve **(A and B)** and PBS + CFA **(C)** immunised mice (Day 18) and stained with isotype control or anti-IL-33 (Amec Red). White matter **(w)** and grey matter **(g)** are indicated with arrows.

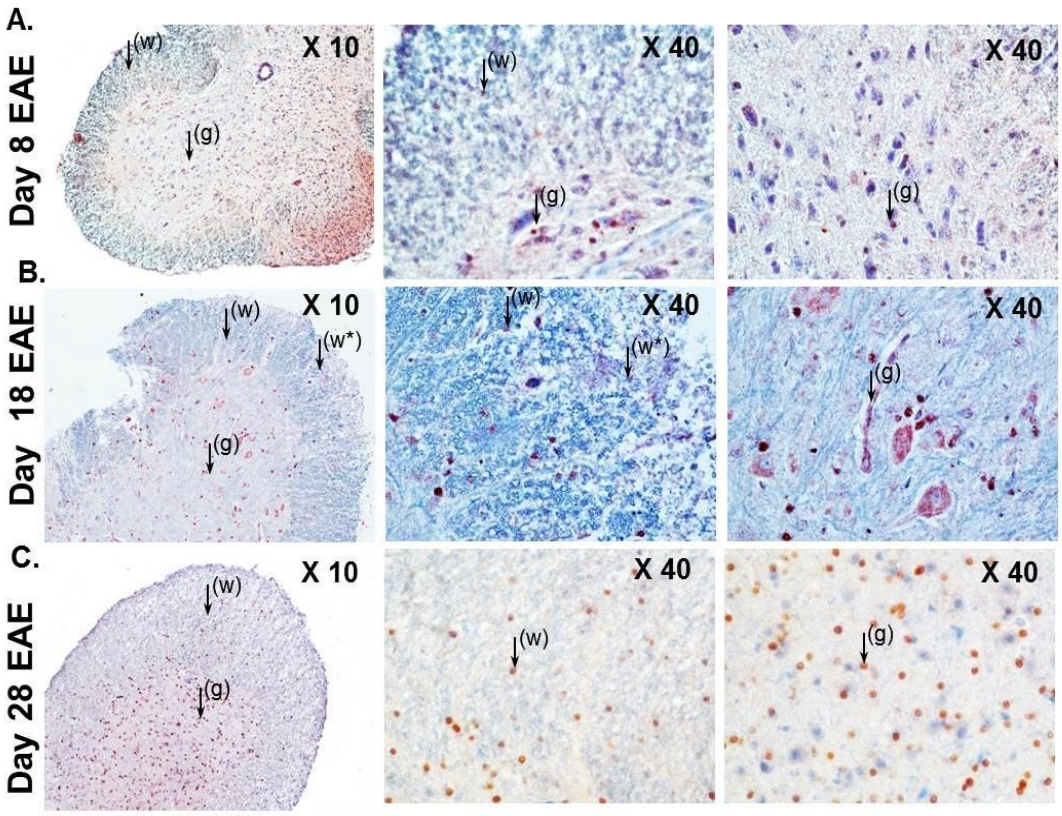

Figure 3.8 IL-33 expression on EAE spinal cord sections. Spinal cords were harvested and stained for IL-33 (DAB, brown) at day 8 **(A)** day 18 **(B)** and day 28 **(C)** post immunisation. Normal white matter **(w)**, white matter with areas of cell infiltration/ inflammation **(w*)** and grey matter **(g)** are indicated by arrows.

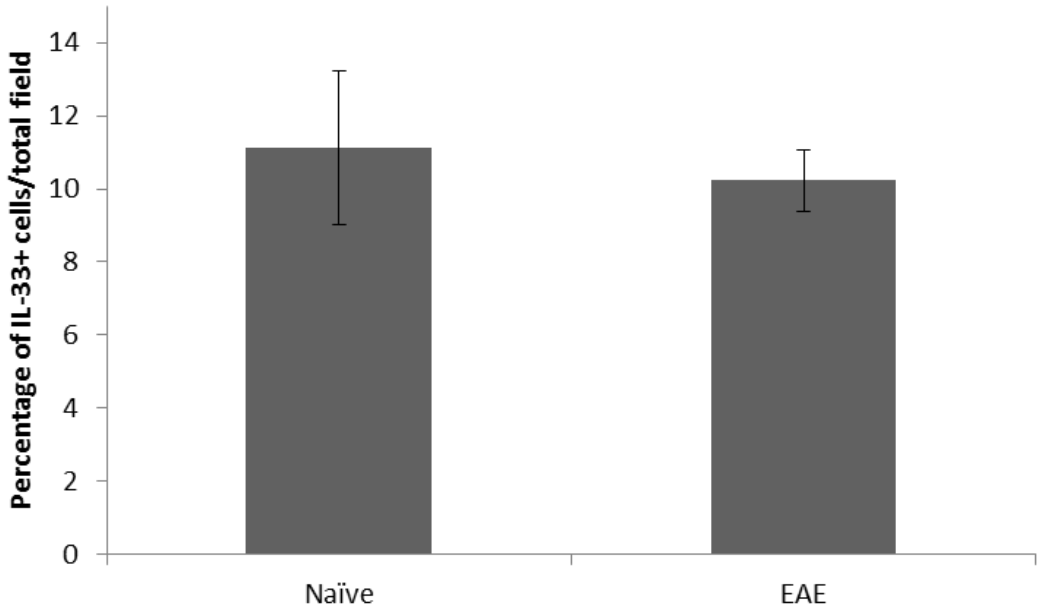

Figure 3.9 Quantitative analysis of IL-33 expression in naive and EAE spinal cord. Spinal cord sections from C57BL/6 naïve and EAE immunised mice were stained for IL-33 and quantified using image J. Data represents mean ± S.E.M, n=3

Previous studies have identified, the cortex (Kidd et al. 1999), ventricular regions (Hart et al. 1998) and the corpus callosum (Jagessar, Heijmans, Bauer, et al. 2012) as regions where lesions are present within MS patients. Therefore I proceeded to analyse the expression of IL-33 within these areas. IL-33 was expressed in different regions of brain sections (Table 3.1) however, these will not be the main focus of this thesis. Figure 3.10 shows that IL-33-positive cells were observed in the cortex, ventricular regions and particularly in the corpus callosum. A similar pattern and level of IL-33 staining was observed in the brain tissues of day 18 EAE mice (Figure 3.11).

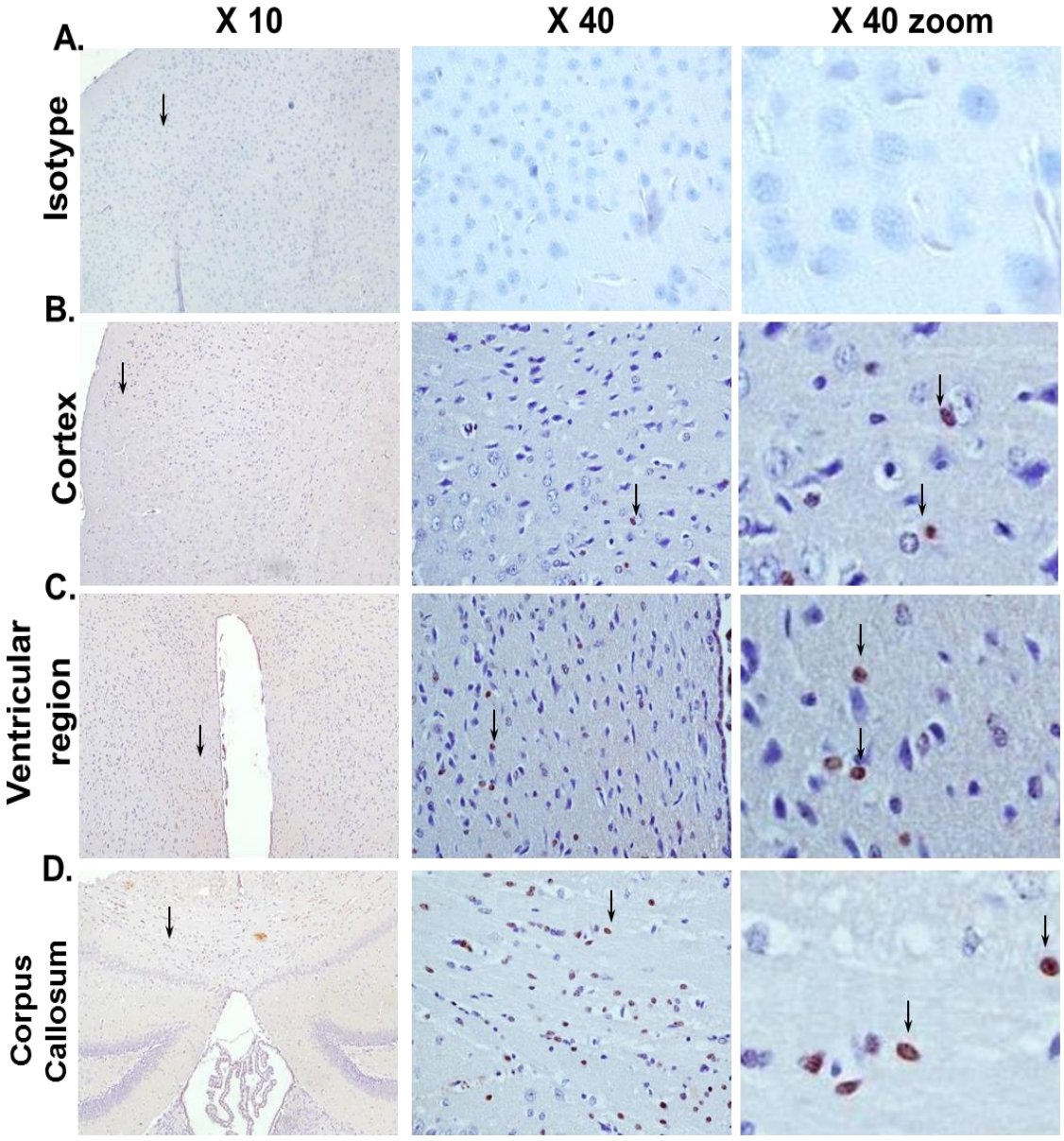

Figure 3.10 IL-33 expression in naive brain tissues. Brains were harvested from naïve C57BL/6 mice and stained with an isotype control or anti-IL-33 (Amec Red) within the cortex **(A, B)**, ventricular regions **(C)** and corpus callosum **(D)**. Arrows indicate the regions of magnification.

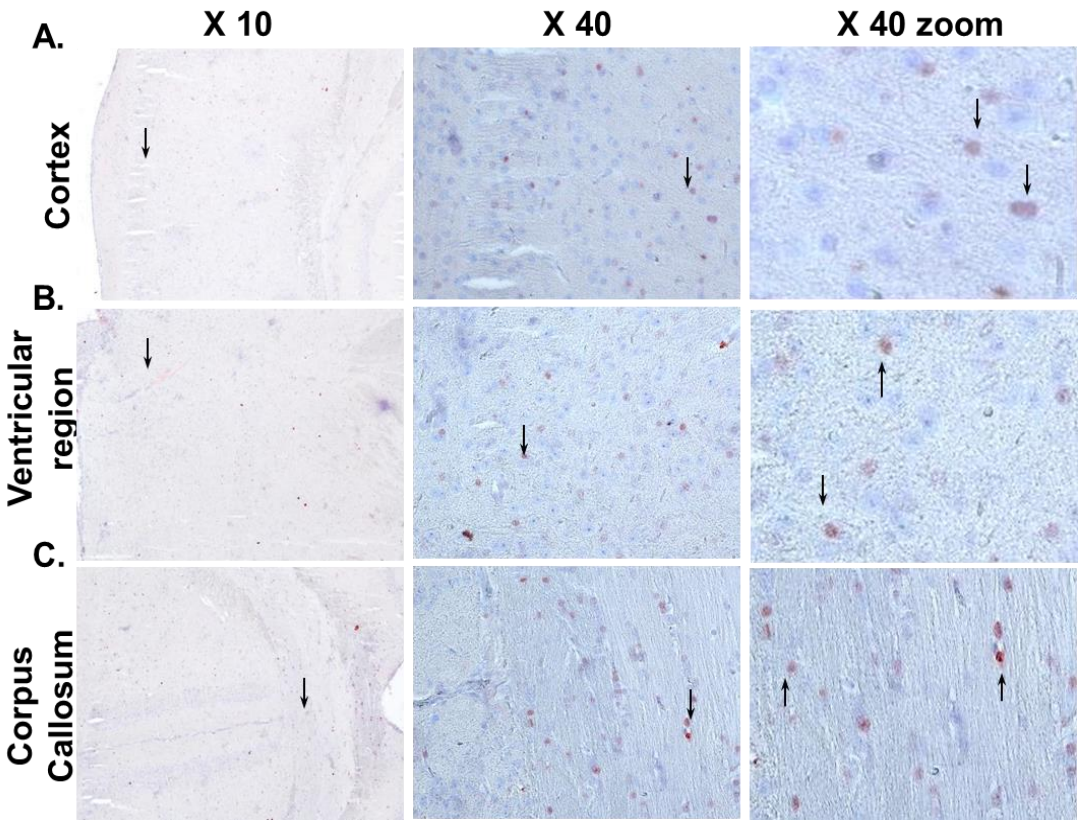

Figure 3.11 IL-33 expression in EAE brain tissues. Brain was harvested from EAE day 18 mice and stained with an isotype control or anti-IL-33 (Amec Red) within the cortex **(A)**, ventricular regions **(B)** and **(C)** corpus callosum. Arrows indicated the regions of magnification.

Table 3.1. IL-33 expression in C57BL/6 brain tissues. IL-33 was observed throughout the mouse brain to varying degrees, detail in the table below (Key: + low expression, ++ moderate expression).

Brain Region	IL-33
Olfactory bulb (GrO)	+
Orbitofrontal cortex (MO,VO)	+
Prefrontal cortex (PrL)	+
Cg1, Cg2 (Hippocampus)	+
Anterior commissure (aca)	++
Corpus callosum (cc)	++
Entorhinal cortex\cingulate cortex	++
Striatum (CPu)	+
Reticular Thalamus (Rt)	+
Fimbria of hippocampus (fi)	++
Stria terminalis (st)	++
Somatosensory regions (S1FL/HL)	+
polymorph layer DG (PoDG)	+
Stratum lacunosum-moleculare (LMol)	
LDDM (lateral dorsal nucleus)	++
RSA/RSG	+

ST2 expression in the CNS tissues of naïve, PBS and MOG immunised mice

IL-33 signals through the heterodimer receptor ST2 and the IL-1 adapter protein IL-1RAcP. ST2 binding activates the signaling pathway of MYD88, IRAK1/4 and TRAF6 initiating NF-κB, ERK, p38 and JUN (Funakoshi-Tago et al., 2008) allowing for the transcription of IL-33-associated cytokines (IL-6 and IL-5). To understand the function of IL-33 in CNS was also essential to know the expression of ST2 in the CNS resident cells.

Naïve and PBS-immunised spinal cord sections were stained with anti-ST2 antibody, alongside an isotype control (Figure 3.12). The results show the specific staining of ST2 within the white and grey matter of the control spinal cord tissues (day 18 PI). ST2 staining between naïve and PBS-immunised mice were comparable. ST2 showed a cytoplasmic distribution however, from these results ST2 was present within the nucleus of cells as well.

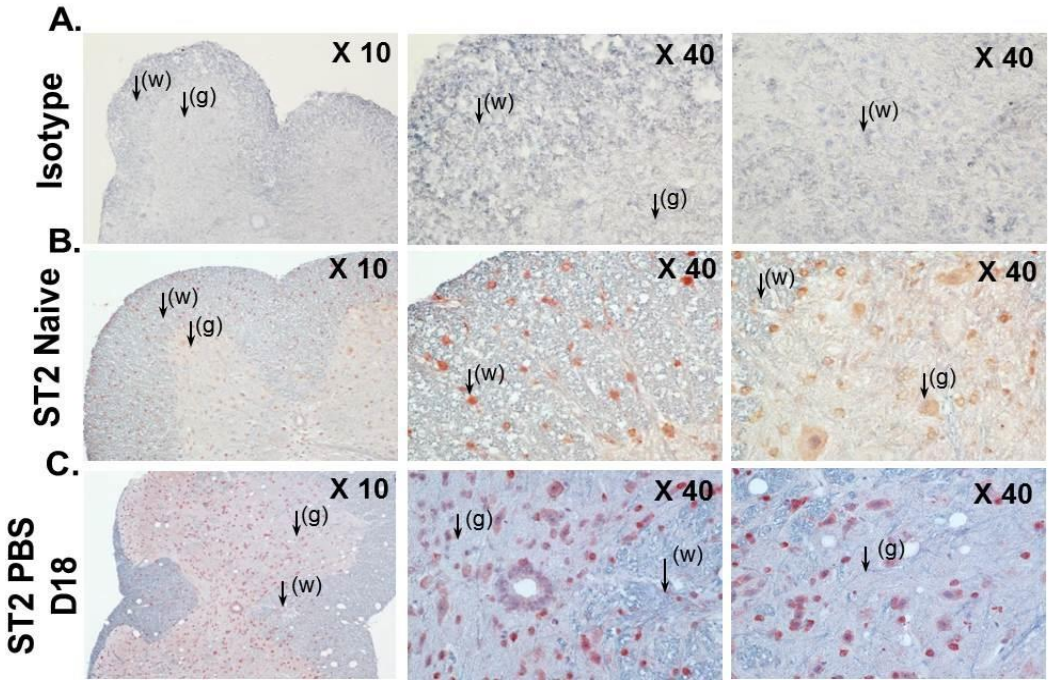

Figure 3.12 ST2 expression on control spinal cord sections. Spinal cords were harvested from naïve **(A and B)** and PBS + CFA **(C)**-immunised mice (Day 18) and stained with isotype control or ST2. White matter **(w)** and grey matter **(g)** are indicated with arrows.

ST2 was next stained within EAE spinal cord sections (Figure 3.13). The protein expression pattern of ST2 at the spinal cord at days 8, 18 and 28 was similar. Figure 3.13 indicates that ST2 was present on neurons as ST2 cytoplasmic staining was observed in cells with a large cytoplasm characteristic of neuronal cell bodies. As the disease progresses and the clinical signs of EAE begin to appear, ST2 staining was enhanced within

lesions (Figure 3.13C, X40 white matter) as well as around the edges of the tissues which coincides with myelin loss and cellular infiltration seen in Figure 3.6. Furthermore, quantitative analysis of the immunohistochemical staining of ST2 spinal cord tissue (Figure 3.14) has shown that there was no significant difference in the expression of ST2 in naïve and EAE tissues.

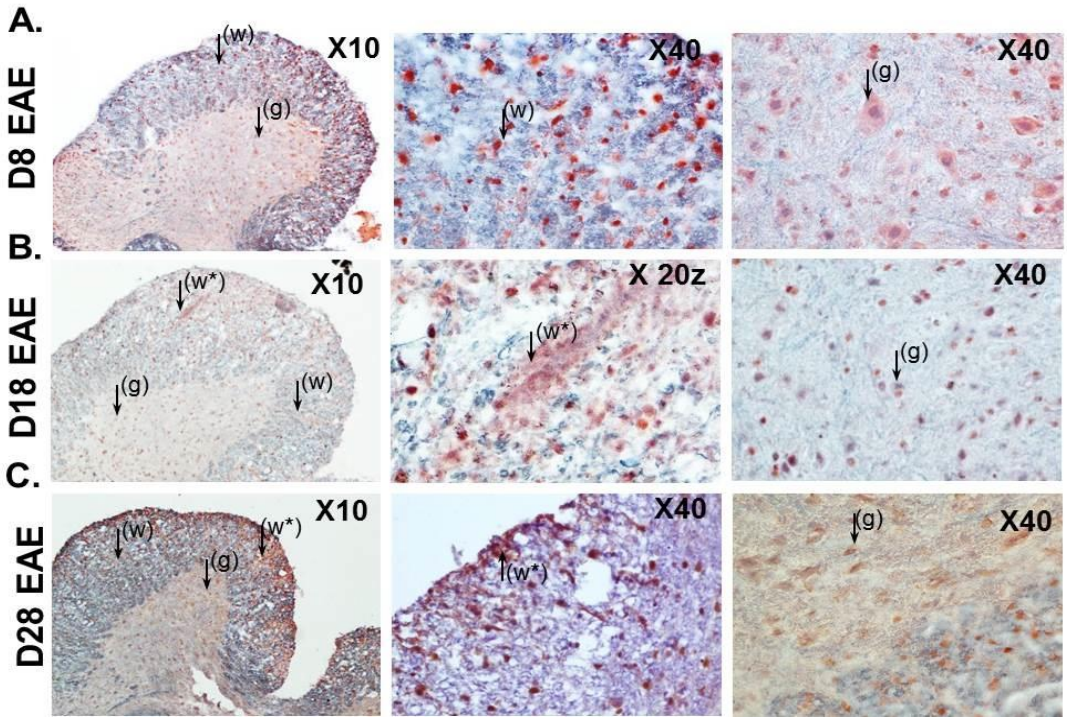

Figure 3.13 ST2 expression on EAE spinal cord sections. Spinal cords were harvested and stained for ST2 at day 8 **(A),** day 18 **(B)** and day 28 **(C)** PI are shown. Normal white matter **(w)**, white matter with areas of cell infiltration/ inflammation **(w*)** and grey matter **(g)** are indicated by arrows.

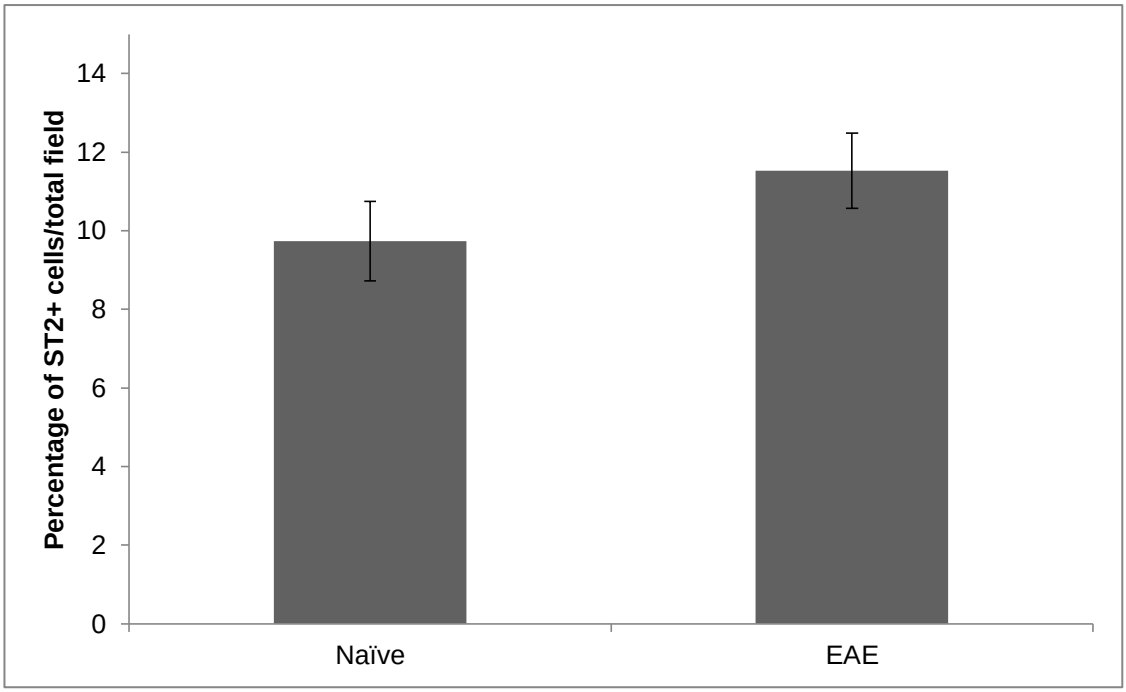

Figure 3.14 Quantitative analysis of ST2 expression in naive and EAE spinal cord. Spinal cord sections from C57BL/6 naïve and EAE immunised mice were stained for ST2 and quantified using image J. Data represents mean ± S.E.M, n=3

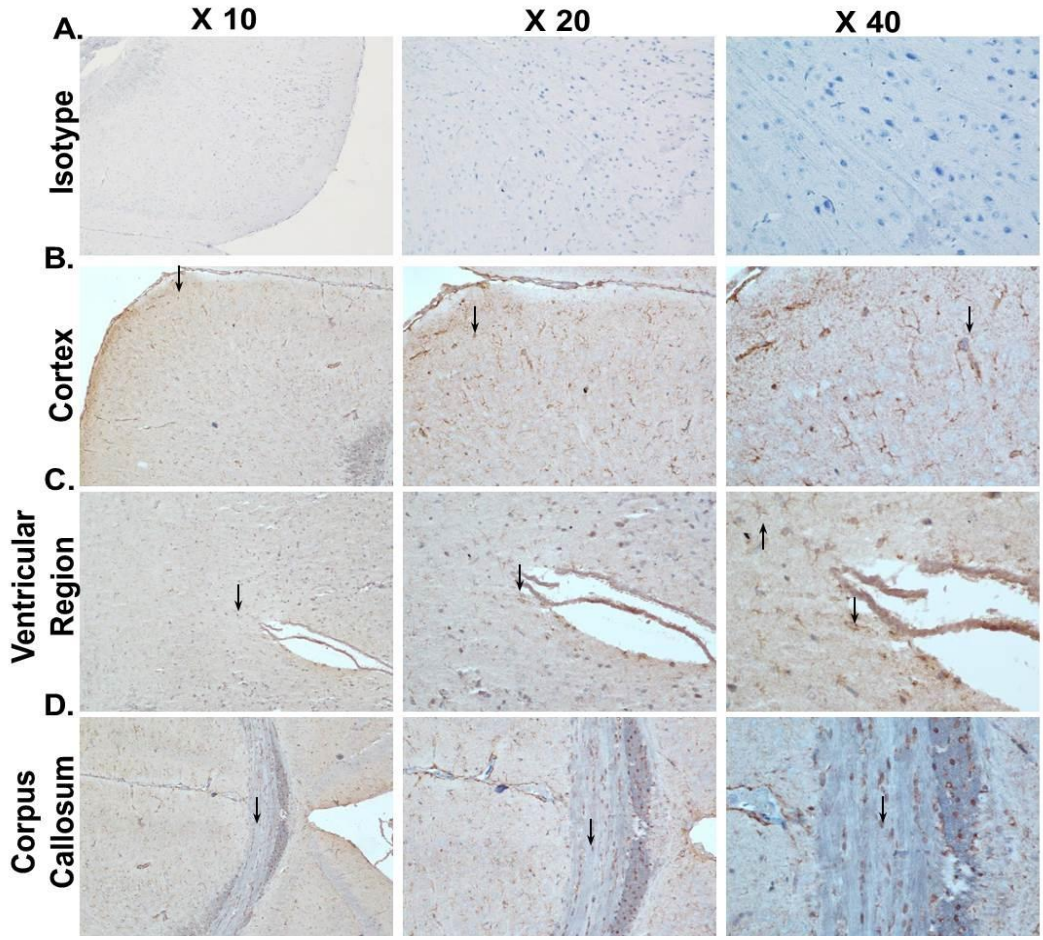

Figure 3.15 ST2 expression in naïve brain tissues. Brains were harvested from naïve C57BL/6 mice and stained for an isotype control **(A)** or ST2 within the cortex **(B)**, ventricular regions **(C)** and corpus callosum **(D)**. Arrows indicated the regions of magnification.

ST2 was then shown to be present within the brain of C57BL/6 control mice (Figure 3.15). Within the cortex of the brain, ST2 staining was cytoplasmic and also stained cellular projections within naïve mice. ST2 was also seen close to ventricles (Figure 3.15C) and within the corpus callosum (Figure 3.15D). However, ST2 was also expressed in other areas of the brain, for details see Table 3.2.

Table 3.2. ST2 expression in C57BL/6 brain tissues. ST2 was observed throughout the mouse brain to varying degrees, detail in the table below (Key: + low expression, ++ moderate expression).
.

Brain Region	ST2
Olfactory bulb (GrO)	
Orbitofrontal cortex (MO,VO)	+
Prefrontal cortex (PrL)	+
Cg1, Cg2 (Hippocampus)	+
Anterior commissure (aca)	
Corpus callosum (cc)	++
Entorhinal cortex	++
Striatum (CPu)	+
Reticular Thalamus (Rt)	+
Fimbria of hippocampus (fi)	++
Stria terminalis (st)	++
Somatosensory regions (S1FL/HL)	+
CA1/CA3 (Hippocampus)	+
polymorph layer DG (PoDG)	+
Stratum lacunosum-moleculare (LMol)	+
LDDM (lateral dorsal nucleus)	+
Substantia nigra (SNC/SNR/SNL)	+

Within EAE brain tissues (Figure 3.16) ST2 staining seems to be up-regulated compared to control mice tissues. Enhanced staining was observed within the cortex especially at the edges of the tissues, where cellular structures were clearly observed. Projection and nuclear ST2 staining within the ventricular region and corpus callosum, was observed within the brain compared to the expression in the spinal cord.

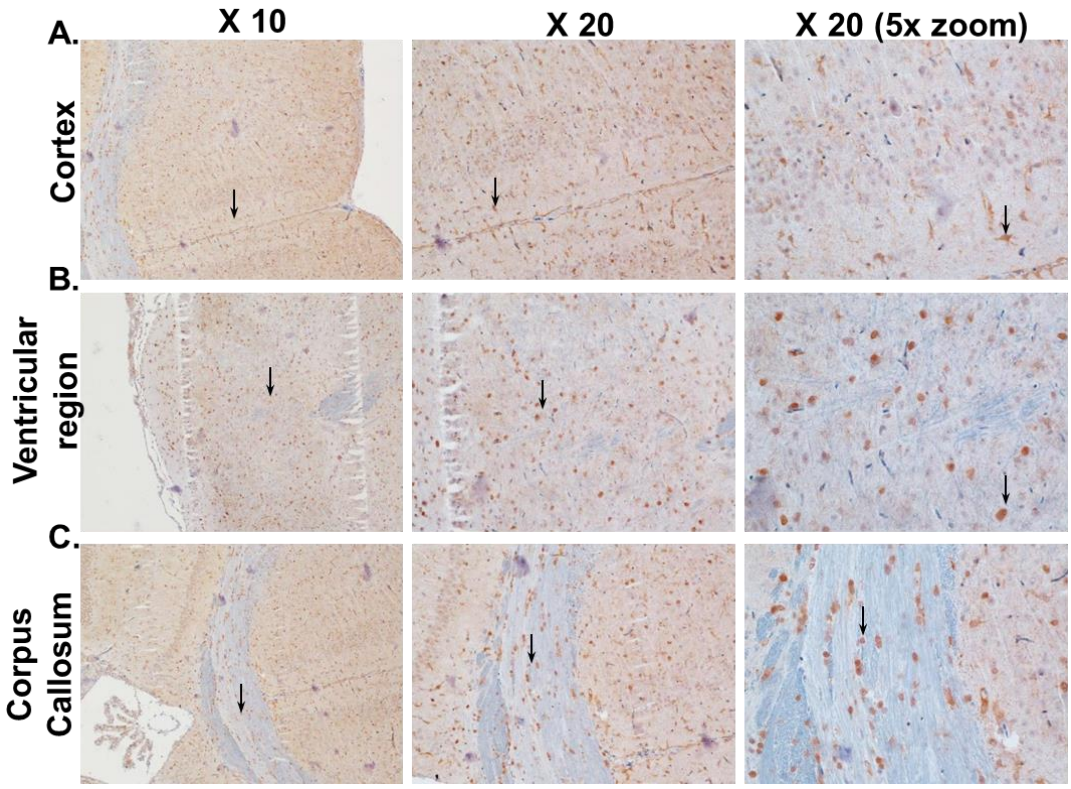

Figure 3.16 ST2 expression in EAE brain tissues. Brain was harvested from EAE day 18 mice and stained for an isotype control or ST2 within the cortex **(A)**, ventricular regions **(B)** and **(C)** corpus callosum. Arrows indicated the regions of magnification.

In conclusion, IL-33 was highly expressed within the spinal cord and brain of both control and EAE mice. However no significant differences in expression were noted. IL-33 showed nuclear staining as well as cytoplasmic staining in CNS resident cells. Similarly, its receptor ST2 was also highly expressed within the spinal cord and brain of control and EAE mice. Similarly to IL-33, there was no significant difference in ST2 protein expression in EAE spinal cord tissues in comparison to naïve tissues. The high expression of IL-33 and ST2 within the CNS tissues suggests that the IL-33/ST2 pathway has an important role in the development of EAE.

3.3 Discussion

EAE is a well-established animal model for research in MS disease because of the similarities in the immunopathological and neuropathological mechanisms. Over the years, EAE has proven to be a valuable tool in obtaining important insights into the immunomechanisms of the MS disease. It has also helped to develop effective clinical treatment for MS patients, e.g. the clinically approved glatiramer acetate and natalizumab (Dhib-Jalbut 2003; Hartung et al. 2002; Jacobs & Beck 2000; Weber et al. 2004; Zamvil & Steinman 1990). In this study, I used the MOG-induced EAE model, to investigate the expression of IL-33 and ST2 within the CNS of C57BL/6 EAE and control mice. After immunisation, the EAE clinical symptoms were monitored and tissues harvested at days 8, 18 and 28 PI for immune response and immunohistochemical analysis. In accordance with previous studies, the EAE disease course was acute and monophasic (Almolda et al. 2011; Farias et al. 2012). The mice began to develop symptoms such as a limp tail and gaited walk at day 9-12, and reached peak of disease at day 18 with both hind limb paralysis and partial fore limb paralysis. EAE mice began to recover from approximately day 20 until day 28.

As described in Chapter 1, systemic infections can cause relapses in MS patients (Moreno et al. 2011). Attenuated bacteria, *Mycobacterium tuberculosis* is used to enhance the clinical symptoms seen in EAE by stimulating IL-17 expression (Emerson et al. 2009; Stockinger & Veldhoen 2007). In this study, control mice (immunised with PBS instead of MOG antigen emulsified with CFA) were not able to induce any signs of CNS inflammation either clinically or histologically. Although peripheral infections enhanced the severity of established MS/EAE, our data suggest that peripheral activation of the immune system was not able to initiate CNS specific inflammation, and antigen-specific activation of immune cells, which is essential for the development of MS and EAE.

Th1 and Th17 cells are the main effector T cells in EAE development. They are primed in the periphery and migrate to the CNS by crossing the BBB, and initiate inflammation within the CNS (Murphy et al. 2010). I evaluated IFN-γ and IL-17 production by the spleen cells in naïve, PBS- and MOG-immunised mice at day 18 PI. The ELISA results showed that the splenocytes from MOG-immunised but not naïve or PBS-immunised mice secreted high levels of IL-17A and IFN-γ after restimulation with MOG_{35-55} in culture. The cells treated with medium alone showed no IL-17A and IFN-γ production for both MOG- and PBS-immunised mice. These results support the evidence that EAE is mainly mediated by Th1/Th17 immune cells (Connor et al. 2009). The spleen cells from MOG-immunised mice have been primed *in vivo* allowing them to recognise the MOG antigen *in vitro* and to produce pro-inflammatory cytokines typical of those seen within the EAE model (Zorzella-Pezavento et al. 2013).

To understand the function of IL-33 in the CNS compartments, I first investigated the expression of IL-33 in spinal cord tissues. My findings reveal that IL-33 was expressed in both white and grey matter in C57BL/6 spinal cord tissues, and that the staining showed both nuclear and cytoplasm localisation of IL-33. The presence of IL-33 in both the cytoplasm and nucleus has previously been shown in several studies identifying different splice variants of IL-33 with different cellular locations (Tsuda et al. 2009; Whitaker et al. 2012). My results also indicated that there was no significant differences in IL-33 expression between naïve and EAE mice within the spinal cord. IL-33 was expressed in low quantities in different regions of the brain, but clustered within the corpus callosum and cortex, these findings are consistent with a previous report which uses a novel IL-33-Lac-Z Gt reporter straining (Pichery et al. 2012a). Similarly to the spinal cord, IL-33 did not seem up-regulated in the brain of control mice (Figure 3.10) when compared to EAE (Figure 3.11).

I proceeded to investigate the expression of ST2 within the CNS. ST2 is a heterodimer receptor and was mainly expressed in the cytoplasm of cells within the grey matter. Additionally, nuclear staining was observed, along with ST2 staining within the white matter of the spinal cord. No significant difference in ST2 staining was observed in the naïve and EAE spinal cord however ST2 infiltrating cells were observed at the peak of the disease. This suggests that ST2 is expressed by infiltrating cells such as Th2 cells (Xu et al. 1998) and M2 macrophages (Kurowska-Stolarska et al. 2009). Consistent with the results from the spinal cord sections, ST2 also appeared upregulated within the CNS of EAE mice, when compared to control mice, despite no cellular infiltration (Stromnes et al. 2008). ST2 was expressed in the cortex, ventricular region and corpus callosum, showing distinct cytoplasm expression, as well as presence within cytoplasmic protrusions.

To conclude, both IL-33 and ST2 are highly expressed within the spinal cord and brain tissues of C57BL/6 mice. No difference in the expression level or pattern of both molecules was observed between naïve and MOG+CFA immunised mice. This is consistent with the clinical and pathological observation that antigen specific inflammation was developed in these mice. This data suggests a role for the IL-33/ST2 signaling pathway in MS/EAE development. However, to further understand the function of IL-33 in CNS diseases, it is important to determine the cellular location of IL-33 and ST2 in the CNS.

4. Expression of IL-33 and ST2 by CNS resident cells

4.1 Introduction

The CNS consists of several resident cells such as the neuron, ODCs, astrocyte and microglia. Within this section I will focus mainly on neurons, astrocytes and microglia.

Neurons do not play an active role in the pathogenesis of MS and EAE. However, through bystander damage or via specific targeting, neurons and axons are also damaged. Furthermore, as a result of MS pathology, the demyelination of axons renders neurons and axons vulnerable to damage.

Microglia are activated very early in CNS injury (before any other glial cell) and are extremely sensitive to even slight changes in their microenvironment such as differences in ion homeostasis (Kreutzberg 1996). Microglia constitutively express MHC II molecules as well as co-stimulatory molecules CD80 and CD86, indicating an important role for microglia in the presentation of antigens to T cells (Satoh et al. 1995; Gerritse et al. 1996). Moreover, microglia are thought to present antigens to naïve T cells in the EAE mouse model of MS as well as secreting cytokines (IL-12, IL-23 and IL-17) associated with the differentiation and activation of Th1 and Th17 cells (thus driving pathology).

Astrocytes can respond to CNS injury such as inflammation or demyelination through a process called astrogliosis, which can often lead to scar formation. On the other hand, astrocytes can also support the re-growth of axons.

Astrocytes produce cytokines such as IL-1, IL-6, IL-10 and TGF-β, and chemokines such as CCL5, MCP-1, CCL2, IL-8 and IP-10 during inflammation (Dong & Benveniste 2001). Depending on the environmental milieu, this could result in a Th1, Th2 or a Th17 mediated response. Furthermore, the secretion of NGF from astrocytes can also alter the development of EAE (Fok-seang et al. 1998).

From the results in chapter 3, it was shown that IL-33 and ST2 proteins are widely expressed within the white and grey matters of CNS tissues of naïve and EAE mice. This suggests that they are likely to be present on resident CNS cells such as astrocytes, neurons or microglia. To determine the role of IL-33 within the CNS compartment, it is important to identify the CNS cells which express IL-33 and/or its receptor ST2.

The aims of this chapter are therefore:

1. Determine the localisation of IL-33 and ST2 within the spinal cord of naïve and EAE mice;

2. Determine the localisation of IL-33 and ST2 within the brain of naïve and EAE mice.

4.2 Results

IL-33 expression on murine neurons

Firstly, I investigated the expression of IL-33 on neuron cells by staining IL-33 (DAB) in conjunction with NeuN (Vector® blue). NeuN stains the nucleus and on occasions the cytoplasm of most neurons. The data shows that in naïve mice (Figure 4.1A and B) approximately 25% of $NeuN^+$ cells expressed IL-33 within the grey matter of the spinal cord (Figure 4.3). There was no co-localisation of IL-33 on neurons within the white matter due to the absence of neuronal cell bodies within this region. This was also confirmed using fluorescent staining (Figure 4.1C) on frozen sections.

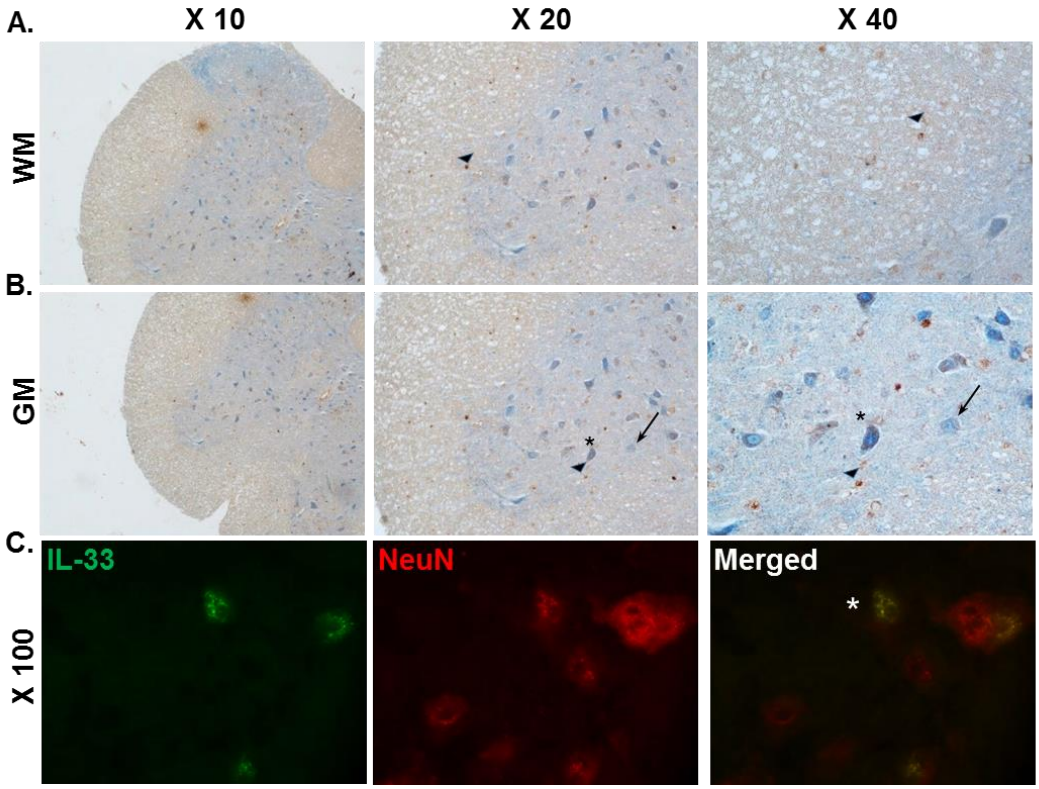

Figure 4.1 IL-33 expression on neurons in naïve mouse spinal cord. Spinal cords were harvested from naïve C57BL/6 mice and stained for IL-33 (brown/ green) and NeuN (blue/red) in white matter (WM) **(A)** and grey

matter (GM) **(B) (C)** (fluorescent staining on frozen sections). Images show IL-33^{+} (arrowhead), NeuN^{+} (arrow) and IL-33^{+}NeuN^{+} (asterisk) cells.

Consistent with the staining data in naïve tissues, approximately 40% of IL-33^{+} neurons within the grey matter (Figure 4.2B and C), but not within the white matter, were observed in EAE spinal cord tissues (Figure 4.2A). Double fluorescence staining of IL-33 and NeuN in EAE spinal cords further confirmed the expression of IL-33 by neuron cells in grey matter (Figure 4.2C). There was no significant difference between the protein expression of IL-33 within the naïve and EAE spinal cord neurons (Figure 4.3).

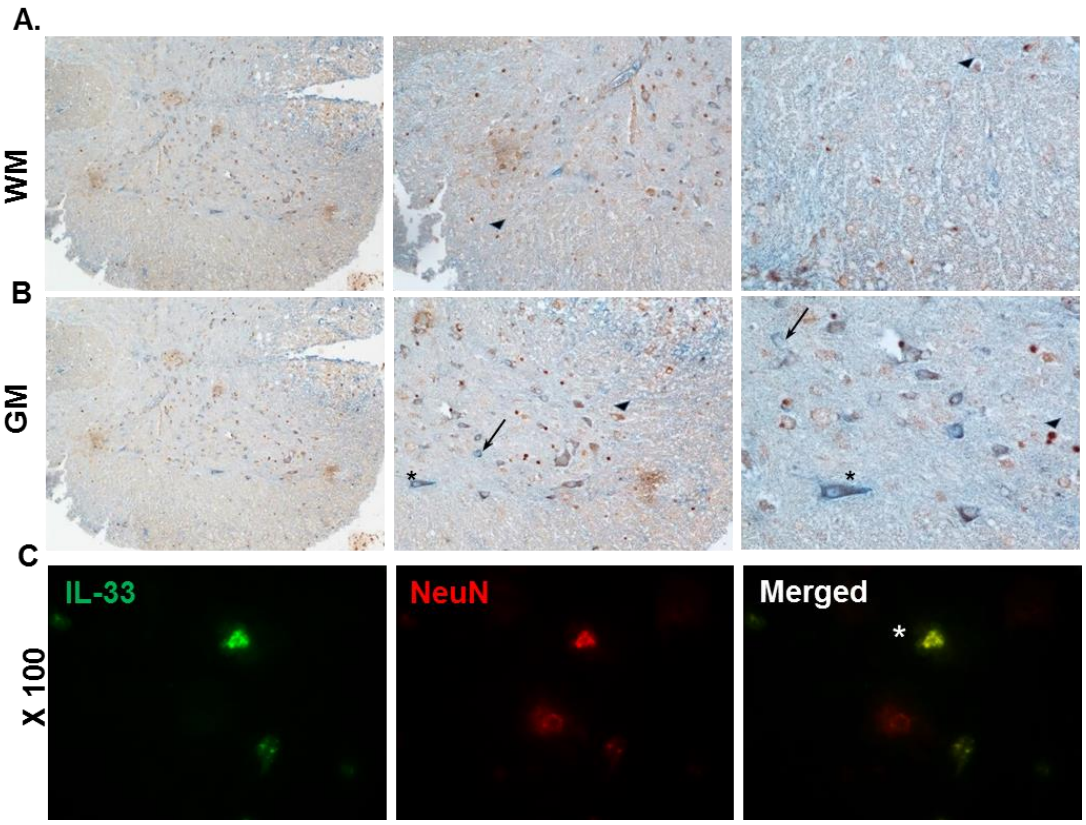

Figure 4.2 IL-33 expression on neurons in EAE spinal cord. Spinal cords were harvested from EAE mice at day 18 and stained for IL-33 (brown/ green) and NeuN (blue/ red) in white matter (WM) **(A)** and grey matter (GM) **(B)** and GM **(C)** (fluorescent staining on frozen sections). Images show IL-33^{+} (arrowhead), NeuN^{+} (arrow) and IL-33^{+}NeuN^{+} (asterisk) cells.

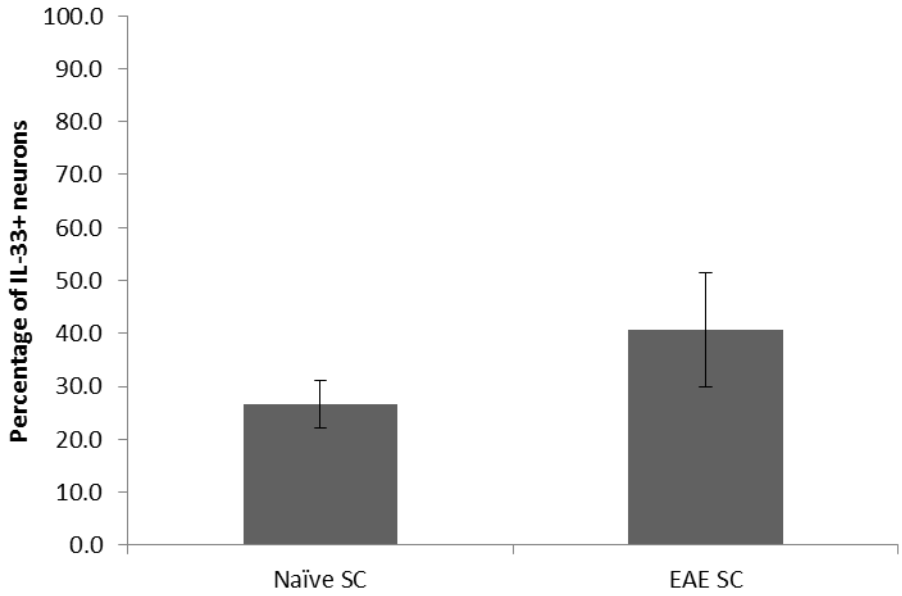

Figure 4.3 The Percentage of IL-33+ neurons in naïve and EAE spinal cord. Spinal cord sections from C57BL/6 naïve and EAE immunised mice were stained for IL-33 and NeuN (neurons) and quantified using image J, cell counter. Data represents mean ± S.E.M, n=2

Upon examination of the colocalisation in naïve brain samples (Figure 4.4), the images showed that only a small number of neuron cells express IL-33 in the cortex, with staining in the ventricular regions, and striatum. In the brain tissues of EAE mice (Figure 4.5), similar levels of IL-33 expression were observed in the cortex. Furthermore, the numbers of IL-33$^+$ neurons are also increased within the cortex and striatum areas, but not within the ventricular region.

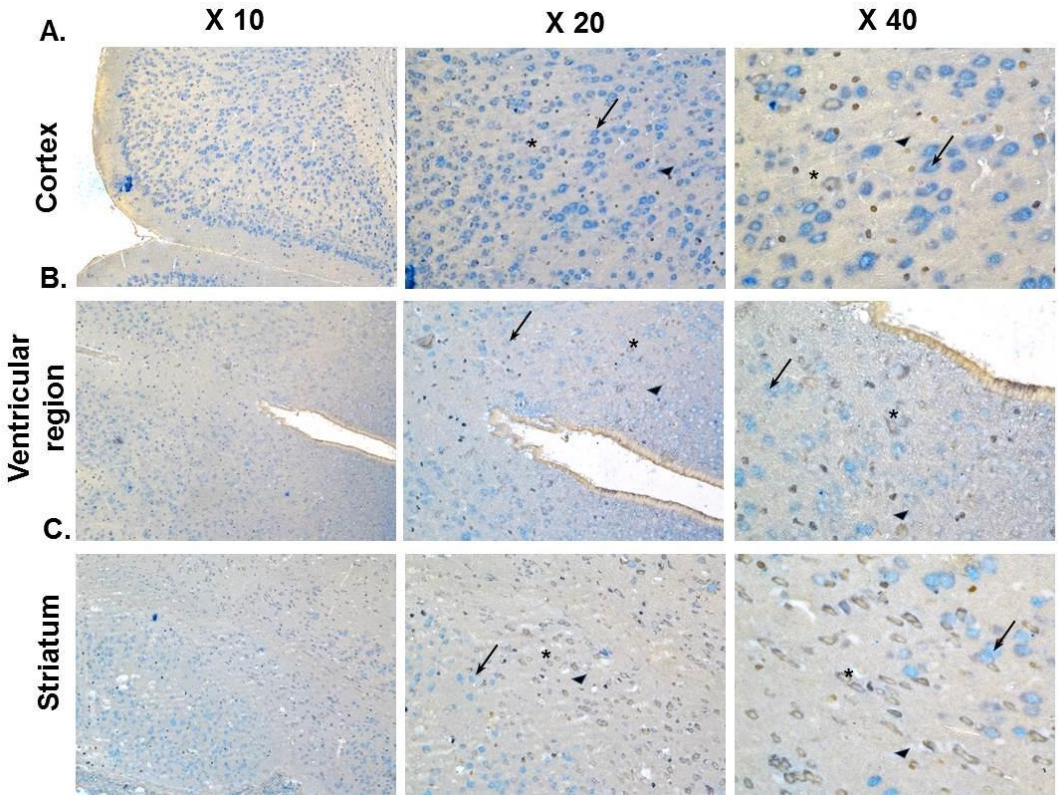

Figure 4.4 IL-33 expression on neurons in naïve brain. Brain tissues were harvested from naïve C57BL/6 mice and stained with IL-33 (DAB) and NeuN (Vector® blue) within the cortex **(A),** corpus callosum **(B)** and striatum **(C).** Images show IL-33$^+$ (arrowhead), NeuN$^+$ (arrow) and IL-33$^+$NeuN$^+$ (asterisk) cells.

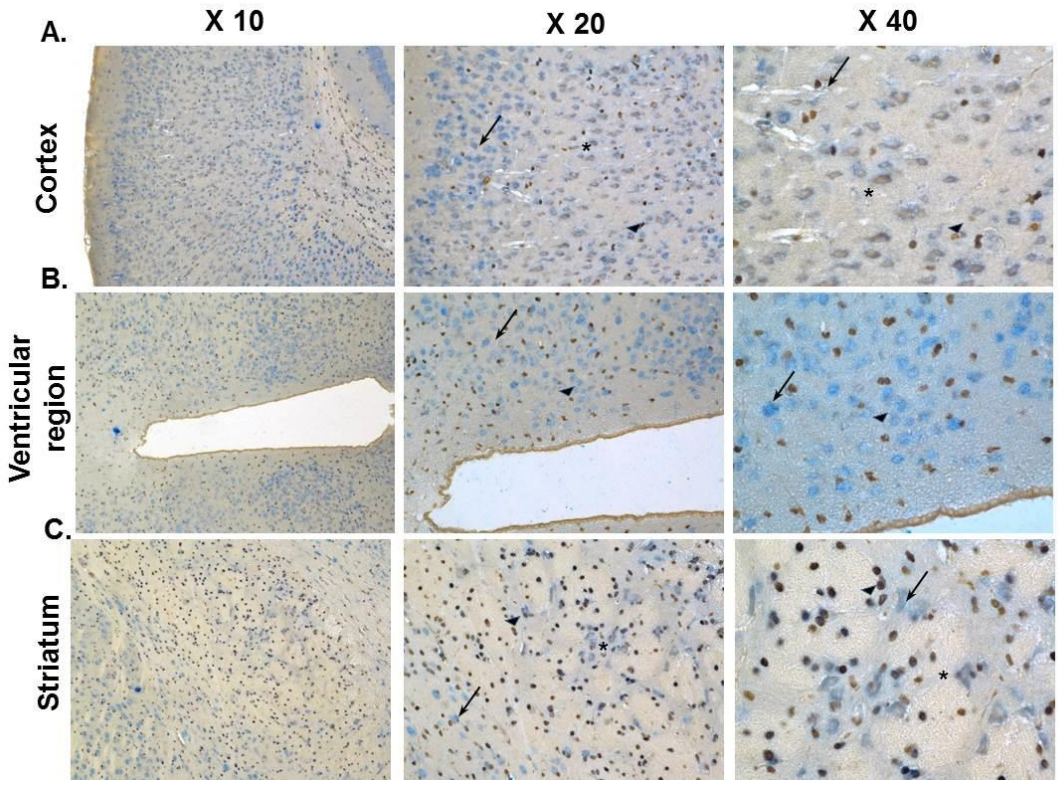

Figure 4.5 IL-33 expression on neurons in EAE brain. Brain tissues were harvested from EAE C57BL/6 mice at peak of disease (day 18) and stained for IL-33 (DAB) and NeuN (Vector® blue) within the cortex **(A),** corpus callosum **(B)** and striatum **(C).** Images show IL-33^{+} (arrowhead), NeuN^{+} (arrow) and IL-33^{+}NeuN^{+} (asterisk) cells.

IL-33 expression on murine astrocytes

To determine the expression of IL-33 on astrocytes within the murine spinal cord, I used double immunohistochemical and immunofluorescent staining. As described in Chapter 2, spinal cord tissues were stained for IL-33 (DAB/ FITC) and glial fibrillary acidic protein GFAP (Vector® blue/ TRITC). The data showed that within the grey matter regions of naïve spinal cord (Figure 4.6B) approximately 50% of GFAP^{+}astrocytes expressed the IL-33 protein, additionally, IL-33 was expressed by other CNS resident cells. When performing the dual staining in the spinal cord tissues of EAE mice (Figure

4.6C and D), the expression of IL-33 significantly decreased in the EAE and naïve tissues (Figure 4.7), possibly as a result of a negative feedback mechanism. IL-33 was also expressed by cells in the white matter regions, no co-localisation of IL-33 within astrocytes was observed within this region in naïve or EAE spinal cord tissues. The colocalisation of IL-33 within astrocytes in the grey matter region, but not in the white matter, suggests that IL-33 is only present in a specific sub-population of astrocytes, and other CNS cells that express also IL-33 (Middeldorp et al. 2009).

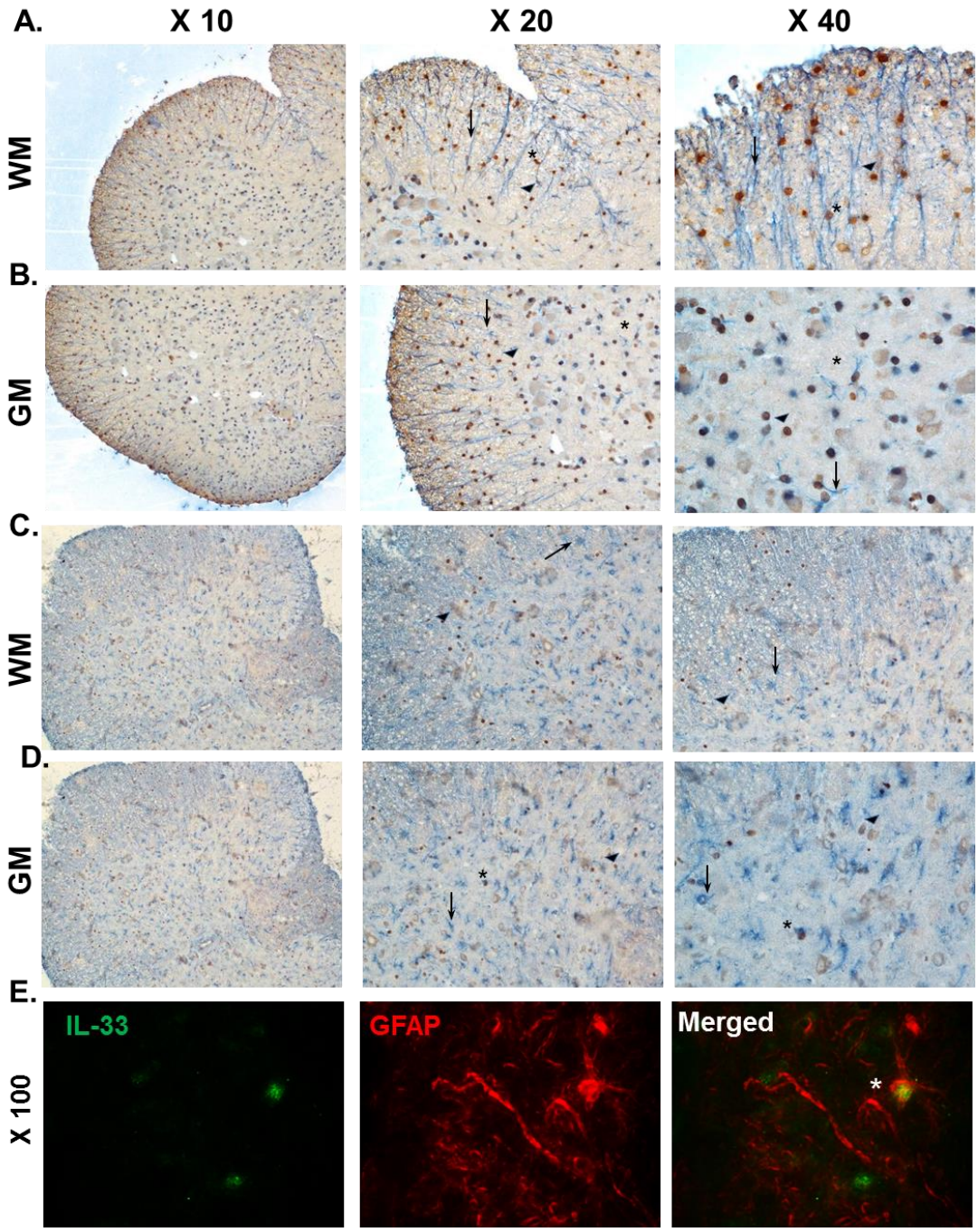

Figure 4.6 IL-33 expression on astrocytes in naïve and EAE mouse spinal cord tissues. Spinal cords were harvested from naïve **(A and B)** and EAE **(day 18 PI) (C and D)** mice and tissue sections were stained for IL-33 (DAB, brown) and GFAP (Vector®-blue). EAE spinal cord sections were also stained with anti-IL-33 (FITC, green) and anti-GFAP (TRITC, red) **(E)** using fluorophore-labelled antibodies. Images show IL-33^{+} (arrowhead), GFAP^{+} (arrow) and IL-33^{+}GFAP^{+} (asterisk) cells.

As IL-33 is highly expressed by both brain and spinal cord tissues, I also examined the colocalisation of IL-33 within astrocytes in brain tissues of naïve and EAE mice. Despite the anatomical differences between the spinal cord and the brain, and the fact that less inflammation is presented in the brain tissues of MOG-induced EAE mice, similar results were observed in the brain to those obtained within the spinal cord tissues. These images have shown that IL-33 is expressed by astrocytes. Interestingly, this also highlights that there are regional differences associated with the levels of IL-33 co-localisation within astrocytes. In the cortex, ventricular region and corpus callosum regions of naïve murine brain, most astrocytes did not express IL-33, and there were many IL-33^{+}GFAP^{-} cells. This suggests that IL-33 is expressed by many other CNS cells in these regions. (Figure 4.8A, B and C). In the hippocampal area astrocytes expressed IL-33, with fewer IL-33^{+}GFAP^{-} cells (Figure 4.8D). Within EAE brain tissues (Figure 4.9), there was an up-regulation of GFAP expression when compared to expression in naïve brain. This suggests inflammation - induced activation and proliferation of astrocytes (astrogliosis) *in vivo* (Sofroniew 2009). Furthermore, there are IL-33^{+} astrocytes present within the cortex and ventricles, which was not observed in the naïve brain. Again, IL-33^{+} astrocytes were observed in the hippocampus region.

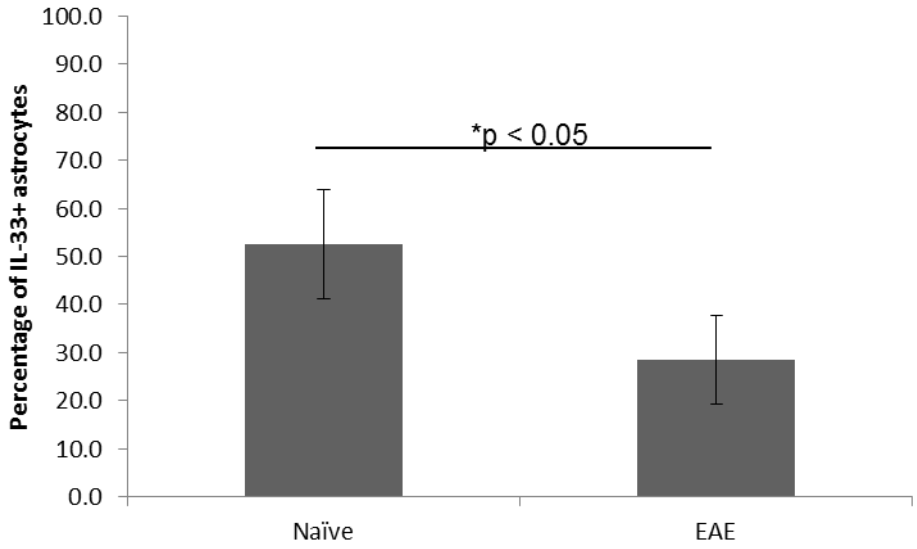

Figure 4.7 Percentage of IL-33+ astrocytes within naïve and EAE spinal cord. Spinal cord sections from C57BL/6 naïve and EAE immunised mice were stained for IL-33 and GFAP (astrocytes) and quantified using image J, cell counter. Data represents mean ± S.E.M, n=2.

were treated with either medium (control) or IL-33 from day 12 until day 28. At day 28 the coverslips were fixed and stained for Iba1 at day 12, 18 and 28 (A). The percentage $Iba1^{+}$ cells was then calculated (B). Data represent mean ± S.E.M, n=3

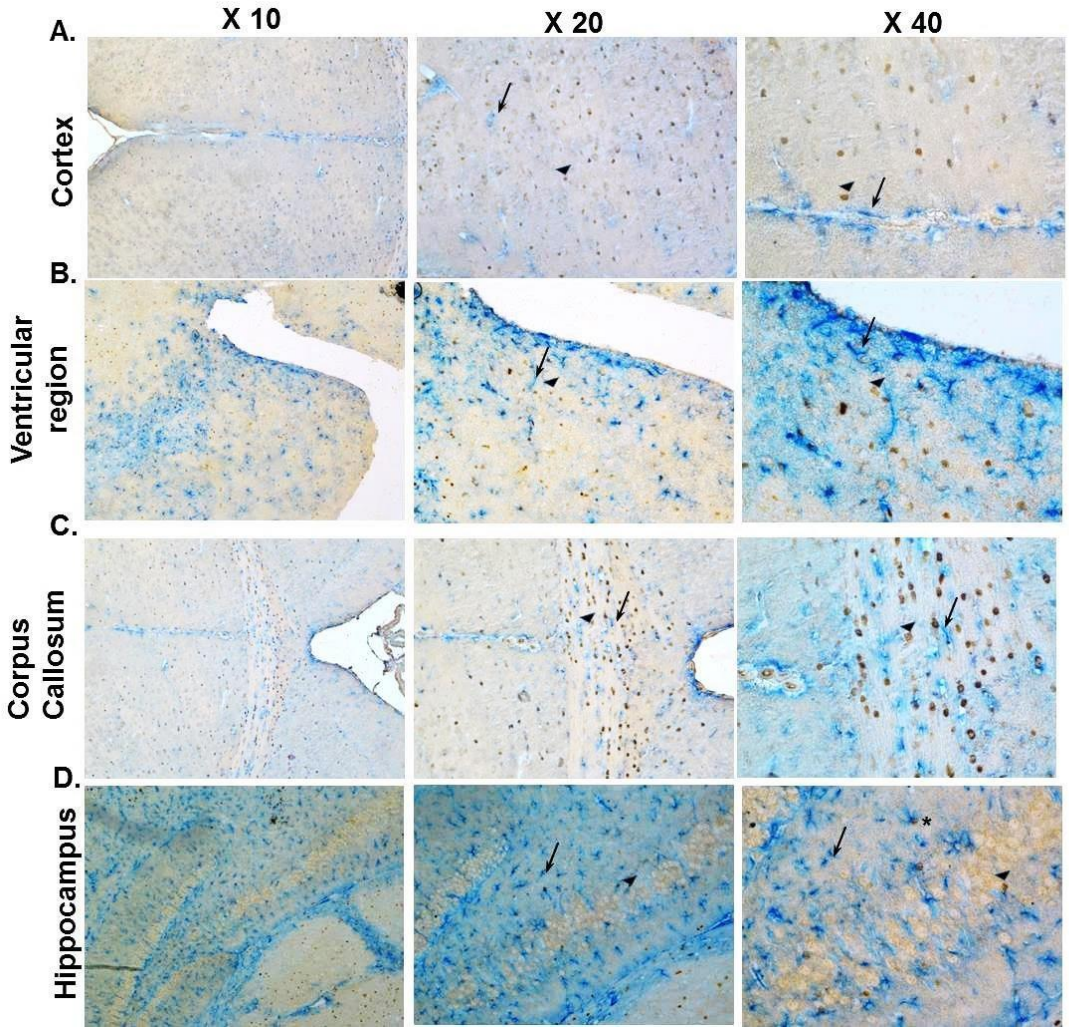

Figure 4.8 IL-33 expression on astrocytes in naïve brain. Brain tissues were harvested from naïve C57BL/6 mice and double-stained for IL-33 (DAB, brown) and GFAP (Vector®blue). Images show IL-33^{+} (arrowhead), GFAP^{+} (arrow) and IL-33^{+}GFAP^{+} (asterisk) cells within the cortex **(A)** ventricular regions **(B),** corpus callosum **(C)** and hippocampus **(D).**

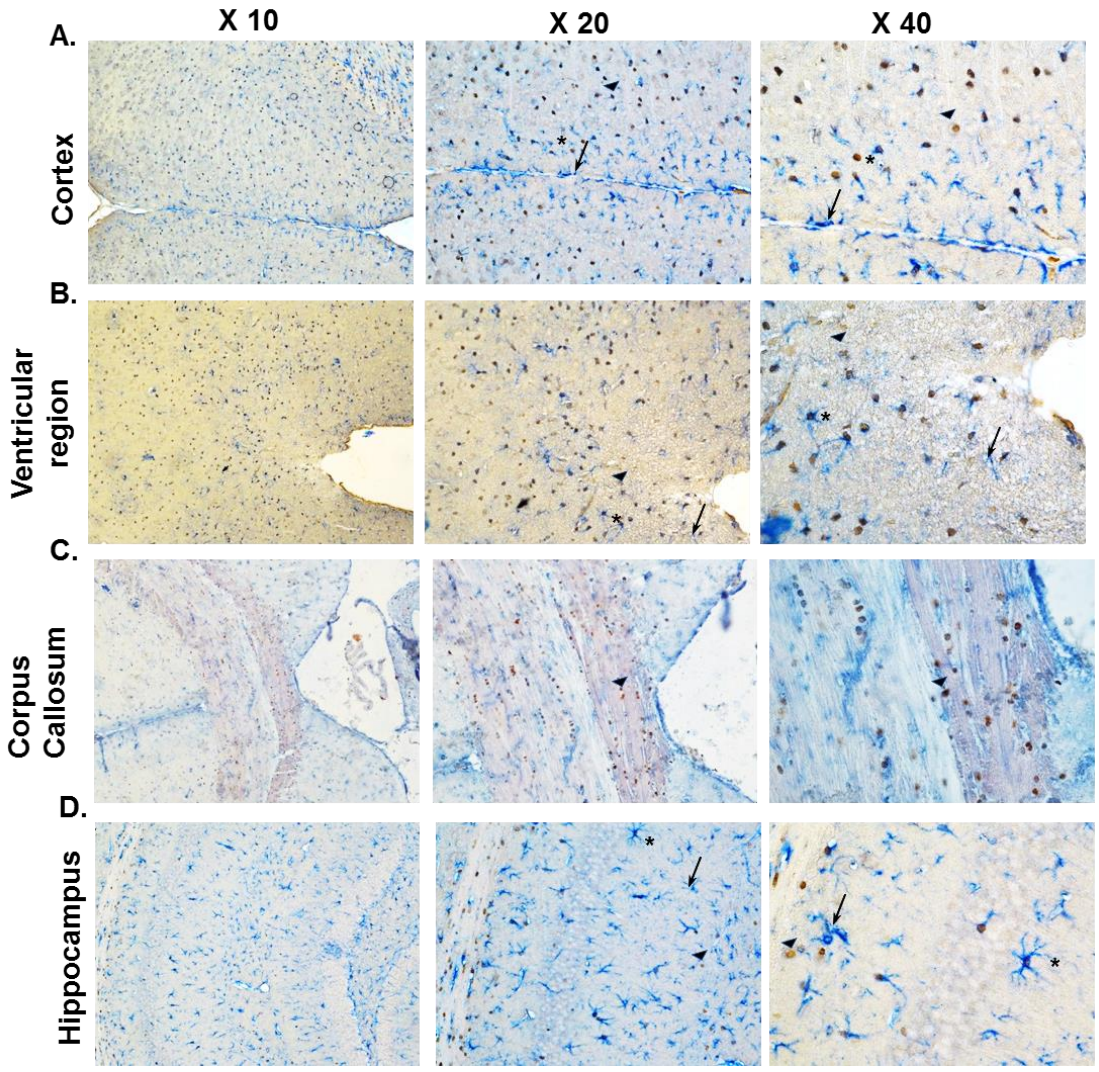

Figure 4.9 IL-33 expression on astrocytes in EAE brain. Brains were harvested from EAE C57BL/6 mice (day 18) and stained for IL-33 (DAB, brown) and GFAP (Vector® blue). Images show IL-33$^+$ (arrowhead), GFAP$^+$ (arrow) and IL-33$^+$GFAP$^+$ (asterisk) cells within the cortex (A) ventricular regions (B) corpus callosum (C) and hippocampus (D).

IL-33 expression on murine microglia

To further determine the cellular location of IL-33 within the brain and spinal cord, IL-33 was co-stained with the microglial marker Iba1. Within the spinal cord of naïve and EAE mice (Figure 4.10), Iba1$^+$ microglia were distributed in the grey and white matters of spinal cord tissues. Interestingly, my double staining data showed that IL-33 was not co-localised with microglia within

naïve or EAE spinal cord tissues. This is confirmed by the data from brain tissues of naïve (Figure 4.11) and EAE mice (Figure 4.12) that also show that IL-33 did not co-localise with Iba1^{+} microglia.

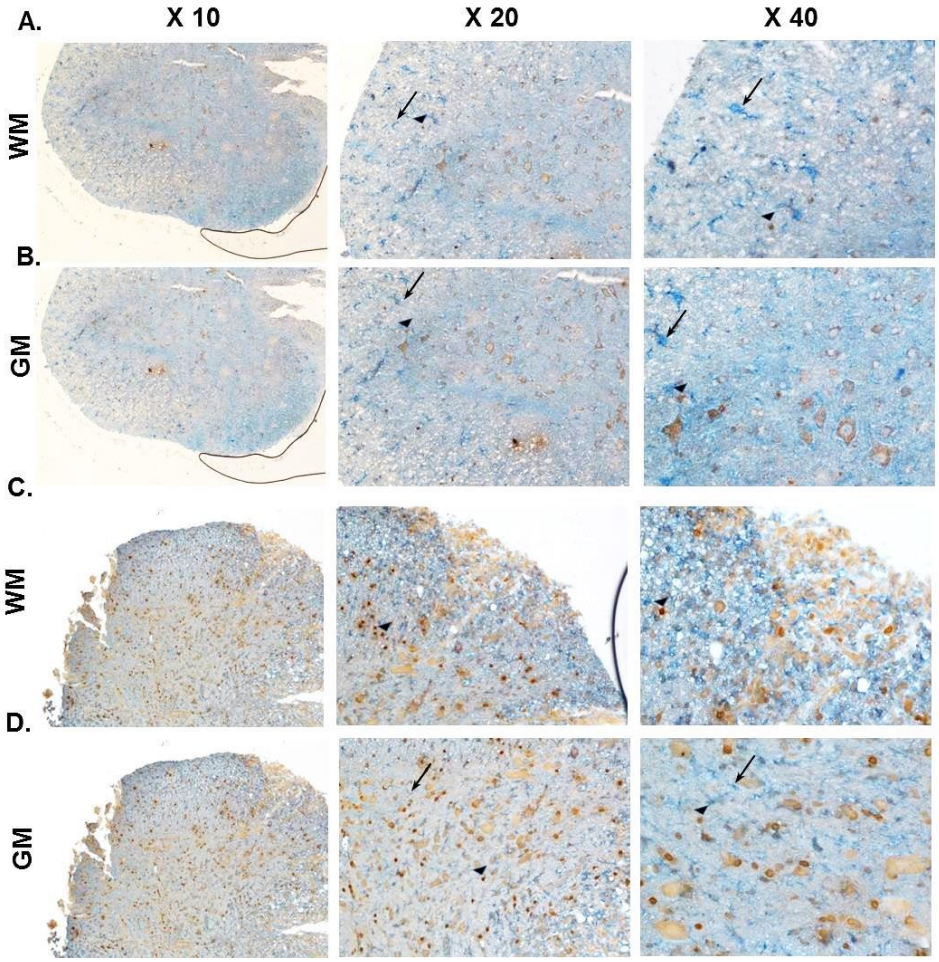

Figure 4.10 IL-33 expression on microglia in naïve and EAE spinal cord. Spinal cords were harvested from naïve **(A and B)** and EAE **(C and D)** EAE mice (Day 18) and stained for IL-33 and Iba1. Images show IL-33^{+} (arrowhead) and Iba1^{+} (arrow) cells.

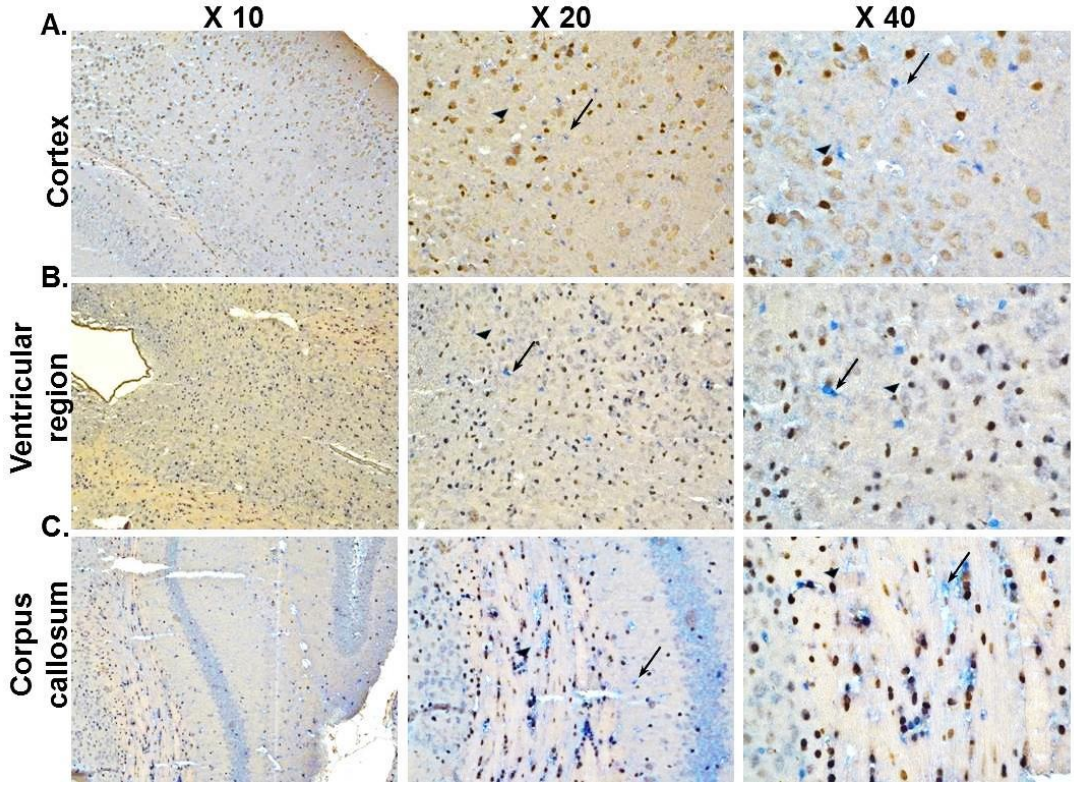

Figure 4.11 IL-33 expression on microglia in naïve brain. Brains from naïve mice were harvested and stained for IL-33 (DAB, brown) and Iba1 (Vector ® blue) within the cortex **(A),** ventricular region **(B)** and the corpus callosum **(C).** Images show IL-33^{+} (arrowhead) and Iba1^{+} (arrow) cells.

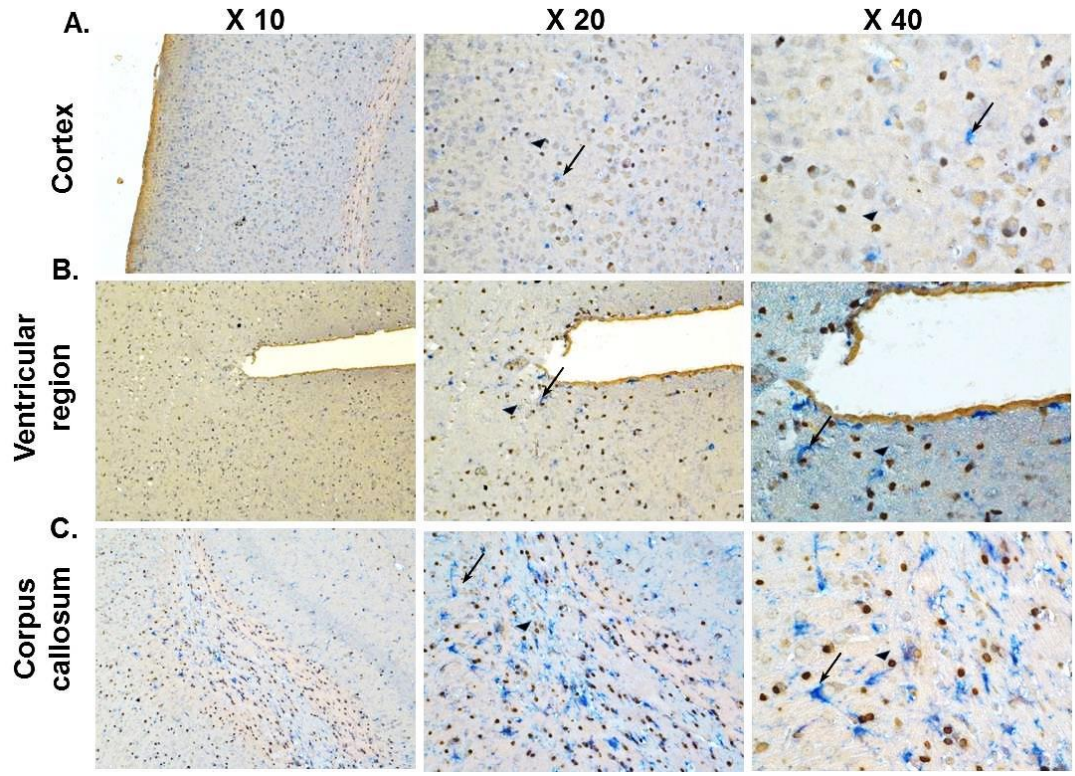

Figure 4.12 IL-33 expression on microglia in EAE brain. Brains from EAE mice were harvested and stained for IL-33 (DAB, brown) and Iba1 (Vector® blue) within the cortex **(A)** ventricular region **(B)** and the corpus callosum **(C).** Images show IL-33^{+} (arrowhead) and Iba1^{+} (arrow) cells.

Understanding the localisation of IL-33 within CNS cells is important to determine the function of IL-33 in the CNS compartment and in CNS diseases such as MS. The double staining of IL-33 with CNS cell markers suggests that IL-33 is present on neurons and astrocytes within naïve and EAE spinal cord sections. Furthermore, within the brain, IL-33 was also present on neurons within the cortex. There was no difference in the expression levels or patterns of IL-33 on neurons between EAE and naïve brain sections. Within the brain of naïve mice, fewer IL-33^{+} astrocytes were found, whilst the number of astrocytes increased in CNS tissues of EAE mice, suggesting that during EAE IL-33 is upregulated on astrocytes within the brain.

ST2 expression on murine neurons

I proceeded to investigate the expression of the IL-33 receptor ST2 on CNS resident cells. The expression of ST2 on neurons was first investigated within the spinal cord and brain of naïve and EAE mice.

ST2 was present on neurons within the grey matter of the spinal cord, however no localisation was observed within the white matter due to the lack of neuronal cell bodies in this region (Figure 4.13). In the spinal cord tissues of EAE mice (Figure 4.14), ST2 was confirmed to be colocalised with $NeuN^{+}$ neuron cells in the grey matter regions. Quantitative analysis of the immunohistochemical staining has shown no difference in the percentage of ST2 expressing neurons in naïve and EAE spinal cord tissues (Figure 4.15).

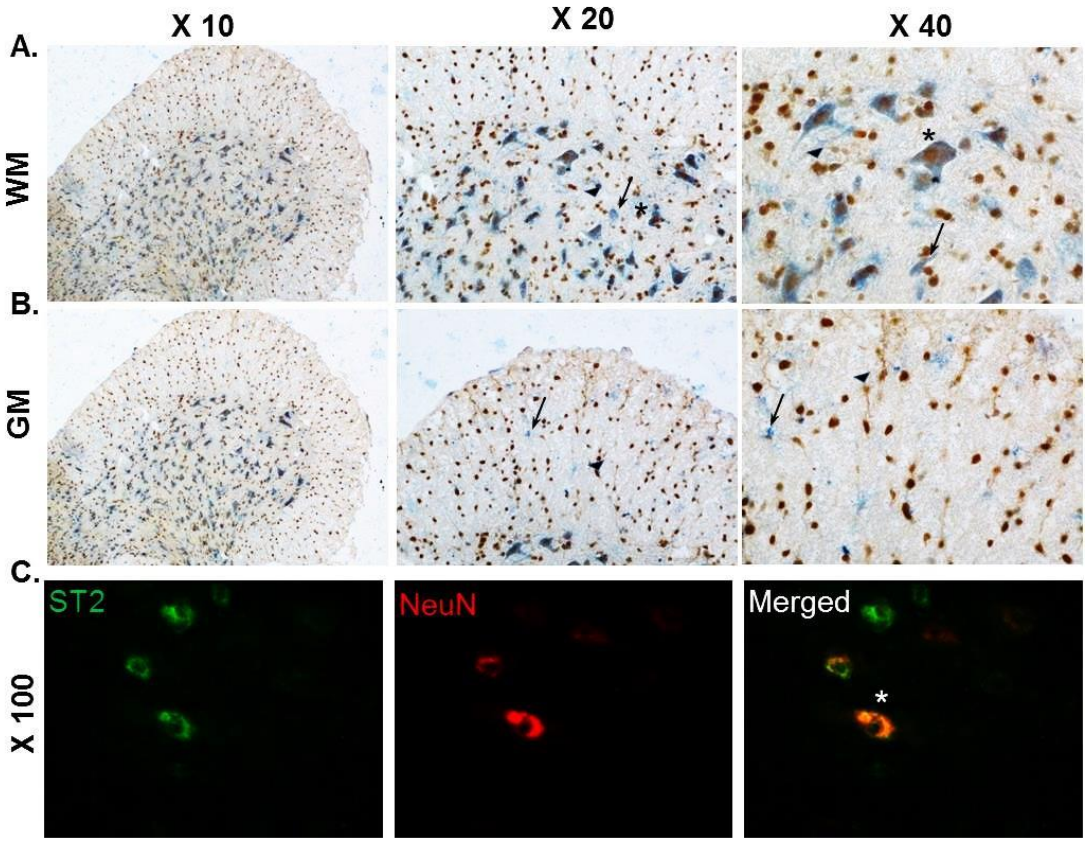

Figure 4.13 ST2 expression on neurons in naïve spinal cord. Spinal cords were harvested from naïve mice stained for ST2 (brown/ green) and

NeuN (blue/ red) by immunohistochemical (A) and (B) and fluorescent staining (C). Images show $ST2^+$ (arrowhead), $NeuN^+$ (arrow) and $ST2^+NeuN^+$ (asterisk) cells.

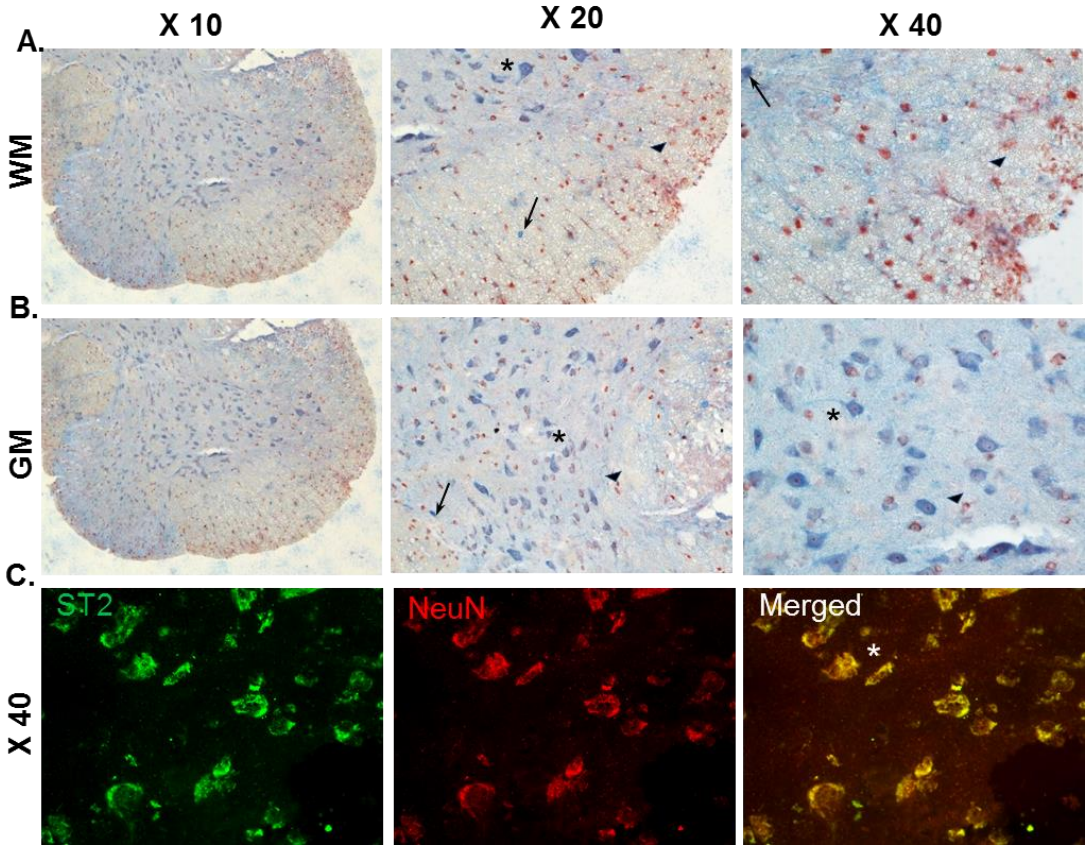

Figure 4.14 ST2 expression on neurons in EAE spinal cords. Spinal cords were harvested from EAE C57BL/6 mice at day 18 PI and stained with ST2 (red/ green) and NeuN (blue/ red) by immunohistochemical (A, B) and fluorescent staining (C). Images show $ST2^+$ (arrowhead), $NeuN^+$ (arrow) and $ST2^+NeuN^+$ (asterisk) cells.

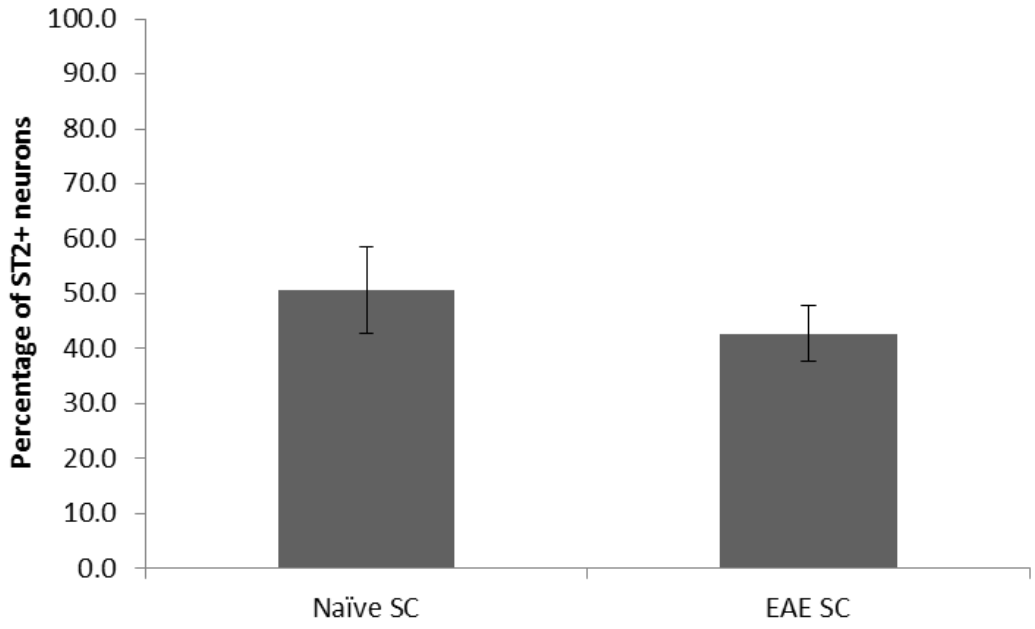

Figure 4.15 Percentage ofST2+ neurons in naïve and EAE spinal cord.Spinal cord sections from C57BL/6 naïve and EAE immunised mice were stained for ST2 and NeuN (neurons) and quantified using image J, cell counter. Data represents mean ± S.E.M, n=3

ST2 expression was also evident within the brain of naive (Figure 4.16) and EAE (Figure 4.17) mice. Double staining results were consistent with the spinal cord showing that ST2 was colocalised with NeuN. These results show that ST2 was expressed by neuron cells in both the naïve and the EAE murine brain. The co-localisation was prominent within the cortex however, fewer $ST2^{+}NeuN^{+}$ cells were observed in the corpus callosum and within the ventricular regions within the brain.

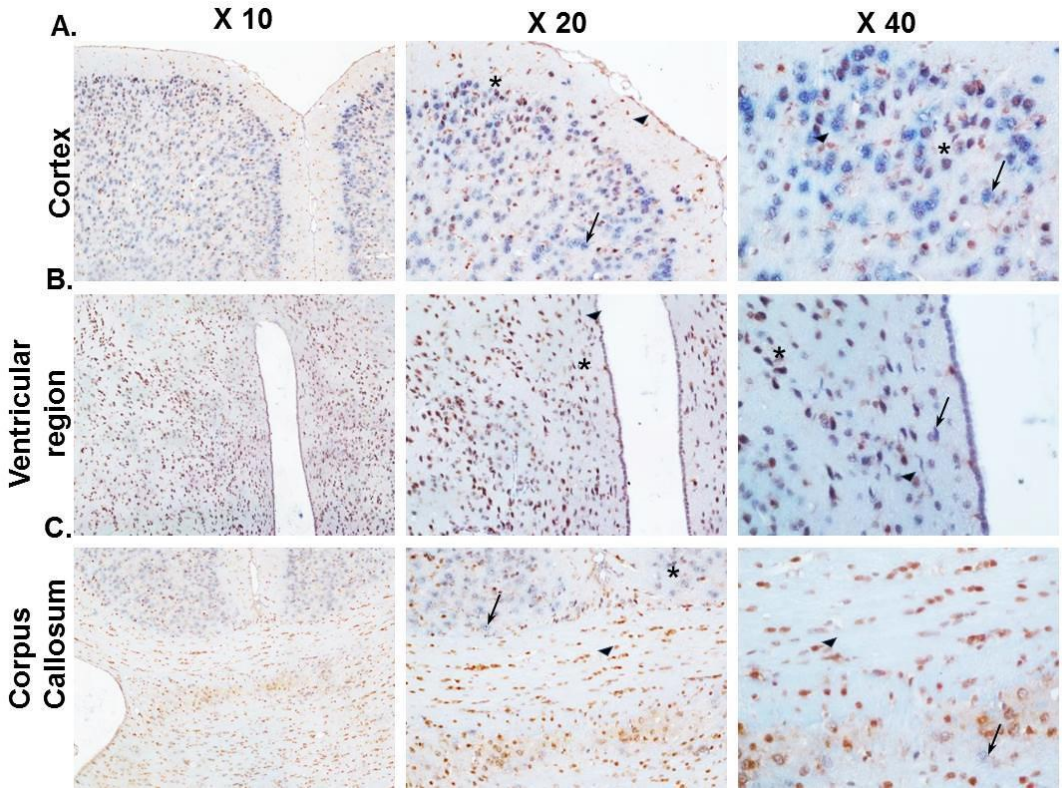

Figure 4.16 ST2 expression on neurons naïve brain. Brains from naïve mice were harvested and stained for ST2 (AEC, red) and NeuN (Vector® blue). Images show $ST2^{+}$ (arrowhead), $NeuN^{+}$ (arrow) and $ST2^{+}NeuN^{+}$ (asterisk) cells within the cortex **(A)** ventricular region **(B)** and the corpus callosum **(C).**

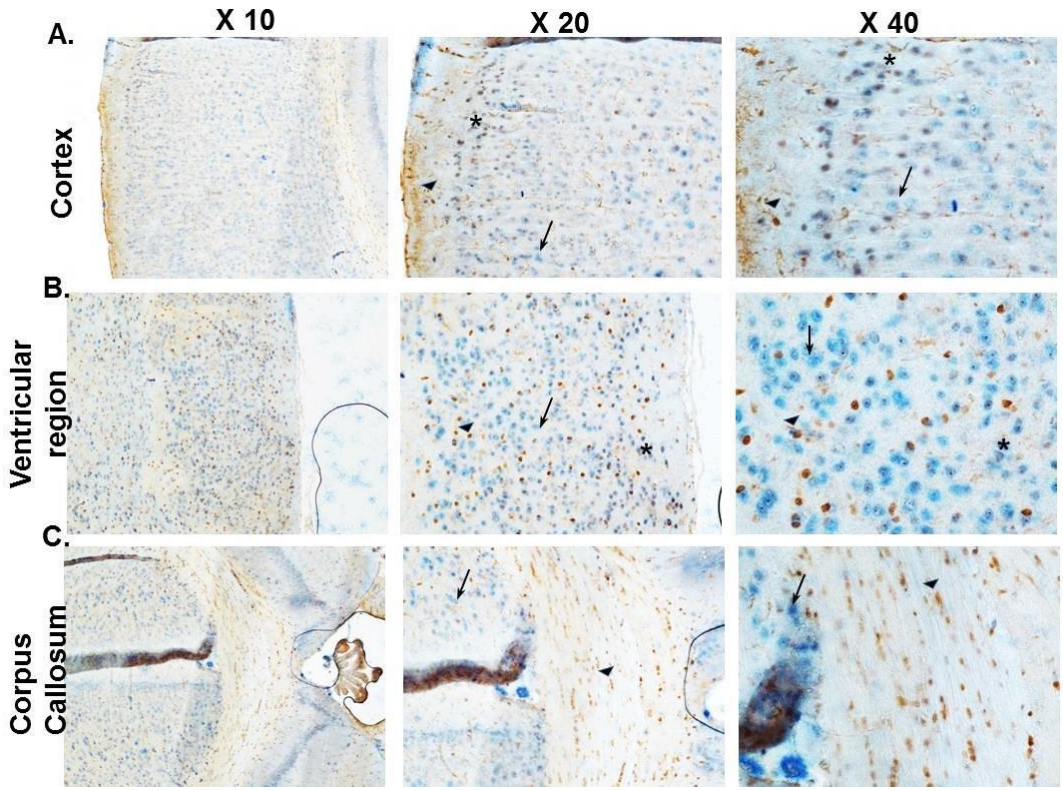

Figure 4.17 ST2 expression on neurons in EAE brain. Brains from EAE mice (day 18) were harvested and stained for ST2 (DAB, brown) and NeuN (Vector® blue). Images show $ST2^+$ (arrowhead), $NeuN^+$ (arrow) and $ST2^+NeuN^+$ (asterisk) cells within the cortex **(A)** ventricular region **(B)** and the corpus callosum **(C).**

ST2 expression on murine astrocytes

The expression of ST2 on astrocytes was determined within the spinal cord using the GFAP astrocyte marker (Figure 4.18). ST2 was expressed within the grey and white matter of the spinal cord and co-localised with astrocytes within the grey matter of naïve mice. ST2 was also present on astrocytes within EAE spinal cord, however there was a significant decrease (Figure 4.19) in ST2 expressing astrocytes suggesting that ST2 is reduced on astrocytes in inflamed conditions.

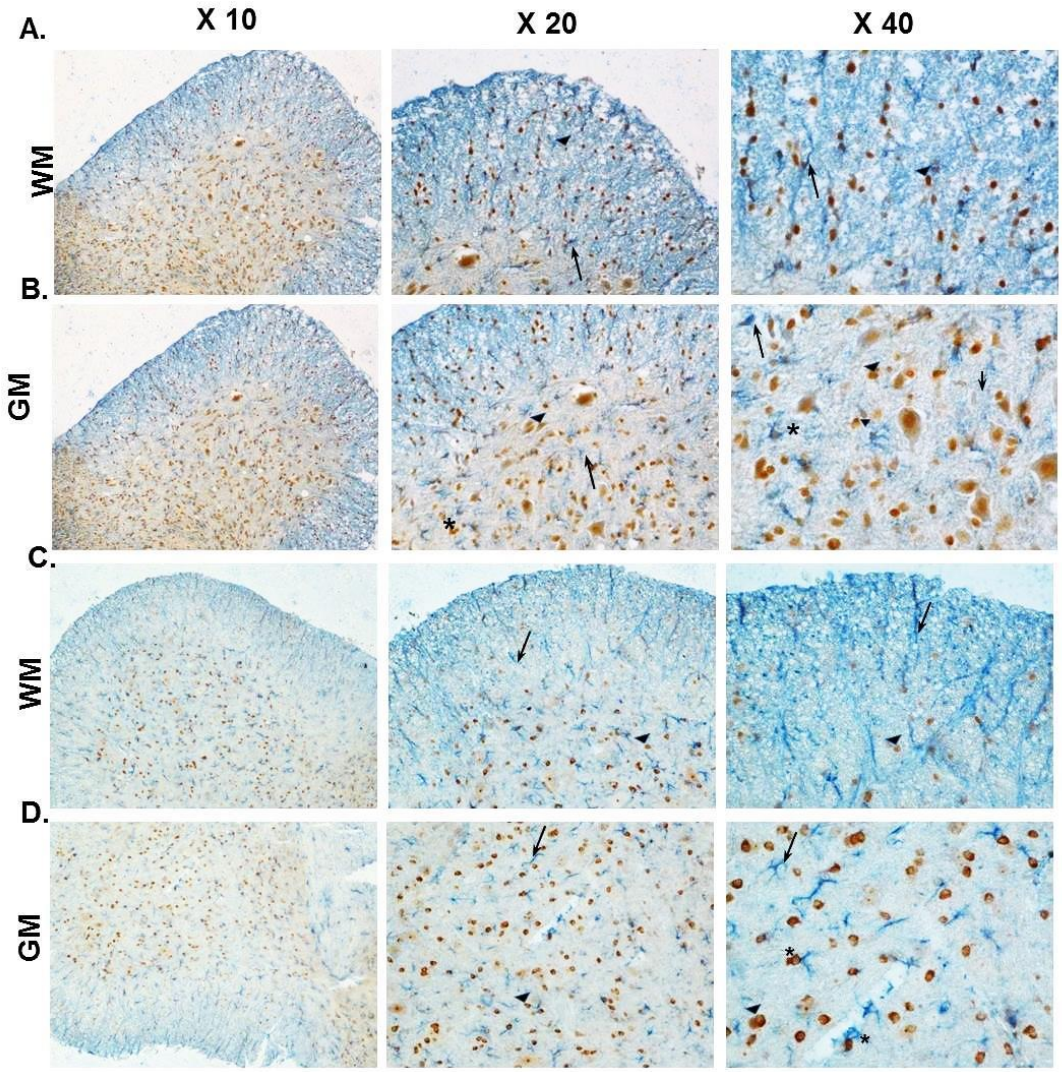

Figure 4.18 ST2 expression on astrocytes in naïve and EAE spinal cord. Spinal cords were harvested from naïve **(A, B)** and EAE **(C,D)** mice (Day 18) and stained for ST2 (DAB, brown) and GFAP (Vector® blue). Images show $ST2^+$ (arrowhead), $GFAP^+$ (arrow) and $ST2^+GFAP^+$ (asterisk) cells.

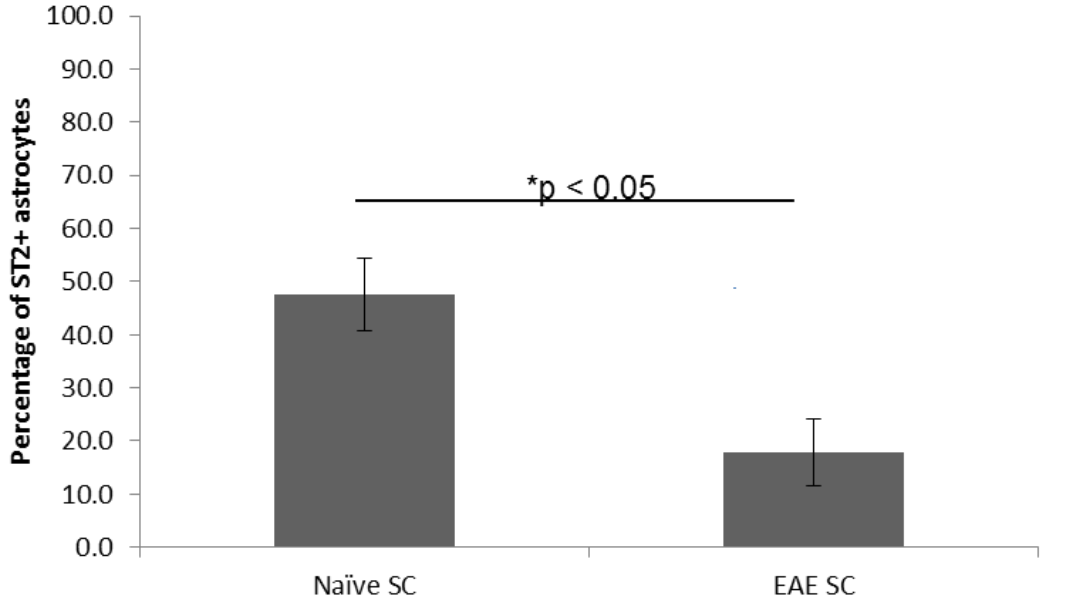

Figure 4.19 Percentage of ST2+ astrocytes in naïve and EAE spinal cords. Spinal cord sections from C57BL/6 naïve and EAE immunised mice were stained for ST2 and GFAP (astrocytes) and quantified using image J, cell counter. Data represents mean ± S.E.M, n=3

The expression of ST2 on $GFAP^+$ astrocytes was more obvious within the brain (Figure 4.20) than spinal cord. $ST2^+$ astrocytes were found within the cortex (although mainly restricted to the edge of the tissue), ventricular regions and corpus callosum. Furthermore, the cingulum, which lies under the corpus callosum, also expressed $ST2^+GFAP^+$ astrocytes. Within EAE brain, ST2 expression on astrocytes was found to be similar (Figure 4.21), the staining was most pronounced on the edge of the cortex. From this it can be seen that ST2 was present on $GFAP^+$ astrocytes in both a healthy and an inflammatory environment within the CNS. From these results, it can be concluded that there are $ST2^+GFAP^+$ cells as well as single positive ST2 and GFAP cells present within the brain.

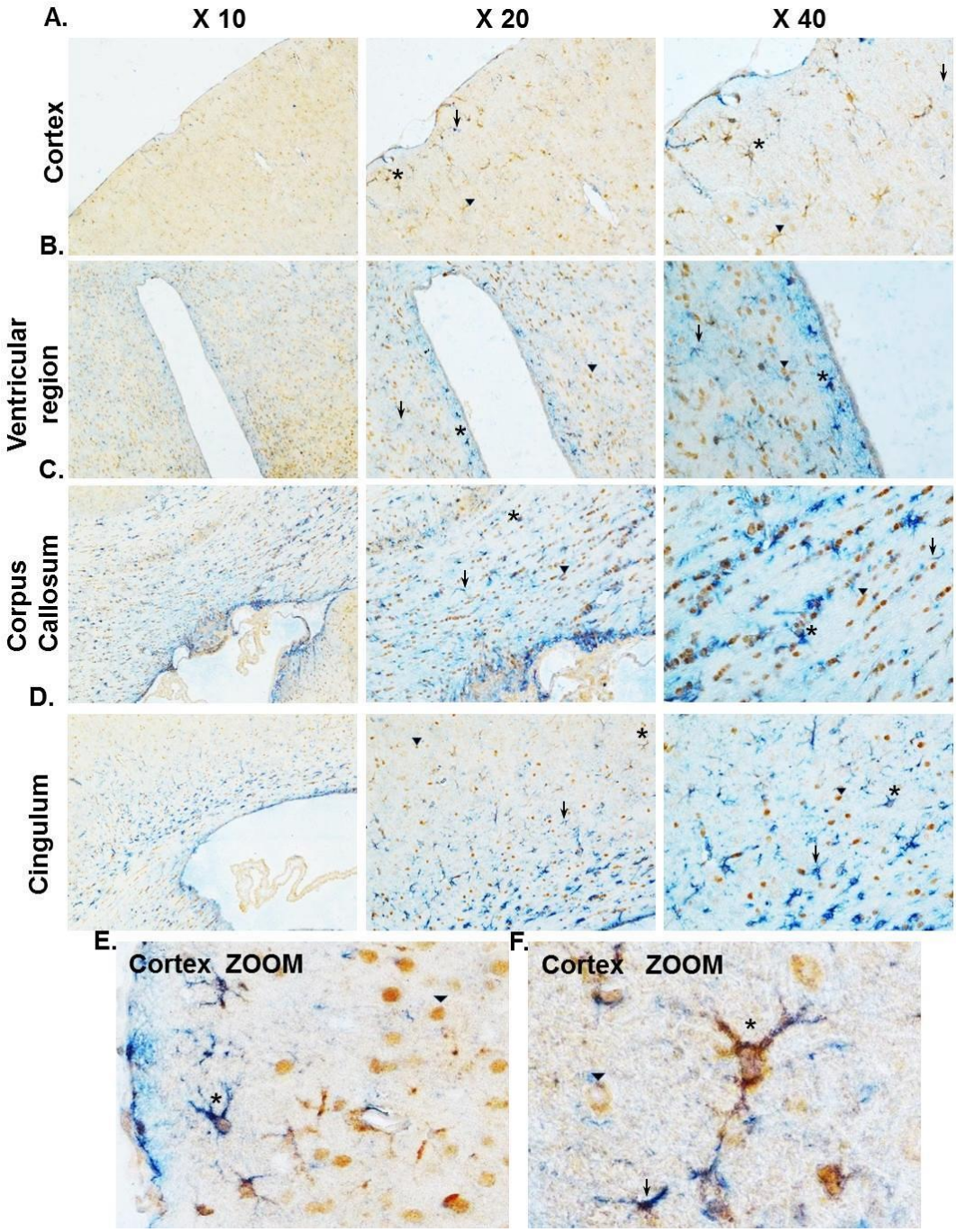

Figure 4.20 ST2 expression on astrocytes in naïve brain. Brains were harvested from naïve mice and stained for ST2 (DAB, brown) and GFAP (Vector® blue). Images show $ST2^+$ (arrowhead), $GFAP^+$ (arrow) and $ST2^+GFAP^+$ (asterisk) cells within the cortex **(A),** ventricular regions **(B)**, corpus callosum **(C)** and cingulum **(D)**. Images E and F depict areas of the cortex taken at x40 magnification, which were further amplified using digital zoom.

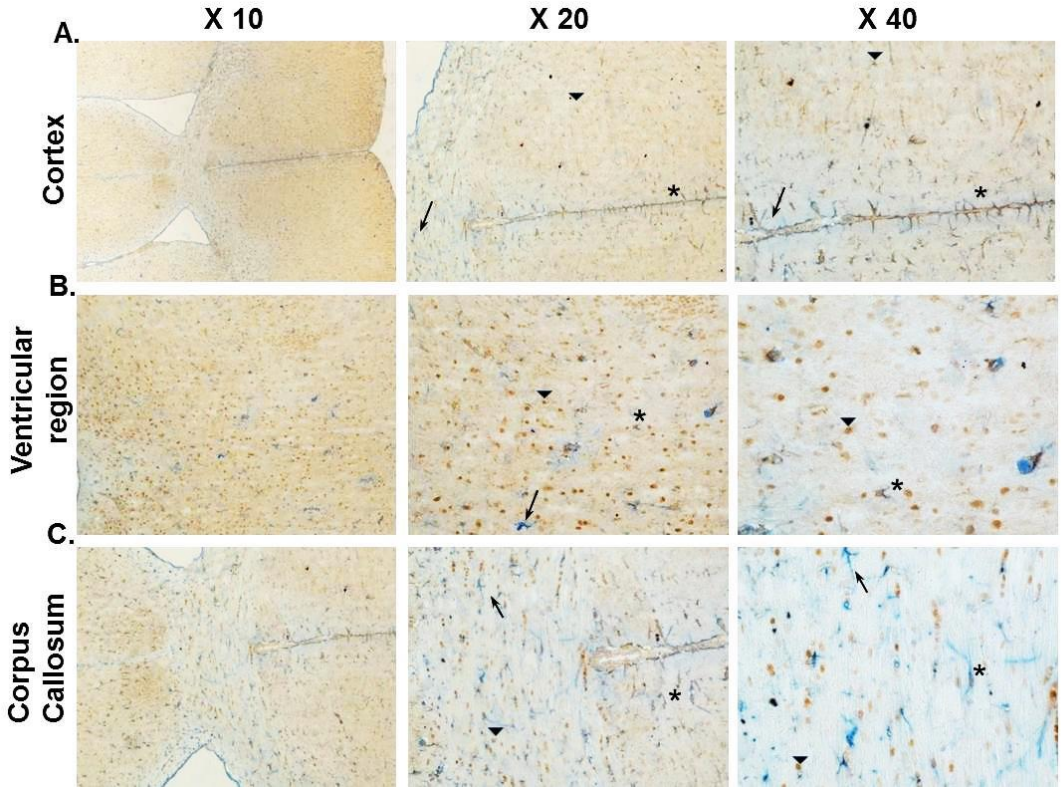

Figure 4.21 ST2 expression on astrocytes in EAE brain. Brains were harvested from EAE mice and stained for ST2 (DAB, brown) and GFAP (Vector® blue). Images show $ST2^+$ (arrowhead), $GFAP^+$ (arrow) and $ST2^+GFAP^+$ (asterisk) cells within the cortex **(A),** ventricular regions **(B)** and corpus callosum **(C)**.

ST2 expression on murine microglia

To conclude this section of investigation, I studied the expression of ST2 on microglial cells within the spinal cord and brain. ST2 was expressed by microglia within the naïve spinal cord (Figure 4.22). Furthermore, within EAE mice, ST2 was not colocalised with microglia cells in the white or grey matter (Figure 4.22). Within the cortex, ventricular region and corpus callosum of brain sections ST2 was not expressed within microglia, in naïve or EAE mice (Figure 4.23 and 4.24 respectively).

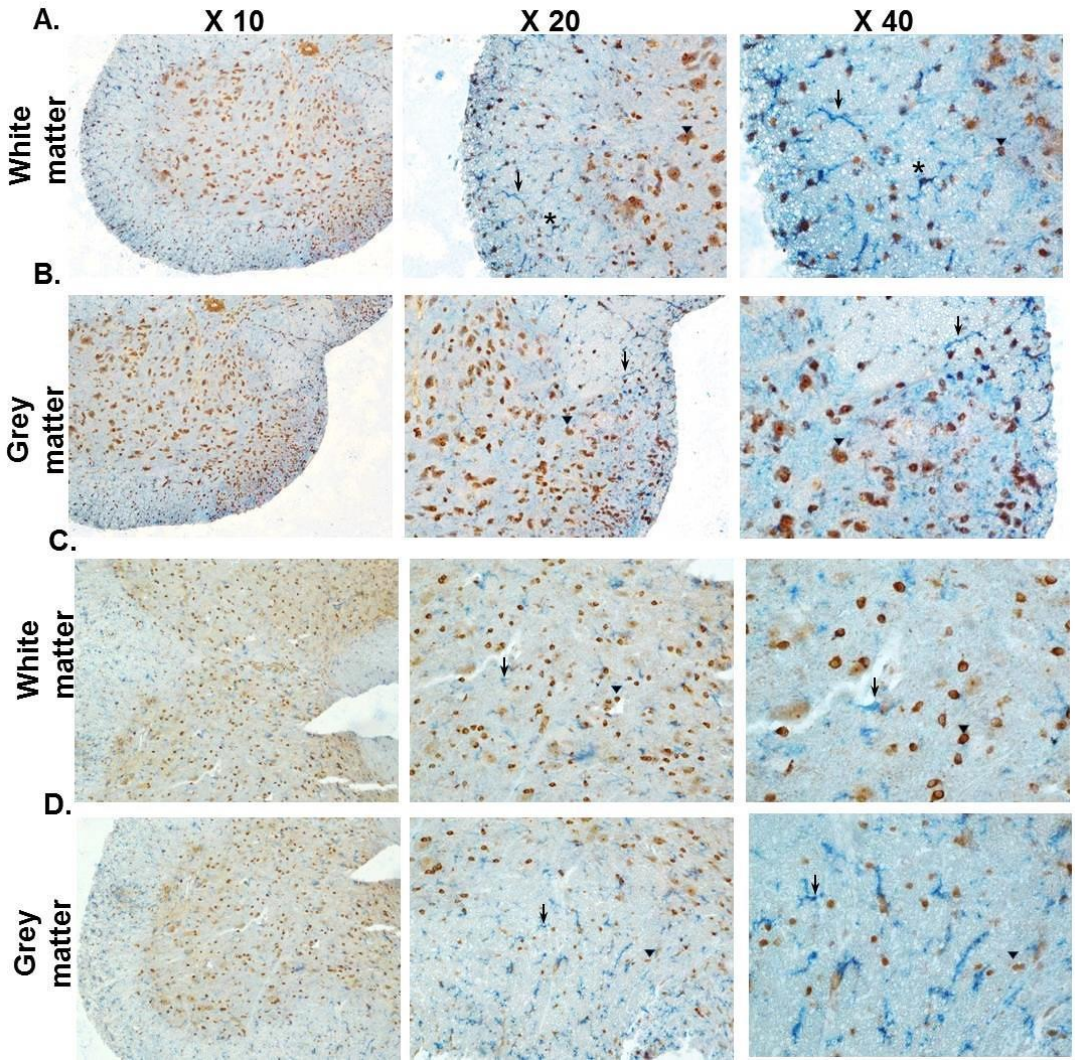

Figure 4.22 ST2 expression on microglia in naïve and EAE spinal cord. Spinal cords were harvested from naïve **(A and B)** and EAE **(C and D)** mice (Day 18) and stained for ST2 (DAB, brown) and Iba1 (Vector® blue). Images show $ST2^+$ (arrowhead), $Iba1^+$ (arrow) and $ST2^+Iba1^+$ (asterisk) cells.

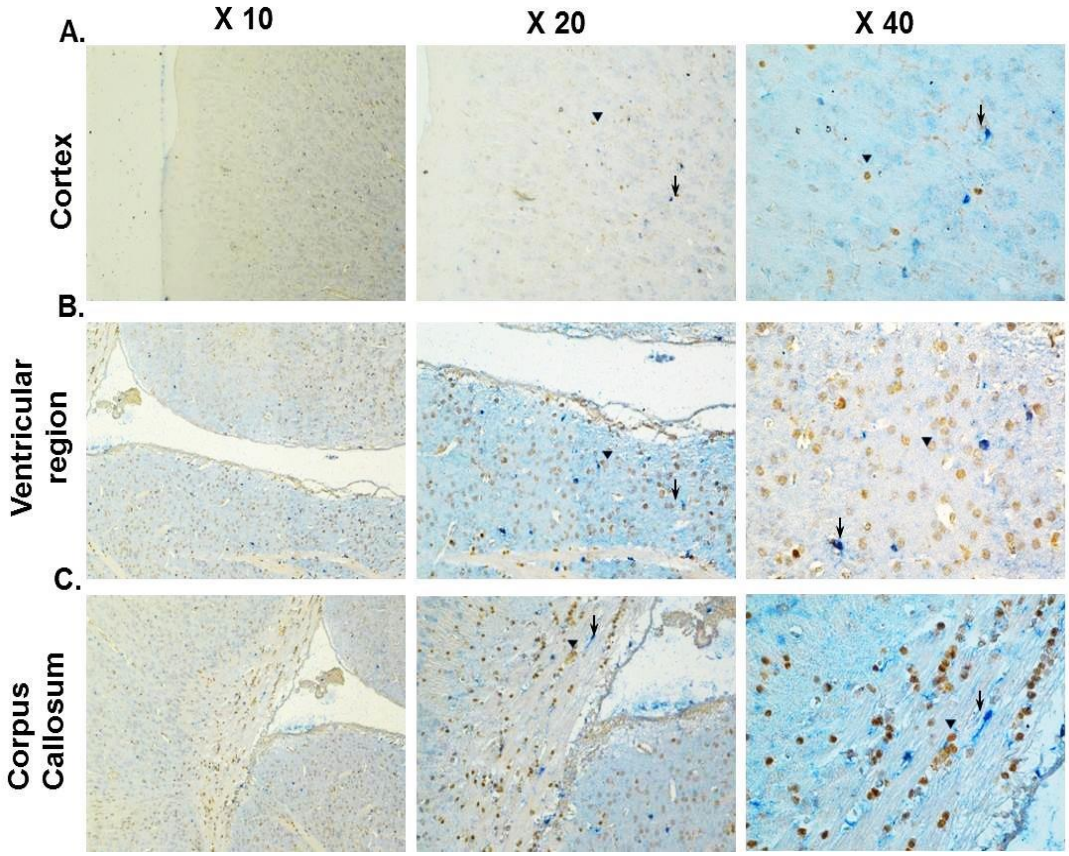

Figure 4.23 ST2 expression on microglia in naïve brain. Brains from naïve mice were harvested and stained for ST2 (DAB, brown) and Iba1 (Vector ® blue) within the cortex **(A)** ventricular region **(B)** and the corpus callosum **(C).** Images show $ST2^{+}$ (arrowhead) and $Iba1^{+}$ (arrow) cells.

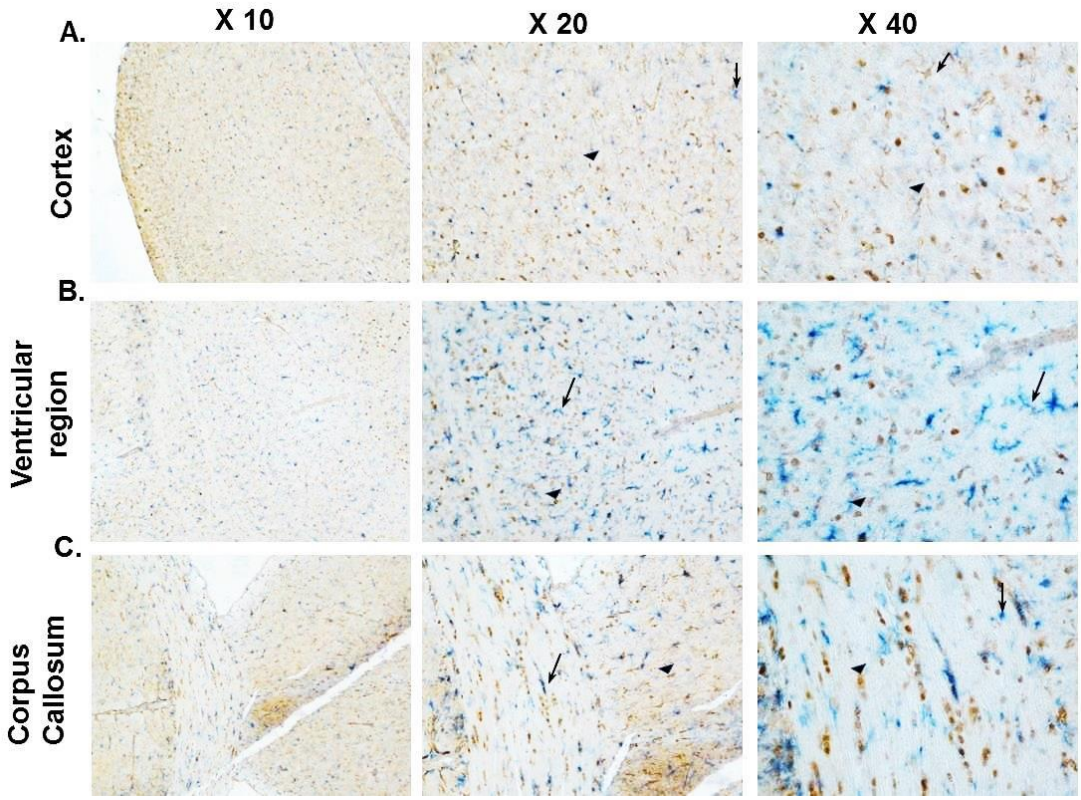

Figure 4.24 ST2 expression on microglia in EAE brain. Brains from EAE mice were harvested on day 18 and stained for ST2 (DAB, brown) and Iba1 (Vector® blue). Images show $ST2^+$ (arrowhead) and $Iba1^+$ (arrow) cells within the cortex (A) ventricular region (B) and the corpus callosum (C).

To summarise, ST2 is present on microglia at the protein level within the spinal cord and brain. Together, with our previous studies (Jiang et al. 2012), the data has shown that ST2 was expressed astrocytes in both the spinal cord and brain tissues of naïve and EAE mice. ST2 was more predominantly expressed by neuron cells within the spinal cord and to a lesser extent within the brain.

4.3 Discussion

The images generated here confirm that both IL-33 and ST2 are highly expressed by murine brain and spinal cord tissues (Schmitz et al. 2005; Jiang et al. 2012). I then examined the expression of the molecules in the CNS resident cells.

IL-33 was expressed by astrocytes and neurons, suggesting that it likely to be expressed by a subset of astrocytes and neurons within the spinal cord and brain. Quantitative analysis of the immunohistochemical staining showed no significant difference in the percentage of IL-33^{+} neurons within naïve and EAE spinal cord. The percentage of IL-33^{+} astrocytes however, decreased during EAE, suggesting down regulation of the IL-33/ST2 pathway during extreme inflammation. Within the brain of naïve mice, IL-33 was co-localised with neurons within the cortex, striatum and within the ventricular region: however, within EAE mice only the cortex and striatum showed co-localisation, this may be due to the release of IL-33 from neurons within the ventricles during inflammation (Pfaff & Kintner 1998) although mRNA analysis has shown no detection of IL-33 within neurons (Yasuoka et al. 2011).

IL-33 was also localised to astrocytes within the hippocampus of naïve tissues but fewer IL-33^{+} cells are expressed by astrocytes within the cortex, ventricular region and corpus callosum. In contrast, in EAE brain tissues, the number of IL-33 and GFAP double positive astrocytes was increased within these regions. My results regarding IL-33 expression by astrocytes are consistent with a previous study investigating the expression of IL-33 on human tissue sections (Yasuoka et al. 2011) and the mRNA expression within culture (Hudson et al. 2008). From the work of Hudson et al, IL-33 was shown to be dependent on ATP for release from cells after PAMP up-regulation (Hudson et al. 2008). It has previously been shown that after IL-33

is released, a decrease in IL-33 expression within cells can be seen (Kakkar et al. 2012). This suggests that the levels of IL-33 protein expression in tissues and cells are dependent on several factors such as the environmental milieu and the presence of ATP.

As expected, IL-33 was not expressed by microglia in naïve or EAE CNS tissues. This result is consistent with several studies showing that IL-33 was not present within microglia at an mRNA (Yasuoka et al. 2011) or at a protein level on microglia using immunohistochemical staining (Hudson et al. 2008).

Interestingly, ST2 was also expressed by a subgroup of neurons and astrocytes within the spinal cord and brain of both naïve and EAE mice. ST2 expression on neurons did not alter between naïve and EAE tissues however ST2 expressing astrocytes decreased in EAE tissues. It is unknown why astrocytes would down regulate ST2 in pathogenic conditions. However, a possible explanation could be that ST2 is not expressed on reactive/ proliferating astrocytes. ST2 could also be down regulated on astrocytes as a result of a decreased expression of IL-33 on astrocytes. ST2 cDNA was not detected on primary neuron cultures, although the ST2 adaptor protein IL-1RAcP was detected (Andre et al. 2005; Yasuoka et al. 2011). Both of these studies were conducted on cortical neurons harvested from embryonic cortices. An explanation for this could be that embryonic neurons may express different mRNA and markers compared to adult murine cortex and spinal cord, as seen with IL-33 (Wicher et al. 2013). Furthermore, the neuron cells were cultured in isolation from other resident cells within the CNS and are therefore not representative of the CNS environment *in vivo*. However, the results in this section show that the staining pattern of ST2 in astrocytes within the brain was mainly cytoplasmic and within projections, whereas no $ST2^+$ projections were seen within the spinal cord. This difference could be attributed to the spinal cord and brain possessing distinct microenvironments (Pierson & Simmons 2012). Alternatively, depending on the plane of the

section, astrocytes can appear as nuclei with a thin cytoplasm or thick primary processes (Shannon et al. 2007). $ST2^{+}GFAP^{+}$ astrocytes are particularly evident within the endothelial layer of the cortex. These astrocytes may be interacting with endothelial cells and pericytes which form the BBB (Abbott et al. 2006; Abbott et al. 2010). These results are consistent with other studies which showed ST2 mRNA was detected in astrocytes (Andre et al. 2005; Yasuoka et al. 2011). Therefore, it is possible that IL-33 may interact with the BBB via $ST2^{+}$ astrocytes in an autocrine manner and play a role in the permeability of the BBB.

My results have shown that ST2 was not located on $Iba1^{+}$ microglia cells in naïve or EAE spinal cord or brain tissues. These results are consistent with another study which detected no ST2 cDNA on secondary cultures of microglia (Andre et al. 2005). However, a previous study, using microglia derived from mixed glia cultures, have reported ST2 mRNA to be present on microglia (Yasuoka et al. 2011). The differences seen here could be due to the difficultly in producing a 100% microglia population when shaking the cells from a mixed glial culture. Other cells such as astrocytes may contaminate the cultures, which thrive in most conditions. Thus astrocyte growth could account for this discrepancy.

In summation this study determined the colocalisation of IL-33 and ST2 in CNS resident cells, and these results will help us to understand the intrinsic CNS specific functions of IL-33/ST2 pathway in normal and diseased conditions.

5. Expression of IL-33 and ST2 in the brain of MS patients

5.1 Introduction

IL-33 has also been identified in a number of CNS diseases. Jones et al., have shown that IL-33 is significantly up-regulated in T. gondii-infected mice (Jones et al. 2010). Furthermore, IL-33 is present on chromosome 9p24, which is a chromosome of interest with regards to Alzheimer's disease (AD). Polymorphisms of chromosome 9p24 has been associated with a higher risk of developing AD (Chapuis et al. 2009). Interestingly, the target gene for subarachnoid haemorrhage also encodes IL-33 (Inoue & Takeda 1999) and ST2 was upregulated in the CSF of patients who have had a subarachnoid haemorrhage (Kanda et al. 2006).

Some studies have even investigated IL-33 and ST2 within MS and EAE. Most importantly IL-33 has been identified on astrocytes within MS lesions (Yasuoka et al. 2011). These results suggest a pathogenic role for IL-33 in EAE and MS. This is further re-iterated by the administration of anti-IL-33 antibody to EAE mice potentiating the disease (Li et al. 2012a). However, studies within our group have shown that the timing of IL-33 administration was crucial and IL-33 treatment can attenuate the EAE disease course by reducing IL-17 and IFN-γ (Jiang et al. 2012).

Most studies on MS have been conducted using EAE in mice however, it is important to determine how this translates into MS patients. Although EAE has been a very useful tool in understanding the immunopathogenesis of MS and potential drug targets, there are still species differences, which cannot be ignored. Within this thesis, I have determined IL-33/ST2 expression in

vivo using C57BL/6 mice. To complete our understanding of IL-33 expression and possible function with the CNS, it is important to look at the expression within MS and healthy brain samples. Although this has been addressed briefly (Yasuoka et al. 2011; Christophi et al. 2011) these studies only employed acute MS lesion tissues using a single patient and did not address the expression of ST2. A more extensive investigation into the protein levels of IL-33 and ST2 in an array of different MS sample types and ages are needed. To perform this work I had the privilege of working alongside the MS pathologist Professor Lassmann, who offered his expertise and access to his extensive MS tissue archive at the University of Vienna, Austria. From data presented within this thesis is was envisaged that IL-33 would be upregulated within the MS tissue samples compared to the control tissues and if these data correlated with the mouse model IL-33 would be expressed on neurons and astrocytes.

The aims of this chapter are therefore:

1. To determine the expression of IL-33 and ST2 in healthy and MS (acute and chronic) patient brain tissues of varying ages.

2. To determine the cellular location of IL-33 and ST2 in healthy and MS patient brain tissues.

5.2 Results

Having characterised the expression and colocalisation of IL-33 and ST2 in both healthy and diseased (EAE) tissue (Chapter 4), I sought to determine expression of IL-33 and ST2 within human control and MS tissues.

Specificity of IL-33 immunohistochemical staining in human tissue

Previous studies have indicated that IL-33 is expressed within the lungs, on epithelial and endothelial cells, and has a role in the pathology of asthma (Kurowska-Stolarska et al. 2009; Moussion et al. 2008). Therefore, we reasoned that human lung tissues is an accurate positive control tissue in these experiments (details of all samples are described in Chapter 2 Materials and Methods). All tissues were stained with anti-IL-33 or matching isotype control antibody, to determine any background, which arises from immunohistochemical staining. Consistent with recent literature (Carriere & Roussel 2007), the anti-IL-33 antibody stained lung tissues showing distinct endothelial staining mainly in the cell nucleus, while no staining was observed in the tissues stained with the isotype control (Figure 5.1). These data confirmed the specificity of the anti-IL-33 antibody for human tissues; next I examined its expression in human CNS tissue samples.

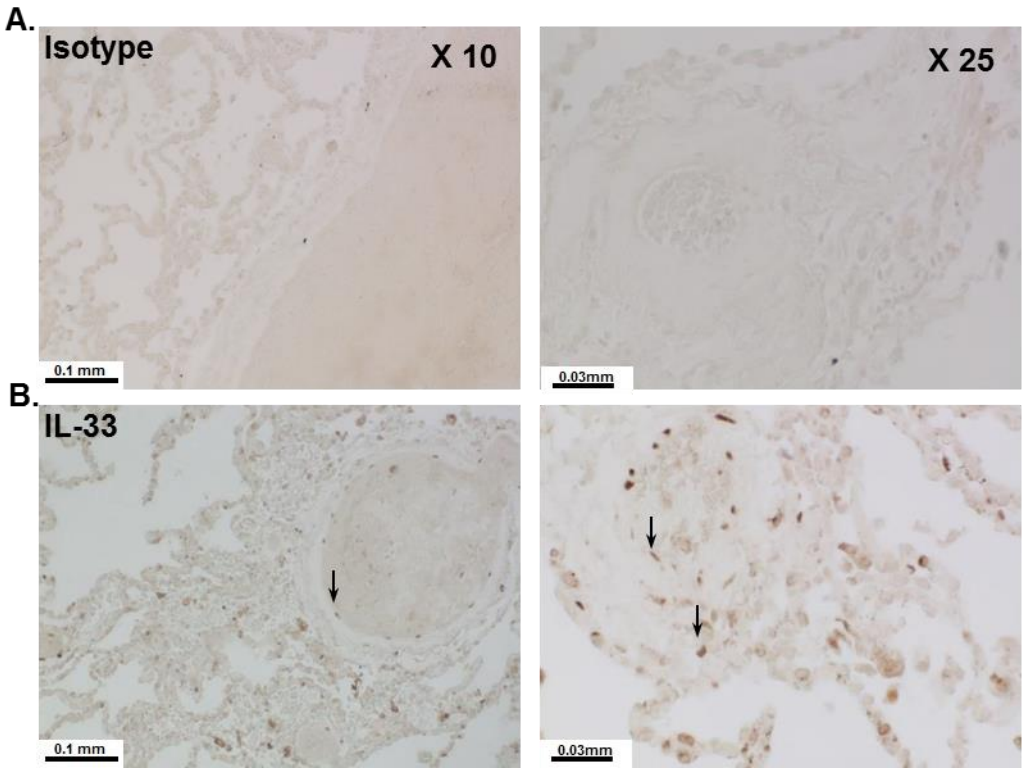

Figure 5.1 Expression of IL-33 in human lung tissues. Sections of human lung (sample Y 256-08-3) samples were stained with either isotype control (A) or anti-human IL-33 antibody (B).

Expression of IL-33 in normal cortex and NAWM brain tissues in human

I next studied the expression of IL-33 in young and aged control brain cortex and NAWM. To determine whether there was an age-related expression difference in CNS samples, all normal and lesion brain samples were divided up into young (<40yrs) and aged (>40yrs) groups in this study.

In young control brain samples (e.g. <40yrs) (Figure 5.2), IL-33 staining showed a distinct cellular pattern within the cortex and punctate staining in the normal appearing white matter (NAWM). IL-33 staining within the cortex was more pronounced than within the NAWM, with distinctive cellular

structures and protrusions in all samples examined (n=7) (Figure 5.2). Similar data were obtained from the aged brain samples suggesting there was little difference in IL-33 expression in young and aged adult brain tissues.

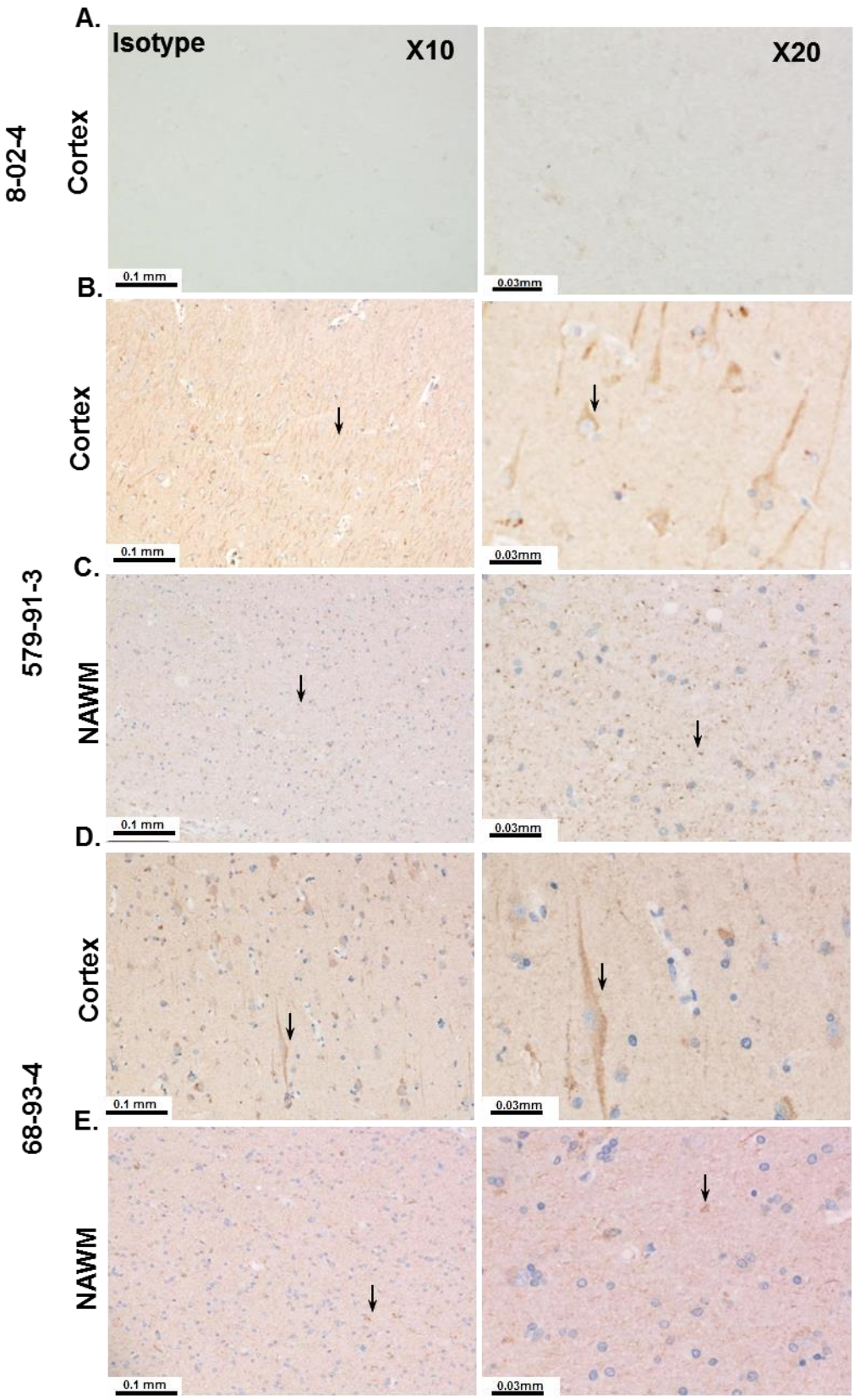
A.
Isotype
X10
X20
8-02-4
Cortex
0.1 mm
0.03mm
B.
Cortex
0.1 mm
0.03mm
C.
579-91-3
NAWM
0.1 mm
0.03mm
D.
Cortex
0.1 mm
0.03mm
68-93-4
E.
NAWM
0.1 mm
0.03mm

Figure 5.2 Expression of IL-33 in normal cortex and WM brain tissues. Normal brain was stained with isotype control antibody (sample 8-02-4) (A), or anti-IL-33 in the cortex (B and D) and WM (C and E) of young (sample 579-91-3) and aged (sample 68-93-4). Arrows indicate IL-33 staining.

Expression of IL-33 in acute MS lesions patients

To understand whether the expression of IL-33 in MS lesions correlated with disease activities, I next stained for IL-33 within acute MS lesions. Acute MS lesions are defined by the presence of perivenular inflammation with demyelination, while axonal loss occurs in the later chronic progressive stage of the disease and is responsible for, the permanent disability (Tievsky et al. 1999).

Expression of IL-33 was determined in acute MS samples from young patients within the cortex, NAWM and lesions (Figure 5.3A, B and C respectively). As with the control samples (Figure 5.2), IL-33 expression was more pronounced within the cortex, with punctate staining observed in the NAWM. Within the acute lesion severe tissue damage can be observed, compared to the NAWM. Low levels of IL-33 expression were observed within the acute lesion in both, the cytoplasm and nucleus of cells. Likewise, within aged acute MS patient samples (Figure 5.4), IL-33 was more prominent within the cortex with distinct cellular and protrusion-like staining. The NAWM also showed punctate staining consistent with previous control and young acute samples. This staining pattern was consistent across all samples obtained from seven different acute MS patients.

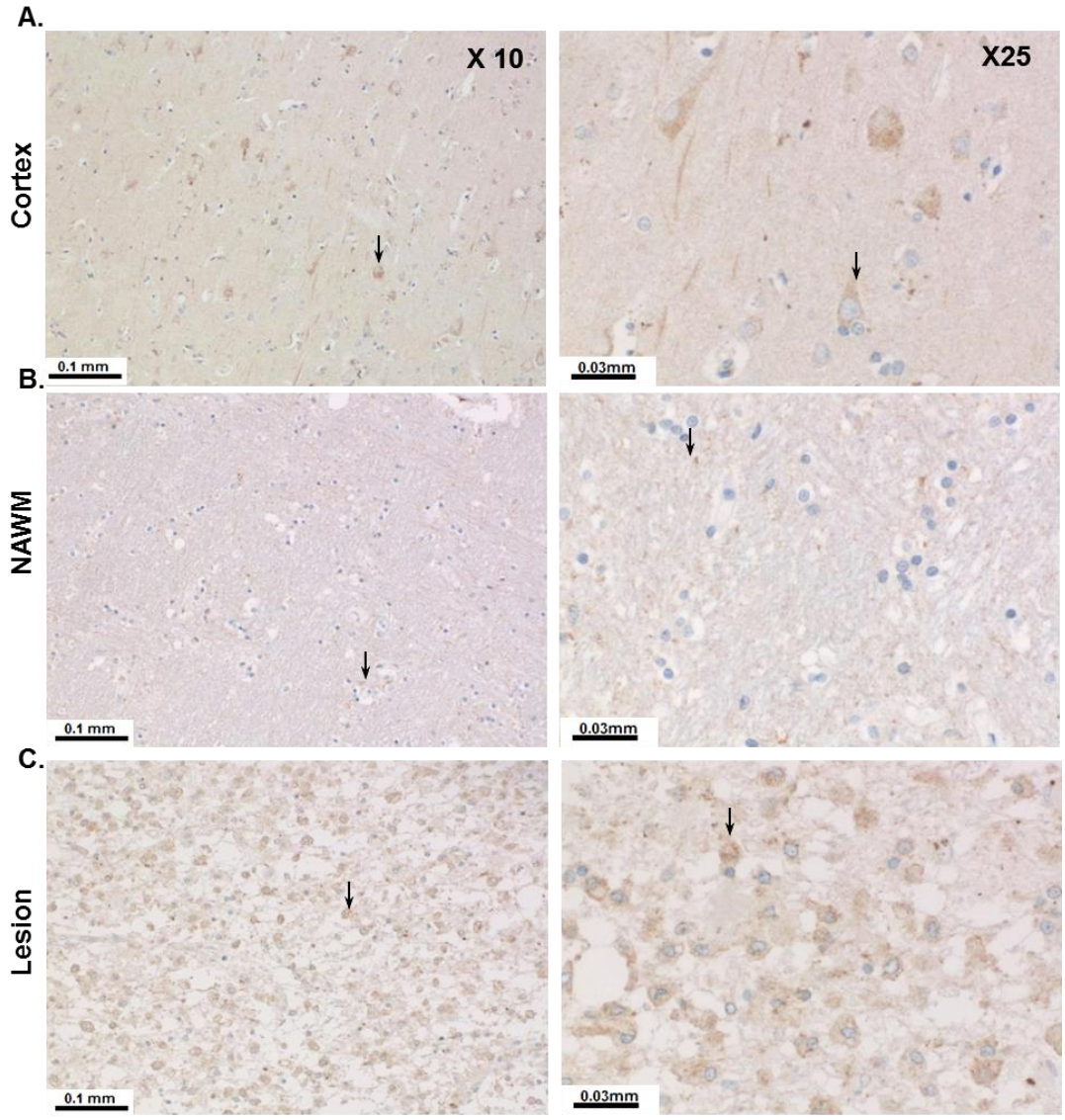

Figure 5.3 IL-33 expression within young acute MS lesion brain. Brain sample A01 144 was stained for IL-33 in the cortex (A), NAWM (B) and site of the WM lesion (C). Arrows indicate IL-33 staining.

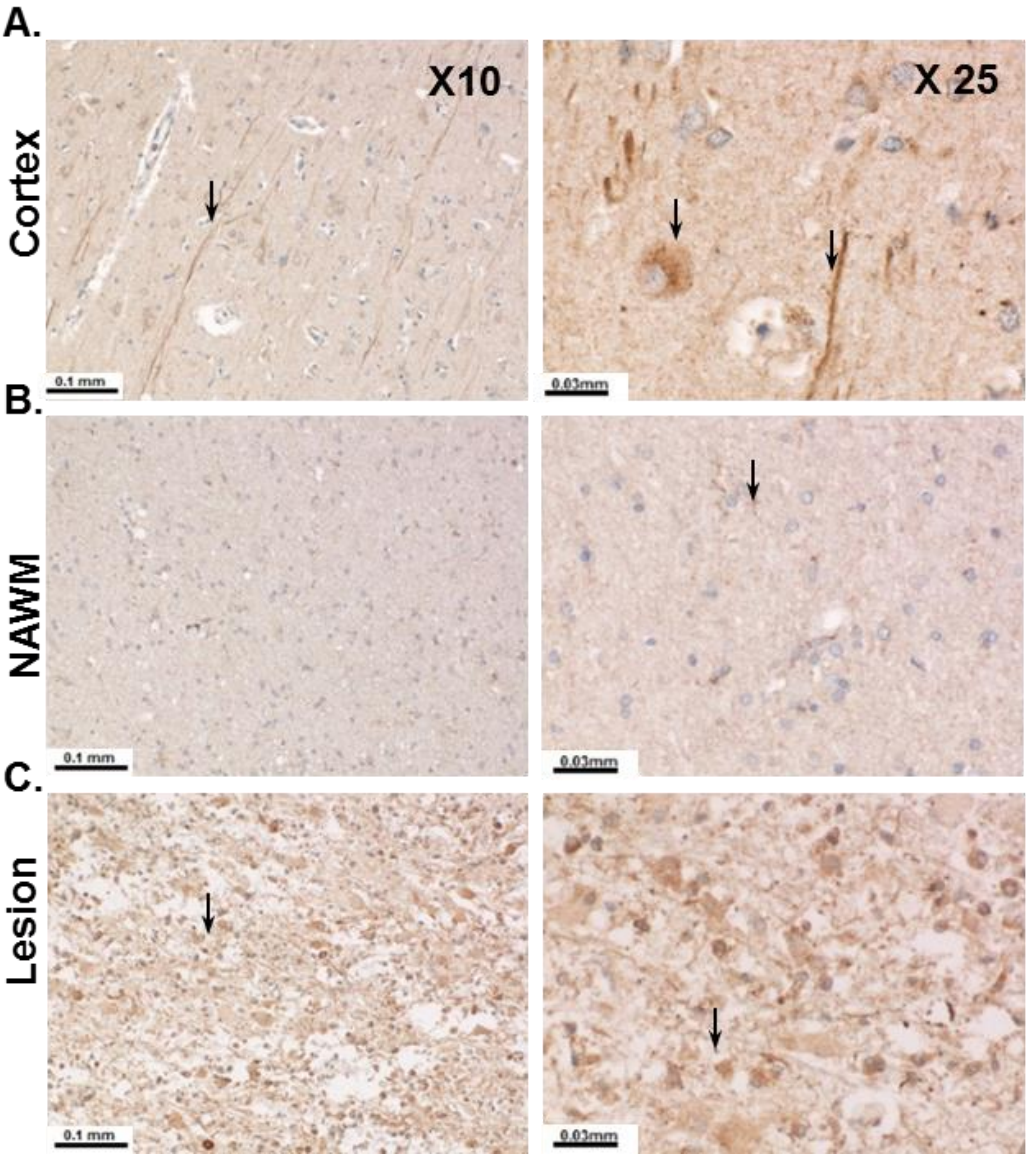

Figure 5.4 IL-33 expression within aged acute MS lesion brain. Brain sample 70-93-6 was stained for IL-33 in the cortex (A), NAWM (B) and site of WM lesion (C). Arrows indicate IL-33 staining.

Expression of IL-33 in chronic MS samples

Chronic MS lesions often develop after several acute MS relapses and result in complete loss of myelin, and severe damage to axons and glia cells (Tievsky et al. 1999; Chang et al. 2008). IL-33 expression was next determined within young chronic MS samples (Figure 5.6). IL-33 staining in the cortex was consistent with previous IL-33 staining seen within control and acute MS samples. Furthermore, low level punctate staining was observed within the NAWM suggesting that there are very few IL-33^{+} cells in NAWM tissues. The chronic lesion had reduced cell numbers, likely due to the extensive damage, after active inflammation as a result of MS relapses. The structure of the lesion was less 'net-like' and the tissue is noticeable inactive due to the lack of infiltrating cells. Within the chronic lesion the expression of IL-33 is dramatically reduced compared to the acute lesion site (Figure 5.3 and 5.4).

In tissues from aged chronic MS patients (Figure 5.6), cytoplasmic and protrusion/ fiber-like structures were observed within the cortex. Within the NAWM sparse IL-33 staining was observed and the staining within the cortex and NAWM was fainter than that of the younger patient samples. This pattern of staining was consistent in all samples examined (n=7).

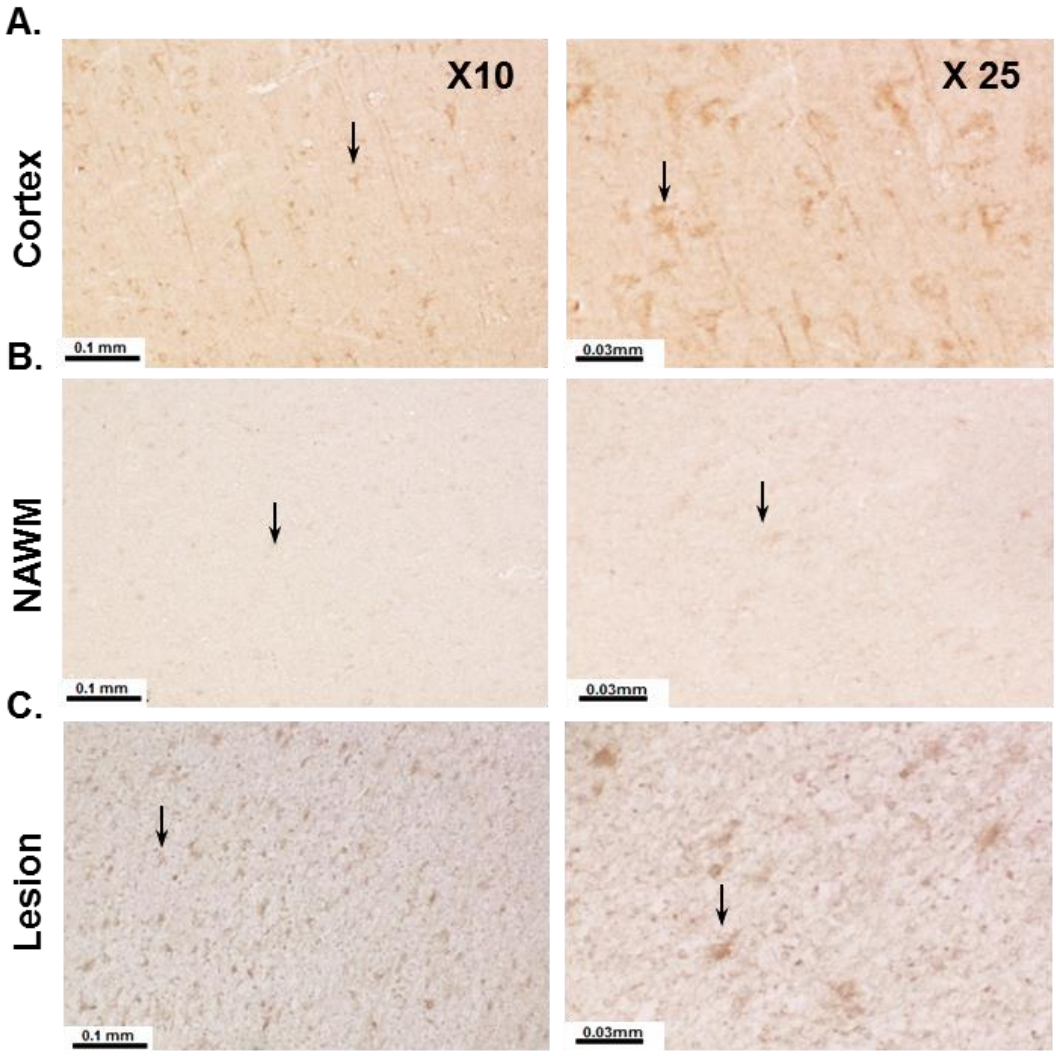

Figure 5.5 IL-33 expression within young chronic MS lesion. Brain sample 67-05-9 was stained for IL-33 in the cortex (A), NAWM (B) and site of WM lesion (C). Arrows indicate IL-33 staining.

My results have shown that IL-33 was present in the cytoplasm of cells within the normal cortex of brain samples from healthy patients, acute MS patients or chronic MS patients with no age related difference (Figure 5.7). The intensity of IL-33 staining was variable within the tissue types and different age groups making it difficult to determine a trend in IL-33 staining. In acute (young) lesions, the cytoplasmic expression of IL-33 was down regulated compared to its expression in cortex and NAWM of the same patients

however aged patients did not show this reduction (Figure 5.7). In aged chronic MS tissues there was a significant reduction in IL-33 staining not seen in the young chronic MS patients. Furthermore, IL-33 expression within the cortex of healthy controls was significantly higher than acute and chronic MS tissues. This data suggest IL-33 is closely linked with CNS inflammation and demyelination, which often occurs in the acute stage of MS disease.

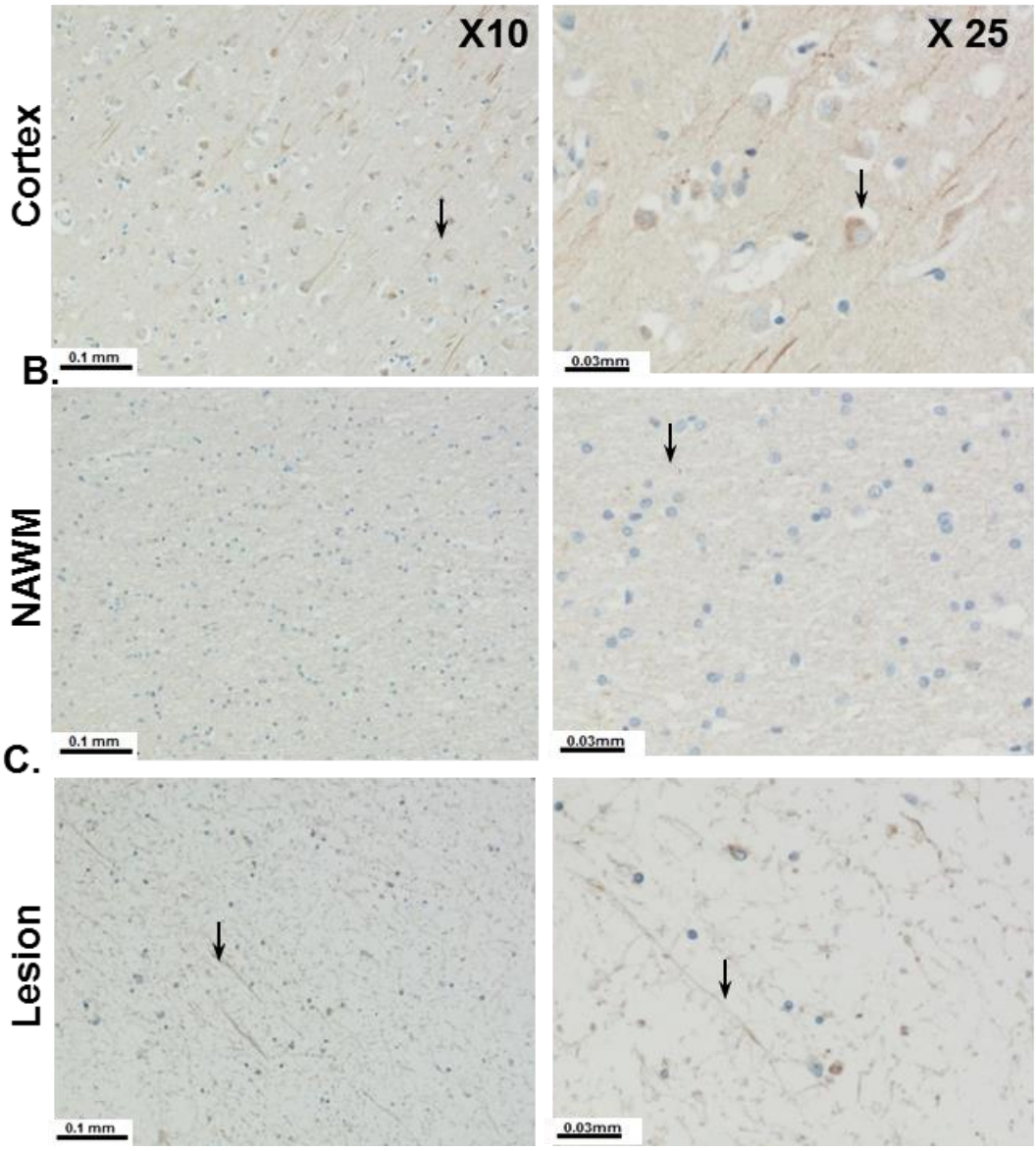

Figure 5.6 IL-33 expression within aged chronic MS lesion brain. Brain sample 285-81-1 was stained for IL-33 in the cortex (A), NAWM (B) and site of WM lesion (C). Arrows indicate IL-33 staining.

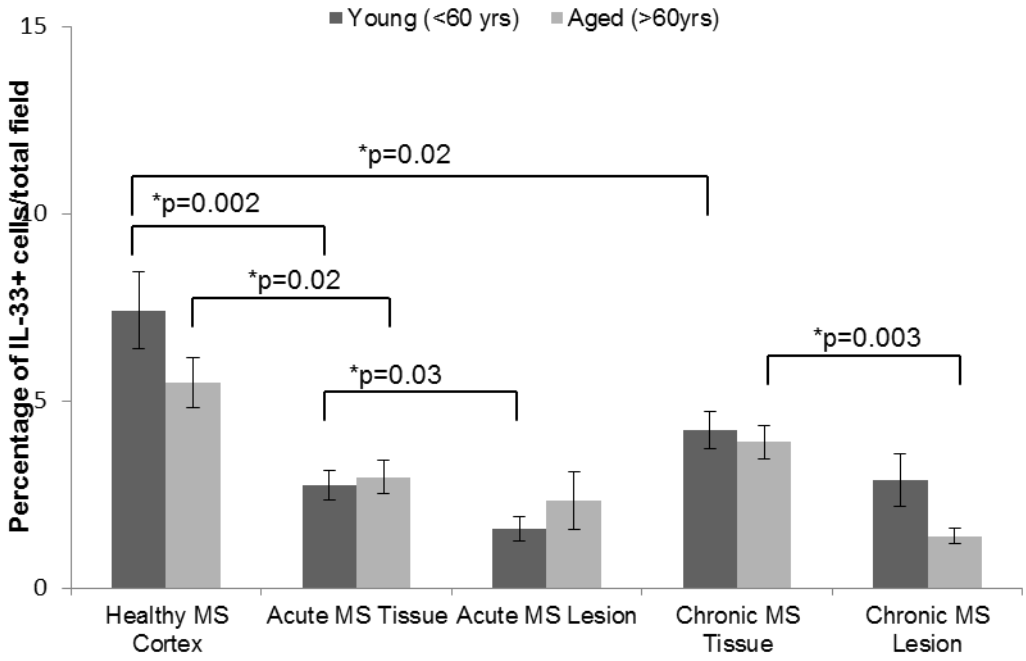

Figure 5.7 Percentage of IL-33^{+} cells in healthy, acute MS and chronic MS brain tissues. Brain sections were taken from healthy cortex, acute MS lesion and acute MS tissue (distal from lesion), chronic MS tissue (distal from lesion) and chronic MS lesion. Tissue sections were stained for IL-33 using immunohistochemical staining and quantified using image J. Data represents mean ± S.E.M, n=7

IL-33 expression on neurons, astrocytes, microglia and ODCs

I next determined the localisation of IL-33 within the resident cells of the CNS. In chapter 4, I used anti-NeuN antibody to stain murine neuron cells, however the anti-human IL-33 antibody in use was unable to be employed in conjunction with the anti-NeuN antibody due to the antibody cross-reactivity with the anti-IL-33 antibody. Instead I used SMI-32, an antibody, which binds to non-phosphorylated neurofilament H (masked when phosphorylated) thus, allowing for the visualisation of neuronal cell bodies, dendrites and thick axons but not thin axons. SMI-32 was used in conjunction with SMI-31 (binds phosphorylated axons) for visualisation of both thick and thin axons, as well as neuronal cell bodies. The results show that IL-33 co-localised with most SMI-31/32^{+} neurons within both the control cortex and WM lesion (Figure 5.8). Both the axon and soma of several axons stained both blue and brown indicating co-localisation within the cortex of control tissues. This indicates that IL-33 was expressed by neurons within control cortex brain tissues. Within the acute MS lesion (Figure 5.8C and D) IL-33 was also observed to co-localise with SMI-31/32^{+} neurons. As this tissue sample was derived from an acute lesion there was a lot of tissue damage and the neurons/axons (blue) are miss-sharpen and with axonal swelling. Despite the damage observed the anti-IL-33 antibody also stained neurons.

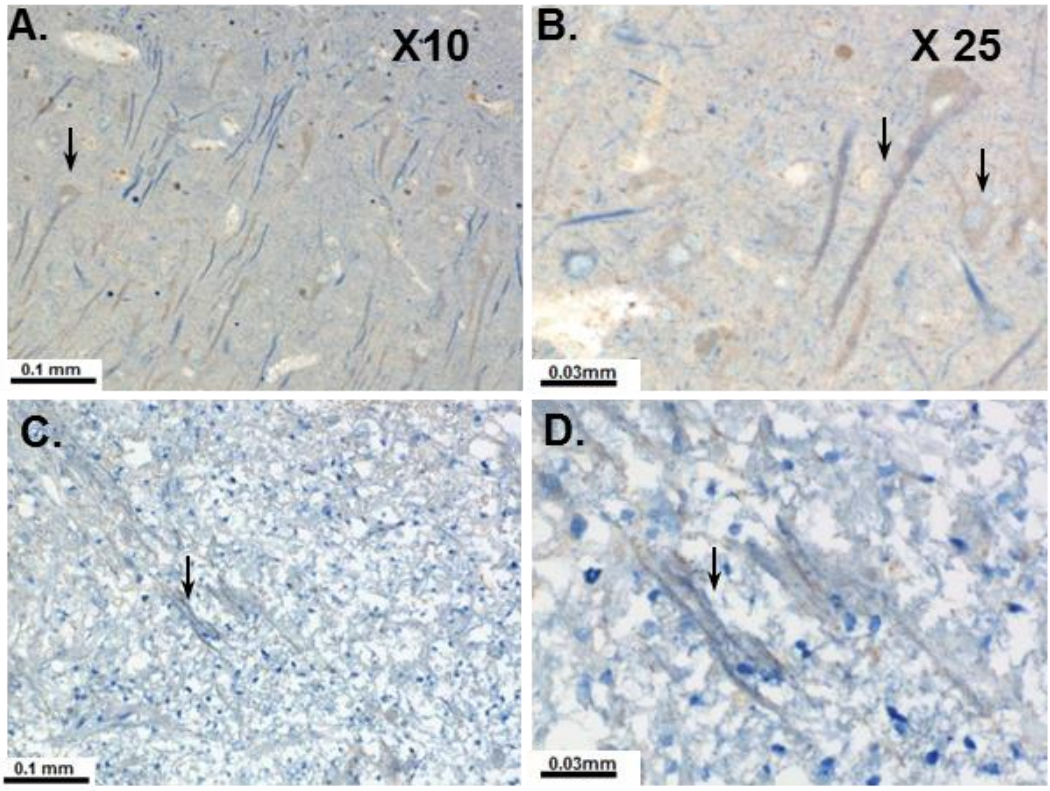

Figure 5.8 IL-33 and axons/neurons in control brain and MS lesion. Both tissues were stained for IL-33 (brown) and SMI-31/SMI-32 (blue) in control cortex (68-93-4) (A and B) and in an acute lesion (90-09-6) (C and D). Arrows indicate IL-33 staining.

Microglia have previously been identified within the lesion site in MS tissues (Ulvestad et al. 1994). On the one hand, they are involved in tissue destruction through expression and production of inflammatory molecules such as TNF-α, IL-1β, IL-2, IL-6 and IL-12. On the other hand, they are involved in scavenging of dead cells and myelin debris, and tissue repair (Goldmann & Prinz 2013). I thus examined the localisation of IL-33 on microglia cells in the normal and lesion sample of MS patients. The double fluorescence staining data showed that IL-33 was mainly present on the neuron/axon-like structures previously seen within the lesion. However, a few microglia did stain positive for IL-33 protein (Figure 5.9). Confocal microscopy provided a platform, which allowed the separation of the layers of tissue and visualise anti-IL-33 antibody binding at a cellular level. The

majority of Iba1^{+} microglia cells are IL-33^{-} suggesting the microglia are not the main source of IL-33 within the MS brain.

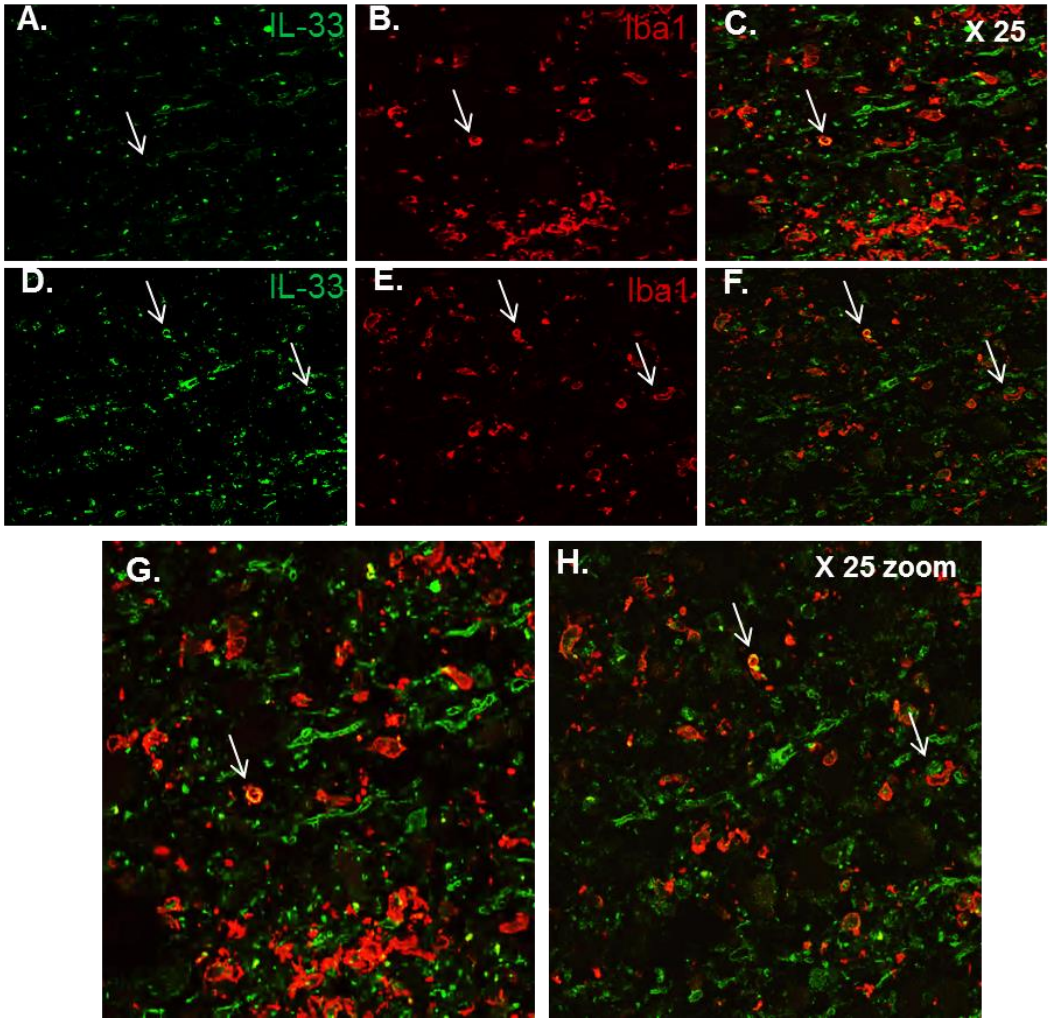

Figure 5.9 Fluorescent staining for IL-33 and the microglia marker Iba1 in acute MS lesion. Tissues were stained for IL-33 (green) and Iba1 (red) within the active lesion (70-93-6). Images A–C and D-F show different regions of the active lesion with anti-IL-33 (A and D), anti-Iba1 (B and E) and merged images (C and F). Image G is an enlarged image of C and image H is an enlarged image of F.

I next investigated whether IL-33 was present within ODCs (CA II) and astrocytes (GFAP) in the acute lesions of MS patients. Data in Figure 5.9 showed that most CAII^{+} ODCs are not IL-33^{+} within the acute lesion of the

MS sample. Furthermore, GFAP^{+} astrocytes also did not express IL-33 within the acute lesion site contrary to previous findings within the literature (Yasuoka et al. 2011; Christophi et al. 2011).

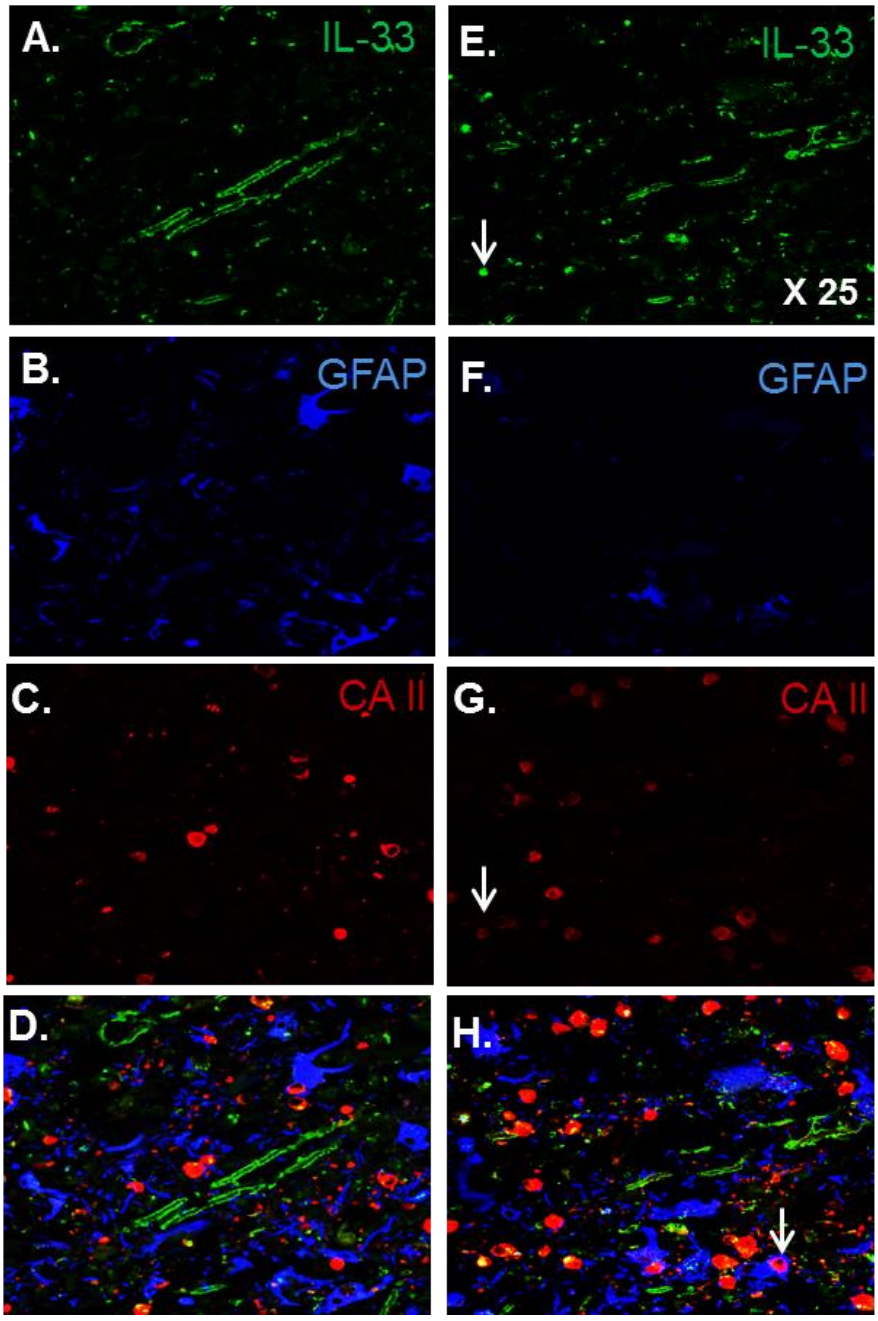

Figure 5.10 IL-33, CA II and GFAP in acute MS lesion. Acute MS lesions (70-9-36) were stained for IL-33 (A and E), GFAP (B and F) and CA II (C and G); images were then combined (D and H respectively).

Specificity of ST2 immunohistochemical staining in human tissue

Anti-human ST2 antibody was first tested using control lung tissues together with a matching isotype control antibody. Figure 5.11 shows that the isotype control generated no specific staining whereas ST2-specific staining was evident on epithelial/ endothelial cells and mononuclear cells within the lung. This confirmed the specificity of anti-ST2 antibody for human tissues, which was then used to characterise ST2 expression in MS CNS tissues.

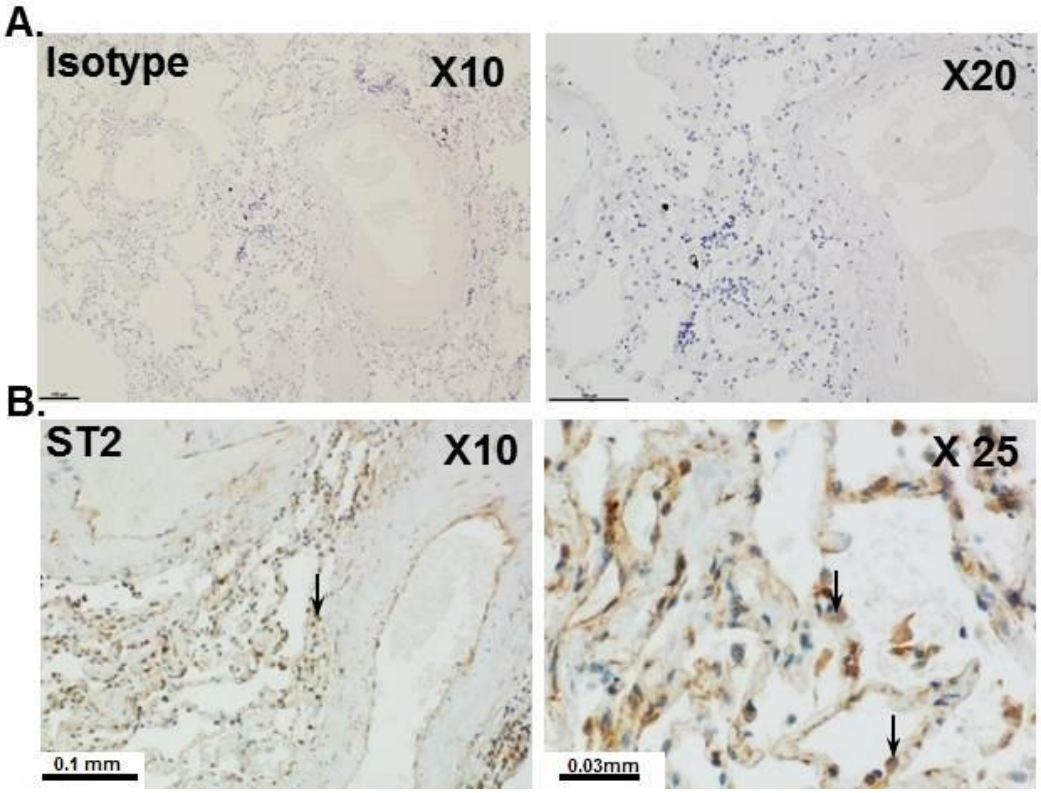

Figure 5.11 ST2 expression on human lung tissue. Sections of human lung (sample Y 256-08-3) were stained with either rabbit isotype control (A) or anti-human ST2 (B).

ST2 within control brain samples

Next I investigated the expression of ST2 in young and aged healthy brain sections. In the normal cortex, the isotype control antibody gave no staining as expected (Figure 5.12A). In contrast, within healthy control brain sections, ST2 showed diffuse distribution throughout the cortex (Figure 5.12B), which was not observed when employing the antibody isotype control. Within the NAWM of normal brain sections, a diffuse staining was also observed; however, the staining appeared more granular in this region, revealing the outline of cells (Figure 5.12C, as indicated by arrow). Within the aged healthy control sections an identical expression pattern can be seen (Figure 5.12). In addition, the staining appears to outline cortical neurons and axons/dendrites within the cortex.

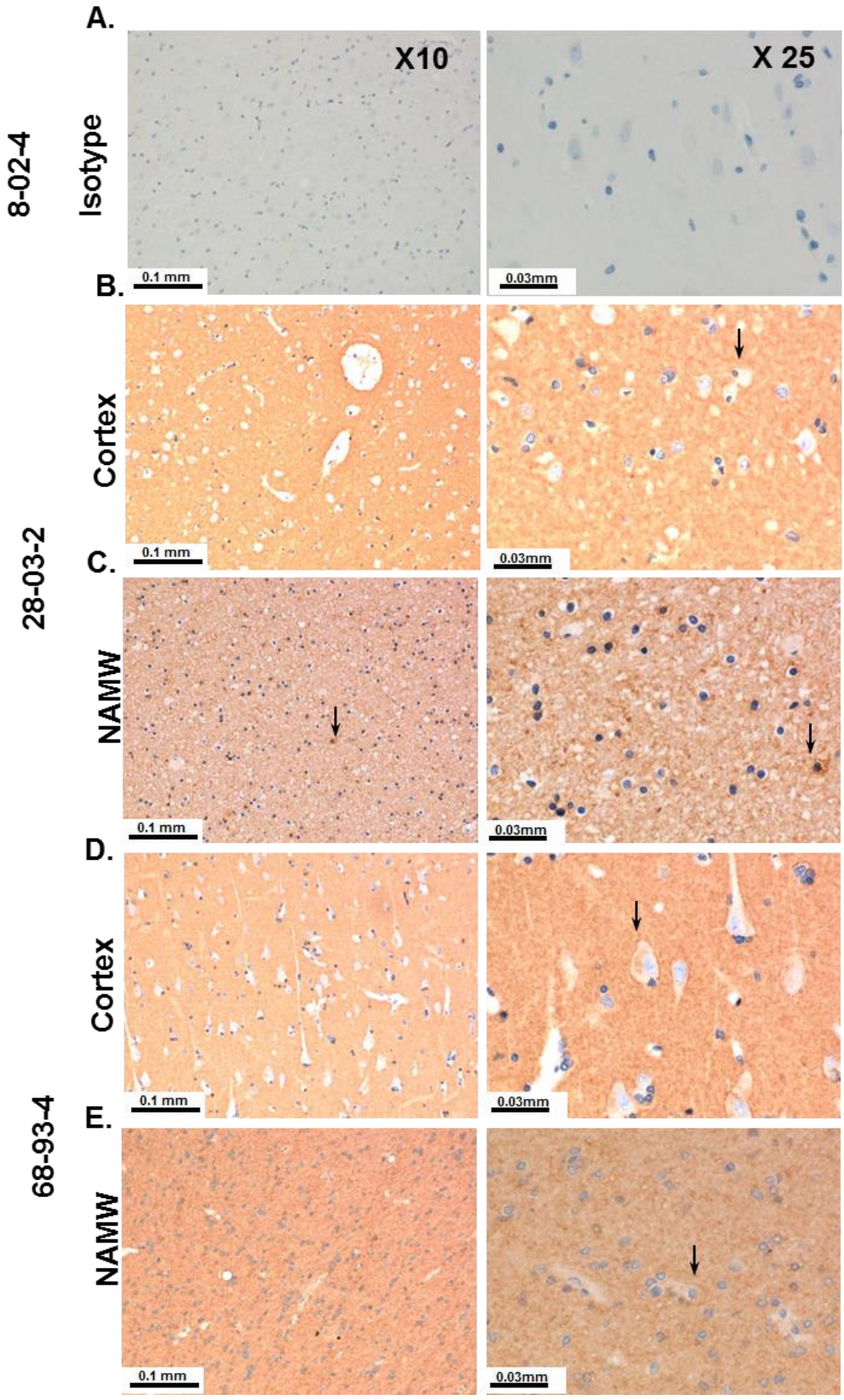
A.
X10
X 25
8-02-4
Isotype
0.1 mm
0.03mm
B.
Cortex
0.1 mm
0.03mm
28-03-2
C.
NAMW
0.1 mm
0.03mm
D.
Cortex
0.1 mm
0.03mm
68-93-4
E.
NAMW
0.1 mm
0.03mm

Figure 5.12 Expression of ST2 in normal cortex and NAWM brain tissues. Normal brain was stained with isotype control antibody (sample 8-02-4) (A), or anti-ST2 in the cortex (B and D) and NAWM (C and E) of young (sample 28-03-2) and aged (sample 68-93-4). Arrows indicate IL-33 staining.

Expression of ST2 in acute MS lesions

ST2 expression was next determined within young acute MS tissues (Figure 5.13). As seen in the healthy CNS samples (Figure 5.12), ST2 expression was diffuse within young acute human MS tissues in both the cortex and NAWM. Within this particular section it was identified by a histologist that tissue A01-144 represented a demyelinating lesion (identified by immunohistochemical staining during the characterisation of these tissues). The results have shown ST2 present on filament structures indicating that ST2 may be expressed on degenerating myelin (Figure 5.13C) and within cells present in the lesion. The cortical expression of ST2 within aged acute brain sections (Figure 5.14) was very similar to the expression within the healthy control sections (Figure 5.12) suggesting ST2 expression was not altered within the cortex of this sample. ST2 showed a diffuse expression within the cortex and a granular staining within the NAWM (Figure 5.14). This was accompanied by high ST2 expression on degenerating myelin; however, within the lesion more specific cellular staining was observed as well as fiber-like projections.

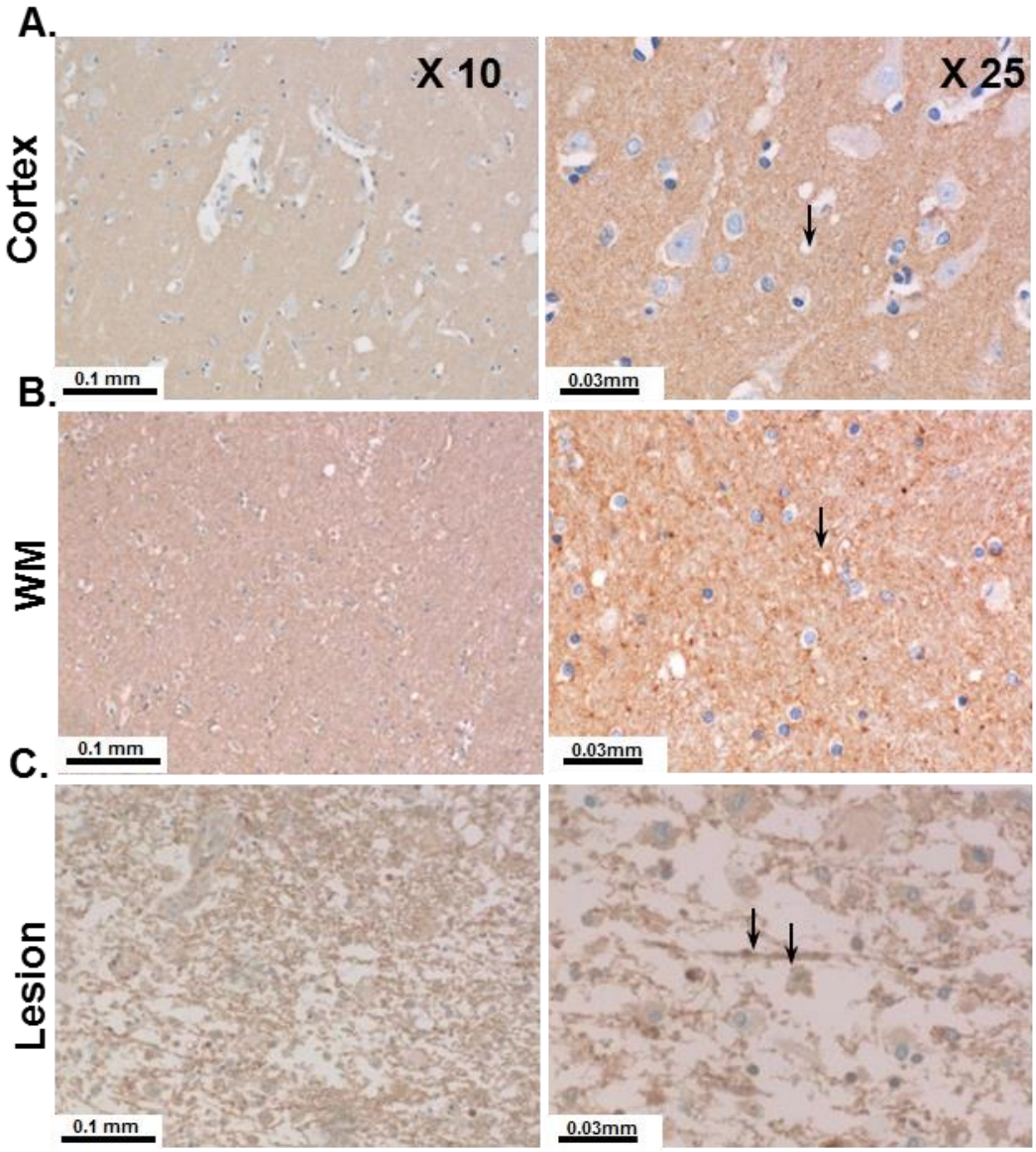

Figure 5.13 ST2 expression on young acute MS human brain. Brain sample A01-144 was stained for ST2 in the cortex (A), NAWM (B) and site of lesion (C).

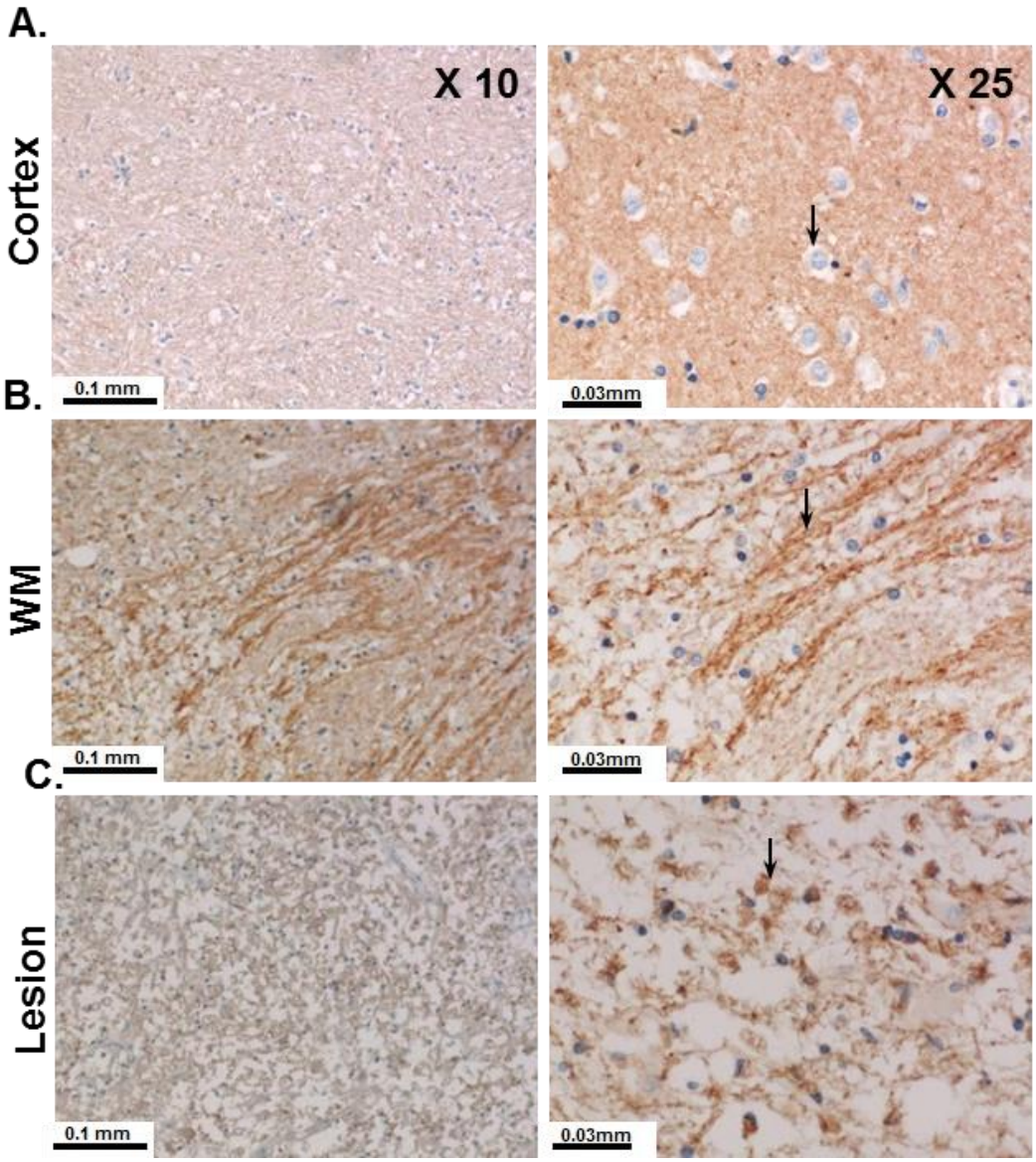

Figure 5.14 ST2 expression on aged acute MS human brain. Brain sample 90-09-6 was stained for ST2 in the cortex (A), NAWM (B) and site of lesion (C).

Expression of ST2 in chronic MS lesions

In chronic MS samples of young patients (Figure 5.15), ST2 expression was diffuse within the cortex and WM as previously described. However, within the lesion site, more specific ST2 staining was observed which was also seen in the acute lesion samples (Figures 5.13 and 5.14). Similar results were observed in chronic samples of aged MS patients (Figure 5.16) with diffuse staining of ST2 in the cortex and white matter, but fiber like $ST2^{+}$ structures in the lesions.

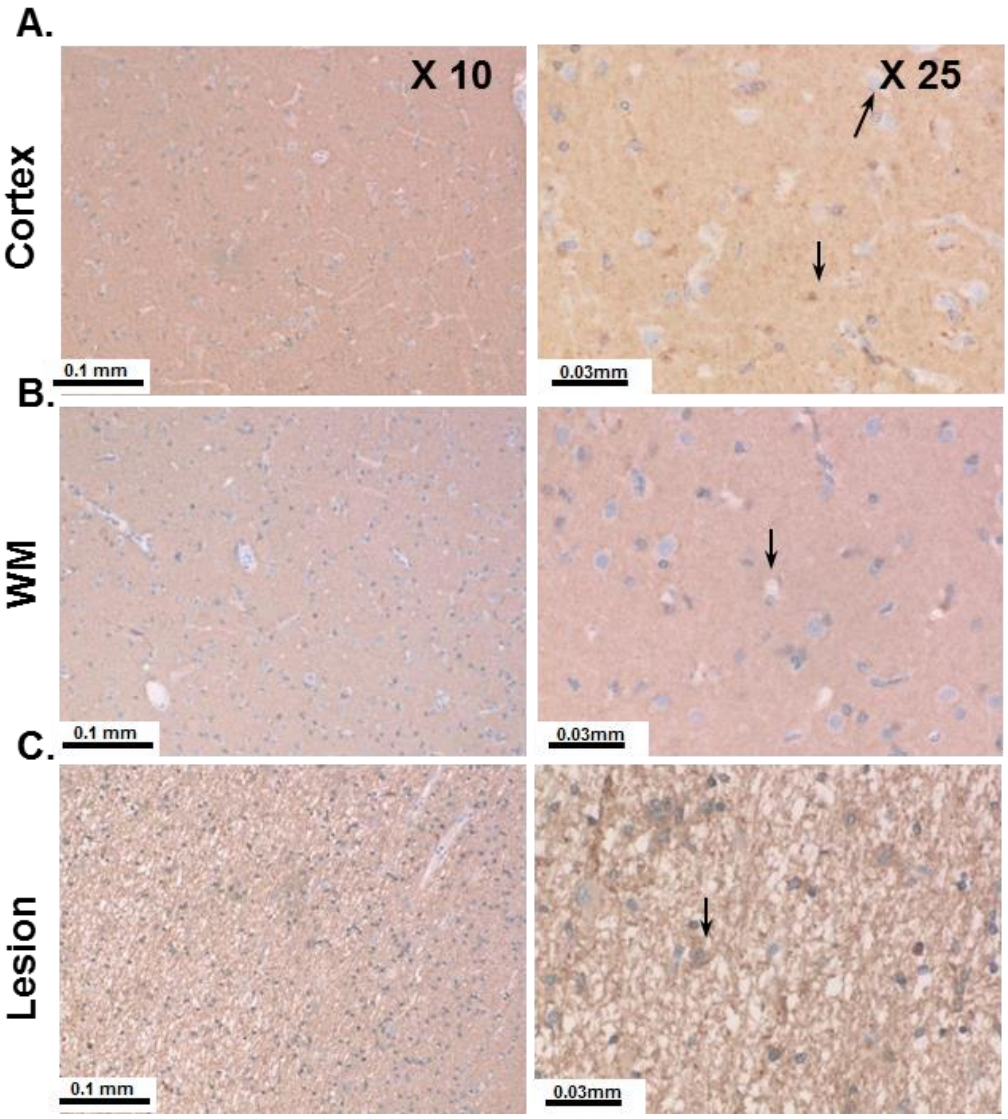

Figure 5.15 ST2 expression on young chronic MS human brain. Brain sample 67-05-9 was stained ST2 in the cortex (A), NAWM (B) and site of lesion (C).

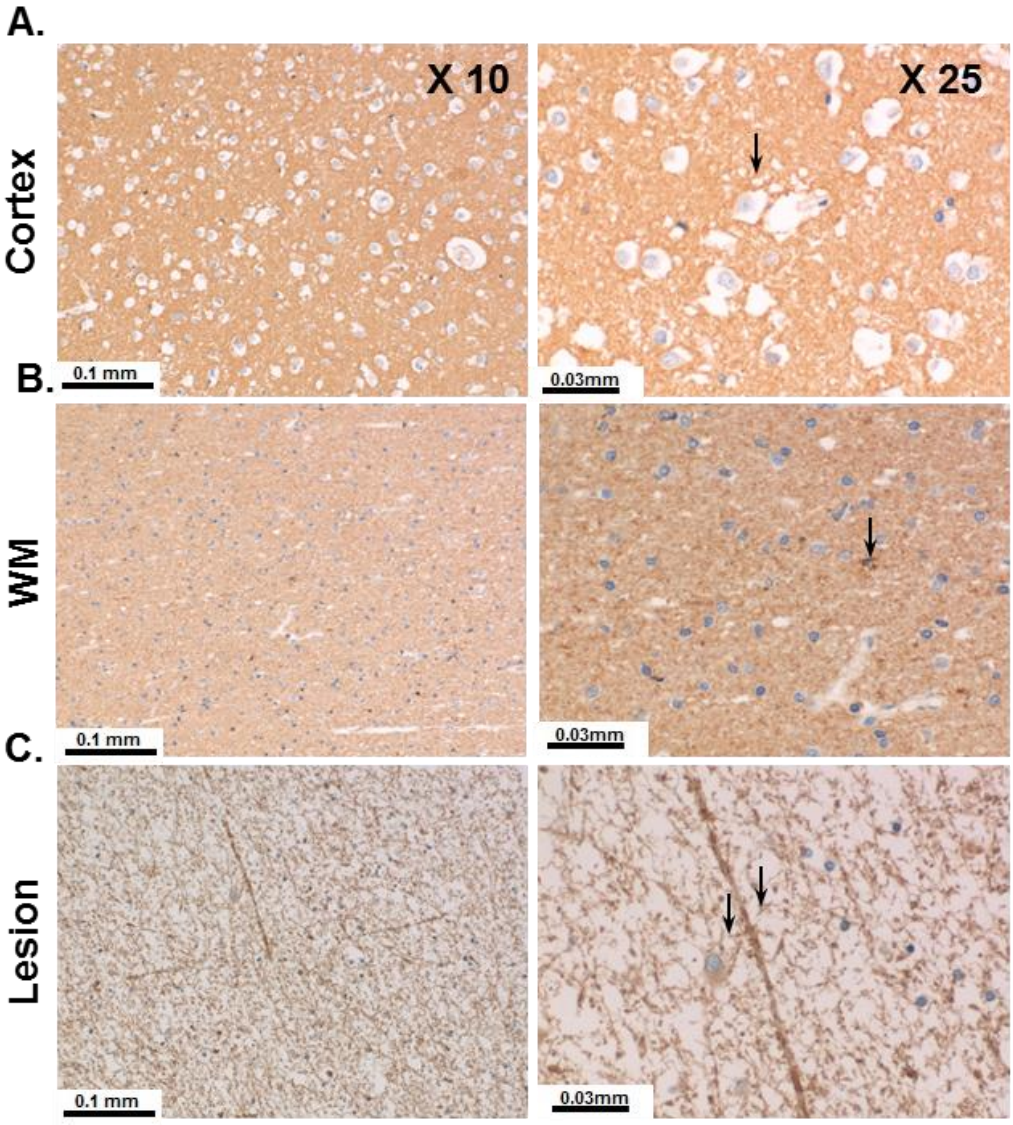

Figure 5.16 ST2 expression on aged chronic lesion human brain. Brain sample 285-81-1 was stained for ST2 in the cortex (A), NAWM (B) and site of lesion (C).

The co-localisation of ST2 on CNS resident cells

To determine the localisation of ST2 on the 'fiber-like' structures seen in acute and chronic lesions of MS patients, ST2 was stained alongside anti-SMI-31 and anti-SMI-32 antibodies, which stain axons and the neuronal cell bodies respectively. The double fluorescence staining in MS lesion samples (Figure 5.17) showed ST2 was present on axons or around the axons in a similar manner as myelin. ST2 was previously shown within the cytoplasm of cells within the lesion site (Figure 5.14). To test whether microglia cells in the lesions expressed ST2, I next stained for ST2 together with CD68, a marker for microglia/ macrophages. This marker was used instead of Iba1 due to the cross reactivity of the anti-Iba1 with anti-ST2 antibody. The results indicate that ST2 did not co-localise with CD68 (Figure 5.18), suggesting microglia are not the source of ST2 in the lesion. The expression of ST2 around the axons within the lesion, suggest ST2 may be involved in myelin damage or repair in MS disease. Next, I determined whether the ODCs express ST2 using the ODC marker CAII. Figure 5.19 showed that ST2 is present in a small subset of $CAII^{+}$ ODCs however; most CAII ODCs did not express ST2. Astrocytes are involved in MS inflammation and lesion formation thus I investigated the expression of ST2 on astrocytes (GFAP) but found no evidence to suggest that ST2 is present within astrocytes in acute MS lesion samples (Figure 5.19).

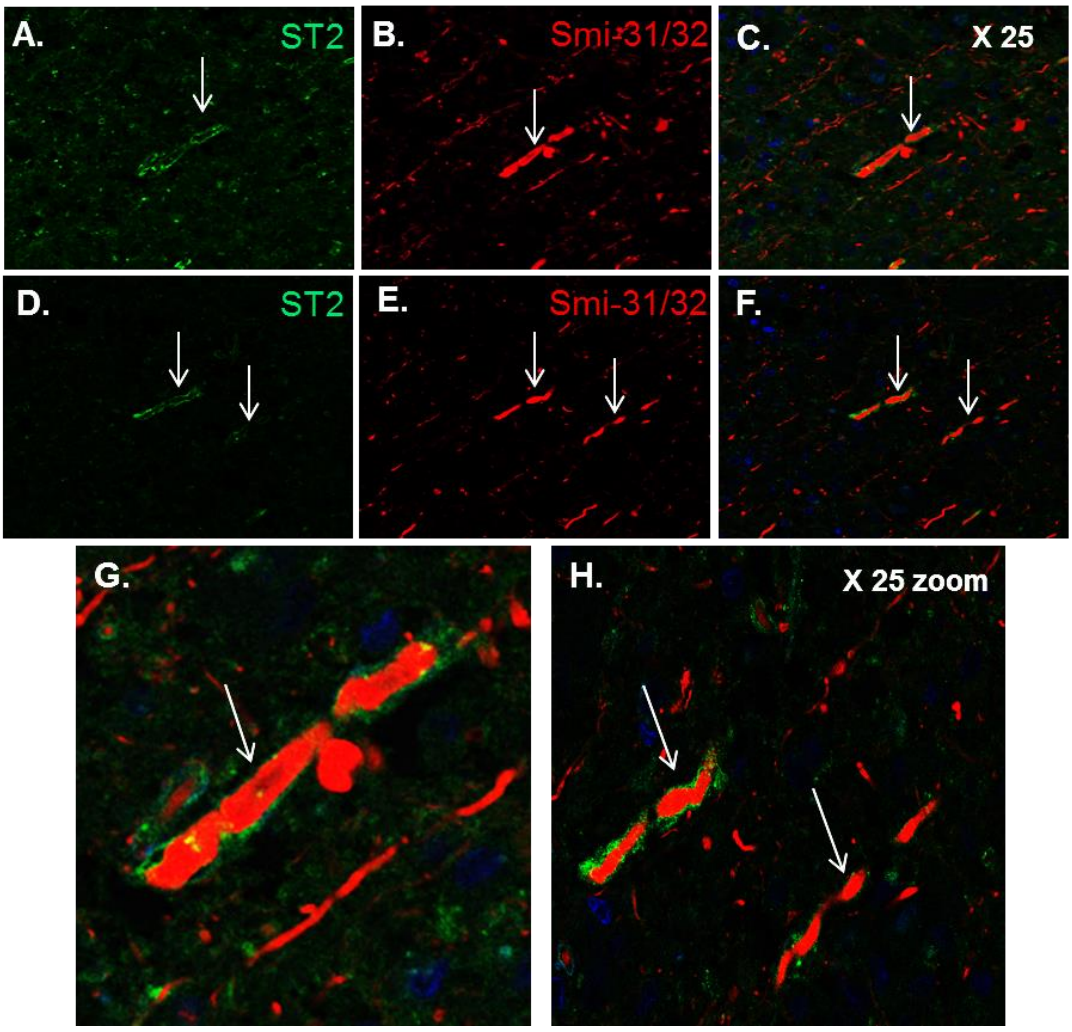

Figure 5.17 Double staining of ST2 and SMI-31/32 in MS lesions. Acute MS lesion (70-93-6) was stained with anti-ST2 (green), anti-SMI-31/32 (red) within regions (A) and (B). Images C and D are enlarged regions of interest from (A) and (B) respectively.

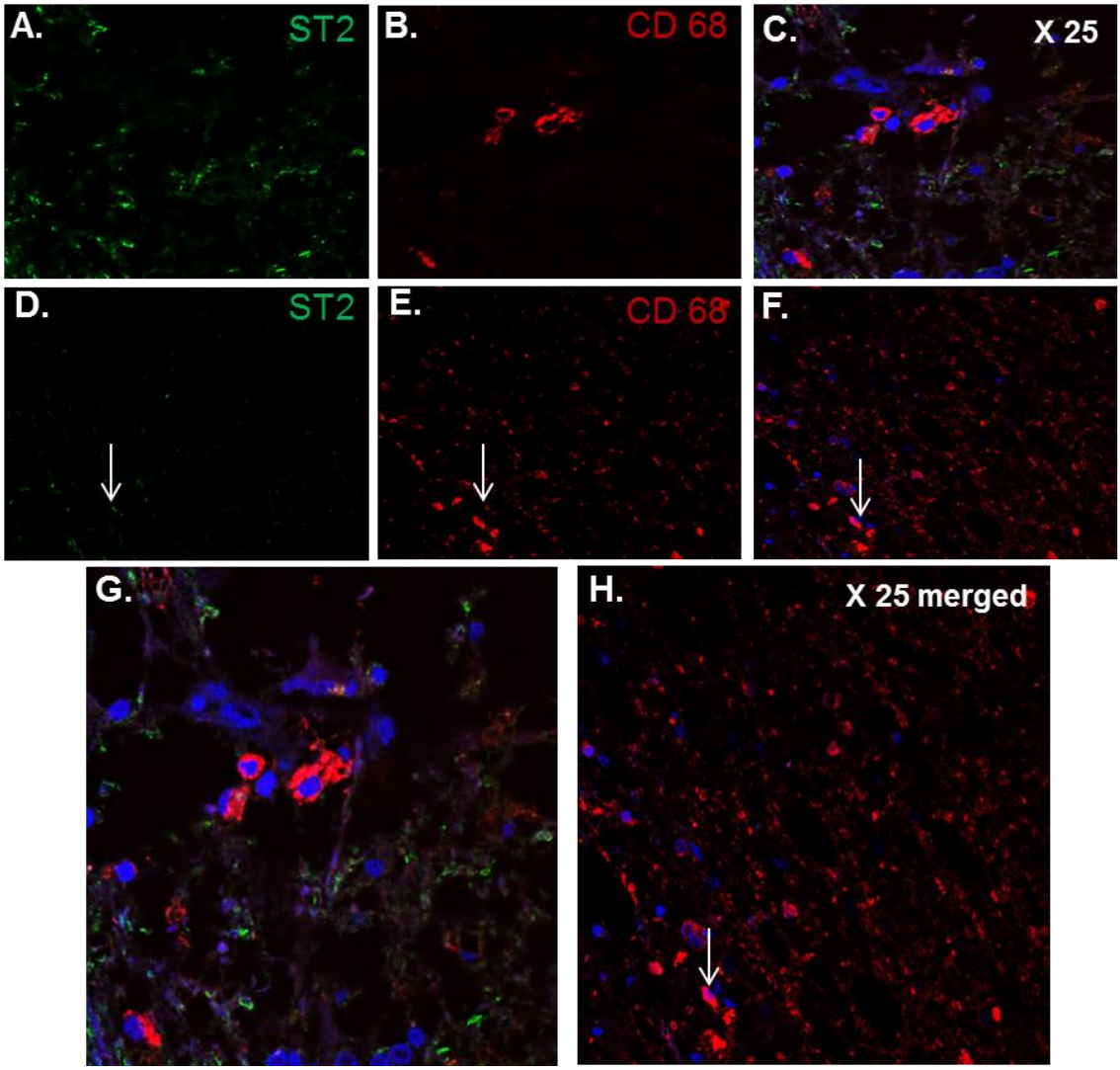

Figure 5.18 ST2 and CD68 in MS lesion. Acute MS tissue (90-09-3) was stained for ST2 (green) or CD 68 (red) within regions (A) and (B). Images C and D are enlarged regions of interest from (A) and (B) respectively. Cellular nuclei were also stained with DAPI (blue).

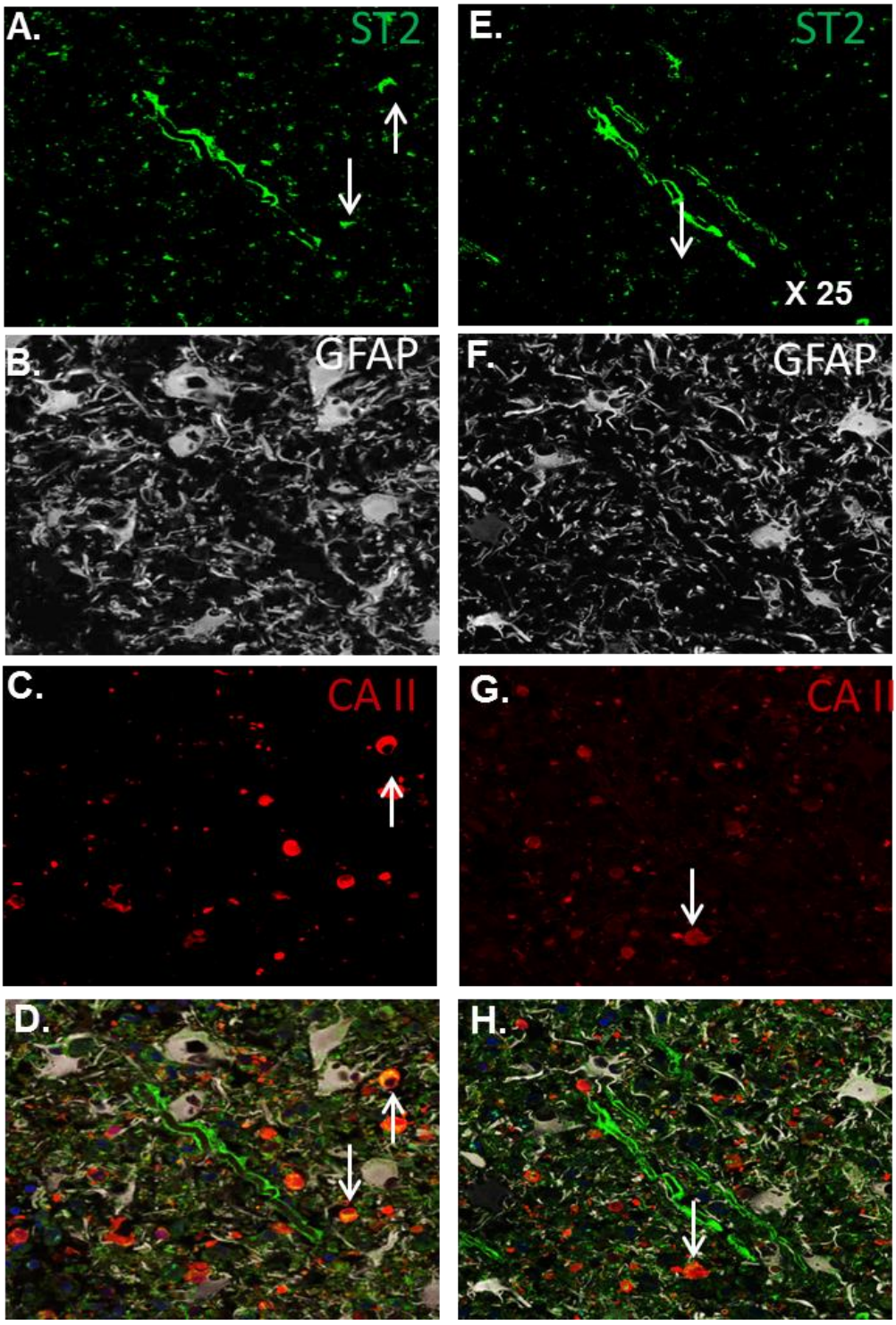

Figure 5.19 ST2, CA II and GFAP in MS lesions. Acute MS sample (70-93-6) was stained for ST2 (green), CA II (red) and GFAP (white) in regions (A-D) and (B-H).

5.3 Discussion

IL-33 has been implicated in the CNS inflammation associated with subarachnoid haemorrhage and may have a protective role in Alzheimer's disease (Yu et al. 2012) and amyotrophic lateral sclerosis (Lin et al. 2012). However, with regards to its role in MS disease, data from EAE studies are currently contradictory. A report by Li et al, has shown that IL-33 is pathogenic and the neutralisation of IL-33 attenuated EAE (Li et al. 2012b). On the other hand, our own study has demonstrated a protective role for IL-33 in EAE by dampening down IL-17 and IFN-γ production (Jiang et al. 2012). To help understand the role of IL-33 in MS disease, I investigated the expression of IL-33 and its receptor ST2 in control and MS brain samples.

IL-33 has been identified on astrocytes within EAE and MS samples (Yasuoka et al. 2011; Christophi et al. 2012). However, less information is available about the location of the ST2 molecule in CNS cells. While studies suggested that ST2 is solely expressed by CNS astrocytes, others reported the presence of ST2 on astrocytes and microglia (Yasuoka et al. 2011; Hudson et al. 2008). To our knowledge, no study has identified ST2 protein expression in human CNS tissues.

IL-33 has several characteristics in common with the alarmin High-mobility group box 1 (HMGB1). Both alarmins have nuclear expression; move from the nucleus to the cytoplasm and are then secreted; are expressed constitutively on most cells and have a role in intracellular gene expression as well as being secreted as an alarmin (Faraco et al. 2007). IL-33 staining within the cortex of normal brains showed pronounced cytoplasmic staining which co-localised with neurons and axons not seen in the NAWM. Although, IL-33 has been identified within the nucleus of cells, a recent study has shown that IL-33 can traffic, between the nucleus and cytoplasm of cells (Tsuda et al. 2012a) and has also been visualised in vesicles in a similar

manner as HMGB1 (Tsuda et al. 2012b; Gardella et al. 2002). IL-33 may be expressed in vesicles within axons which travel along the length of the axons after which it is released into the synaptic cleft to alert other neurons and resident cells of damage (alarmin) (Tsuda et al. 2012b; Gardella et al. 2002; Al-Bassam et al. 2012).

ST2 expression showed diffuse staining within the control human brain, which differed to the astrocytic staining within the mouse brain (Chapter 4). Despite the cortical ST2 staining resembling that of non-specific binding, i.e. not characteristic of specific cellular structures, the isotype controls showed no staining at all suggesting that the staining observed was specific. Although no conclusions can be drawn from the ST2 staining it is important to note that no other study has shown ST2 expression in CNS at a protein level which is unusual as IL-33 has been extensively studied, perhaps the reason for this is the unusual staining pattern ST2 presents within the human brain.

The quantification of the IL-33 staining in the cortex and lesion site of healthy patients, acute and chronic MS patients indicated no age related difference in IL-33 protein expression. Despite this, differences in staining was observed. IL-33 expression within healthy patient cortex was significantly higher than IL-33 expressed in the cortex of acute and chronic MS brain tissue. Furthermore, young acute tissues had a reduced IL-33 expression in the lesion site compared to the cortex (not noted in aged acute tissue). In aged chronic tissue a reduction in IL-33 was also seen in the lesion (not noted in young chronic tissues). The reduction in IL-33 staining could be a result of IL-33 release from cells as a danger signal or potentially the death of IL-33 expressing cells during acute and chronic inflammation.

My findings have shown IL-33 to be present within the cell body of neurons and along the axons in CNS cortex tissues and the lesion sites of chronic samples. As previously mentioned ST2 is part of the IL-1 family of receptors

and shares IL-1RAcP with IL-1RI to exert intracellular effects. Within mouse cultures IL-1RI and IL-1RAcP have been identified on primary neuronal cells, astrocytes, microglial and ODCs (Andre et al. 2005). The double staining data showed a similar pattern of ST2 expression in MS lesions. ST2 often co-localised with SMI-31/32 indicating the presence of ST2 on or around axons. ST2 could be expressed on the surface of the axons during stress as the morphology of the axons seen in this sample shows axonal swelling and damage. I also observed that the higher the level of damage seen in the axons (i.e. the swollen and broken axonal shape) the stronger the ST2 signal. On axons less swollen ST2 staining was not as apparent. Alternatively ST2 could be expressed around the damaged axons suggesting that it may be present on the myelin rather than on the axons.

Next I investigated whether IL-33 was expressed on $CAII^+$ ODCs and results suggest that a subset of $CAII^+$ODCs express IL-33. IL-33 expression on ODCs has also been shown using murine glial cultures detecting $Olig2^+IL\text{-}33^+$ cells (Wicher et al. 2013). Wicher *et al* determined that IL-33 was not expressed on embryonic tissues but was only present during late embryogenesis and in glial cultures grown from postnatal tissues (Wicher et al. 2013) suggesting a role for IL-33 in development. Similarly, ST2 was seen to co-localise with ODCs expressing CAII. The presence of IL-33 and ST2 on ODCs implies that IL-33 may work in an autocrine fashion to modulate myelination or homeostasis within the CNS ODCs. ODCs are very sensitive to stress furthermore, the IL-33/ST2 signaling cascade has shown to be mechanically activated in cardiac fibroblasts (Sanada et al. 2007). It is possible that IL-33 and ST2 are upregulated and activate the signaling pathways in ODCs within the lesion site due to the enhanced mechanical stress the cells are under.

IL-33 was also investigated for expression on astrocytes (GFAP), similarly no staining was observed on astrocytes within the lesion site. The opposite was observed by Christophi *et al.,* who identified IL-33 to be expressed within

human MS patient brain NAWM (Christophi et al. 2012). Furthermore, IL-33 mRNA was detected in astrocytes *in vivo* (Yasuoka et al. 2011) and *in vitro (*Hudson et al. 2008),my *in vivo* results (Chapter 4) also suggest the protein expression of IL-33 on astrocytes. These differences could be due to regional variations, IL-33 is expressed in cells at a certain stage in the cell cycle beyond which it is not observed (Küchler et al. 2008). Although IL-33 was not co-localised with GFAP in these tissues MS is a heterogenetic disease and therefore the analysis of more samples may show IL-33 astrocyte expression. Our detection methods also may not have been sensitive enough to detect low levels of IL-33.

As ST2 was seen to be expressed on the surface of astrocytes at a mRNA level (Andre et al. 2005; Yasuoka et al. 2011) within murine brain in chapter 2 and in previous studies (Hudson et al. 2008) it was expected that this expression would also be seen within the human brain. However, the results showed that there were no $GFAP^{+}ST2^{+}$ cells within the lesion site of the acute MS sample. ST2 could be present on a particular subset of astrocytes not expressed within this region. From previous results in mice ST2 was not present on all astrocytes and it was mainly astrocytes associated with the endothelium and blood vessels and therefore potentially only expressed on protoplasmic astrocytes instead of fibrous.

Microglia are the first line of defense within the CNS, and scavenge dead cells, axons and myelin (McPhail et al. 2004). Previously, IL-33 has been identified on alveolar macrophages (Mizutani et al. 2013). Similarly, IL-33 was expressed by a subset of, but not all $CD68^{+}$ microglia/macrophages. IL-33 has not been previously shown to be expressed by microglia however, IL-33 has been seen to cause the proliferation and activation of microglia in culture (Yasuoka et al. 2011). Interestingly, ST2 has previously been seen to be present on macrophages (AAM) (Kurowska-Stolarska et al. 2009; Brint et al. 2004) and microglia at a mRNA and protein level (Yasuoka et al. 2011). Despite this, our results in EAE showed no protein expression of ST2 on

Iba1^{+} microglia within naïve and EAE spinal cord *in vivo* and *in vitro*. Furthermore, when an acute MS sample, abundant in macrophage/ microglia activity within the lesion, was stained for CD68 (microglia marker) and ST2 no cell was found to be double positive suggesting that microglia and macrophages within the brain lesions are ST2^{-}. The cellular expression of ST2 seen within the lesion is most likely the consequence of scavenging macrophages/microglia engulfing ST2^{+} axons/ myelin that have been destroyed. Alternatively, microglia may express ST2 at an mRNA level but not at a detectable protein level within the human brain.

As the patient ages their ability to withstand stress and damage declines and thus degeneration can occur as a result. Age is an important risk factor in many diseases and thus it is important where possible to identify if there is a link between the expression of genes related to age. Indeed a study by Glass et al., has identified 5 out of 10 brain regions showing age-related difference of gene expression (Glass et al. 2013). For example, a study investigating age-dependent changes in HMGB1 has shown that the localisation and protein expression of this molecule changes in an age-dependent manner (Enokido et al. 2008). As IL-33 is regarded as an alarmin molecule with similar characteristics to HMGB1, I therefore divided the human brain samples into young (<40 yrs) and aged (>40 yrs) groups and studied the expression of IL-33 and ST2 in these tissues. The results however, have shown no obvious difference in the staining between young and aged control samples.

6. The Effect of IL-33 on CNS myelination

6.1 Introduction

In previous chapters, I investigated the expression of IL-33 and ST2 within the spinal cord and brain of EAE and healthy mice. IL-33 was expressed on astrocytes and neurons in both the spinal cord and brain of naïve and EAE mice, but without noticeable upregulation in EAE tissues. Similarly, ST2 was also expressed on astrocytes and neurons within the spinal cord and brain of EAE and control mice. In human CNS tissues, IL-33 was detected on neurons, whilst ST2 was observed in regions around damaged axons in MS samples; suggesting co-localisation with the axon or myelin. Interestingly ST2 was also expressed by ODCs in the lesion. These results suggested a possible role for IL-33/ST2 pathway in CNS remyelination during the development of MS disease. Within this chapter, I investigated the role of IL-33 in CNS myelination within the CNS, utilising a myelinating culture system established within the lab of Professors Barnett and Linington, at Glasgow University.

Often, animal models are used to aid our understanding of the mechanisms underlying disease and the associated pathology. In vitro models are further utilised to investigate interactions at a cellular level. Moreover, they create opportunities for manipulations which may not be possible *in vivo* (Kipp et al. 2012). Several CNS tissue culture systems exist such as aggregated tissue culture (Berglund et al. 2004), organotypic (Ghoumari et al. 2003) dissociated primary mixed cell culture (Fex Svenningsen et al. 2003)and recombinant cell culture (Fitzner et al. 2006). The culture system used for this study – myelinating culture system – involves astrocytes, neurons, axon formation,

microglia and ODCs. The system has previously been validated by Thomson et al, (Thomson et al. 2008a) who showed that myelination began after 15 days in vitro (DIV). However, the major wave of myelination occurred between 17 and 23 DIV. Between 23 and 28 DIV there was an increase in the number of axons myelinated and the thickness of the enveloping myelin and Nodes of Ranvier. Internodes were also found to be developed along the axons within these cultures (Sorensen et al. 2008).

As the mixed glial myelinating culture system most accurately reflects the myelination of axons in vivo, it was chosen to investigate the role of IL-33 in demyelinating MS disease. Due to rat and murine IL-33 being 90% similar (Sanada et al. 2007), it was hypothesised that using mouse rIL-33, would also act on $ST2^{+}$ rat cells. We further tested the effect of IL-33 in a mouse myelinating culture system as we used mouse EAE model in this study. We (Chapter 5) and others (Christophi et al. 2012) have shown IL-33 to be upregulated in the acute lesions of MS samples. Other functional studies have shown a protective role for IL-33 in different CNS disease models such as T. gondii infection (Jones et al. 2010)and EAE (Jiang et al. 2012). Although both studies determined the important effect of IL-33 on the function of peripheral immune system, thus the impact on disease development, little is known about the exact role of IL-33 in CNS function. Therefore the aims of this chapter are to:

1. Characterise both the rat and mouse in vitro myelinating culture system.

2. Determine the cellular expression of IL-33 and ST2 on CNS cells within the in vitro myelinating culture.

3. Investigate the effect of IL-33 on rat and mouse myelination and axonal density.

4. Determine the effect of IL-33 on the astrocytes, ODCs and microglia within the mouse culture system.

6.2 Results

To fully understand the mechanistic action of IL-33 within cultures I firstly established the cellular expression of IL-33 and ST2 on CNS resident cells that exist within rat and mouse cultures; including neurons, astrocytes ODCs and microglia.

Expression of IL-33 and ST2 in CNS culture cells

To determine the expression of IL-33 and ST2 on the CNS cells in the rat myelinating culture system, rat cells were cultured onto coverslips. These were removed from culture at day 28, fixed and stained for IL-33 and ST2, along with antibodies specific for neurons (NeuN), astrocytes (GFAP), microglia (ED1) and ODCs (O4). The results show that ST2 was expressed by some $NeuN^+$ neuron cells (Figure 6.1A), but not $ED1^+$ microglia (Figure 6.1B) or $GFAP^+$ astrocytes in the rat cultures (Figure 6.1D). Although this was consistent with my in vivo results for ST2 expression in neuron cells in mouse, the negative expression of ST2 by microglia and astrocytes in this rat culture system does not agree with my in situ staining data and previous findings using mouse tissues (Yasuoka et al. 2011; Andre et al. 2005), Currently there has been no extensive characterisation published regarding the expression of IL-33 and ST2 in rat CNS tissues and cells. Therefore it is difficult to identify which set of results was accurate. Furthermore, due to cross-reactivity between antibodies - which I experienced during this investigation, ED1 had to be used to label microglia, instead of Iba1. ED1 however, identifies activated microglia and therefore is not a true representation of the expression of ST2 on resting microglia.

As ST2 was shown to be expressed by some ODC in human CNS tissues and as ODC are the myelinating cells in CNS, I next determined the expression of ST2 on ODCs using the O4 marker. The results show that ST2 co-localises with $O4^+$ projections (fibre-like structures) extending from the ODC cell body (Figure 6.1C) indicating that IL-33/ST2 may play an important role in CNS myelination. To determine the IL-33 producing cells, I also stained for IL-33 within the rat cultures (Figure 6.1F). IL-33 expression however, did not differ from the isotype control (Figure 6.1E) indicating non-specific binding; as a result the localisation of IL-33 in vitro was inconclusive.

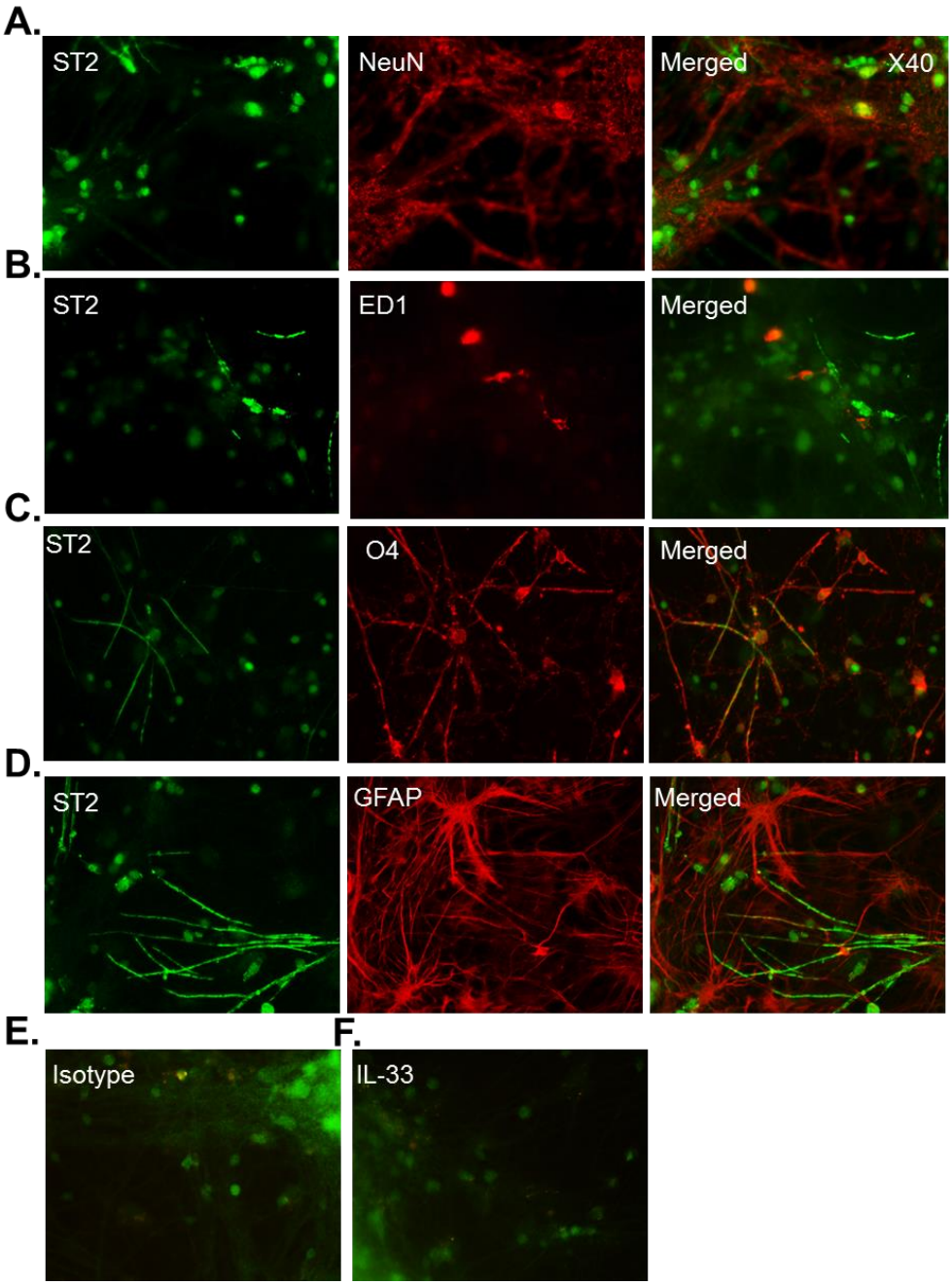

Figure 6.1 Expression of ST2 and IL-33 in CNS cells in rat myelinating culture. Rat myelinating cultures were stained for ST2 in combination with NeuN (A), ED1 (B), O4 (C) and GFAP (D), rat isotype control (E) and IL-33 alone (F).

A similar approach was taken to determine the expression of ST2 and IL-33 within the mouse cultures using fluorescent staining (Figure 6.2). The ST2 single staining was consistent with the morphology of astrocytes (star shape,

images not shown); this was confirmed by GFAP staining (Figure 6.2B). However, ST2 was not stained in conjunction with other cell markers, as the single staining and double staining (Chapter 3 and 4) showed conclusively that ST2 was present solely on astrocytes in the mouse culture system. Similarly to the observation in IL-33 expression in rat culture cells, IL-33 was not detected above background level in this culture system, despite the use of several different antibodies.

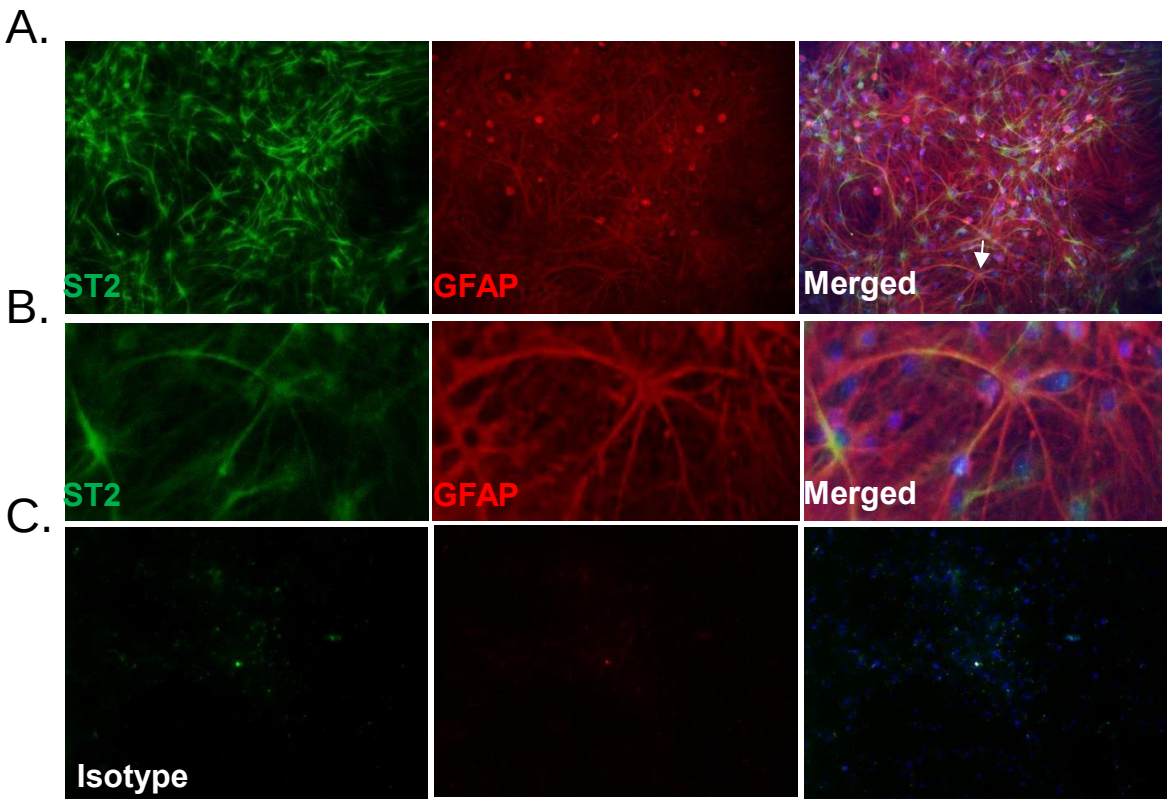

Figure 6.2 ST2 protein expression on CNS cells in mouse myelinating culture. Mouse myelinating cultures were stained for ST2 in combination with GFAP x 20 (A), zoomed imaged (B) and isotype control.

Characterisation of rat myelinating culture system

To investigate the effect of IL-33 on myelination, it was important to characterise the number of ODCs within untreated rat cultures (Figure 6.3). The cultures were stained at regular intervals during the development of the culture (12, 18 and 28 DIV) to get an accurate representation of ODC development within the culture system. During the different stages of development ODCs express distinct markers. Perinatal progenitors express NG2 and PDGFα; late progenitors express NG2, PDGFα and O4. As a pre-myelinating ODC, markers such as GalC, O4 and PLP begin to be expressed. Finally, the ODCs become mature, myelinating cells and expresses GalC, MBP, PLP and MOG (Levine et al. 2001). In addition to the Olig2 expression (early ODC marker) MBP was used as a mature ODC marker. This data showed that the percentage of MBP^{+}ODCs per field was significantly increased ($t_{(2)}$ = 2.45 p = 0.0059) on day 28 when compared to 12 and 18 DIV. Interestingly, $Olig2^{+}$ cells significantly increased from day 12 to day 18 ($t_{(2)}$ = 2.45 p<0.0001) and its population percentage remained the same until 28DIV (Figure 6.3C).

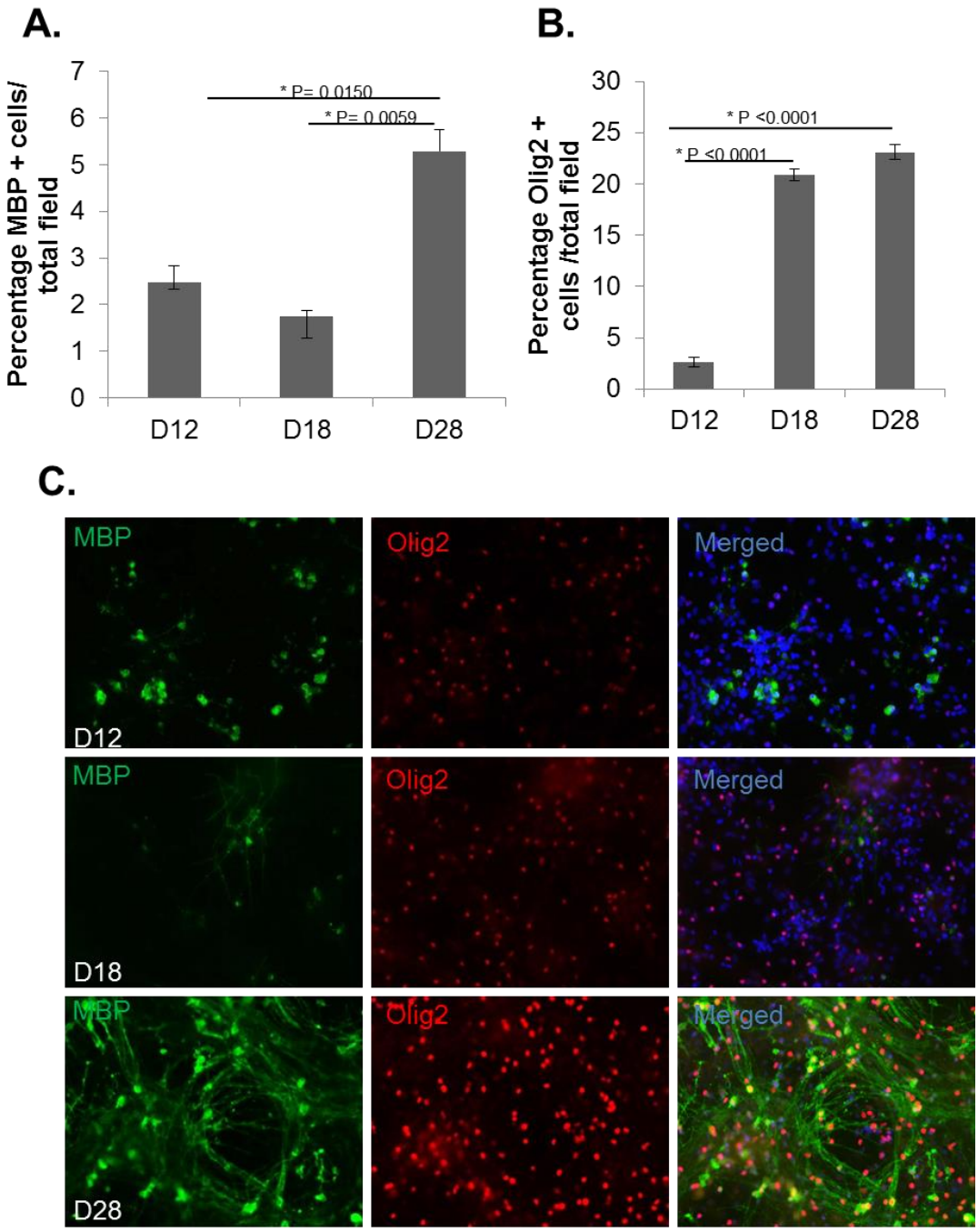

Figure 6.3 Oligodendrocyte expression in rat myelinating cultures. Rat myelinating cultures were stained for Olig2 (early ODC marker) and MBP (late ODC marker) at day 12, 18 and 28. The percentage MBP (A) and Olig2^{+} cells (B) was calculated and representative images taken (C). Data represents the mean ± S.E.M, n= 3. Statistically significant results according to Student's t-test are indicated.

Microglia are regarded as important immune residence cells within the CNS. They are constantly surveying the environment for slight changes which could cause an imbalance of the CNS homeostasis (Kreutzberg 1996). Microglia are also involved in clearing cell debris and pathogens like any other tissue macrophage (Kanazawa et al. 2002). Moreover, in a recent study microglia were identified to be involved in the promotion of myelination (Pang et al. 2013). Although ST2 was only expressed by a very small portion of microglia cells in this EAE study, other reports suggested that ST2 is expressed by microglia at mRNA and protein level (Yasuoka et al. 2011). Furthermore, microglia have also been seen to proliferate and increase their phagocytic properties in response to IL-33 in culture (Yasuoka et al. 2011). Thus, the characterisation of microglia within the rat culture system was vital to aid understanding of the rat culture system as a whole. The percentage of microglia was assessed at day 12, 18 and 28 DIV by staining for Iba1. Throughout the culture system from day 12 to day 28, the number of microglia was slightly increased but with no statistically significant difference (Figure 6.4A & 6.4B) ($F_{2,14} = 1.2425$, $P=0.32$). The data showing their numbers remained the same throughout the culture. This result suggests they most likely contribute to axonal myelination indirectly by maintaining the culture homeostasis.

As mentioned previously, a bed of astrocytes was required to support rat spinal cord cells, which in turn supports the culture system and enhances myelination as a result (Sorensen et al. 2008). Consequently, there were large numbers of astrocytes present throughout the culture visualised using anti-GFAP antibody (Figure 6.4C). As GFAP primarily stains the main branches of the astrocyte projections, rather than the nucleus or cytoplasm, it is difficult to ascribe staining to a given cell. Thus individual astrocytes are not readily distinguished from one another and accurate quantification was not possible. However, images were taken at 12 and 28 DIV to qualitatively assess the astrocyte monolayer at these time points. The astrocyte monolayer showed extensive coverage of the coverslips and was consistent

between 12 and 28 DIV suggesting numbers did not fluctuate during the course of the culture system (Figure 6.4C).

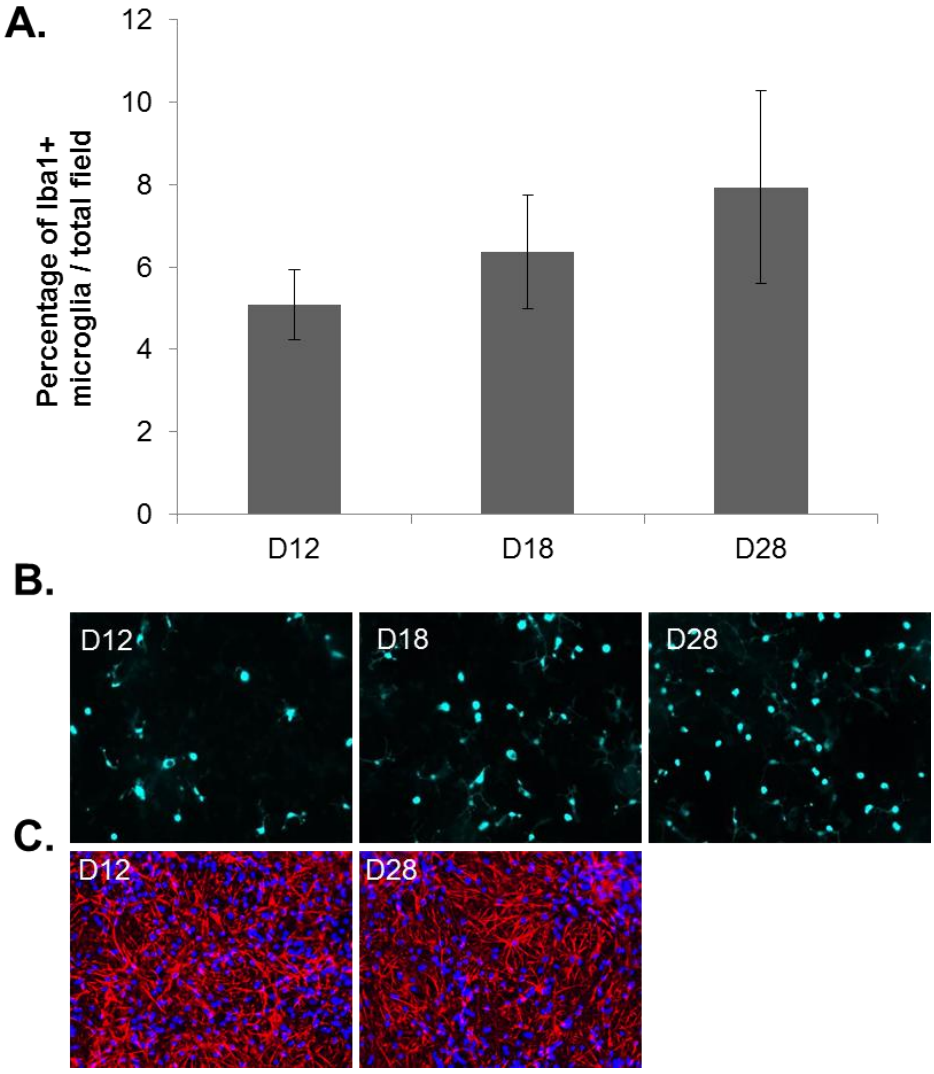

Figure 6.4 The percentage expression of microglia and astrocytes in rat myelinating cultures. Coverslips were fixed and stained for Iba1 at day 12, 18 and 28. The percentage $Iba1^{+}$ microglia was calculated (A) and representative images were shown at the time points indicated (B). Rat myelinating cultures were stained with GFAP and DAPI (nuclei stain, blue) (C) at day 12 and day 28. Data represent the mean ± S.E.M, n= 3.

I next characterised the axonal growth and myelin production by immunofluorescent staining for SMI-31 and MBP respectively (Figure 6.5). Within the rat cultures there was no significant difference in axonal density at

12, 18, or 28 DIV (Figure 6.5A) confirming that a constant level of viable neuron cells were maintained throughout the culture period used in these experiments. As expected, due to the presence of insulin in the culture medium (see Chapter 2, Materials and Methods), at 12 DIV no myelin was observed. After removal of insulin (12 DIV) myelination of the axons by the ODCs began and by 28 DIV a significant increase in MBP expression was observed when compared with 12 and 18 DIV (Figure 6.3). Due to the increase in MBP producing ODCs (Figure 6.3) there was also a significant increase ($t_{(2)}$ = 2.45 p = 0.0155) in the percentage of myelinated (MBP^{+}) axons at day 28 compared to days 12 and 18 (Figure 6.5B, 6.5C).

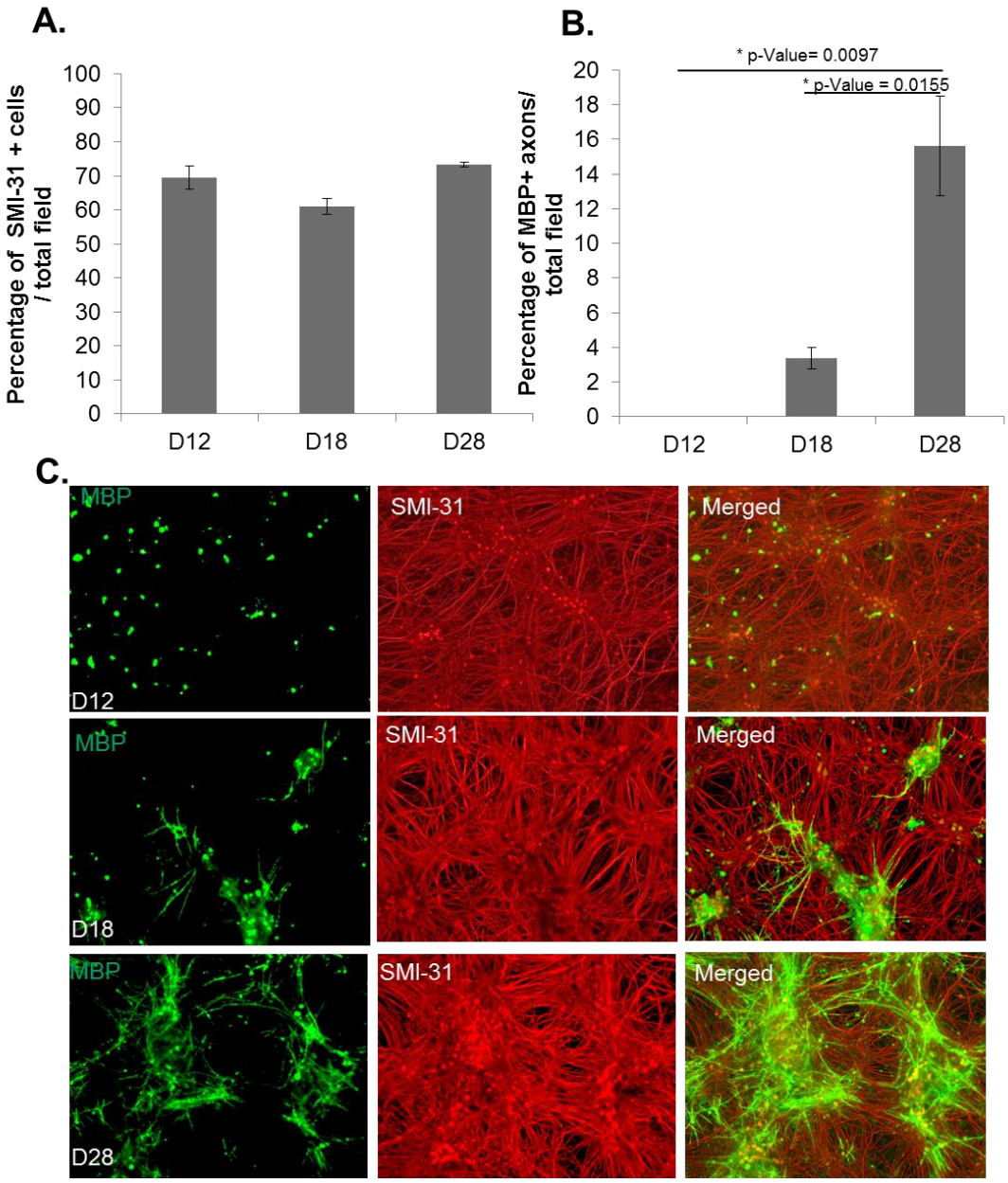

Figure 6.5 Characterisation of axons and myelin within rat myelinating culture. Astrocytes were bedded down onto coverslips upon which spinal cord was added and cultured for up to 28 days. Coverslips were stained for MBP (myelin) and SMI-31 (axons) at day 12, 18 and 28 DIV. Percentage axonal density (A) and percentage myelinated axons (B) were calculated from the images taken (C). Data represent the mean ± S.E.M, n= 2.

In conclusion, $Olig2^+$ ODCs begin to proliferate after day 12 and the removal of insulin from the culture system. In contrast, up until days 18 MBP^+ ODC numbers did not change, after which there was a significant increase. In contrast both microglia and astrocyte did not show a significant increase during the course of the myelin culture. Furthermore, the axonal densities between days 12 and 28 also remained the same while after day 12 myelination began after day 12 IV and the percentage of myelinated axonal was significantly increased between 18 and 28 DIV.

Whilst the culture system can be applied to both rat and mouse tissue, there are differences in the preparation of the cultures between the species which could influence the interpretation of the data. For example, a monolayer of astrocytes is required to support the axons and enhance myelination in the rat but not the mouse myelin culture system (Sorensen et al. 2008; Thomson et al. 2008). This monolayer makes the culture more robust, the mouse cultures also have astrocytes however, the abundance of astrocytes in the rat cultures must be considered when interpreting results. Differences are apparent in the morphology and 'behaviour' of mouse and rat astrocytes in culture. Experiments utilising scratch cultures, involving the activation of the astrocyte monolayer by 'scratching' with a needle, revealed a higher number of proliferating astrocytes ($Ki67^+$ astrocytes) in cultures from rat when compared to mouse. Furthermore, rat astrocytes expressed higher levels of GFAP and vimentin typical of reactivity in vitro (Puschmann et al. 2010) than mouse cultures. Interestingly, although fewer mouse astrocytes were present when compared to rat astrocytes, they were found to be larger (Puschmann et al. 2010). Differences between the species in other CNS cell types have also been reported; mouse OPCs were shown to be less motile than rat OPCs and had shorter projections in vitro (Horiuchi et al. 2010). Furthermore, quantitative analysis of rat and mouse whole brain cultures showed differences between stem cell proliferation, in response to differentiation factors (Ray & Gage 2006). Thus, it should be acknowledged that although rat and mouse cultures are similar, there could be significant variations

between the species. For this reason, my experiments were initially conducted in rat cultures and then moved to the mouse cultures to compare variations between species.

Here, the first step was to characterise the culture system. This data showed that the myelination and axonal density within the mouse culture system were very similar to that of the rat culture (Figure 6.6). Axonal density, which was shown with SMI-31 staining, (Figure 6.6A) revealed changes in the axonal organisation. At 12 DIV, $SMI31^{+}$ axons appeared disorganised and sparse unlike standard axons which are arranged in neat bundles projecting from the neuronal cell body (Figure 6.6C). As the cultures progressed, the axons became dense and formed more organised structures, with several axons bunching together and extending from dense neuronal clusters. Similarly to the rat culture, myelin begins to form after day 12, due to the withdrawal of insulin from the growth medium (Figure 6.6B). Initially the production of myelin was slow showing no significant increase between days 12 and 18. However, by 28 DIV the percentage of myelinated axons was significantly increased ($t_{(2)}$ = 2.45 p = 0.0016). Overall, the percentage of myelination seen in the mouse cultures was lower than that observed in the rat system (Figure 6.5B and 6.6B); however; the minimum threshold of 2% myelination (required for cultures to be deemed viable for experimental purpose) was met at 28 DIV. Furthermore, the axonal density was also lower within the mouse cultures and could therefore account for less myelination.

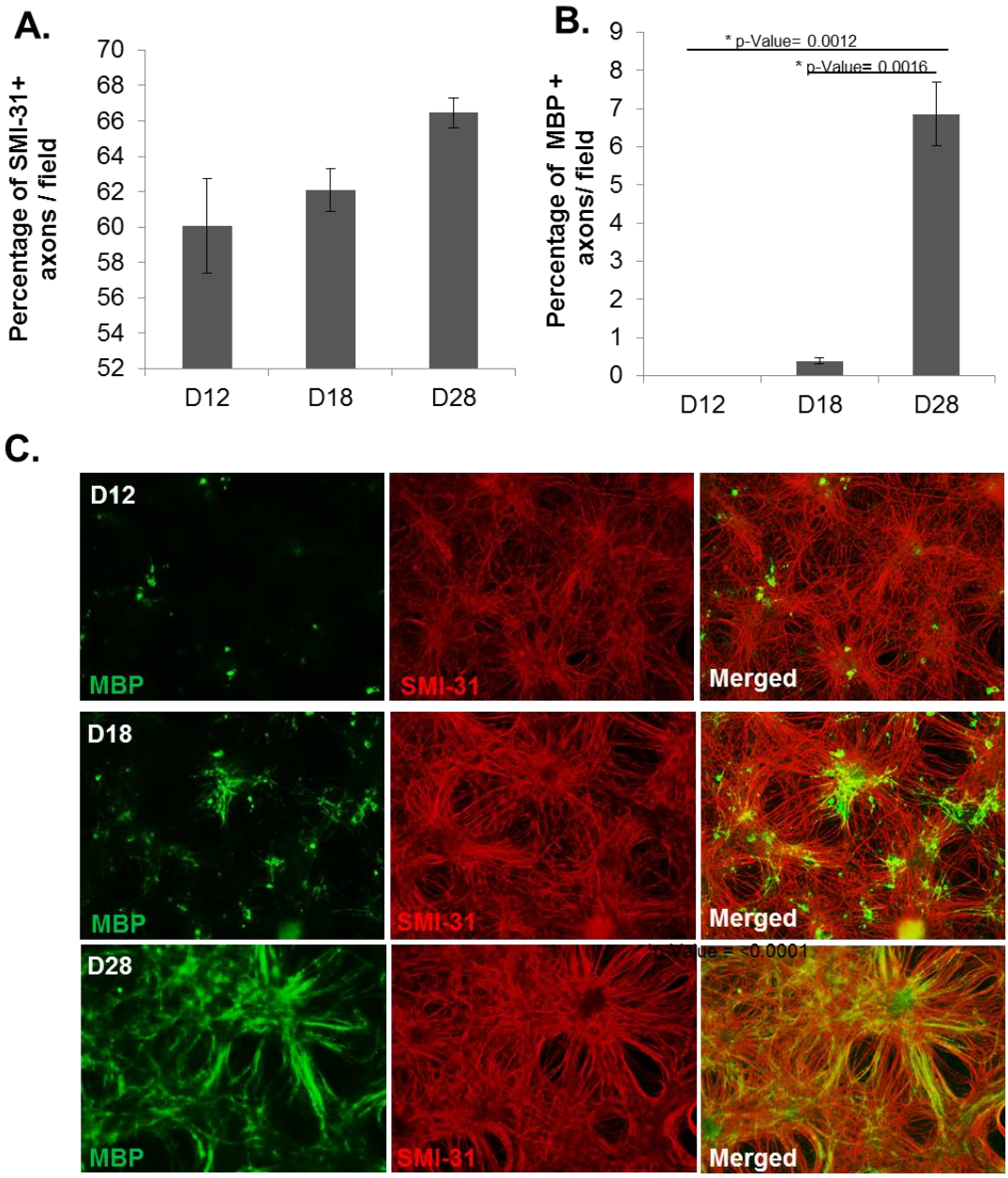

Figure 6.6 The characterisation of axons and myelin in the mouse myelinating culture. Coverslips were stained for MBP (myelin) and SMI-31 (axons) at various time points. Percentage axonal density (A) and percentage myelinated axons (B) were calculated from the images taken (C). Data represent the mean ± S.E.M, n= 3.

The effect of IL-33 on myelination

After characterising the culture systems, I proceeded to investigate the effect of IL-33 on the axonal density and myelination in both the rat and mouse cultures. In an attempt to determine the functional role of IL-33 in CNS myelination, cultures were treated with recombinant IL-33 and the proportion of myelinated axons was analysed. Recombinant IL-33 was added to the cultures at 12 DIV by removing half the medium and adding fresh medium containing 100ng of IL-33 three times a week. Cells on coverslips were then fixed and stained with anti-MBP (myelin) and anti-SMI-31 (axons) at 28 DIV for rat and mouse cultures (Figure 6.7 & 6.8 respectively). Within the rat culture (Figure 6.7) there was no significant difference between the axonal densities of control and IL-33-treated cultures as shown by the percentage of SMI-31^{+} axons (Figure 6.7A) suggesting IL-33 does not affect neuron cell growth and axonal formation. However, the percentage of MBP^{+} axons showed a significant reduction in myelination ($t_{(2)}$ = -7.19 p-Value = 0.0188) when compared to control cultures (Figure 6.7B). Representative images (Figure 6.7C) illustrate the reduction in myelination observed within IL-33-treated rat cultures. A similar result was observed within the mouse myelinating culture system. It was also found that there was no significant difference in axonal density could be observed between control and IL-33 treated groups (Figure 6.8A). In contrast to the rat cultures, IL-33 treatment had a non-significant effect in the percentage of myelinated axons in the mouse culture system (Figure 6.8B) however, this result could be attributed to the variability of the culture system.

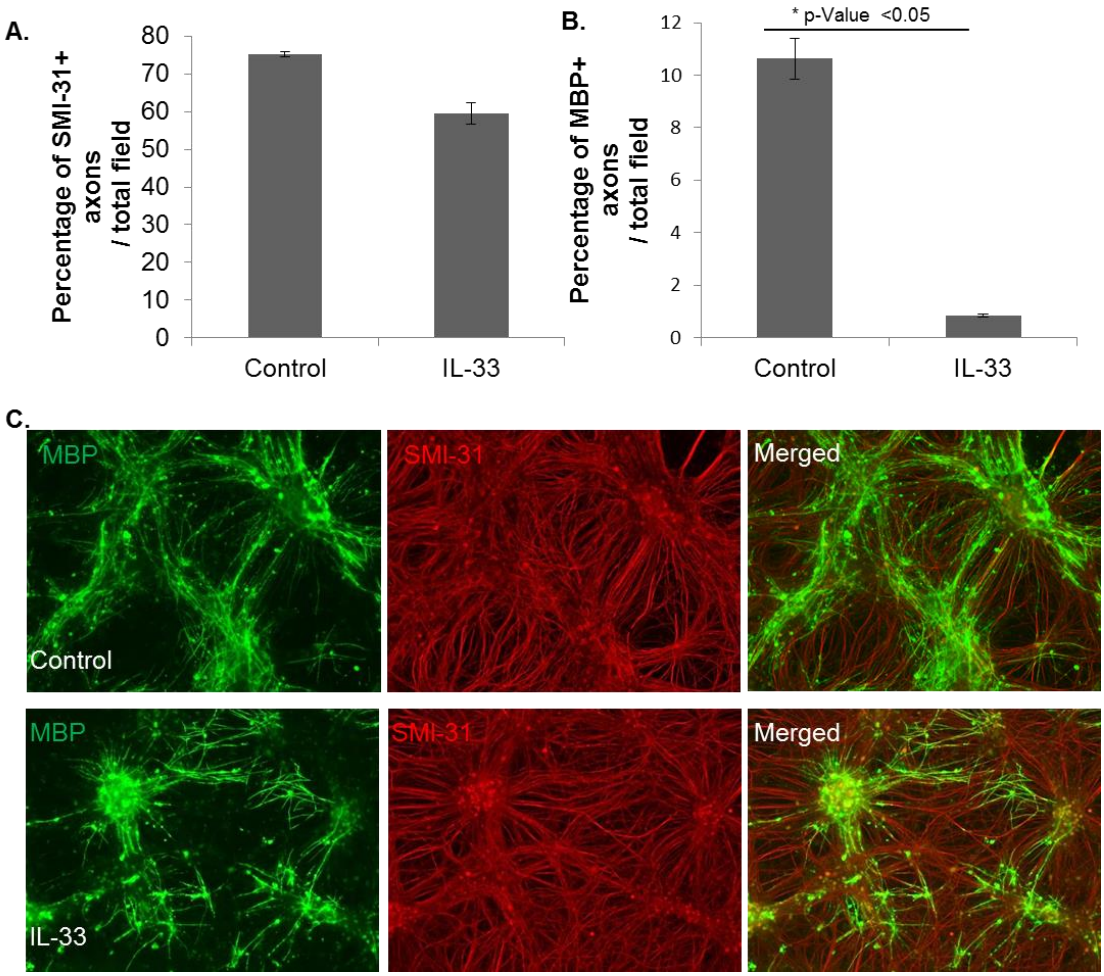

Figure 6.7 The effect of IL-33 on CNS myelination in rat myelinating culture. At day 12 cultures were either treated with medium alone (control) or 100ng of IL-33. Coverslips were stained for MBP (A) and SMI-31 (B) at day 12, 18 and 28 DIV. Percentage axonal density and myelinated axons were calculated from the images taken (C). Data represent the mean ± S.E.M, n= 2.

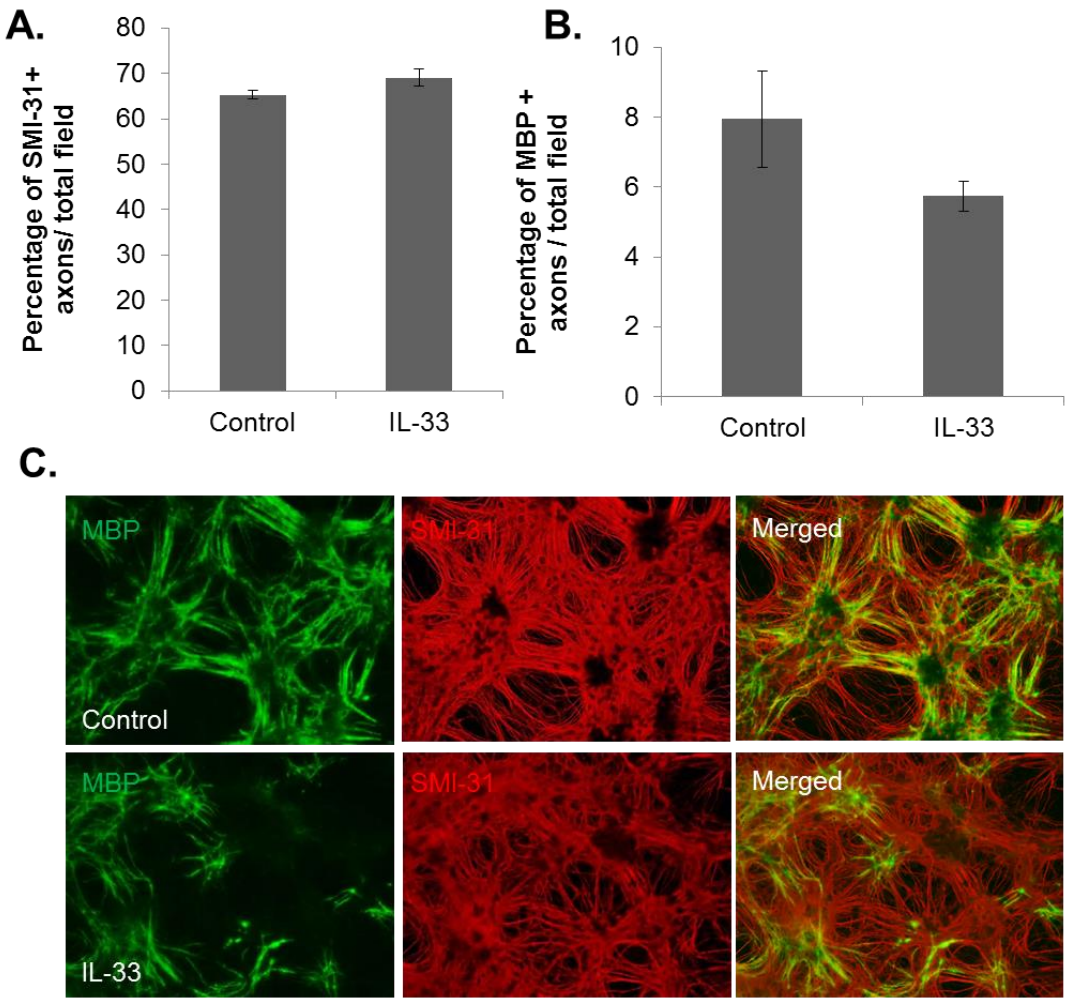

Figure 6.8 The effect of IL-33 on myelination in the mouse CNS culture. At day 12 cultures were either treated with medium alone (control) or 100ng of IL-33. Coverslips were stained for SMI-31 (A) and MBP (B) at day 28. Percentage axonal density and myelinated axons were calculated from the images taken (C). Data represent the mean ± S.E.M, n= 3.

To understand the underlying mechanisms of IL-33's contribution to myelination, I further investigated the effect of IL-33 on the individual CNS cell population in the mouse cultures by assessing; ODC development and maturation, microglia cell number, and astrocyte morphology in the culture (with and without IL-33 treatment at various timpoints).

As mentioned for rat culture system, Olig2 is an early ODC marker and my data showed that the percentage of $Olig2^+$ cells remained constant throughout the 28 days in culture, and again no difference was observed between the control and IL-33-treated mouse culture (D28, p value=0.5539).

The effect of IL-33 on the percentage of MBP^+ cells / total field was then assessed. The data (Figure 6.9) showed that the percentages of MBP^+ ODCs significantly increased from day 12 to day 18 (ANOVA Days In Vitro $F_{2,15} = 9.88$ p= 0.002) in both IL-33-treated and control groups, and that the levels were maintained from day 18 to day 28. However, there was no significant difference between the control and IL-33-treated cells; suggesting that IL-33 does not alter the number of myelinating MBP^+ ODCs.

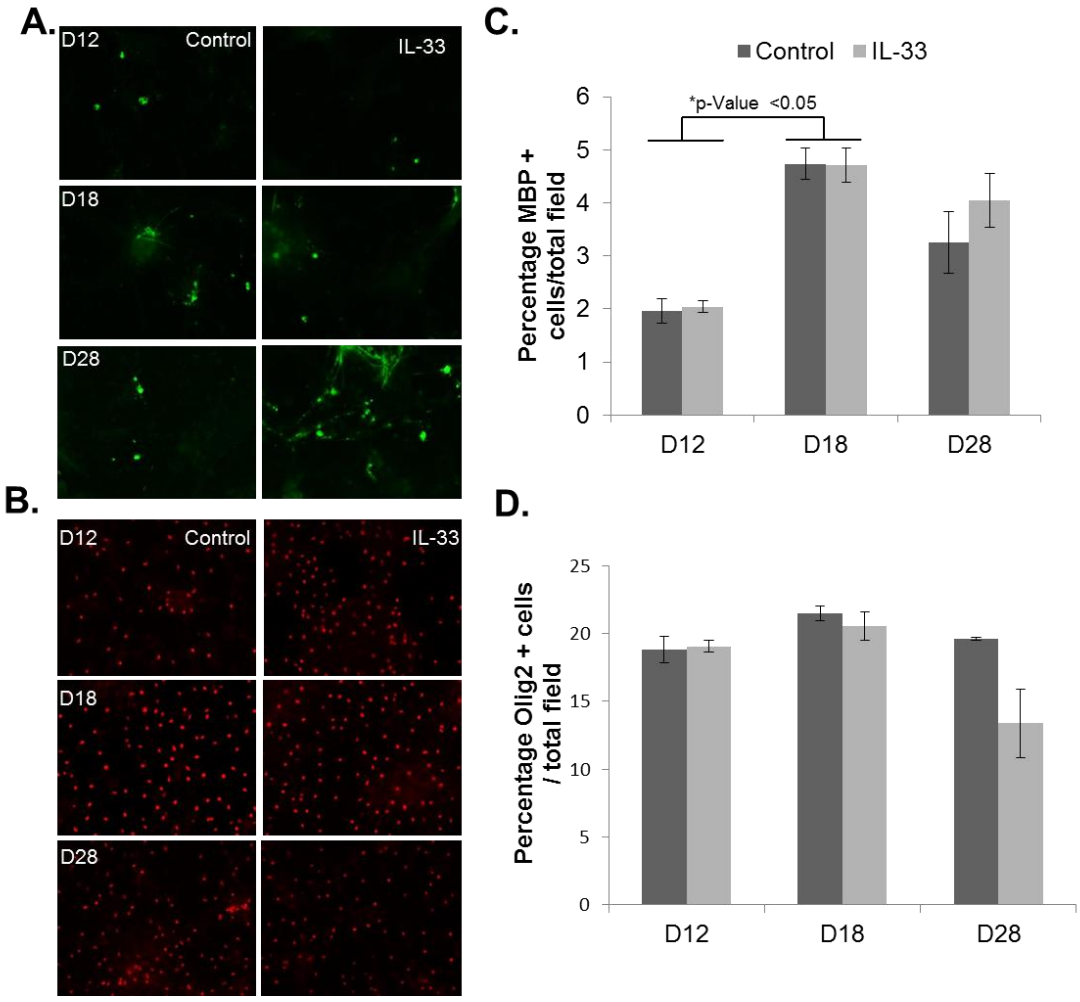

Figure 6.9 ODC expression in mouse myelinating cultures. Mouse cultures were stained for MBP (A) and Olig2 (B) at day 12, 18 and 28 and imaged at X20 magnification. The percentage of MBP^+ (C) and $Olig2^+$ (D) cells / totally number of cells per field of view was calculated. Data represent the mean ± S.E.M, n=3.

I next investigated the effect of IL-33 on $Iba1^+$ microglia within both cultures (Figure 6.10). In the control cultures the percentage of $Iba1^+$ microglia cells/total cell number in each field was increased but with no statistical difference (Day In Vitro $F_{2,14} = 1.2425$ p=0.32) for the duration of the culture. In the IL-33-treated microglia there was no significant difference between the time points (D28, p= 0.0556), despite this there is a trend for IL-33 to reduce microglia (Iba1). Interestingly, the microglia morphology (Figure 6.10A) was very similar between the two groups at day 12, with most cells appearing

round, but at day 18 the control microglia were found to have a ramified structure characteristic of resting, patrolling microglia. This morphology allows microglia to move freely around the environment and detect changes in molecules such as ions or cytokines (Kreutzberg 1996). IL-33 treated microglia have a more pronounced activated morphology (rounded cell body); consistent with macrophages and the ability to phagocytose (Kreutzberg 1996).

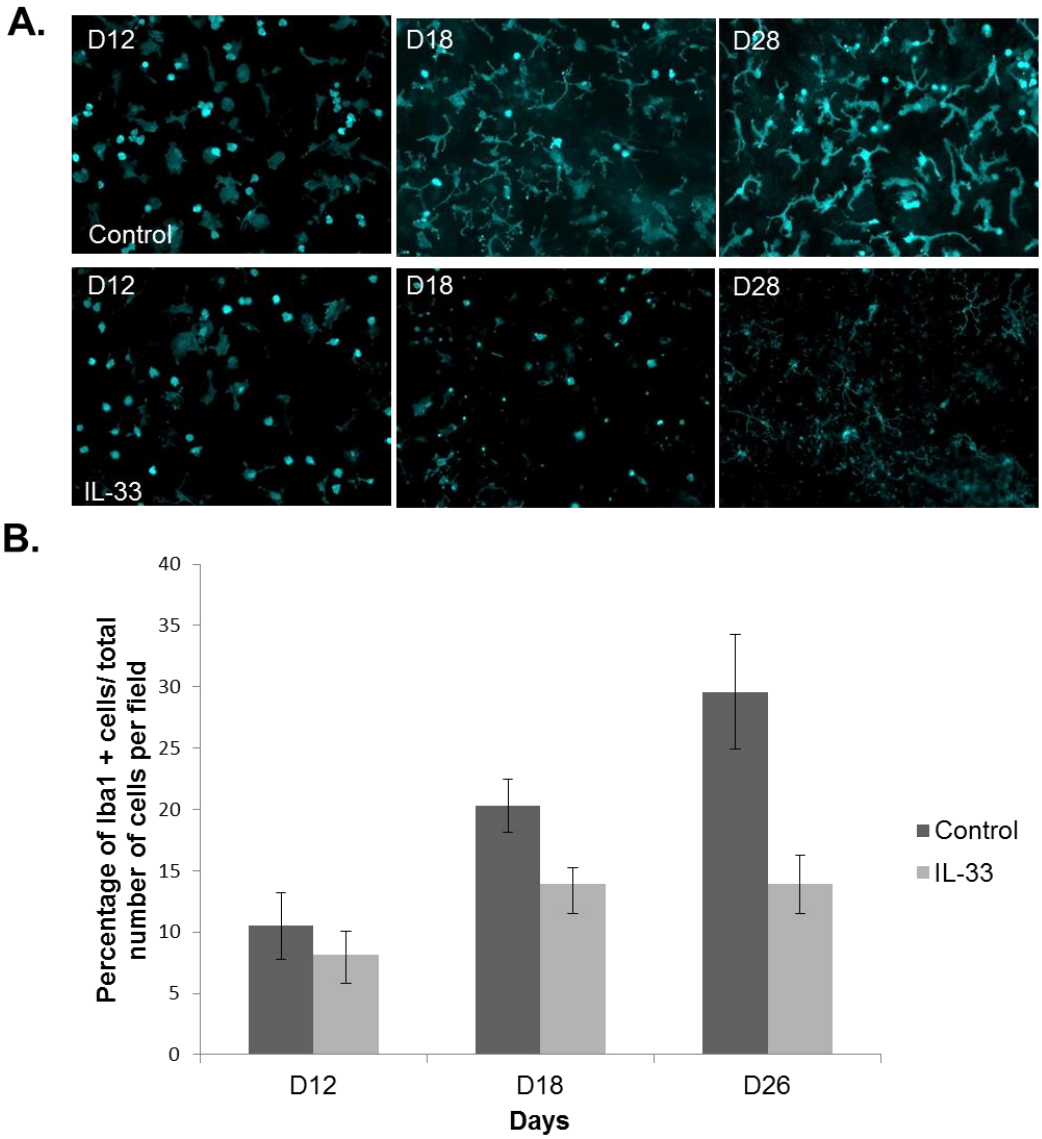

Figure 6.10 The effect of IL-33 on Iba1$^+$ microglia in mouse myelinating cultures. Mouse cultures were treated with either medium (control) or IL-33 from day 12 until day 28. At day 28 the coverslips were fixed and stained for Iba1 at day 12, 18 and 28 (A). The percentage Iba1$^+$ cells was then calculated (B). Data represent mean ± S.E.M, n=3

The exclusive expression of ST2 on astrocytes in mouse cultures (Figure 6.2) indicates that IL-33 has the potential to influence this cell population. To determine the effect of IL-33 on astrocytes (Figure 6.11), the myelinating cell culture was treated with IL-33 or medium alone and stained for GFAP at day 12, 18 and 28. Due to the number of cells and staining pattern it was difficult

to calculate the percentage of astrocytes, however morphological differences were assessed visually. At day 12 the control and IL-33 astrocytes were found to look similar; with a large body and short projections. At day 18 the astrocyte cell bodies were smaller and the projections were long and slender. This morphology was also apparent at day 28. Thus the data suggests that IL-33 does not have obvious effect on astrocyte cell growth or morphology, future studies with specific astrocyte markers for activated or reactive astrocytes could provide more definitive information.

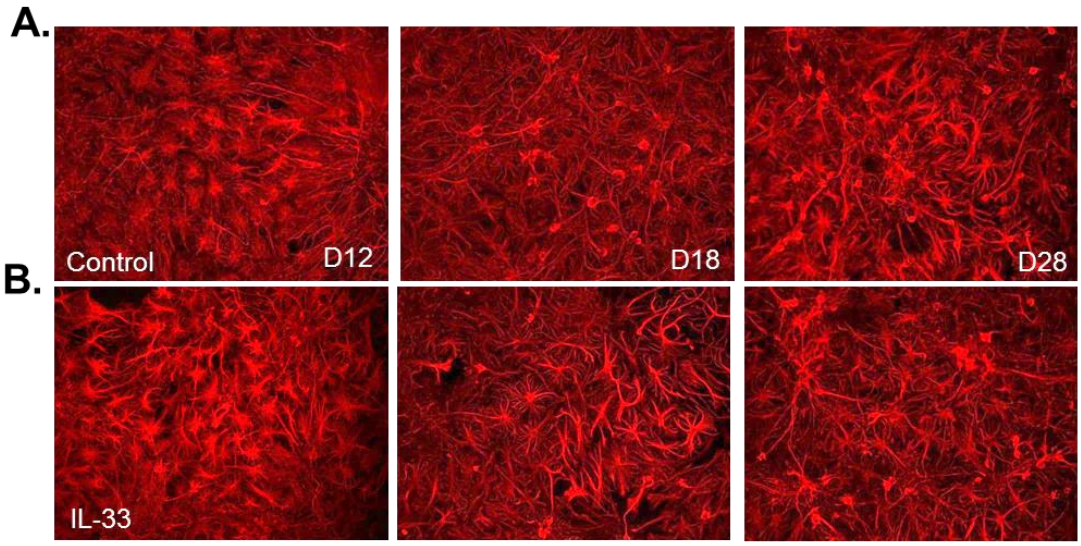

Figure 6.11 The effect of IL-33 on astrocytes in rat mixed culture. At day 12 cultures were either treated with medium alone (A) or 100ng of IL-33 (B). Coverslips were stained with GFAP (X20 magnification) at days 12, 18 and 28 DIV. Data shown are representative of three independent experiment (n=3).

In conclusion, I used rat and mouse myelinating culture systems to study the effect of IL-33 on CNS axonal density and myelination. Despite the difference between the two cultures, the characterisation of the axonal density and percentage of myelinated axons were found to be comparable for both cultures. The data from the rat myelinating culture system suggest that some neuron cells and ODCs express ST2. Surprisingly, within the mouse system, ST2 was found to be present on astrocytes. IL-33 treatment inhibited

myelination within the rat and mouse cultures, with a significant difference recorded in the rat culture system.

6.3 Discussion

The data presented within this chapter shows the presence of axons, neurons, ODCs and microglia within the cultures. My results showed myelination did not occur until after the removal of insulin from the growth medium at 12 DIV. The rat myelinating cultures showed a normal structure and morphology of neurons, as well as axons. ODCs are able to actively myelinate axons within the culture system resulting in 10-20% myelination at day 28 DIV. Within the mouse myelinating cultures, axonal density was consistent between days 12 and 28 and myelination did not begin until after the insulin was removed at day 12 of the cultures, peaking at approximately 10% at day 28.

Although the kinetics of myelination were similar for rat and mouse cultures, the percentage of both axons and myelinated axons were found to be approximately 10% less in the mouse cultures than the rat cultures. An important factor to consider when comparing cultures between rat and mouse is that a layer of neurosphere-derived astrocytes supports rat CNS tissue. Astrocytes can have an important effect on myelination; which was more pronounced when spinal cord tissues were plated on top of reactive or activated astrocytes, when compared to quiescent cells (Nash et al. 2011). Furthermore, astrocytes secrete factors which promote or hinder myelination (Moore et al. 2011). Astrocytes can enhance the differentiation of O-2A progenitors into ODCs through the effect of astrocyte-derived Platelet Derived Growth Factor (PDGF) (Moore & Goldberg 2011). Thus, this extra layer of neurosphere-grown astrocytes (cultured two weeks prior to the addition of spinal cord) could be the result of the enhanced stability of the rat cultures; resulting in additional axons, and as a result, increased myelinated

axons. Despite the differences noted, both systems provided a useful in-vitro model to investigate myelination.

Previously, IL-33 has been detected on astrocytes in other mixed glial cultures systems (Christophi et al. 2011; Yasuoka et al. 2011). Within the rat myelin cultures, IL-33 treatment dramatically reduced the percentage of myelinated axons. During the characterisation of the rat myelin culture system at day 18, control cultures only had approximately 3% of myelinated axons. Furthermore, by day 28 in the IL-33-treated cultures, there was no increase in the initial level of myelination that had occurred prior to treatment. This suggests that myelination was not reduced but prevented. The axonal density was not significantly reduced indicating that IL-33 did not decrease myelination by damaging or reducing axonal density. For the mouse myelinating culture system, the axonal density was unaffected by treating the cultures with IL-33, unlike the rat system. It is unclear whether this difference was due to variations in species or due to the variable nature of the cultures.

Microglial cells are the resident macrophages within the CNS and are very responsive to changes in their environment which disrupt homeostasis (Kreutzberg 1996). Activated microglia secrete reactive oxygen and nitrogen species resulting in damage and potentially neurodegeneration (Neher et al. 2012). Within the cultures IL-33 was not seen to be expressed by microglia as shown in previous research (Yasuoka et al. 2011), they are unlikely to be a source of IL-33 in vivo. Furthermore, IL-33 was not found to co-localise with microglia in EAE (Chapter 4) or MS (Chapter 5) control or diseased tissues. The potential for IL-33 to directly act on microglia depends upon the expression of the receptor ST2. In previous studies ST2 mRNA has been detected on some microglia cells and treatment with IL-33 resulted in the proliferation and phagocytic activity of microglia and cytokine production (Yasuoka et al. 2011). However, the results from this chapter has shown ST2 was expressed on ODC projections (rat) and astrocytes (mouse) (Figure 6.1 and 6.2 respectively) but not microglia. The disagreement of IL-33 and ST2

expression in cells and tissues could depend upon whether proteins or mRNA is examined (Yasuoka et al. 2011). One possible explanation for this would be that microglia also express ST2 mRNA; but not at a protein level in these cultures. However, another explanation would be that if there were only low levels of ST2 present on cells in these cultures, IHC staining may not be sensitive enough to detect it.

The effect of IL-33 on microglia was non-significant ($p=0.0556$). In addition to the non-significant effect on microglial staining, my data showed that IL-33 treatment did not significantly affect the numbers of astrocytes within the mouse culture. The morphology of the astrocytes at day 12 in both the control and IL-33 treated astrocytes reflects large cell bodies with short projections. This is likely to be representative of activated astrocytes since activated astrocytes create a better environment for myelination and thus aid the culture (Sorensen et al. 2008). At day 18 and 28 both the control and IL-33-treated cultures contained reactive astrocytes. It was not possible to quantify the astrocytes accurately, due to GFAP staining on the branches rather than cell body.

IL-33 is regarded as an alarmin, which is released upon necrosis/apoptosis, thus alerting the neighbouring cells to react to the damage in the tissues (Lamkanfi & Dixit 2009). Therefore addition of exogenous IL-33 to the cultures could mimic in-vivo danger signals and result in an increase in reactive astrocytes. This has been shown for another alarmin (HMGB1), located within the nucleus of epithelial cells is known to be released from astrocytes (Pedrazzi et al. 2014). HMGB1-treated astrocytes increased GFAP and vimentin. Moreover, HMGB1 was found to increase the enzyme COX-1, which is essential in inflammatory responses. This indicates that HMGB1 selectively activates astrocytes in a pro-inflammatory manner. HMGB1 also increased CCL5 and CCL2 production; these molecules are involved in the activation and migration of microglia ((Pedrazzi et al. 2014)). By analogy, IL-33's properties as an alarmin could initiate a pro-inflammatory

environment by activating astrocytes through binding to ST2 on their surface seen to be present on astrocytes in EAE tissues (Chapter 4).

IL-33 may have beneficial or detrimental role in CNS myelination depending on the cytokine microenvironment: IL-33 could either promote myelination or alert immune cells to destroy ODC sheaths resulting in demyelination. ST2 is highly upregulated in areas of myelin damage in MS CNS samples (chapter 5). Furthermore in control rat cultures, staining for ST2 and ODC markers showed that ST2 was expressed on the projections of 04^+ ODCs, and the treatment of rat cultures with recombinant IL-33 resulted in a dramatic reduction of myelinated axons when compared to cultures that received medium alone. A similar but non- significant reduction was also observed in the mouse cultures. Further mechanism studies suggest that IL-33 did not affect the percentage of MBP and Olig2 positive ODCs in the mouse culture system. Therefore, the data suggests that the IL-33 does not affect the development and proliferation of ODCs but rather affects their myelinating function.

7. General Discussion

IL-33 is an immunomodulatory cytokine that has been shown to play important roles in the development of several CNS diseases. It has been shown to be associated with various CNS diseases such as AD, ALS and T.gondii infection, indicating a clear role for IL-33 in neurodegenerative diseases and neuroinflamamtion (Chapuis et al. 2009; Yu et al. 2012; Jones et al. 2010; Lin et al. 2012).

The IL-33/ST2 signaling pathway also plays an important role in the development of MS disease as IL-33 is upregulated in MS plasma and on astrocytes in MS plaques, periplaques and NAWM of MS patients, when compared to normal control patients (Yasuoka et al. 2011; Christophi et al. 2011). We previously reported that IL-33 mRNA was highly expressed by CNS spinal cord tissues and IL-33 treatment attenuates EAE development through promoting a Th2 response and alternatively activated macrophage (AAM) polarisation (Jiang et al. 2012). In this thesis I investigated the expression of IL-33 and ST2 proteins within the CNS of naïve and EAE mice as well as determining a functional role for IL-33 in myelination in the CNS. In vivo and *in vitro* models are important as they can provide insight into MS, which would otherwise be difficult to obtain. However, these experiments must then translate into the human disease in order to examine the importance of IL-33 in immunomodulation in MS. Determining the expression of IL-33 and ST2 within different lesion types also provided a unique opportunity to apply this research directly to the clinical field. Table 7.1 summarises the expression of IL-33 and ST2 within mouse and human CNS tissues.

Table 7.1 Summary of IL-33 and ST2 staining in Murine and Human CNS tissues

Molecule	Murine Spinal Cord				Murine Brain					
	Naïve		EAE		Naïve			EAE		
	WM	GM	WM	GM	Cortex	Ventricular Region	Corpus Callosum	Cortex	Ventricular Region	Corpus Callosum
IL-33	++	++	++	++	+	+	+	+	+	+
ST2	++	++	+++	++	++	++	++	++	++	++

	Murine Spinal Cord						Murine Brain					
	Naïve			EAE			Naïve			EAE		
	Astro	Micro	Neurons	Astro	Micro	Neurons	Astro	Micro	Neurons	Astro	Microglia	Neurons
IL-33	+	-	++	+	-	++	+	-	++	++	-	++
ST2	++	-	++	++	-	++	++	-	+	++	-	+

	Healthy Human Brain		Acute Multiple Sclerosis Brain			Chronic Multiple Sclerosis Brain		
	Cortex	WM	Cortex	NAWM	Lesion	Cortex	NAWM	Lesion
IL-33	+++	+	+++	+	++	+++	+	+
ST2	+++ (diffuse)	+++ (diffuse)	+++ (diffuse)	+++ (diffuse)	++	+++ (diffuse)	+++ (diffuse)	++

	Multiple Sclerosis Brain			
	Axons	ODC	Astro	Micro
IL-33	++	+	-	+
ST2	++	+	-	-

+ little staining, ++ moderate staining, +++ substantial staining

The expression of IL-33 and ST2 within the CNS

Consistent with previous reports (Schmitz et al. 2005; Jiang et al. 2012), my results have confirmed that IL-33 is highly expressed within the spinal cord grey and white matter, of both naïve and EAE mice. IL-33 was found to be present within the cortex, ventricular regions and corpus callosum of naïve and EAE mice which is consistent with the reports of others (Pichery et al. 2012). Despite IL-33 being found throughout the CNS, this study focused upon the aforementioned regions, due to their importance in lesion formation. My IL-33 staining in the spinal cord and brain of EAE tissues showed both nuclear and cytoplasmic staining, despite early reports suggesting that IL-33 was solely located within the nucleus (Carriere & Roussel 2007). Recent studies (Tsuda et al. 2012a) have also confirmed the presence of the IL-33 protein in both nuclear and cytoplasmic fractions. Their study confirmed that IL-33 constructs lacking exon 3 were cytoplasmic, however IL-33 constructs lacking exon 4 or 5 or 4/5 were nuclear located. In the case of IL-33, one particular IL-33 splice variant lacking the exon 3 has been described as 'constitutively active' (Hong et al. 2011). Kakkar's study showed that IL-33 displays an 'inter-organelle flux', allowing nuclear IL-33 to gradually move to the cytoplasm over time to be packaged into vesicles, which may be ATP-dependent (Tsuda et al. 2012b; Kouzaki et al. 2013). This was confirmed in a previous *in vitro* study which found that IL-33 was only released by glial cells after PAMP stimulation in an ATP-dependent manner (Hudson et al. 2008).

Despite repeated detection of the expression of IL-33 in CNS tissues in mice and in humans, it was not possible to detect its expression on CNS cells within the myelinating cultures. Previous reports have stated that IL-33 has been detected on astrocytes in other mixed glial cultures systems (Christophi et al. 2011; Yasuoka et al. 2011). However, a recent study (using the same antibodies as used in this thesis) has shown that IL-33 was not detected in C56BL/6 embryonic tissues (CNS or PNS) until embryonic day 19 (E19) (Wicher et al. 2013). As the cultures used in this thesis were created from

E13 embryos (see Material and Methods) this could account for the lack of IL-33 staining observed. These results suggest that IL-33 is highly expressed in the nucleus and cytoplasm of cells within the spinal cord and brain of naïve and EAE mice. In normal and MS brain tissue; IL-33 stained the cytoplasm of cells as well as cellular projections and fiber-like structures within the cortex of both normal and MS tissues. Furthermore, there was a significant reduction in IL-33 staining in healthy cortex compared to acute and chronic MS cortex despite the lesion being expressed distal to the cortex suggesting that a vast environmental change occurs during inflammation which effects cells distal from the inflammation site as well as the cells involved.

The IL-33 receptor is a heterodimer consisting of ST2 and IL-1RAcP (Chackerian et al. 2013). Here, I compared the expression of ST2 in spinal cord and brain tissues of naïve, PBS-treated and MOG immunised EAE mice. Within the spinal cord my results showed that ST2 was expressed on cells in the white matter however, more extensive ST2 staining was observed within the grey matter. On numerous occasions, this staining was found to be both nuclear (suggesting an alternative signaling pathway), and cytoplasmic (which is characteristic of this heterodimer receptor). ST2 has several splice variants (Tominaga et al. 1999) which have not been studied to the same extent as the ST2 transmembrane ligand. It is possible that the different ST2 staining could be due to a ST2 splice variant being localised to the nucleus. While the expression pattern and level of ST2 in CNS resident cells of EAE spinal cord tissues was similar to that of naïve mice, within the white matter of EAE tissues $ST2^+$ infiltrating cells were observed. As ST2 is expressed by Th2 cells (Xu et al. 1998) and M2 macrophages (Kurowska-Stolarska et al. 2009), the infiltrating cells could be $ST2^+$Th2 cells $ST2^+$ macrophages entering from the periphery (Brint et al. 2004) during inflammation. The difference observed is likely to be due to the EAE mouse model employed within this experiment here; which is characterised by major inflammation within the spinal cord tissues but very little inflammation in the brain (Stromnes et al. 2008).

Surprisingly, my data of ST2 expression within human control brains showed diffuse staining which differed to the specific cellular staining observed within the mouse brain. Despite the cortical ST2 staining resembling that of non-specific binding, the isotype controls showed no staining, suggesting that the staining observed was specific. Although no definite conclusions could be drawn from this staining, it is important to note that no other study has shown ST2 expression in the CNS at a protein level. This is surprising, as IL-33 has been extensively studied - perhaps the reason for this is due to the unusual staining pattern ST2 presents within the human brain. The expression of ST2 within the cortex and NAWM in acute and chronic MS samples did not change when compared to the control samples. However, ST2 expression was shown on fiber structures within acute lesions and to a lesser extent in chronic lesions. ST2 is present on Th2 cells (Löhning et al. 1998) which are associated with protection in EAE. An explanation for the lack of increase ST2 within the lesions could be the lack of Th2 cells in the lesion site of MS tissues and EAE brain when compared to EAE spinal cord that has shown obvious $ST2^+$ cellular infiltration.

IL-33 and ST2 within neurons in MS and EAE

Neurons are the main structural unit within the CNS, ODCs myelinate the neurons to enhance the conduction of impulses throughout the CNS and periphery (Caldwell et al. 2000; Craner et al. 2004; Greene et al. 1988). In MS, both the myelin produced by the ODCs and the ODCs themselves are the main target of autoreactive T and B cells. The damage to myelin and ODCs leaves the neuron and axons vulnerable to further damage and subsequently results in axonal atrophy and neuron degeneration. The significantly high levels of IL-33 expression in CNS tissues indicate that IL-33 may have unique CNS specific functions (Schmitz et al. 2005).

To further understand the role it may play in MS and EAE, I used double fluorescence staining to identify which CNS cells express IL-33 and ST2. I

co-stained neurons (NeuN) with anti-IL-33 and anti-ST2 in control and EAE mice. NeuN is widely used as a neuronal marker as it is present on almost all neurons (Mullen et al. 1992).

IL-33 was expressed on neurons within naive and EAE mice within the grey matter of the spinal cord. Within the brain of naïve mice IL-33 also co-localised with neurons within the cortex, striatum and ventricular region; however within EAE mice, only the cortex showed co-localisation. This may have been due to the release of IL-33 from neurons within the ventricles (Pfaff & Kintner 1998). Using normal control and MS brain samples I observed IL-33 expressing neurons and axons within the cortex, as well as within the lesion site of MS patients. Little IL-33^{+} neurons were observed within the NAWM - potentially due to the lack of neuronal cell bodies in this region. IL-33 was however present on damaged neurons within the MS lesions sites.

IL-33 can move between the nucleus and cytoplasm of cells (Tsuda et al. 2012b), and has also been visualised in vesicles in a comparable manner as HMGB1, a similar alarmin to IL-33 (Tsuda et al. 2012a; Gardella et al. 2002). In the EAE and human CNS IL-33 could be expressed in vesicles in the neuron which travel along the length of the axons after which it is released into the synaptic cleft to signal/ alert other neurons or local astrocytes (Tsuda et al. 2012a; Gardella et al. 2002; Al-Bassam et al. 2012).

Since IL-33 acts through binding to its receptor ST2, I proceeded to examine the expression of ST2 on neurons. Within the naïve and EAE spinal cords of C57BL/6 mice, ST2 was found to be present within the cytoplasm of several neurons, especially neurons with a large cytoplasm (suggesting they may be motor neurons). In naïve and EAE brains, ST2 can also be seen to co-localise with NeuN^{+} neurons within the cortex and ventricular regions. However, there are still many neurons which do not express ST2, suggesting

that only a sub population of neurons express this receptor. Importantly, when I investigated the localisation of ST2 within the MS lesion site it often co-localised with SMI-31/32, indicating the presence of ST2 on or around axons. ST2 could be expressed on the surface of the axons during stress as the morphology of the axons seen in this sample show axonal swelling and damage. We also observed that the higher the level of damage seen in the axons (i.e. the swollen and broken axonal shape) the stronger the ST2 signal. Alternatively ST2 could be expressed around the damaged axons, suggesting that it may be present on the myelin rather than on the axons.

IL-33 and ST2 within ODCs in MS and EAE

To further understand the role IL-33 and ST2 plays in MS, I co-stained ODCs (CAII) with anti-IL-33 and anti-ST2 in MS tissue and MBP/O4 in rat myelinating cultures. Furthermore, using mouse myelinating cultures the effect of IL-33 on early (Olig2) and late (MBP) markers was assessed using fluorescent imaging.

I investigated whether IL-33 was expressed on $CAII^+$ ODCs within human brain tissues; the results have suggested that a small number of $CAII^+$ODCs express IL-33 within the MS lesion site. IL-33 expression on ODCs has also been shown when using murine glial cultures detecting $Olig2^+IL\text{-}33^+$ cells (Wicher et al. 2013). Wicher *et al* determined that IL-33 was only present during late embryogenesis and in glial cultures grown from postnatal tissues (Wicher et al. 2013) suggesting a role for IL-33 in development. ST2 was expressed by some $CAII^+$ ODCs within MS lesion tissues. The results in chapter 6 also demonstrated that within the *in-vitro* rat myelinating system ST2 was localised on $O4^+$ ODC projections. These results suggest that IL-33 might have an important role in CNS demyelination or remyelination, therefore contributing to the development of MS/EAE. Overall, the presence of IL-33 and ST2 on ODCs implies that IL-33 may work in an autocrine fashion to modulate myelination or homeostasis within the CNS ODCs.

In this study, an *in vitro* culture system was used to investigate the role of IL-33 in CNS myelination. The myelinating culture system is a diverse culture system which uses embryonic tissues to create a CNS microenvironment closely, mimicking that observed *in vivo* by the presence of microglia, neurons, astrocytes, ODCs, OPCs axons, myelin and Nodes of Ravier. Within the rat myelin cultures, IL-33 treatment dramatically reduced the percentage of myelinated axons. The axonal density was not significantly decrease, indicating that IL-33 did not reduce myelination by damaging or reducing axonal density. For the mouse myelinating culture system, the axonal density was also not affected by treating the cultures with IL-33 (a similar, but non-significant, result was seen in mouse). Immunohistochemical staining of ST2 in the culture CNS cells was used to show that ST2 was present on ODC projections within the rat cells. Surprisingly ST2 was only shown to be present on astrocytes but not on ODCs within the mouse system, which may account for the difference observed in the effect of IL-33 on myelination. Within mouse cultures, the percentage of MBP and Olig2 positive ODCs was unaffected by IL-33 treatment throughout indicating that it is unlikely that IL-33 acts to inhibit ODC proliferation. As the expression of ST2 was not confirmed on mouse ODCs and there was no obvious effect of IL-33 on ODC number, the potential effect of IL-33 on myelination, could be due to the indirect effect of IL-33 on other cells in the culture.

The expression and function of IL-33 and ST2 on astrocytes in MS and EAE

Astrocytes are often considered to be analogous to epithelial cells for the CNS and thus may express IL-33 and ST2. As previous reports have indicated, both IL-33 and ST2 are expressed throughout the body on epithelial cells (Pichery et al. 2012b). Using the astrocyte marker GFAP I co-stained for IL-33 and ST2 in the EAE model, human tissue and the *in vitro* myelinating culture system. IL-33 was found to be expressed within the nucleus of the majority of the astrocytes, but not all, within naïve and EAE

mouse spinal cord sections. Quantitative analysis has shown that IL-33 was reduced in EAE spinal cord compared to naïve, this is most likely due to the release from cells or the death of IL-33 expressing cells. My results suggest that IL-33 was not expressed on astrocytes within the cortex, ventricular region and corpus callosum in control mice brain. However, some colocalisation was observed on astrocytes within the hippocampus, highlighting that IL-33 may be expressed by a subgroup of astrocytes which are distributed in different regions of CNS. Interestingly, within EAE brain, the cortex, ventricular region and the hippocampus all contained IL-33^{+}GFAP^{+} astrocytes, yet the corpus callosum remained relatively astrocyte free. This is a result of microglia being the main cell which monitors this area (Gehrmann et al. 1995). Within human MS tissues IL-33 was also co–stained with astrocytes (GFAP). However, no staining was observed on astrocytes within the MS brain. This result was contrary to that observed by Christophi *et al.,* who identified IL-33 to be expressed within human MS patient brain NAWM (Christophi et al. 2012). MS is heterogeneous therefore IL-33 may be upregulated at different points throughout the disease in different patients. Furthermore there could be other contributing factors relating to the expression of IL-33 on astrocytes for example the location of the astrocytes or the gender and age of the patient. IL-33 mRNA has previously been detected in astrocytes *in vivo* (Yasuoka et al. 2011) and *in vitro* (Hudson et al. 2008). There may be more subtypes of astrocytes than those that have been currently characterised, thus it is also possible that a small subgroup of astrocytes (Shibasaki et al. 2014), express IL-33. Alternatively, these differences could be due to regional variations, or due to the possibility that IL-33 may only be expressed in cells at a certain stage in the life cycle, beyond which it is not observed (Küchler et al. 2008).

Following from the colocalisation studies, I proceeded to use immunohistochemical staining for ST2 and GFAP which revealed ST2 to be expressed on astrocytes within the grey matter of both naïve and EAE spinal

cord sections. Similar to IL-33, ST2 expressing astrocytes were reduced in EAE spinal cord. As this is also shown in the IL-33 staining it suggests a negative feedback mechanism may come into play to reduce the IL-33/ST2 signaling pathway or the expression is due to the death of ST2 expressing astrocytes. ST2 staining within the brain has shown$ST2^+GFAP^+$ astrocytes in the cortex, ventricular regions, corpus callosum and cingulum of naïve C57BL/6 mice. This agrees with previous reports that ST2 mRNA was detected in astrocytes (Andre et al. 2005; Yasuoka et al. 2011). $ST2^+GFAP^+$ astrocytes were found to be particularly evident within the endothelial layer of the cortex in the EAE mice suggesting that these astrocytes may interact with endothelial cells and pericytes which form the BBB. ST2 has been shown to be expressed by endothelial (and epithelial) cells (Yagami et al. 2010) membrane receptor involved in the initiation of angiogenesis and vascular permeability due to the binding of IL-33 (Choi et al. 2009). Therefore it is possible that IL-33 may interact with the BBB via $ST2^+$ astrocytes in an autocrine manner and play a role in the permeability of the BBB and enhancing inflammation. However, ST2 was not localised to astrocytes within the brain of control or MS brain samples. From the results discussed above, there is a clear indication that IL-33 may function in the CNS compartment via its receptor ST2 on astrocytes.

IL-33 treatment does not significantly affect the numbers of astrocytes within the mouse culture. No difference between the control and IL-33-treated cultures from day 18 to 28 was observed as both cultures contained reactive (large cell bodies and short projections) astrocytes. IL-33 is regarded as an alarmin, which is released upon necrosis/apoptosis, thus alerting the neighboring cells to react to the damage in the tissues (Lamkanfi & Dixit 2009). Therefore, addition of exogenous IL-33 to the cultures could mimic *in-vivo* danger signals similar to HMGB1 released by astrocytes (Pedrazzi et al. 2014). As a result, this is likely to lead to an increase in reactive astrocytes. HMGB1-treated astrocytes were previously found to increase levels of GFAP and vimentin (Pedrazzi et al. 2007). This indicates that HMGB1 selectively

activates astrocytes in a pro-inflammatory manner. HMGB1 also increased levels of CCL5 and CCL2, which are involved in the activation and migration of microglia (Pedrazzi et al. 2014). By analogy, IL-33's properties as an alarmin could initiate a pro-inflammatory environment by activating astrocytes through binding to ST2 on their surface. The presence of IL-33 on astrocytes within the brain and spinal cord of EAE mice (chapter 4) and the reduction of axonal myelination in the IL-33 treated rat *in vitro* system suggest that astrocytes may play important roles in regulating myelination in MS/EAE (Moore et al. 2011) the mechanisms for which are yet to be established. IL-33 has been previously shown to regulate the effects of TNF-α (Kunisch et al. 2012) which in turn induces IL-33 production (Taniguchi et al. 2013). IL-33 could reduce the production of myelin as TNF-α has previously been reported to induce myelin and ODC damage *in vitro* (Nash et al. 2011; Akassoglou et al. 1998) and the production of TNF by glial cells binds to the p55TNFR, resulting in ODC apoptosis, demyelination and plaque formation (Akassoglou et al. 1998).

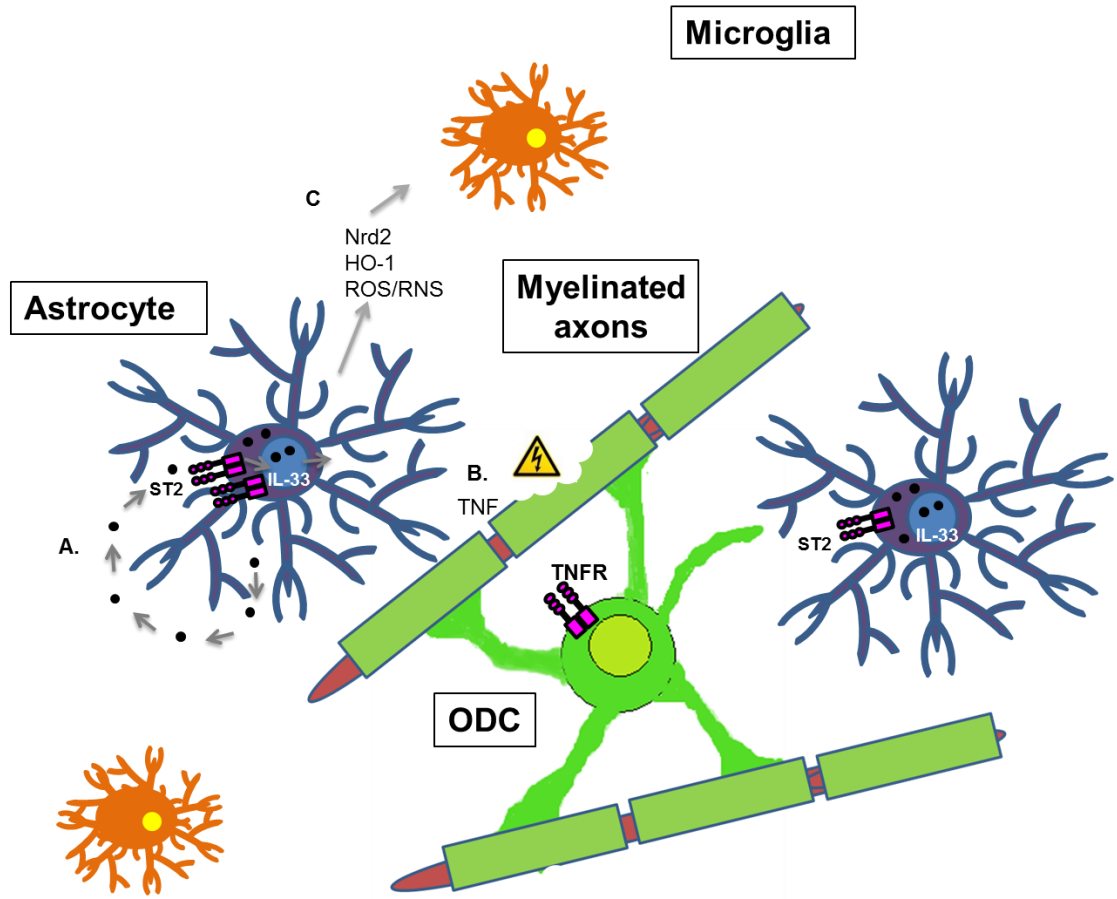

Figure 7.1. Potential roles for IL-33 within the CNS. There may be several potential roles for IL-33 within the CNS. IL-33 could be released by astrocytes under pathogenic conditions and activate astrocytes via an autocrine loop by binding to ST2 present on the astrocyte surface (A). IL-33 activation of astrocytes could also lead to the secretion of TNF-α, which binds the TNFR on ODCs resulting in ODC apoptosis and demyelination (B). Activated astrocytes release Nrd2, HO-1, ROS/RON, which can activate microglia and result in microglia proliferation and phagocytosis (C).

The expression and function of IL-33 and ST2 on microglia in MS and EAE

My results showed that IL-33 did not co-localise with Iba1^{+} microglia within naïve or EAE spinal cord sections. Furthermore, within naïve and EAE brain sections, IL-33 was also not expressed in the cortex, ventricular region or corpus callosum. IL-33 was expressed by many but not all

$CD68^+$microglia/macrophages within the brain of MS patients (chapter 5). This result is consistent with the work of Yasuoka et al and Hudson et al, who demonstrated that IL-33 mRNA was not present within microglia *in vitro*. (Yasuoka et al. 2011; Hudson et al. 2008).

Interestingly, ST2 has previously been observed to be present on macrophages (AAM) (Kurowska-Stolarska et al. 2009; Brint et al. 2004) and microglia at an mRNA and protein level *in vitro* (Yasuoka et al. 2011). In the myelinating cultures (chapter 6) ST2 was only expressed by the ODC projections (rat) and astrocytes (mouse), but not on microglia cells. Despite previous reports suggesting that ST2 is expressed by microglia (Yasuoka et al. 2011), ST2 was not colocalised with Iba1 in the white matter or the grey matter of naïve and EAE spinal cord. Similar results were observed in the cortex, ventricular regions or corpus callosum regions of brain tissues of naïve and EAE mice (chapter 4). Furthermore, in an acute MS sample, abundant in macrophage/ microglia activity within the lesion, was stained for CD68 (microglia marker) and ST2 (chapter 5). No cell was double positive suggesting that microglia and macrophages within the brain lesions are $ST2^-$. The cellular expression of ST2 observed within the lesion is likely a consequence of macrophage/ microglia scavenging $ST2^+$ axons/ myelin that have been destroyed. These results are consistent with the work of Andre et al who detected no ST2 cDNA on secondary cultures of mouse microglia (Andre et al. 2005). A possible explanation for why these studies do not yield the same results as Yasuoka *et al*., is that microglia may express ST2 at an mRNA level, but not at a detectable protein level within the human brain.

Although ST2 may not be expressed by microglia cells, it is possible that IL-33 has an indirect effect on microglia cell differentiation and function. In my mouse myelinating cultures, the effect of IL-33 treatment on microglia was not significant ($p=0.0556$). However, a trend for IL-33 treatment causing a reduction in the percentage of $Iba1^+$ microglial was evident. Previous studies have shown that astrocytes can indirectly affect microglia. Astrocytes have

been reported to secrete factors (Nrd2, HO-1, ROS/RNS) which can induce anti-oxidant gene expression and impact on the activation state of microglia (Shih et al. 2006). Furthermore, astrocyte-derived ATP released during injury can activate local microglia by potentiating the calcium wave generated from astrocytes to microglia (Davalos et al. 2005; Schipke et al. 2002). This results in the proliferation and migration of microglia (Davalos et al. 2005) and aids phagocytosis (Fang et al. 2009). Thus, IL-33 may act upon $ST2^+$ astrocytes (Stolarski et al. 2010; Hudson et al. 2008) to initiate the release of cytokines from astrocytes, which may alter the activation state of microglia (DeWitt et al. 1998). Furthermore, it is also possible that there were only low levels of ST2 present on these cultures (Yasuoka et al. 2011) and IHC staining may not be sensitive enough to detect it. Western blot analysis would be one possible future route to further examine ST2 protein expression within these cultures.

Limitations of In Vitro data in the context of MS

Despite the obvious benefits of in vitro studies touched upon in chapter 6 there are also limitations to this research. Although one of the benefits is the ease at which the cells can be manipulated to test a certain hypotheses, this can also be a disadvantage as we are creating and environment which may never occur in vivo. Specifically, the limitation of the in vitro data presented within this thesis would be the administration of IL-33 into the myelinating culture system. Recombinant IL-33 was added to the cultures during a healthy state, not during inflammation, and therefore does not reflect accurately what would happen within an inflammatory environment as seen in EAE and MS. Furthermore, cultures were treated with IL-33 at day 12, at the beginning of myelination, although this information is helpful with regards to the effect of IL-33 on myelination. It has limited standing when determining the purpose of IL-33 during MS as the axons in MS patients will have been myelinated prior to the inflammation. Thus IL-33 should also be administered after myelination has already finished. Despite these limitations in vitro

cultures are vital to our research and have provided great insight into the potential mechanisms of IL-33 within the CNS.

Future Experiments

To further understand the role of IL-33/ST2 pathway in CNS function, future experiments would need to identify the specific subsets of neurons and astrocytes which express IL-33 and ST2. This could be achieved using neuron-specific enolase (NSE) or MAP-2 (microtubule associated protein -2) for mature neurons, ßIII tubulin for differentiating neurons or DCX (Doublecortin), which is widely expressed by migrating neurons. Alternatively, markers for GABAergic interneurons (Gad65), dopamingeric neurons (TH), mature motor neurons ChAT (choline acetyltransferase) or Calbindin/Pax-2 for cortical/ spinal interneurons would provide the extra information needed to determine the exact location of ST2/IL-33 on neurons.

The exact effect of IL-33 on astrocytes in the cultures would be examined by PCR or by analysing the astrocyte reactive markers (vimentin) and utilising FACs analysis to determine if IL-33 effects the activation state of astrocytes. Future studies could also investigate the effect of IL-33 on the proliferation of different CNS resident cells using BrdU endpoints, in normal and pathological environments. The inhibitory effect of IL-33 on myelination is both surprising and interesting; this data provides more insights into the function of IL-33 in CNS damage and/or repair and its potential role in MS disease development.

Concluding Remarks

IL-33 and ST2 have shown to be expressed on neurons in EAE tissues (chapter 4) which has also translated into MS patient samples (chapter 5). In ALS, which results in motor neuron apoptosis, it has previously been shown that IL-33 is reduced in patients compared to healthy controls (Lin et al.

2012). Our results can add to these findings suggesting that IL-33 is reduced in ALS patients as a result of apoptotic IL-33^{+} neurons. MS is characterised with axonal demyelination with some neurodegeneration but infrequent neuron apoptosis. This can account for the similarity in IL-33 expression between MS and control patients. IL-33 has been shown to be elevated in MS serum (Christophi et al. 2012) which could be a result of neuron degeneration/ apoptosis. These results suggest a potential role for IL-33 to be a biomarker for neuronal degeneration and apoptosis. This information could aid the diagnosis of the specific subtype of MS. For example, as MS progresses, more neurons will be damaged as a result of the repeated myelin damage. As patients progresses (detailed in chapter 1) different clinical therapies are required. It is important to determine which stage of the disease the patient is currently displaying. The presence or absence of IL-33 may result in patients receiving the treatment they need to reduce the progression or attenuate the symptoms presented. Overall the research presented in this thesis provides a step forward in understanding the role for IL-33 in the mouse CNS and within MS, and in finding new therapeutic strategies for patients.

8. Bibliography

Abbott, N. et al., 2010. Structure and function of the blood-brain barrier. *Neurobiol Dis*, 37(1), pp.13–25.

Abbott, N.J., Rönnbäck, L. & Hansson, E., 2006. Astrocyte-endothelial interactions at the blood-brain barrier. *Nature reviews. Neuroscience*, 7(1), pp.41–53.

Acosta, M., Gioia, G. & Silva, A., 2006. Neurofibromatosis type 1: new insights into neurocognitive issues. *Curr Neurol Neurosci Rep*, 6(2), pp.136–43.

Akaoka, H. et al., 2001. Functional changes in astrocytes by human T-lymphotrophic virus type 1 T-lymphocytes. *Virus Res*, 78(1-2), pp.57–66.

Al-Bassam, S. et al., 2012. Differential trafficking of transport vesicles contributes to the localization of dendritic proteins. *Cell Reports*, 2(1), pp.89–100.

Alderson, M. & Tough, T., 1995. Fas ligand mediates activation-induced cell death in human T lymphocytes. *The Journal of Immunology*, 181.

Ali, S. et al., 2011. The dual function cytokine IL-33 interacts with the transcription factor NF-κB to dampen NF-κB-stimulated gene transcription. *Journal of Immunology*, 187(4), pp.1609–16.

Alizadeh, M. et al., 2003. Genetic interaction of CTLA-4 with HLA-DR15 in multiple sclerosis patients. *Annals of Neurology*, 54(1), pp.119–22.

Almolda, B. et al., 2011. Increase in Th17 and T-reg lymphocytes and decrease of IL22 correlate with the recovery phase of acute EAE in rat. *PloS one*, 6(11), p.e27473.

Alves-Filho, J.C. et al., 2010. Interleukin-33 attenuates sepsis by enhancing neutrophil influx to the site of infection. *Nature Medicine*, 16(6), pp.2–7.

Andre, R. et al., 2005. Regulation of expression of the novel IL-1 receptor family members in the mouse brain. *Journal of Neurochemistry*, 95(2), pp.324–30.

Andreiuolo, F. et al., 2009. GFAPdelta immunostaining improves visualization of normal and pathologic astrocytic heterogeneity. *Neuropathology*, 29(1), pp.31–9.

Araque, A. et al., 1999. Tripartite: glia, the unacknowledged partner. *Trends Neurosciences*, 22(5), pp.208–15.

Astier, A.L. et al., 2006. Alterations in CD46-mediated Tr1 regulatory T cells in patients with multiple sclerosis. *The Journal of Clinical Investigation*, 116(12), pp.1–6.

Badovinac, V. et al., 1998. Interleukin-1 receptor antagonist suppresses experimental autoimmune encephalomyelitis (EAE) in rats by influencing the activation and proliferation of encephalitogenic cells. *Journal of Neuroimmunology*, 85(1), pp.87–95.

Barres, B. a et al., 1993. Multiple extracellular signals are required for long-term oligodendrocyte survival. *Development*, 118(1), pp.283–95.

Battistini, L. et al., 2003. CD8+ T cells from patients with acute multiple sclerosis display selective increase of adhesiveness in brain venules : a critical role for P-selectin glycoprotein ligand-1. *Blood*, 101(12), pp.4775–4782.

Bauer, M. et al., 2009. Beta1 integrins differentially control extravasation of inflammatory cell subsets into the CNS during autoimmunity. *Proceedings of the National Academy of Sciences of the United States of America*, 106(6), pp.1920–5.

Beauvillain, C. et al., 2008. Neonatal and Adult Microglia Cross-Present Exogenous Antigens. *Glia*, 77, pp.69–77.

Bennett, J. et al., 2010. Blood-brain barrier disruption and enhanced vascular permeability in the multiple sclerosis model EAE. *Journal of Neuroimmunology*, 229(1-2), pp.180–91.

Berglund, C.M.D. et al., 2004. Characterization of long-term mouse brain aggregating cultures: evidence for maintenance of neural precursor cells. *The Journal of Comparative Neurology*, 474(2), pp.246–60.

Bettelli, E. et al., 2004. Loss of T-bet, but not STAT1, prevents the development of experimental autoimmune encephalomyelitis. *The Journal of Experimental Medicine*, 200(1), pp.79–87.

Bettelli, E., Korn, T. & Kuchroo, V.K., 2008. Th17: The third member of the effector T cell Trilogy Estelle. *Current Opinions in Immunology*, 19(6), pp.652–657.

Bieber, A.J., Kerr, S. & Rodriguez, M., 2003. Efficient central nervous system remyelination requires T cells. *Annals of neurology*, 53(5), pp.680–4.

Billiau, A. & Matthys, P., 2001. Modes of action of Freund ' s adjuvants in experimental models of autoimmune diseases. *Journal of Leukocyte Biology* , 70, pp.849–860.

Bitsch, a et al., 2000. Acute axonal injury in multiple sclerosis. Correlation with demyelination and inflammation. *Brain : a journal of Neurology*, 123 Pt 6, pp.1174–83.

Braughlers, J.M., Duncan, L.A. & Chase, R.L., 1986. The Involvement of Iron in Lipid Peroxidation. *Society*, 261(22), pp.10282–10289.

Brehm, M. a., Daniels, K. a. & Welsh, R.M., 2005. Rapid Production of TNF- following TCR Engagement of Naive CD8 T Cells. *The Journal of Immunology*, 175(8), pp.5043–5049.

Brinkmann, B., Agarwal, A. & Sereda, M., 2008. Neuregulin-1/ErbB signaling serves distinct functions in myelination of the peripheral and central nervous system. *Neuron*, 59(4), pp.581–595.

Brint, E.K. et al., 2002. Characterization of signaling pathways activated by the interleukin 1 (IL-1) receptor homologue T1/ST2. A role for Jun N-terminal kinase in IL-4 induction. *The Journal of Biological Chemistry*, 277(51), pp.49205–11.

Brint, E.K. et al., 2004. ST2 is an inhibitor of interleukin 1 receptor and Toll-like receptor 4 signaling and maintains endotoxin tolerance. *Nature Immunology*, 5(4), pp.373–9.

Bulek, K. et al., 2009. The essential role of single Ig IL-1 receptor-related molecule/Toll IL-1R8 in regulation of Th2 immune response. *Journal of Immunology*, 182(5), pp.2601–9.

Bushong, E. a et al., 2002. Protoplasmic astrocytes in CA1 stratum radiatum occupy separate anatomical domains. *The Journal Of Neuroscience : The Official Journal Of The Society For Neuroscience*, 22(1), pp.183–92.

Cabarrocas, J. et al., 2003. Effective and selective immune surveillance of the brain by MHC class I-restricted cytotoxic T lymphocytes. *European Journal of Immunology*, 33(5), pp.1174–82.

Caldwell, J.H. et al., 2000. Sodium channel Na(v)1.6 is localized at nodes of ranvier, dendrites, and synapses. *Proceedings of the National Academy of Sciences of the United States of America*, 97(10), pp.5616–20.

Carriere, V. & Roussel, L., 2007. IL-33, the IL-1-like cytokine ligand for ST2 receptor, is a chromatin-associated nuclear factor in vivo. *Proceedings of the National Academy of Sciences*, 104(1), pp.2–7.

Cavanillas, M.L. et al., 2010. Polymorphisms in the IL2, IL2RA and IL2RB genes in multiple sclerosis risk. *European Journal of Human Genetics : EJHG*, 18(7), pp.794–9.

Cayrol, C. & Girard, J., 2009. The IL-1-like cytokine IL-33 is inactivated after maturation by caspase-1. , 106(22).

Cepok, S. et al., 2005. Short-lived plasma blasts are the main B cell effector subset during the course of multiple sclerosis. *Brain : a Journal of Neurology*, 128(Pt 7), pp.1667–76.

Chackerian, A. a et al., 2007. IL-1 receptor accessory protein and ST2 comprise the IL-33 receptor complex. *Journal of Immunology* 179(4), pp.2551–5.

Chang, A. et al., 2008. Neurogenesis in the chronic lesions of multiple sclerosis. *Brain : a Journal of Neurology*, 131(Pt 9), pp.2366–75.

Chapuis, J. et al., 2009. Transcriptomic and genetic studies identify IL-33 as a candidate gene for Alzheimer's disease. *Molecular psychiatry*, 14(11), pp.1004–1016.

Charles, P. et al., 2000. Negative regulation of central nervous system myelination by polysialylated-neural cell adhesion molecule. *Proceedings of the National Academy of Sciences of the United States of America*, 97(13), pp.7585–90.

Chen, W.C. & Chen, C.C., 1998. ATP-induced arachidonic acid release in cultured astrocytes is mediated by Gi protein coupled P2Y1 and P2Y2 receptors. *Glia*, 22(4), pp.360–70.

Cho, I.-H. et al., 2008. Role of microglial IKKbeta in kainic acid-induced hippocampal neuronal cell death. *Brain : a Journal of Neurology*, 131(Pt 11), pp.3019–33.

Choi, Y. et al., 2009. Interleukin-33 induces angiogenesis and vascular permeability through ST2 / TRAF6-mediated endothelial nitric oxide production. *Vascular*, 114(14), pp.3117–3126.

Choi, Y.-S. et al., 2012. Nuclear IL-33 is a transcriptional regulator of NF-κB p65 and induces endothelial cell activation. *Biochemical and Biophysical Research Communications*, 421(2), pp.305–311.

Christophi, G.P. et al., 2011. Interleukin-33 upregulation in peripheral leukocytes and CNS of multiple sclerosis patients. *Clinical Immunology (Orlando, Fla.)*.

Christophi, G.P. et al., 2012. Interleukin-33 upregulation in peripheral leukocytes and CNS of multiple sclerosis patients. *Clinical Immunology (Orlando, Fla.)*, 142(3), pp.308–19.

Coetzee, T. et al., 1996. Myelination in the Absence of Galactocerebroside and Sulfatide : Normal Structure with Abnormal Function and Regional Instability University of North Carolina at Chapel Hill. *Cell* , 86, pp.209–219.

Colton, C. a & Gilbert, D.L., 1987. Production of superoxide anions by a CNS macrophage, the microglia. *FEBS letters*, 223(2), pp.284–8.

Comabella, M. & Khoury, S.J., 2012. Immunopathogenesis of multiple sclerosis. *Clinical Immunology (Orlando, Fla.)*, 142(1), pp.2–8.

Connor, R.A.O. et al., 2009. Cutting Edge : Th1 Cells Facilitate the Entry of Th17 Cells to the Central Nervous System during Experimental Autoimmune. *Journal of Immunology*, 181(6), pp.3750–3754.

Conti, B. et al., 1999. Cultures of astrocytes and microglia express interleukin 18. *Brain research. Molecular Brain Research*, 67(1), pp.46–52.

Craner, M.J. et al., 2004. Co-localization of sodium channel Nav1.6 and the sodium-calcium exchanger at sites of axonal injury in the spinal cord in EAE. *Brain : a Journal of Neurology*, 127(Pt 2), pp.294–303.

Cua, D.J. et al., 2003. Interleukin-23 rather than interleukin-12 is the critical cytokine for autoimmune inflammation of the brain. *Nature*, 421(6924), pp.744–8.

Dabertrand, F. et al., 2013. Prostaglandin E2, a postulated astrocyte-derived neurovascular coupling agent, constricts rather than dilates parenchymal arterioles. *Journal Of Cerebral Blood Flow And*

***Metabolism : Official Journal Of The International Society Of Cerebral Blood Flow And Metabolism*, 33(4), pp.479–82.**

Damsker, J.M., Hansen, A.M. & Caspi, R.R., 2010. Th1 and Th17 cells: adversaries and collaborators. *Annals of the New York Academy of Sciences*, 1183, pp.211–21.

Davies, C. a et al., 1999. The progression and topographic distribution of interleukin-1beta expression after permanent middle cerebral artery occlusion in the rat. *Journal Of Cerebral Blood Flow And Metabolism : Official Journal Of The International Society Of Cerebral Blood Flow And Metabolism*, 19(1), pp.87–98.

Deb, C. et al., 2010. CD8+ T cells cause disability and axon loss in a mouse model of multiple sclerosis. *PloS one*, 5(8), p.e12478.

Devraj, K. et al., 2013. GLUT-1 Glucose Transporters in the Blood-Brain Barrier: Differential Phosphorylation. *Journal of Neurosciences*, 89(12).

Dhib-Jalbut, S., 2003. Glatiramer acetate (Copaxone®) therapy for multiple sclerosis. *Pharmacology & Therapeutics*, 98(2), pp.245–255.

Dinarello, C. a, 2011. Interleukin-1 in the pathogenesis and treatment of inflammatory diseases. *Blood*, 117(14), pp.3720–32.

Edwards, S. et al., 1998. Clinical relapses and disease activity on magnetic resonance imaging associated with viral upper respiratory tract infections in multiple sclerosis. *Journal of Neurology, Peurosurgery, and psychiatry*, 64(6), pp.736–41.

Elices, M.J. et al., 1990. VCAM-1 on activated endothelium interacts with the leukocyte integrin VLA-4 at a site distinct from the VLA-4/fibronectin binding site. *Cell*, 60(4), pp.577–84.

Emerson, M.R. et al., 2009. Enhancing the Ability of Experimental Autoimmune Encephalomyelitis to Serve as a More Rigorous Model

of Multiple Sclerosis through Refinement of the Experimental Design. *Comparative Medicine*, 59(2), pp.112–128.

Endharti, A.T. et al., 2005. Cutting edge: CD8+CD122+ regulatory T cells produce IL-10 to suppress IFN-gamma production and proliferation of CD8+ T cells. *Journal of Immunology*, 175(11), pp.7093–7.

Enokido, Y. et al., 2008. Age-dependent change of HMGB1 and DNA double-strand break accumulation in mouse brain. *Biochemical and Biophysical Research Communications*, 376(1), pp.128–33.

Faingold, C.L., 2004. Emergent properties of CNS neuronal networks as targets for pharmacology: application to anticonvulsant drug action. *Progress in Neurobiology*, 72(1), pp.55–85.

Falnes, P.Ø. & Sandvig, K., 2000. Penetration of protein toxins into cells. *Current Opinion in Cell Biology*, pp.407–413.

Faraco, G. et al., 2007. High mobility group box 1 protein is released by neural cells upon different stresses and worsens ischemic neurodegeneration in vitro and in vivo. *Journal of Neurochemistry*, 103(2), pp.590–603.

Farias, A.S. et al., 2012. Proteome analysis of spinal cord during the clinical course of monophasic experimental autoimmune encephalomyelitis. *Proteomics*, 12(17), pp.2656–62.

Farooqi, N., Gran, B. & Constantinescu, C.S., 2010. Are current disease-modifying therapeutics in multiple sclerosis justified on the basis of studies in experimental autoimmune encephalomyelitis? *Journal of Neurochemistry*, 115(4), pp.829–44.

Ferber, I.A. et al., 1996. Mice with a Disrupted IFN-y Gene Are Susceptible to the Induction of Experimental Autoimmune Encephalomyelitis (EAE). *The Journal of Immunolgy*, (156), pp.0–2.

Fex Svenningsen, A. et al., 2003. Rapid method for culturing embryonic neuron-glial cell cocultures. *Journal of Neuroscience Research*, 72(5), pp.565–73.

Ffrench-Constant, C. & Miller, R., 1986. Molecular specialization of astrocyte processes at nodes of Ranvier in rat optic nerve. *The Journal of Cell Biology*, 102(March), pp.844–852.

Fitzner, D. et al., 2006. Myelin basic protein-dependent plasma membrane reorganization in the formation of myelin. *The EMBO Journal*, 25(21), pp.5037–48.

Fodstad, H., 2002. The neuron saga. *International Congress Series*, 1247, pp.645–650.

Foote, a K. & Blakemore, W.F., 2005. Inflammation stimulates remyelination in areas of chronic demyelination. *Brain : a journal of Neurology*, 128(Pt 3), pp.528–39.

Frank, M.G. et al., 2006. mRNA up-regulation of MHC II and pivotal pro-inflammatory genes in normal brain aging. *Neurobiology of Aging*, 27(5), pp.717–22.

Funakoshi-Tago, M. et al., 2008. TRAF6 is a critical signal transducer in IL-33 signaling pathway. *Cellular signalling*, 20(9), pp.1679–86.

Furtado, G.C. et al., 2008. Swift Entry of Myelin-Specific T lymphocytes into the Central Nervous System in Spontaneous Autoimmune. *The Journal of Immunolgy*, (181), pp.4648–4655.

Gardella, S. et al., 2002. The nuclear protein HMGB1 is secreted by secretory pathway. , 3(10), pp.995–1001.

Gerritse, K. et al., 1996. CD40-CD40 ligand interactions in experimental allergic encephalomyelitis and multiple sclerosis. *Proceedings of the National Academy of Sciences of the United States of America*, 93(6), pp.2499–504.

Ghoumari, a. M. et al., 2003. Progesterone and its metabolites increase myelin basic protein expression in organotypic slice cultures of rat cerebellum. *Journal of Neurochemistry*, 86(4), pp.848–859.

Gifford, G.E. & Lohmann-Matthes, M.L., 1987. Gamma interferon priming of mouse and human macrophages for induction of tumor necrosis factor production by bacterial lipopolysaccharide. *Journal of the National Cancer Institute*, 78(1), pp.121–4.

Glass, D. et al., 2013. Gene expression changes with age in skin, adipose tissue, blood and brain. *Genome biology*, 14(7), p.R75.

Gocke, A.R. et al., 2007. T-bet regulates the fate of Th1 and Th17 lymphocytes in autoimmunity. *Journal of Immunology*, 178(3), pp.1341–8.

Goldmann, T. & Prinz, M., 2013. Role of Microglia in CNS Autoimmunity. *Clinical and Developmental Immunology* , 2013(88).

Goverman, J. et al., 1993. Transgenic mice that express a myelin basic protein-specific T cell receptor develop spontaneous autoimmunity. *Cell*, 72(4), pp.551–60.

Grabovsky, V. et al., 2000. Subsecond induction of alpha4 integrin clustering by immobilized chemokines stimulates leukocyte tethering and rolling on endothelial vascular cell adhesion molecule 1 under flow conditions. *The Journal of Experimental Medicine*, 192(4), pp.495–506.

Greene, D.A., Lattimer, S.A. & Sima, A.A.F., 1988. Regulation Involved in Pathogenesis. , 37(June), pp.688–693.

Griffin, G.K. et al., 2012. IL-17 and TNF-α sustain neutrophil recruitment during inflammation through synergistic effects on endothelial activation. *Journal of Immunology (Baltimore, Md. : 1950)*, 188(12), pp.6287–99.

Halassa, M.M. et al., 2007. Synaptic islands defined by the territory of a single astrocyte. *The Journal of Neuroscience : the official journal of the Society for Neuroscience*, 27(24), pp.6473–7.

Handel, A.E., Lincoln, M.R. & Ramagopalan, S. V, 2011. Of mice and men: experimental autoimmune encephalitis and multiple sclerosis. *European Journal of Clinical Investigation*, 41(11), pp.1254–8.

Hart, B. t, Bauer, J. & Muller, H., 1998. Histopathological characterization of magnetic resonance imaging-detectable brain white matter lesions in a primate model of multiple sclerosis: a correlative study in. *The American Journal of Pathology,* 153(2), pp.649–663.

Hartung, H.-P. et al., 2002. Mitoxantrone in progressive multiple sclerosis: a placebo-controlled, double-blind, randomised, multicentre trial. *Lancet*, 360(9350), pp.2018–25.

Hayakawa, H. et al., 2007. Soluble ST2 blocks interleukin-33 signaling in allergic airway inflammation. *The Journal of Biological Chemistry*, 282(36), pp.26369–80.

Hayes, C.E., 2000. Vitamin D: a natural inhibitor of multiple sclerosis. *The Proceedings of the Nutrition Society*, 59(4), pp.531–5.

Hensiek, a E. et al., 2002. HLA-DR 15 is associated with female sex and younger age at diagnosis in multiple sclerosis. *Journal of Neurology, Neurosurgery, and Psychiatry*, 72(2), pp.184–7.

Hilgetag, C.C. & Barbas, H., 2009. Are there ten times more glia than neurons in the brain? *Brain structure & function*, 213(4-5), pp.365–6.

Hirota, K. et al., 2007. Preferential recruitment of CCR6-expressing Th17 cells to inflamed joints via CCL20 in rheumatoid arthritis and its animal model. *The Journal of Experimental Medicine*, 204(12), pp.2803–12.

Hirotani, T. et al., 2005. Regulation of lipopolysaccharide-inducible genes by MyD88 and Toll/IL-1 domain containing adaptor inducing IFN-beta. *Biochemical and Biophysical Research Communications*, 328(2), pp.383–92.

Hofstetter, H.H. et al., 2003. Autoreactive T cells promote post-traumatic healing in the central nervous system. *Journal of Neuroimmunology*, 134(1-2), pp.25–34.

Höftberger, R. et al., 2004. Expression of major histocompatibility complex class I molecules on the different cell types in multiple sclerosis lesions. *Brain pathology (Zurich, Switzerland)*, 14(1), pp.43–50.

Hong, J. et al., 2011. Identification of Constitutively Active Interleukin 33 (IL-33) Splice Variant *Journal of Biological Chemistry*, 33, pp20078-20087

Horiuchi, M. et al., 2010. Differing in vitro survival dependency of mouse and rat NG2+ oligodendroglial progenitor cells. *Journal of Neuroscience research*, 88(5), pp.957–70.

Horiuchi, M. et al., 2006. MEK-ERK signaling is involved in interferon-gamma-induced death of oligodendroglial progenitor cells. *The Journal of Biological Chemistry*, 281(29), pp.20095–106.

Huang, W.-X., Huang, P. & Hillert, J., 2004. Increased expression of caspase-1 and interleukin-18 in peripheral blood mononuclear cells in patients with multiple sclerosis. *Multiple Sclerosis*, 10(5), pp.482–487.

Hudson, C.A. et al., 2008. Induction of IL-33 expression and activity in central nervous system glia. *Journal of Leukocyte Biology*, 84, pp.631–643.

Humphreys, N.E. et al., 2008. IL-33, a Potent Inducer of Adaptive Immunity to Intestinal Nematodes Neil. *The Veterinary Clinics of North America. Small animal practice*, 39(6), pp.1091–107, vi–vii.

Huxley, B.Y.A.F. & Stampfli, A.D.R., 1948. Evidence For Saltatory Conduction in Peripheral Myelinated Nerve Fibres. *Journal of Physiology* , (1946), pp.315–339.

Inoue, I. & Takeda, J., 1999. Identification of Genes Differentially Expressed in Canine Vasospastic Cerebral Arteries After Subarachnoid Hemorrhage. *Journal of Cerebral Blood Flow and Metabolism*, pp.1279–1288.

Izumi, Y. et al., 1998. An Atypical PKC Directly Associates and Colocalizes at the Epithelial Tight Junction with ASIP, a Mammalian Homologue of. *The Journal of Cell Biology*, 143(1), pp.95–106.

Jacobs, L. & Beck, R., 2000. Intramuscular interferon beta-1a therapy initiated during a first demyelinating event in multiple sclerosis. *The England Journal of Medicine*, 343(13), pp.898–904.

Jagessar, S.A., Heijmans, N., Oh, L., et al., 2012. Antibodies against human BLyS and APRIL attenuate EAE development in marmoset monkeys. *Journal of Neuroimmune Pharmacology : the official journal of the Society on NeuroImmune Pharmacology*, 7(3), pp.557–70..

Jagessar, S.A., Heijmans, N., Bauer, J., et al., 2012. B-Cell Depletion Abrogates T Cell-Mediated Demyelination in an Antibody-Nondependent Common Marmoset Experimental Autoimmune Encephalomyelitis Model. *Journal of Neuropathology and Experimental Neurology*, 71(8), pp.716–728.

Jagessar, S.A., Heijmans, N., Blezer, E.L.A., et al., 2012. Unravelling the T-cell-mediated autoimmune attack on CNS myelin in a new primate EAE model induced with MOG 34 – 56 peptide in incomplete adjuvant. *European Journal of Immunology*, pp.217–227.

Jarjour, A.A. et al., 2003. Netrin-1 Is a Chemorepellent for Oligodendrocyte Precursor Cells in the Embryonic Spinal Cord vitro in the absence of either netrin-1 or DCC . These findings

indicate that netrin-1 is a repellent cue for migrating OPs in the embryonic. *Journal of Neuroscience*, 23(9), pp.3735–3744.

Jessen, K.R. & Mirsky, R., 1983. Astrocyte-like glia in the peripheral nervous system: an immunohistochemical study of enteric glia. *The Journal of Neuroscience : the official journal of the Society for Neuroscience*, 3(11), pp.2206–18.

Jiang, H.-R. et al., 2012. IL-33 attenuates EAE by suppressing IL-17 and IFN-γ production and inducing alternatively activated macrophages. *European Journal of Immunology*, 42(7), pp.1804–14.

Jones, L. a et al., 2010. IL-33 receptor (T1/ST2) signalling is necessary to prevent the development of encephalitis in mice infected with Toxoplasma gondii. *European Journal of Immunology*, 40(2), pp.426–36.

De Jong, B. a. et al., 2002. Production of IL-1β and IL-1Ra as risk factors for susceptibility and progression of relapse-onset multiple sclerosis. *Journal of Neuroimmunology*, 126(1-2), pp.172–179.

JR, Connor. & SL, M., 1996. Relationship of iron to oligodendrocytes and myelination. *Glia*, 17(2), pp.83–83.

Jurewicz, A. et al., 2005. Tumour necrosis factor-induced death of adult human oligodendrocytes is mediated by apoptosis inducing factor. *Brain : a Journal of Neurology*, 128(Pt 11), pp.2675–88.

Kai, H. et al., 2006. Critical role of M. tuberculosis for dendritic cell maturation to induce collagen-induced arthritis in H-2b background of C57BL/6 mice. *Immunology*, 118(2), pp.233–9.

Kakkar, R. et al., 2012. Interleukin 33 as a Mechanically Responsive Cytokine Secreted by Living Cells. *The Journal of Biological Chemistry*, 287(9), pp.6941–6948.

Kanazawa, H. et al., 2002. Macrophage/microglia-specific protein Iba1 enhances membrane ruffling and Rac activation via phospholipase

C-gamma -dependent pathway. *The Journal of Biological Chemistry*, 277(22), pp.20026–32.

Kanda, M. et al., 2006. Elevation of ST2 protein levels in cerebrospinal fluid following subarachnoid hemorrhage. *Acta neurologica Scandinavica*, 113(5), pp.327–33.

Karakus, N. et al., 2013. Association of interleukin (IL)-4 gene intron 3 VNTR polymorphism with multiple sclerosis in Turkish population. *Human Immunology*, 74(9), pp.1157–60.

Kebir, H. et al., 2009. Preferential recruitment of interferon-gamma-expressing TH17 cells in multiple sclerosis. *Annals of neurology*, 66(3), pp.390–402.

Kenealy, S.J., Pericak-Vance, M. a. & Haines, J.L., 2003. The genetic epidemiology of multiple sclerosis. *Journal of Neuroimmunology*, 143(1-2), pp.7–12.

Kerstetter, a E. et al., 2009. Inhibition of CXCR2 signaling promotes recovery in models of multiple sclerosis. *Experimental neurology*, 220(1), pp.44–56..

Kidd, D. et al., 1999. Cortical lesions in multiple sclerosis. *Brain : a journal of neurology*, 122 Pt 1, pp.17–26.

Kipp, M. et al., 2012. Experimental in vivo and in vitro models of multiple sclerosis: EAE and beyond. *Multiple Sclerosis and Related Disorders*, 1(1), pp.15–28.

Kivisäkk, P. et al., 1999. High numbers of perforin mRNA expressing CSF cells in multiple sclerosis patients with gadolinium-enhancing brain MRI lesions. *Acta Neurologica Scandinavica*, 100(1), pp.18–24.

Knopf, P.M. et al., 1998. Antigen-dependent intrathecal antibody synthesis in the normal rat brain: tissue entry and local retention of

antigen-specific B cells. *Journal of Immunology (Baltimore, Md. : 1950)*, 161(2), pp.692–701.

Kobayashi, K. et al., 2013. Minocycline selectively inhibits M1 polarization of microglia. *Cell death & disease*, 4(3), p.e525..

Kohm, A.P. et al., 2002. Cutting Edge:CD4+CD25+ Regulatory T Cells Suppress Antigen-Specific Autoreactive Immune Response and Central Nervous System Inflammation During Active Experimental Autoimmune Encephalomyelitis. *The Journal of Immunology,169, pp4712-4716*

Komai-Koma, M. et al., 2007. IL-33 is a chemoattractant for human Th2 cells. *European Journal of Immunology*, 37(10), pp.2779–86.

Kondo, Y. et al., 2008. Administration of IL-33 induces airway hyperresponsiveness and goblet cell hyperplasia in the lungs in the absence of adaptive immune system. *International Immunology*, 20(6), pp.791–800.

Kreutzberg, G.W., 1996. Microglia: a sensor for pathological events in the CNS. *Trends in Neurosciences*, 19(8), pp.312–8.

Kroenke, M. a et al., 2008. IL-12- and IL-23-modulated T cells induce distinct types of EAE based on histology, CNS chemokine profile, and response to cytokine inhibition. *The Journal of Experimental Medicine*, 205(7), pp.1535–41.

Krzisch, M. et al., 2014. Pre-existing astrocytes form functional perisynaptic processes on neurons generated in the adult hippocampus. *Brain Structure & Function*.

Küchler, A.M. et al., 2008. Nuclear interleukin-33 is generally expressed in resting endothelium but rapidly lost upon angiogenic or proinflammatory activation. *The American Journal of Pathology*, 173(4), pp.1229–42.

Kuerten, S. & Angelov, D.N., 2008. Comparing the CNS morphology and immunobiology of different EAE models in C57BL/6 mice - a step towards understanding the complexity of multiple sclerosis. *Annals of Anatomy*, 190(1), pp.1–15.

Kuhlmann, T., Lassmann, H. & Brück, W., 2008. Diagnosis of inflammatory demyelination in biopsy specimens: a practical approach. *Acta Neuropathologica*, 115(3), pp.275–87.

Kunisch, E. et al., 2012. IL-33 regulates TNF-α dependent effects in synovial fibroblasts. *International Journal of Molecular Medicine*, 29(4), pp.530–40.

Kuno, R. et al., 2005. Autocrine activation of microglia by tumor necrosis factor-alpha. *Journal of Neuroimmunology*, 162(1-2), pp.89–96.

Kurowska-Stolarska, M. et al., 2009. IL-33 amplifies the polarization of alternatively activated macrophages that contribute to airway inflammation. *Journal of Immunology*, 183(10), pp.6469–77.

Kurowska-Stolarska, M. et al., 2008. IL-33 induces antigen-specific IL-5+ T cells and promotes allergic-induced airway inflammation independent of IL-4. *Journal of Immunology*, 181(7), pp.4780–90.

Kurth, F. et al., 2014. Neuroprotective effects of testosterone treatment in men with multiple sclerosis. *NeuroImage. Clinical*, 4, pp.454–60.

Lamkanfi, M. & Dixit, V.M., 2009. IL-33 raises alarm. *Immunity*, 31(1), pp.5–7.

Lang, D. et al., 1998. The type II IL-1 receptor interacts with the IL-1 receptor accessory protein: a novel mechanism of regulation of IL-1 responsiveness. *Journal of Immunology*, 161(12), pp.6871–7.

Langrish, C.L. et al., 2005. IL-23 drives a pathogenic T cell population that induces autoimmune inflammation. *The Journal of Experimental Medicine*, 201(2), pp.233–40.

Lehner, P.J. & Cresswell, P., 2004. Recent developments in MHC-class-I-mediated antigen presentation. *Current Opinion in Immunology*, 16(1), pp.82–89.

Levin, L.I. et al., 2011. of Epstein-Barr Virus Antibody Titers and Initial Onset of Neurological Symptoms in Multiple Sclerosis. *Nutrition*, 293(20), pp.2496–2500.

Levine, J.M., Reynolds, R. & Fawcett, J.W., 2001. The oligodendrocyte precursor cell in health and disease. *Trends in Neurosciences*, 24(1), pp.39–47.

Li, M. et al., 2012a. IL-33 blockade suppresses the development of experimental autoimmune encephalomyelitis in C57BL/6 mice. *Journal of Neuroimmunology*, 247(1-2), pp.25–31.

Li, M. et al., 2012b. IL-33 blockade suppresses the development of experimental autoimmune encephalomyelitis in C57BL/6 mice. *Journal of Neuroimmunology*, 247(1-2), pp.25–31.

Li, Z. et al., 2004. The importance of dendritic mitochondria in the morphogenesis and plasticity of spines and synapses. *Cell*, 119(6), pp.873–87.

Liebner, S. et al., 2008. Wnt/beta-catenin signaling controls development of the blood-brain barrier. *The Journal of Cell Biology*, 183(3), pp.409–17.

Liew, F.Y., Pitman, N.I. & McInnes, I.B., 2010. Disease-associated functions of IL-33: the new kid in the IL-1 family. *Nature reviews. Immunology*, 10(2), pp.103–10.

Lim, S.Y. & Constantinescu, C.S., 2010. Current and future disease-modifying therapies in multiple sclerosis. *International Journal of clinical practice*, 64(5), pp.637–50.

Lin, C.Y. et al., 2012. Reduced levels of interleukin 33 and increased levels of soluble ST2 in subjects with amyotrophic lateral sclerosis. *Journal of Neuroimmunology*, 249(1-2), pp.93–5.

Lingel, A. et al., 2009. Structure of IL-33 and its interaction with the ST2 and IL-1RAcP receptors--insight into heterotrimeric IL-1 signaling complexes. *Structure*, 17(10), pp.1398–410.

Link, H. & Huang, Y.-M., 2006. Oligoclonal bands in multiple sclerosis cerebrospinal fluid: an update on methodology and clinical usefulness. *Journal of Neuroimmunology*, 180(1-2), pp.17–28.

Löhning, M. et al., 1998. T1/ST2 is preferentially expressed on murine Th2 cells, independent of interleukin 4, interleukin 5, and interleukin 10, and important for Th2 effector function. *Proceedings of the National Academy of Sciences of the United States of America*, 95(12), pp.6930–5.

Lorenz, P. et al., 2003. Oxyresveratrol and resveratrol are potent antioxidants and free radical scavengers: effect on nitrosative and oxidative stress derived from microglial cells. *Nitric Oxide*, 9(2), pp.64–76.

Losy, J. & Niezgoda, A., 2001. IL-18 in patients with multiple sclerosis. , 3(9), pp.171–173.

Lucchinetti, C. et al., 2000. Heterogeneity of multiple sclerosis lesions: implications for the pathogenesis of demyelination. *Annals of Neurology*, 47(6), pp.707–17.

Lüthi, A.U. et al., 2009. Suppression of interleukin-33 bioactivity through proteolysis by apoptotic caspases. *Immunity*, 31(1), pp.84–98.

MacDonald, B.T., Tamai, K. & Ke, X., 2009. Wnt/b-catenin signalling: components, mechanisms, and disease. *National Institute of Health*, 17(1), pp.9–26.

Magliozzi, R. et al., 2007. Meningeal B-cell follicles in secondary progressive multiple sclerosis associate with early onset of disease and severe cortical pathology. *Brain : a Journal of Neurology*, 130(Pt 4), pp.1089–104.

Marin-Padilla, M., 2011. Neurons and Associated Cells. In *The Human Brain: Prenatal Development and Structure*. pp. 11–39.

Martin, D. & Near, S.L., 1995. Protective effect of the interleukin-1 receptor antagonist (IL-1ra) on experimental allergic encephalomyelitis in rats. *Journal of Neuroimmunology*, 61(2), pp.241–5.

Martinon, F., Burns, K. & Tschopp, J., 2002. The inflammasome: a molecular platform triggering activation of inflammatory caspases and processing of proIL-beta. *Molecular cell*, 10(2), pp.417–26.

Masamune, A. et al., 2010. Nuclear expression of interleukin-33 in pancreatic stellate cells. *American Journal of Physiology. Gastrointestinal and Liver Physiology*, 299(4), pp.G821–32.

Mascarucci, P. et al., 1998. Glutamate release in the nucleus tractus solitarius induced by peripheral lipopolysaccharide and interleukin-1 beta. *Neuroscience*, 86(4), pp.1285–90.

Massacesi, L. et al., 2005. Efficacy of azathioprine on multiple sclerosis new brain lesions evaluated using magnetic resonance imaging. *Archives of Neurology*, 62(12), pp.1843–7.

Matsumura, K. & Yamagata, K., 1996. Endothelial cells of the rat brain vasculature express cyclooxygenase-2 rnRNA in response to systemic interleukin-1 ~ : a possible site of prostaglandin synthesis responsible for fever (COX-2). *Brain Research*, 733, pp.263–272.

Matusevicius, D. et al., 1998. Interleukin-12 and perforin mRNA expression is augmented in blood mononuclear cells in multiple sclerosis. *Scandinavian journal of Immunology*, 47(6), pp.582–90.

McLaren, J.E. et al., 2010. IL-33 reduces macrophage foam cell formation. *Journal of Immunology (Baltimore, Md. : 1950)*, 185(2), pp.1222–9.

McLaughlin, K. a et al., 2009. Age-dependent B cell autoimmunity to a myelin surface antigen in pediatric multiple sclerosis. *Journal of Immunology (Baltimore, Md. : 1950)*, 183(6), pp.4067–76.

McMahon, E.J. et al., 2005. Epitope spreading initiates in the CNS in two mouse models of multiple sclerosis. *Nature Medicine*, 11(3), pp.335–9.

McPhail, L.T. et al., 2004. The contribution of activated phagocytes and myelin degeneration to axonal retraction/dieback following spinal cord injury. *The European Journal of Neuroscience*, 20(8), pp.1984–94

McTigue, D.M. & Tripathi, R.B., 2008. The life, death, and replacement of oligodendrocytes in the adult CNS. *Journal of Neurochemistry*, 107(1), pp.1–19.

Mead, R.J. et al., 2002. The membrane attack complex of complement causes severe demyelination associated with acute axonal injury. *Journal of Immunology*, 168(1), pp.458–65.

Menard, L.C. et al., 2007. B cells amplify IFN-gamma production by T cells via a TNF-alpha-mediated mechanism. *Journal of Immunology*, 179(7), pp.4857–66.

Mi, S. et al., 2005. LINGO-1 negatively regulates myelination by oligodendrocytes. *Nature Neuroscience*, 8(6), pp.745–51.

Middeldorp, J. et al., 2009. Specific human astrocyte subtype revealed by affinity purified GFAP antibody; unpurified serum cross-reacts with neurofilament-L in Alzheimer. *PloS one*, 4(11), p.e7663.

Miller, A.M. et al., 2008. IL-33 reduces the development of atherosclerosis. *The Journal of Experimental Medicine*, 205(2), pp.339–46.

Miller, A.M. et al., 2010. Interleukin-33 induces protective effects in adipose tissue inflammation during obesity in mice. *Circulation Research*, 107(5), pp.650–8.

Miller, D.J. et al., 1994. Monoclonal autoantibodies promote central nervous system repair in an animal model of multiple sclerosis. *The Journal of neuroscience : the official journal of the Society for Neuroscience*, 14(10), pp.6230–8.

Miller, R., 1996. Oligodendrocyte origins. *Trends in neurosciences*, pp.92–96.

Miyagishi, R. et al., 2003. C–C chemokine receptor 2 gene polymorphism in Japanese patients with multiple sclerosis. *Journal of Neuroimmunology*, 145(1-2), pp.135–138.

Mizutani, N., Nabe, T. & Yoshino, S., 2013. Interleukin-33 and alveolar macrophages contribute to the mechanisms underlying the exacerbation of IgE-mediated airway inflammation and remodelling in mice. *Immunology*, 139(2), pp.205–18.

Moore, D.L. & Goldberg, J.L., 2011. Multiple transcription factor families regulate axon growth and regeneration. *Developmental Neurobiology*, 71(12), pp.1186–1211.

Moreno, B. et al., 2011. Systemic inflammation induces axon injury during brain inflammation. *Annals of Neurology*, 70(6), pp.932–42.

Mori, I. et al., 2001. Impaired microglial activation in the brain of IL-18-gene-disrupted mice after neurovirulent influenza A virus infection. *Virology*, 287(1), pp.163–70.

Moritz, D.R. et al., 1998a. The IL-1 receptor-related T1 antigen is expressed on immature and mature mast cells and on fetal blood

mast cell progenitors. *Journal of Immunology (Baltimore, Md. : 1950)*, 161(9), pp.4866–74.

Moritz, D.R. et al., 1998b. The IL-1 receptor-related T1 antigen is expressed on immature and mature mast cells and on fetal blood mast cell progenitors. *Journal of Immunology*, 161(9), pp.4866–74.

Morris-Downes, M.M. et al., 2002. Pathological and regulatory effects of anti-myelin antibodies in experimental allergic encephalomyelitis in mice. *Journal of Neuroimmunology*, 125(1-2), pp.114–24.

Mosmann, T.R. & Sad, S., 1996. The expanding universe of T-cell subsets: Th1, Th2 and more. *Immunology today*, 17(3), pp.138–46.

Moussion, C., Ortega, N. & Girard, J., 2008. The IL-1-Like Cytokine IL-33 Is Constitutively Expressed in the Nucleus of Endothelial Cells and Epithelial Cells In Vivo : A Novel " Alarmin "? Plos one, 3(10), pp.1–8.

Mouzannar, R. et al., 2001. Hydrogen peroxide induces rapid digestion of oligodendrocyte chromatin into high molecular weight fragments. *Neurochemistry International*, 38(1), pp.9–15.

Mulligan, S.J. & Macvicar, B.A., 2004. Calcium transients in astrocyte endfeet cause cerebrovascular constrictions. *Letters to Nature*, pp.195–199.

Murphy, A.C. et al., 2010. Infiltration of Th1 and Th17 cells and activation of microglia in the CNS during the course of experimental autoimmune encephalomyelitis. *Brain, behavior, and immunity*, 24(4), pp.641–51.

Najafian, N. et al., 2003. Regulatory functions of CD8 + CD28 – T cells in an autoimmune disease model. *The Journal of Clinical Investigation*, 112(7), pp.1037–1048.

Nandi, A., Estess, P. & Siegelman, M., 2004. Bimolecular complex between rolling and firm adhesion receptors required for cell

arrest; CD44 association with VLA-4 in T cell extravasation. *Immunity*, 20(4), pp.455–65.

Nash, B. et al., 2011. Functional Duality of Astrocytes in Myelination. *The Journal of Neuroscience*, 31(37), pp.13028–13038.

Nashold, F., Miller, D. & Hayes, C., 2000. 1,25-dihydroxyvitamin D3 treatment decreases macrophage accumulation in the CNS of mice with experimental autoimmune encephalomyelitis. *J Neuroimmunol*, 103(2), pp.171–9.

Neher, J.J., Neniskyte, U. & Brown, G.C., 2012. Primary phagocytosis of neurons by inflamed microglia: potential roles in neurodegeneration. *Frontiers in Pharmacology*, p.27.

Nguyen, D. & Stangel, M., 2001. Expression of the chemokine receptors CXCR1 and CXCR2 in rat oligodendroglial cells. *Brain research. Developmental Brain Research*, 128(1), pp.77–81.

Niino, M. et al., 2000. Vitamin D receptor gene polymorphism in multiple sclerosis and the association with HLA class II alleles. *Journal of the Neurological Sciences*, 177(1), pp.65–71.

Nimmerjahn, A., Kirchhoff, F. & Helmchen, F., 2005. Resting microglial cells are highly dynamic surveillants of brain parenchyma in vivo. *Science*, 308(5726), pp.1314–8.

Nogai, a. et al., 2005. Lipopolysaccharide Injection Induces Relapses of Experimental Autoimmune Encephalomyelitis in Nontransgenic Mice via Bystander Activation of Autoreactive CD4+ Cells. *The Journal of Immunology*, 175(2), pp.959–966.

Nowak, E.C. et al., 2009. IL-9 as a mediator of Th17-driven inflammatory disease. *The Journal of experimental medicine*, 206(8), pp.1653–60.

Ohya, W. et al., 2007. Hepatocyte growth factor (HGF) promotes oligodendrocyte progenitor cell proliferation and inhibits its

differentiation during postnatal development in the rat. *Brain Research*, 1147, pp.51–65.

Olitsky, P.K. & Yager, R.H., 1949. Experimental disseminated encephalomyelitis in white mice. *The Journal of Experimental Medicine*, 90(3), pp.213–24.

Olson, J.K. et al., 2001. A virus-induced molecular mimicry model of multiple sclerosis. *The Journal of Clinical Investigation*, 108(2), pp.311–318.

Oppmann, B. et al., 2000. Novel p19 protein engages IL-12p40 to form a cytokine, IL-23, with biological activities similar as well as distinct from IL-12. *Immunity*, 13(5), pp.715–25.

Ousman, S.S. & David, S., 2001. MIP-1 , MCP-1 , GM-CSF , and TNF- ␤ Control the Immune Cell Response That Mediates Rapid Phagocytosis of Myelin from the Adult Mouse Spinal Cord. *Journal of Neuroscience* , 21(13), pp.4649–4656.

Palmer, A.M., 2013. Multiple sclerosis and the blood-central nervous system barrier. *Cardiovascular psychiatry and neurology*, 2013, p.530356.

Pang, Y. et al., 2013. Differential roles of astrocyte and microglia in supporting oligodendrocyte development and myelination in vitro. *Brain and behavior*, 3(5), pp.503–14.

Panitch, H., 1994. Influence of infection on exacerbations of multiple sclerosis. *Ann Neurol*, 36, pp.25–8.

Panitch, H.S. et al., 1987. Exacerbations Of Multiple Sclerosis Interferon. *The Lancet*, pp.893–895.

Papadopoulos, M.C. et al., 2004. Aquaporin-4 facilitates reabsorption of excess fluid in vasogenic brain edema. *FASEB journal : official publication of the Federation of American Societies for Experimental Biology*, 18(11), pp.1291–3.

Pastorelli, L. et al., 2010. Epithelial-derived IL-33 and its receptor ST2 are dysregulated in ulcerative colitis and in experimental Th1/Th2 driven enteritis. *Proceedings of the National Academy of Sciences of the United States of America*, 107(17), pp.8017–22.

Pedrazzi, M. et al., 2014. Selective Proinflammatory Activation of Astrocytes by High-Mobility Group Box 1 Protein Signaling. *Journal of Immunology,* (179), pp8525-8532

Pedrazzi, M. et al., 2007. Selective proinflammatory activation of astrocytes by high-mobility group box 1 protein signaling. *Journal of Immunology*, 179(12), pp.8525–32.

Pellerin, L. & Magistretti, P.J., 1994. Glutamate uptake into astrocytes stimulates aerobic glycolysis: a mechanism coupling neuronal activity to glucose utilization. *Proceedings of the National Academy of Sciences of the United States of America*, 91(22), pp.10625–9.

Perry, V.H., 2004. The influence of systemic inflammation on inflammation in the brain: implications for chronic neurodegenerative disease. *Brain, behavior, and immunity*, 18(5), pp.407–13.

Perry, V.H., Newman, T. a & Cunningham, C., 2003. The impact of systemic infection on the progression of neurodegenerative disease. *Nature reviews. Neuroscience*, 4(2), pp.103–12.

Pfaff, S. & Kintner, C., 1998. Neuronal diversification: development of motor neuron subtypes. *Current opinion in neurobiology*, 8(1), pp.27–36.

Pfeiffer, F. et al., 2011. Claudin-1 induced sealing of blood–brain barrier tight junctions ameliorates chronic experimental autoimmune encephalomyelitis. *Acta Neuropathologica*, 122(5), pp.601–614.

Piccio, L. et al., 2002. Molecular mechanisms involved in lymphocyte recruitment in inflamed brain microvessels: critical roles for P-

selectin glycoprotein ligand-1 and heterotrimeric G(i)-linked receptors. *Journal of immunology*, 168(4), pp.1940–9.

Pichery, M. et al., 2012a. Endogenous IL-33 is highly expressed in mouse epithelial barrier tissues, lymphoid organs, brain, embryos, and inflamed tissues: in situ analysis using a novel Il-33-LacZ gene trap reporter strain. *Journal of immunology*, 188(7), pp.3488–95.

Pichery, M. et al., 2012b. Endogenous IL-33 is highly expressed in mouse epithelial barrier tissues, lymphoid organs, brain, embryos, and inflamed tissues: in situ analysis using a novel Il-33-LacZ gene trap reporter strain. *Journal of immunology*, 188(7), pp.3488–95.

Pichery, M. & Mirey, E., 2012. Highly Expressed in Mouse Epithelial Barrier Tissues, Lymphoid Organs, Brain, Embryos, and Inflamed Tissues: In Situ Analysis Using a Novel Il-33–LacZ Gene Trap. *The Journal of Immunology*, 188, pp.3488–3495.

Piddlesden, S. et al., 1991. Antibody-mediated demyelination in experimental allergic encephalomyelitis is independent of complement membrane attack complex formation. *Clinical and Experimental Immunology*, 83(2), pp.245–50.

Pierson, E. & Simmons, S., 2012. Mechanisms regulating regional localization of inflammation during CNS autoimmunity. *Immunological Review*, 248(1), pp.205–215.

Pirko, I. et al., 2004. In vivo magnetic resonance imaging of immune cells in the central nervous system with superparamagnetic antibodies. *FASEB journal : official publication of the Federation of American Societies for Experimental Biology*, 18(1), pp.179–82.

Pöllinger, B. et al., 2009. Spontaneous relapsing-remitting EAE in the SJL/J mouse: MOG-reactive transgenic T cells recruit endogenous MOG-specific B cells. *The Journal of Experimental Medicine*, 206(6), pp.1303–16.

Powell, E.M. & Geller, H.M., 1999. Dissection of Astrocyte-Mediated Cues in Neuronal Guidance. *Glia* , 83, pp.73–83.

Puschmann, T.B., Dixon, K.J. & Turnley, A.M., 2010. Species differences in reactivity of mouse and rat astrocytes in vitro. *Neuro-Signals*, 18(3), pp.152–63.

Pushparaj, P.N. et al., 2009. The cytokine interleukin-33 mediates anaphylactic shock. *Proceedings of the National Academy of Sciences of the United States of America*, 106(24), pp.9773–8.

Qin, Y. et al., 1998. Clonal expansion and somatic hypermutation of V(H) genes of B cells from cerebrospinal fluid in multiple sclerosis. *The Journal of Clinical Investigation*, 102(5), pp.1045–50.

Ramroodi, N. et al., 2013. Monitoring of active human herpes virus 6 infection in Iranian patients with different subtypes of multiple sclerosis. *Journal of Pathogens*, 2013, p.194932.

Raupach, B. et al., 2006. Caspase-1-mediated activation of interleukin-1beta (IL-1beta) and IL-18 contributes to innate immune defenses against Salmonella enterica serovar Typhimurium infection. *Infection and immunity*, 74(8), pp.4922–6.

Ray, J. & Gage, F.H., 2006. Differential properties of adult rat and mouse brain-derived neural stem/progenitor cells. *Molecular and cellular Neurosciences*, 31(3), pp.560–73.

Reboldi, A. et al., 2009. C-C chemokine receptor 6-regulated entry of TH-17 cells into the CNS through the choroid plexus is required for the initiation of EAE. *Nature immunology*, 10(5), pp.514–23.

Remington, L.T. et al., 2007. Microglial recruitment, activation, and proliferation in response to primary demyelination. *The American Journal of Pathology*, 170(5), pp.1713–24.

Rodriguez, M., 2007. Effectors of demyelination and remyelination in the CNS: implications for multiple sclerosis. *Brain pathology*, 17(2), pp.219–29.

Rovere-Querini, P. et al., 2004. HMGB1 is an endogenous immune adjuvant released by necrotic cells. *EMBO reports*, 5(8), pp.825–30.

Runmarker, B. & Andersen, O., 1995. Pregnancy is associated with a lower risk of onset and a better prognosis in multiple sclerosis. *Brain : a Journal of Neurology*, 118 (Pt 1), pp.253–61.

Sairanen, T.R. et al., 1997. Global forebrain ischemia results in differential cellular expression of interleukin-1beta (IL-1beta) and its receptor at mRNA and protein level. *Journal of Cerebral Blood Flow and Metabolism : official journal of the International Society of Cerebral Blood Flow and Metabolism*, 17(10), pp.1107–20.

Sanada, S. et al., 2007. IL-33 and ST2 comprise a critical biomechanically induced and cardioprotective signaling system. *The Journal of Clinical Investigation*, 117(6).

Satoh, J., Lee, Y. & Kim, S., 1995. T-cell costimulatory molecules B7-1 (CD80) and B7-2 (CD86) are expressed in human microglia but not in astrocytes in culture. *Brain research*, 704, pp.92–96.

Sayed, B. a et al., 2010. Meningeal mast cells affect early T cell central nervous system infiltration and blood-brain barrier integrity through TNF: a role for neutrophil recruitment? *Journal of immunology*, 184(12), pp.6891–900.

Schif-Zuck, S. et al., 2005. Targeted Overexpression of IL-18 Binding Protein at the Central Nervous System Overrides Flexibility in Functional Polarization of Antigen-Specific Th2 Cells. *The Journal of Immunology*, 174(7), pp.4307–4315.

Schmitz, J. et al., 2005. IL-33, an interleukin-1-like cytokine that signals via the IL-1 receptor-related protein ST2 and induces T helper type 2-associated cytokines. *Immunity*, 23(5), pp.479–90.

Schnitzer, J. & Karschin, a, 1986. The shape and distribution of astrocytes in the retina of the adult rabbit. *Cell and tissue research*, 246(1), pp.91–102.

Serafini, B. et al., 2004. Detection of ectopic B-cell follicles with germinal centers in the meninges of patients with secondary progressive multiple sclerosis. *Brain pathology*, 14(2), pp.164–74.

Shannon, C., Salter, M. & Fern, R., 2007. GFP imaging of live astrocytes: regional differences in the effects of ischaemia upon astrocytes. *Journal of Anatomy*, 210(6), pp.684–92.

Shi, G. et al., 2009. Phenotype Switching by Inflammation-Inducing Polarized Th17 Cells, but not by Th1 Cells. *Journal Of Immunology*, 181(10), pp.7205–7213.

Sibley, W.A. & Bamford, C.R., 1985. Clinical Viral Infection and Multiple sclerosis. *The Lancet*, pp.1313–1315.

Sicotte, N.L. et al., 2002. Treatment of multiple sclerosis with the pregnancy hormone estriol. *Annals of Neurology*, 52(4), pp.421–8.

Skulina, C. et al., 2004. Multiple sclerosis: brain-infiltrating CD8+ T cells persist as clonal expansions in the cerebrospinal fluid and blood. *Proceedings of the National Academy of Sciences of the United States of America*, 101(8), pp.2428–33.

Smith, D.E., 2011. The biological paths of IL-1 family members IL-18 and IL-33. *Journal of leukocyte biology*, 89(3), pp.383–92.

Smithgall, M.D. et al., 2008. IL-33 amplifies both Th1- and Th2-type responses through its activity on human basophils, allergen-reactive Th2 cells, iNKT and NK cells. *International immunology*, 20(8), pp.1019–30.

Sofroniew, M. V, 2010. Molecular dissection of reactive astrogliosis and glial scar formation. *Trends in Neuroscience*, 32(12), pp.638–647.

Sorensen, A. et al., 2008. Astrocytes, but not olfactory ensheathing cells or Schwann cells, promote myelination of CNS axons in vitro. *Glia*, 56(7), pp.750–63.

Sospedra, M. & Martin, R., 2005. Immunology of multiple sclerosis. *Annual review of immunology*, 23, pp.683–747.

Spassky, N. et al., 2001. Sonic hedgehog-dependent emergence of oligodendrocytes in the telencephalon : evidence for a source of oligodendrocytes in the olfactory bulb that is independent of PDGFRα signaling. , 5004, pp.4993–5004.

Staudt, V. et al., 2010. Interferon-regulatory factor 4 is essential for the developmental program of T helper 9 cells. *Immunity*, 33(2), pp.192–202.

Steinman, L., 1999. Assessment of animal models for MS and demyelinating disease in the design of rational therapy. *Neuron*, 24(3), pp.511–4.

Steinman, R.M. & Nussenzweig, M.C., 2002. Avoiding horror autotoxicus: the importance of dendritic cells in peripheral T cell tolerance. *Proceedings of the National Academy of Sciences of the United States of America*, 99(1), pp.351–8.

Stevens, B. et al., 2007. The classical complement cascade mediates CNS synapse elimination. *Cell*, 131(6), pp.1164–78.

Stewart, V.C. et al., 2000. Astrocyte-derived nitric oxide causes both reversible and irreversible damage to the neuronal mitochondrial respiratory chain. *Journal of Neurochemistry*, 75(2), pp.694–700.

Stockinger, B. & Veldhoen, M., 2007. Differentiation and function of Th17 T cells. *Current opinion in immunology*, 19(3), pp.281–6.

Stromnes, I.M. et al., 2008. Differential regulation of central nervous system autoimmunity by T(H)1 and T(H)17 cells. *Nature medicine*, 14(3), pp.337–42.

Stromnes, I.M. & Goverman, J.M., 2006. Active induction of experimental allergic encephalomyelitis. *Nature protocols*, 1(4), pp.1810–9.

Stüve, O. et al., 2005. Clinical stabilization and effective B-lymphocyte depletion in the cerebrospinal fluid and peripheral blood of a patient with fulminant relapsing-remitting multiple sclerosis. *Archives of Neurology*, 62(10), pp.1620–3.

Subramanian, S. et al., 2011. Oestrogen-mediated protection of experimental autoimmune encephalomyelitis in the absence of Foxp3+ regulatory T cells implicates compensatory pathways including regulatory B cells. *Immunology*, 132(3), pp.340–7.

Sugama, S. et al., 2007. Stress induced morphological microglial activation in the rodent brain: involvement of interleukin-18. *Neuroscience*, 146(3), pp.1388–99.

Sugawara, S. et al., 2014. Neutrophil Proteinase 3-Mediated Induction of Bioactive IL-18 Secretion by Human Oral Epithelial Cells. *The Journal of Immunology,* (167), pp 6568-6575

Suh, S.W. et al., 2007. Astrocyte Glycogen Sustains Neuronal Activity during Hypoglycemia : Studies with the Glycogen Phosphorylase. *The Journal of Pharmacology and Experimental Therpeutics*, 321(1), pp.45–50.

Sun, D. et al., 2001. Myelin antigen-specific CD8+ T cells are encephalitogenic and produce severe disease in C57BL/6 mice. *Journal of immunology*, 166(12), pp.7579–87.

Sutton, C.E. et al., 2009. Interleukin-1 and IL-23 induce innate IL-17 production from gammadelta T cells, amplifying Th17 responses and autoimmunity. *Immunity*, 31(2), pp.331–41.

Swapna, I. et al., 2006. Phospholipid and cholesterol alterations accompany structural disarray in myelin membrane of rats with

hepatic encephalopathy induced by thioacetamide. *Neurochemistry international*, 49(3), pp.238–44.

Takahashi, Y. et al., 2013. Circumventricular organs and fever. *American Journal of Physiology - Regulatory, Integrative and Comparative Physiology*, 273, pp.1690–1695.

Taniguchi, K. et al., 2013. Interleukin 33 Is Induced by Tumor Necrosis Factor _ and Interferon a in Keratinocytes and Contributes to Allergic Contact Dermatitis. *Journal of Investigational Allergology and Clinical Immunology*, 23(6), pp.428–434.

Thomassen, E. et al., 1998. Binding of interleukin-18 to the interleukin-1 receptor homologous receptor IL-1Rrp1 leads to activation of signaling pathways similar to those used by interleukin-1. *Journal of interferon & cytokine research : the official Journal of the International Society for Interferon and Cytokine Research*, 18(12), pp.1077–88.

Thomson, C.E. et al., 2006. Murine Spinal Cord Explants : A Model For Evaluating Axonal Growth and Myelination In Vitro. *Journal of Neuronscience,* pp.1703–1715.

Thomson, C.E. et al., 2008. Myelinated, synapsing cultures of murine spinal cord--validation as an in vitro model of the central nervous system. *The European Journal of Neuroscience*, 28(8), pp.1518–35.

Tievsky, a L., Ptak, T. & Farkas, J., 1999. Investigation of apparent diffusion coefficient and diffusion tensor anisotrophy in acute and chronic multiple sclerosis lesions. *AJNR. American journal of Neuroradiology*, 20(8), pp.1491–9.

Todorich, B. et al., 2009. Oligodendrocytes and myelination: the role of iron. *Glia*, 57(5), pp.467–78.

Tominaga, S., Kuroiwa, K. & Tago, K., 1999. Presence and expression of a novel variant form of ST2 gene product in human leukemic cell

line UT-7/GM. *Biochemical and Biophysical Research Communications*, 18, pp.14–18.

Tselios, T. et al., 2000. Treatment of Experimental Allergic Encephalomyelitis (EAE) Induced by Guinea Pig Myelin Basic Protein Epitope 72 ± 85 with a Human MBP 87À99 Analogue and E € ects of Cyclic Peptides. *Bioorganic & Medicinal Chemistry*, 8, pp.1903–1909.

Tsuda, H. et al., 2012a. Novel Splice Variants of IL-33: Differential Expression in Normal and Transformed Cells. *The Journal of Investigative Dermatology*, 132(11), pp.2661–4.

Tsuda, H. et al., 2012b. Novel Splice Variants of IL-33: Differential Expression in Normal and Transformed Cells. *The Journal of Investigative Dermatology*, 132(11), pp.2661–4.

Tsuda, M. et al., 2009. IFN-gamma receptor signaling mediates spinal microglia activation driving neuropathic pain. *Proceedings of the National Academy of Sciences of the United States of America*, 106(19), pp.8032–7.

Tsunoda, I. & Fujinami, R., 2010. Neuropathogenesis of Theiler's murine encephalomyelitis virus infection, an animal model for multiple sclerosis. *Journal of Neuroimmune Pharmacology*, 5(3), pp.355–369.

Ulvestad, E. et al., 1994. Reactive microglia in multiple sclerosis lesions have an increased expression of receptors for the Fc part of IgG. *Journal of the Neurological Sciences*, 121(2), pp.125–131.

Uno, H. & Else, G., 1989. Hippocampal Primates Damage Associated. *The Journal of Neuroscience*, pp.1705–1711.

Vajkoczy, P., Laschinger, M. & Engelhardt, B., 2001. α 4-integrin-VCAM-1 binding mediates G protein – independent capture of encephalitogenic T cell blasts to CNS white matter microvessels. *The Journal of Clinical Investigation* , 108(4), pp.557–565.

Venken, K. et al., 2008. Compromised CD4+ CD25(high) regulatory T-cell function in patients with relapsing-remitting multiple sclerosis is correlated with a reduced frequency of FOXP3-positive cells and reduced FOXP3 expression at the single-cell level. *Immunology*, 123(1), pp.79–89.

Warrington, a E. et al., 2000. Human monoclonal antibodies reactive to oligodendrocytes promote remyelination in a model of multiple sclerosis. *Proceedings of the National Academy of Sciences of the United States of America*, 97(12), pp.6820–5.

Watkins, T.A. et al., 2009. Distinct Stages of Myelination Regulated by γ-Secretase and Astrocytes in a Rapidly Myelinating CNS Coculture System. *Neuron*, 60(4), pp.555–569.

Weaver, A. et al., 2005. An elevated matrix metalloproteinase (MMP) in an animal model of multiple sclerosis is protective by affecting Th1/Th2 polarization. *FASEB Journal : official publication of the Federation of American Societies for Experimental Biology*, 19(12), pp.1668–70.

Weber, M.S. et al., 2004. Multiple sclerosis: glatiramer acetate inhibits monocyte reactivity in vitro and in vivo. *Brain : a journal of neurology*, 127(Pt 6), pp.1370–8.

Weinshenker, B.G. et al., 1999. A randomized trial of plasma exchange in acute central nervous system inflammatory demyelinating disease. *Annals of neurology*, 46(6), pp.878–86.

Weissert, R. et al., 1998. MHC haplotype-dependent regulation of MOG-induced EAE in rats. *The Journal of Clinical Investigation*, 102(6), pp.1265–73.

Wergeland, S. et al., 2011. Dietary vitamin D3 supplements reduce demyelination in the cuprizone model. *PloS one*, 6(10), p.e26262.

Werman, a. et al., 2004. The precursor form of IL-1 is an intracrine proinflammatory activator of transcription. *Proceedings of the National Academy of Sciences*, 101(8), pp.2434–2439.

Whitaker, E.L. et al., 2012. Splice Variants of mda-7/IL-24 Differentially Affect Survival and Induce Apoptosis in U2OS Cells: Functional Characterization of mda-7/IL-24 Splice Isoforms. *Cytokine*, 56(2), pp.272–281.

Wicher, G. et al., 2013. Developmental expression of IL-33 in the mouse brain. *Neuroscience letters*, 555, pp.171–6.

Wilhelmsson, U. et al., 2006. Redefining the concept of reactive astrocytes as cells that remain within their unique domains upon reaction to injury. *Proceedings of the National Academy of Sciences of the United States of America*, 103(46), pp.17513–8.

Wojkowska, D.W. et al., 2014. Chemokines during the Initiation of Experimental Model of Multiple Sclerosis. *Mediators of Inflammation* , 2014, pp.1–9.

Wolinsky, J.S., 1999. The mechanisms of lesion genesis in multiple sclerosis? *Brain : a Journal of Neurology*, 122 (Pt 7, pp.1211–2.

Woodworth, C.D. et al., 1995. Interleukin la and tumor necrosis factor a stimulate autocrine amphiregulin expression and proliferation of human. , 92, pp.2840–2844.

Wucherpfennig, K.W. & Strominger, J.L., 1995. Molecular mimicry in T cell-mediated autoimmunity: viral peptides activate human T cell clones specific for myelin basic protein. *Cell*, 80(5), pp.695–705.

Xu, D. et al., 2010. IL-33 exacerbates autoantibody-induced arthritis. *Journal of immunology*, 184(5), pp.2620–6.

Xu, D. et al., 1998. Selective expression of a stable cell surface molecule on type 2 but not type 1 helper T cells. *The Journal of Experimental Medicine*, 187(5), pp.787–94.

Yamazaki, T. et al., 2008. CCR6 Regulates the Migration of Inflammatory and Regulatory T Cells. *The Journal of Immunology*, 181(12), pp.8391–8401.

Yan, H. & Rivkees, S. a, 2002. Hepatocyte growth factor stimulates the proliferation and migration of oligodendrocyte precursor cells. *Journal of Neuroscience Research*, 69(5), pp.597–606.

Yanagawa, Y. et al., 2011. Prostaglandin E(2) enhances IL-33 production by dendritic cells. *Immunology letters*, 141(1), pp.55–60.

Yang, J. et al., 2002. Differential Expression of Cytokines (IL-2 , IFN- g , IL-10) and Adhesion Molecules (VCAM-1 , LFA-1 , CD44) Between Spleen and Lymph Nodes Associates with Remission in Chronic Relapsing Experimental Autoimmune Encephalomyelitis. *Scandinavian Journal of Immunology*, 1, pp.286–293.

Yang, Y.-X. & Lichtenstein, G.R., 2002. Corticosteroids in Crohn's disease. *The American Journal of Gastroenterology*, 97(4), pp.803–23.

Yasuoka, S. et al., 2011. Production and functions of IL-33 in the central nervous system. *Brain research*, 1385, pp.8–17.

Yen, D. et al., 2006. IL-23 is essential for T cell – mediated colitis and promotes inflammation via IL-17 and IL-6. The Journal of Clinical Investigation, 116(5).

Yu, J.-T. et al., 2012. Implication of IL-33 gene polymorphism in Chinese patients with Alzheimer's disease. *Neurobiology of aging*, 33(5), pp.1014.e11–4.

Zamvil, S.S. & Steinman, L., 1990. The T Lymphocyte in Experiemental Allergic Encephalomyelitis. *Annual review of immunology*, pp.579–621.

Zhang, Z. et al., 1998. Cerebral vessels express interleukin 1beta after focal cerebral ischemia. *Brain research*, 784(1-2), pp.210–7.

Zorzella-Pezavento, S.F.G. et al., 2013. Persistent Inflammation in the CNS during Chronic EAE Despite Local Absence of IL-17 Production. *Mediators of Inflammation*, 2013, pp.1–10.